NTNU

Norwegian University of
Science and Technology

Case study of offshore wind farm integration to offshore oil and gas platforms as an isolated system - System Topologies, Steady State and Dynamic Aspects

Maheshkumar Hadiya

Master of Science in Electric Power Engineering
Submission date: July 2011
Supervisor: Kjetil Uhlen, ELKRAFT

Norwegian University of Science and Technology
Department of Electric Power Engineering

NTNU – Trondheim
Norwegian University of
Science and Technology

Case study of offshore wind farm integration to offshore oil and gas platforms as an isolated system

System Topologies, Steady State and Dynamic Aspects

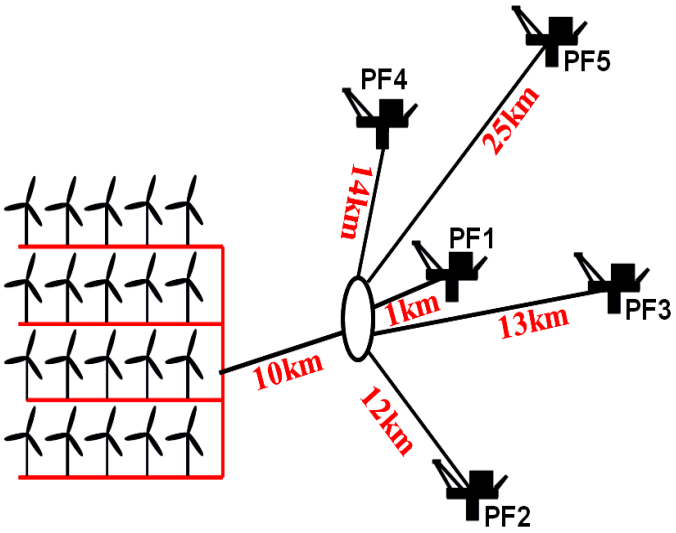

Maheshkumar Hadiya

Master of Science in Electric Power Engineering
Submission date: July 2011
Supervisor: Prof. Kjetil Uhlen, Elkraft NTNU
Co-supervisor: Dr. Wei He, Principal Researcher, Statoil Research Center, Bergen
Firms: Nowitech and Statoil ASA

Norwegian University of Science and Technology
Department of Electric Power Engineering

"This page is Intentionally Left Blank"

PROBLEM DESCRIPTION

In 1998, according to Kyoto protocol signed at Japan, the European countries made a commitment to reducing their CO_2 / NOx emissions as first commitment for period 2020. Based on that, Norway has decided the goal of 20-20, means 20 % wind penetration and 20 % CO2 reduction by 2020 and no net CO_2 emissions by 2050.

This M.Sc. thesis work will be a continuation of the project work performed in the autumn semester 2010 entitled “Specialization Project Work”. The scope of that project work was to study challenges related to integration of offshore wind farm to offshore oil and gas platforms as an isolated system via high voltage AC interconnections.

The objective of thesis shall be to examine reliability and stability issues of an “off grid” isolated system of an offshore wind farm integration to five offshore oil and gas platforms, have different load demands. System stability studies shall be performed, focusing on power quality requirements analysis and following the offshore NORSOK standards for voltage and frequency variations. Various system simulation studies shall be performed, including starting of large induction motors, loss of wind power production, loss of generation at platforms and loss of interconnections between two platforms considering different topology aspects. It is of particular interest to examine various system dynamic aspects and benefits of the integrated system, such as criticality of perturbation events, significance and consequences of wind power penetration, wind power loss and loss of interconnections in the system. A study concerning security of power supply and loss of load could be included by considering different platform connection topologies. Enhancement of dynamic voltage control capability during transient conditions should also be analyzed with application of power electronics equipments like SVC and STATCOM. Simulation should also be performed for two different system voltage levels such as 36kV and 52kV via static power flow analysis and dynamic analysis.

The work shoud be analysed and investigated for proposed system network via dynamic simulation software tool SIMPOW.

Assignment given: 07th February 2011
Supervisor: Prof. Kjetil Uhlen, ELKRAFT NTNU
Submission: July 2011

FOREWORD

This master's thesis work has been done in collaboration with Nowitech and Statoil under ongoing research project work. The work performed in this project was interesting for firms owing to advanced development in the field of deep sea "floating wind turbines" technology, commitment toward fossil energy saving and emission of CO_2 / NOx reduction. It is a continuation of a specialization work autumn 2010 and part of thesis work was performed at Statoil ASA, research center at Bergen.

Trondheim – July, 2011

Maheshkumar Hadiya

ACKNOWLEDGEMENT

Work of thesis was mostly performed in the Department of Electrical Power Engineering at NTNU, Trondheim in collaboration with Nowitech research center at SINTEF and Statoil ASA at Bergen. Partially work was performed at Statoil ASA, Research Center, Bergen. It ends of my two years studies in NTNU - Norway in order to complete master degree in Electrical Power Engineering.

First of all I would like to thank Prof. Kjetil Uhlen, my direct supervisor, for giving me such an opportunity to carry out work under ongoing research activities as part of my master thesis, for his patient guidance, useful suggestions and giving me permission, recommendation and cooperation to perform work at Statoil ASA, Bergen. As a professor in NTNU, his course entitled Power System Stability (TET4180) and Power System Analysis (TET4115), gave motivation to focus my studies on power system stability aspects and wind power system integration kind of specific field.

I would like to thank Dr. Wei He, principal researcher at Statoil ASA, Research Center at Bergen for giving me opportunity by inviting at Statoil to perform partly my thesis work there. I am really grateful to her for made me familiarized with practical information, help to collect necessary technical real data from different departments, valuable inputs and her great support and guidance. I am also thankful to all Research group staff at Statoil for cooperation and help.

I am grateful to Trond Toftevaag, senior researcher at SINTEF Energy Research also professor at NTNU and Harald Svendsen, researcher at SINTEF for giving me a very precious technical guide, his valuable time and made me familiarized with commercial software tool SIMPOW. They spend much time with me for tackling SIMPOW software related problems and technical discussions even though they are not my supervisor.

I would like to thanks SINTEF Energy Research Group and Electrical Power Engineering Department – NTNU for providing me a specific SIMPOW commercial software license of 1000 nodes since my system consists of around 650 nodes large system. I am grateful to my Prof. Kjetil uhlen, Trond Toftevaag and Kurt Salmi, Elkraft NTNU for help me to get access, resolving my technical problems of the tool at any time.

My thanks go to my classmates Anders, Sigurd, Lester and Sachin, we had a lot of discussions, exchange of ideas, thoughts and computer support regarding our master works.

My brother, Nanji and sister in law, Shobhna are to be thanked for making my stay comfortable and enjoyable. I met a lot of people during those two years and I will never forget this foreign experience.

Last but not in least I would like to special thank to my parents for giving me moral support and my wife for supported me all along, I am thankful to all of them.

Maheshkumar Hadiya
Trondheim, July - 2011

SUMMARY

The objective of this thesis work has been to investigate the electric system stability, reliability and power security of an "off-grid" isolated network system integration of an offshore wind farm to offshore oil and gas platforms via HVAC transmission, considering different network topologies for wind power penetration, network losses, application of FACTS devices and different system voltage levels. The system stability studies were performed by steady state and dynamic simulations, analysing different perturbation events in the system.

The power system model under study was established as a continuation of a previous work concerning a single platform system. The model can be seen to represent the Oseberg oilfield in the Norwegian Sea consisting of five offshore platforms. The complete model represents a grid integration of the five offshore platforms with a total load demand of 147MW to an offshore wind farm of 100MW production via HVAC as an isolated system. Wind farm capacity is less but of comparable size to the total load. Each platform has its own offshore power generation units (Gas Turbines - GTs) to cover the load demand at each platform. Load demands were selected based on recently collected real operational power consumption data from Statoil, ASA. In this study, 8 GTs were installed at different specific platforms to cope with the load of 150MW. Three different network topology configurations were considered, denoted Star, Star-F and Meshed. Four types of perturbation/disturbance events were analysed: Starting of 9MW asynchronous motor at Platform4, loss of a GT at Platform4, sudden loss of wind power production and loss of interconnection cable between Platform1 and Plaform4. The dynamic system stability was assessed by measuring frequency and voltage deviations at specific load buses to ensure whether transient deviations were following offshore NORSOK or IEC standards correctly or not.

For each type of disturbances, different topology aspects were considered and analysed for different outages and different cases of percentage of wind power penetration. It could be seen that generators at platforms in all cases were able to regain synchronism by maintaining terminal voltage and power factor within allowed ranges after disturbances caused by Starting of 9MW motor, loss of wind power, loss of a GT and loss of cable. This can be explained because the isolated network system has a strong spinning reserve capacity. But not all studied scenarios were dynamically stable, following NORSOK standards for transient of voltage and frequency variations.

The results showed the importance of an integrated grid system: Starting of big induction motor was found not to give large frequency or voltage deviations compared to the previous study of a single platform system since the integrated system has a larger inertia. Voltage deviations were found most critical in case of starting big motors. In addition, a meshed topology have better performace with less voltage and frequency deviation compared to the other two topologies for all perterbation events and cases.

The results also showed that loss of wind power was more critical at high wind power penetration levels. A 100% sudden loss of wind power gave unacceptable frequency deviations. The study of two different voltage levels, 36kV and 52kV showed that a 52 kV network gave better dynamic stability behaviour compared to the other one. The study of FACTS devices applications showed that a STATCOM was more efficient in dynamic control of voltage than an SVC due to its better reactive power compensation capability at lower voltage, thus improving power transmission capability for the same power ratings.

TABLE OF CONTENTS

LIST OF FIGURES

LIST OF TABLES

1 INTRODUCTION

Wind energy is widely used nowadays in Europe and especially in Denmark where it represents more than 20% of the total production. In Norway, wind power gained a lot of interests in the last decade, now reaches an annual production above 3 TWh.

Europe is one of the best areas for the implementation of offshore wind farms due to shallow waters. Winds are strong and stable in the Baltic and North Sea and thus offshore implementation of wind farms is seen as the development of many future wind farm projects. It is such that offshore wind power could represent 10% of the electricity production of European Union in 2020.

Offshore sites can be found in the South and West of Norway but most of the fjord area is protected by industrial infrastructures. Modern wind farms are installed in shallow waters, at depth up to 50 meters but, most promising places are at water depths from 30 to 150 meters in Norway. Thus, development of large scale offshore wind farm is limited by exploitation of the necessary bases.

Three main types of power transmission technologies available in market for offshore interconnection to grid are: High Voltage Alternating Current (HVAC), Line-Commutated Converter (LCC) based High Voltage Direct Current (HVDC) and Voltage-Source Converters (VSC) based HVDC. HVAC is the easiest and well-known way to make connections. However, reactive power capability of HVAC cables has demoed its limits and HVDC tends to replace most of offshore connections. LCC based HVDC equips most of HVDC transmissions but self commutating converters are also the next step, with VSC already replacing LCC. VSC stations are smaller and thus for high amount of power, it is much easier to install offshore.

1.1 Motivation

Norway has large costal area, good wind condition near by costal area and hence a large potential to produce wind power. Synergy of wind power integaration to electric grid, power produced via wind must be needed to integrated with the electric grid. Limited available source of fossil fuels, more utilization of free uncommitted wind power energy are the motivation points to investigate study of offshore wind power integration to offshore oil and gas platforms. Moving towards green renewable energy to reduce the global warming effect by reducing CO2/NOx emission is also an important motivation for this work.

The introduction of renewable power production into an existing electric grid can results new challenges regarding voltage and frequency deviation, system stability and security of the power supply. As wind is the main source for wind power production, the large wind fluctuations introduce additional challenges as voltage flickering, harmonics and reactive power fluctuations problems. To minimize fluctuations in power, voltage and frequency requires efficient integration of control system. Hence to perform steady state and dynamic analyses to investigate impacts and importance of the integrated system. This report focuses on challenges related to the integration of an"off grid" isolated system of offshore wind farm integration to offshore five oil and gas platforms via HVAC trasmission system.

1.2 Background

As a part of international commitment [1] and response to global warming, Norway has set target for reducing CO_2 / NOx emission in the coming years. Since the electric power supply in Norway is largely dominated by renewable energy in form of hydro power, there is very little scope for emission reductions within this sector. However, there is an exception; nearly all offshore petroleum installations are currently powered by on-site gas turbines. These rely on fossil fuel and contribute significantly to Norwegian carbon emissions. *Klimakur 2020* [2, 3], a recent policy document, has identified electrification of the offshore oil and gas sector as a priority to achieve emission reduction targets in the short term.

Electrification of offshore installations can be realised by subsea power cables from land. A significant reduction in carbon emissions can be achieved if this is combined with added renewable power production on the grid. Electrification options with power from land has been described in reference [4].

An alternative to reducing carbon emissions via electrification from land is to connect offshore petroleum installations directly to offshore power production with or without connection to land. The most realistic offshore deep water power production is currently a floating offshore wind farm [5]. Such an offshore platform/wind farm combination has been identified as a potential match for the offshore petroleum sector's desire for renewable energy with the offshore wind power industry's desire for an early market.

A stand-alone offshore power grid that connects one or more oil and gas platforms with a floating wind farm poses technical challenges that have so far not been fully studied.

1.3 Present study

The present study addresses some of the technical issues related to power system stability, reliability, security and dynamic voltage control owing to integration of offshore wind power to offshore oil and gas platforms following offshore NORSOK and IEC standards as a reference. The project work performed is part of an ongoing research project work under Norwegian Research Centre for Offshore Wind Technology (NOWITECH) work package 4 – grid integration, Task 4.2 – electri grid connection, topology and control in collaboration with Statoil ASA, Norway.

The thsis work performed here, is continuation of previous case study done about to; integration of small offshore wind farm consists of four wind turbine (4x5 MW) to an offshore oil and gas platform with an active load demand of approximately 20 MW [6] as an isolated "off grid" system. This study is extended by, integration of five real offshore oil and gas platforms to an offshore wind farm of 100MW via HVAC power transmission. The wind farm is radially connected by four feeders of five wind turbines in each (4x5x5 MW) [7]. The study also includes different inteconnecation topology configurations of five offshore platforms to investigate security of supply aspects. Three different topologies viz., Star, Star-F, and Mesh topologies have been considered for the study. For such an offshore independent and isolated integrated system there are numerous interesting questions that require to be answered. This study deals with following technical aspects:

- System stability aspect: Steady state and dynamic stability of system
- Power system, security of supply aspect: Different topology view point
- System voltage levels aspect: 36kV and 52kV system comparison
- Dynamic voltage control aspect: SVC and Statcom application strategies

The relative locations of platforms and wind farm have in this study been kept fixed for all the simulation cases according to different topologies. The chosen platforms and windfarm layout is based on the real locations of the Oseberg oilfield platforms in western coast of the Norwegian Sea and the principle that the security of supply and length of interconnecting cables should be minimised. Two system voltage level of 36 kV and 52kV have been considered to examine impact on system stability through voltage and frequency deviation comparison for different perturbations. As mentioned earlier, motivation of thesis is to analyse; power reliability, system stability behavior, security of supply, criticality of perturbation and importance of integrated system with respect to a consistent contingency

perturbation events. Four main classes of perturbations have been focused for static and dynamic simulations study:

- Starting of 9MW induction motor at a platform
- Loss of a Gas Turbine (GT) at a platform
- Sudden loss of wind power production
- Loss of interconnection between to adjacent platforms

Considering different topology aspects for each of the above cases, percentage of wind power penetration or suddent wind power loss for a system are evaluated. The real operationl data of Starting of 9MW induction motor at PF4 taken by UNITECH Power System AS are set as reference data, frequency and voltage deviations have been compared for different network topology aspects with these data. By this way importance of integrated system, against single platform system could be compared and analysed. The effect of different wind production penetration/loss on frequency and voltage deviations, effects on power production at platforms generations have been analyzed and compared following the limitations fixed by NORSOK [8]. Impact of SVC and STATCOM applications at Platform1 to improve voltage transients control and enhancement in system stability for start up of 9MW motor have been performed. All simulations have been performed using the commercial power system dynamic software tool SIMPOW.

1.4 Report Outline

Chapter 2 contains the relevant background theory considered to be importnat for project work. It includes the basics of wind power technology, about grid code, NORSOK and IEC standards for offshore wind technology, theory of reactive power compensation and strategies relevant to dynamic voltage control through application of SVC and STATCOM based FACTS deviceses.

Chapter 3 gives description and basis of the proposed system network, technical details about individual platforms and different network topologies aspects. Chaper 4 gives reference data to this study, obtained from UNITECH Power System AS at one of the real platform and relevent details. Chapter 5 outlines the detailed modeling of the power system network under study. It includes a description of the different types of models used in this study.

Chaper 6 describes static and dynamic simulation work performed for different cases, relevent analysis, results and discussions. Conclusions and future work have been described in Chapter 7.

2 BASIC THEORY

2.1 Over View - Wind turbine technology

The wind turbine technology is differentiates by many way, according to design of wind turbine Horizontal Axis Wind Turbine (HAWT) and Vertical Axis Wind Turbine (VAWT). According to orientation of rotor position, upwind or downwind wind turbine. According to hub design, rigid or teetering. According to number of blades used, usually two or three blades wind turbine. And according to alignment with the wind as free yaw or active yaw. But Wind turbines are mostly classified according to power control strategies, speed control and generator with use of power electronics as below [9].

- **According to power control aspect:**

All wind turbines are designed with some sort of power control. There are different ways to control aerodynamic forces on the turbine rotor and thus to limit the power in very high winds in order to avoid damage to the wind turbine[10].

- Stall control
- Pitch control
- Active stall control

- **According to speed control aspect:**

- Fixed speed wind turbine (conventional control system)
- Variable speed wind turbine (with use of advanced power electronics)

- **According to generator with use of power electronics control aspect:**

- Directly connected Induction generator
- Doubly fed induction generator
- Full convertor connected generator

Stall control*:* - The simplest, most robust and cheapest control method (passive control), The blades are bolted onto the hub at a fixed angle. At high speed the special design of rotor aerodynamics causes the rotor to stall (lose power)

- *Advantages:* - Power control at high wind speed, less power fluctuations compared to fast pitch control.
- *Drawbacks:* - lower efficiency at low wind speeds,

Pitch control*:* - active control, where the blades can be turned out or into the wind when power high or too low, respectively.

- *Advantages:* - Good power control, performance of startup and emergency stop can done easily
- *Disadvantage:* - More Complex, costlier then stall control and more fluctuations in power at high wind speeds and during gusts.

Active stall control*:* - This control is mixing of both above system. At low wind speeds the blades are pitched similar to a pitch-controlled wind turbine and at high wind speeds the blades go into stall, the direction opposite to that of a pitch-controlled turbine.

- *Advantage:* - Smoother power control, less power fluctuations and emergency stops and to start up performs
- *Disadvantage:* - More complexity in mechanism and extra cost for control with active yaw mechanism.

Fixed speed wind turbines

In the early 1990s the standard installed wind turbines operated at fixed speed. That means, regardless of the wind speed, the wind turbines rotor speed is fixed and determined by the frequency of the supply grid, the gear ratio and the generator design.

- *Advantages*: simple, robust and reliable, less expensive
- *Disadvantages*: an uncontrollable reactive power consumption, mechanical stress and limited power quality control and fluctuations (mechanical and electrical).

Variable speed wind turbines

Variable speed wind turbines are designed to achieve maximum aerodynamic efficiency over a wide range of wind speeds. By this way, tip speed ratio is kept constant at predefined value that corresponds to maximum power coefficient. In this system, power converters control the generator speed and try to minimize the fluctuations in the system.

- *Advantages*: increased energy capture, improved power quality, reduced mechanical stress.
- *Disadvantages*: requires more electronic components, increased cost, and power loss in electronic components.

Types of wind turbines

According to the control of the speed and use of generators, wind turbines are classified into four different categories as shown in Figure 1.

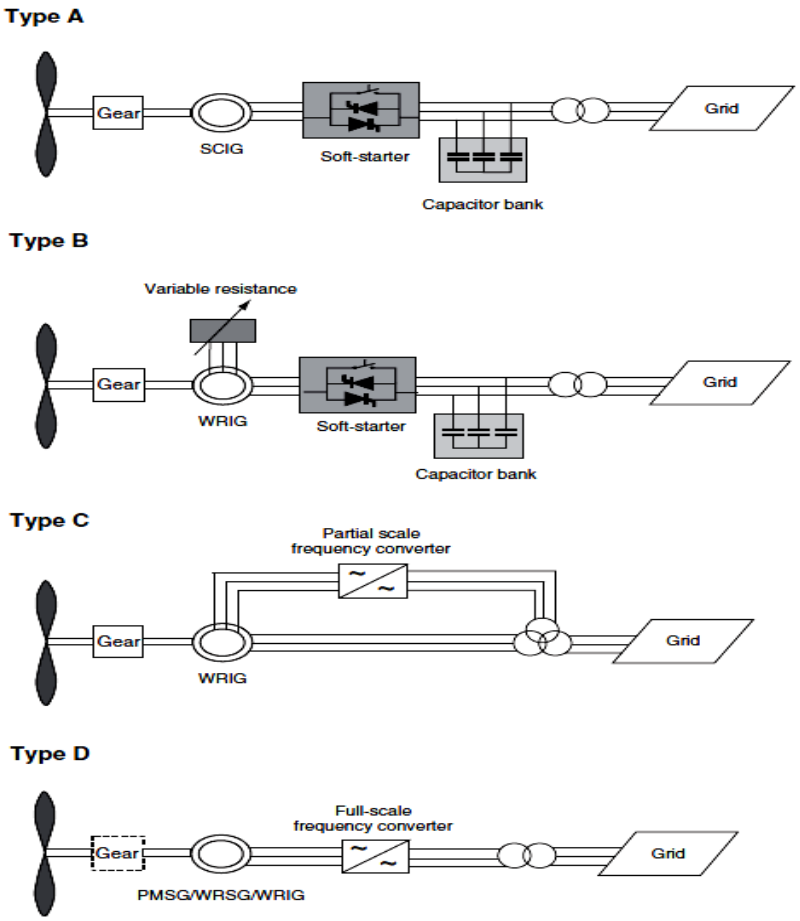

Figure 1: Types of wind turbines A) Fixed speed wind turbine, B) limited variable speed wind turbine, C) variable speed wind turbine using partial scale frequency converter, and D) variable speed wind turbine with full scale frequency converter [10]

A) Fixed speed wind turbine: This configuration is equipped with a squirrel cage induction generator (SCIG) directly connected to the grid via transformer. In this system, Capacitor bank is used for reactive power compensation. Soft starter used for a smoother grid connection with the system.

- *Advantages*: Cheap, simple and robust design.
- *Disadvantages*: this type of wind turbine does not support any speed control.

B) Limited variable speed wind turbine: This configuration corresponds to limited variable speed with variable generator rotor resistance. The Wound Rotor Induction Generator (WRIG) is directly connected to grid via transformer. In this system, Capacitor bank performs

the reactive power compensation by delivering power to the grid. Soft starter used for a smoother grid connection with the system.

Unique feature: variable additional rotor resistance can be changed by an optically controlled converter mounted on the rotor shaft. Thus resistance is controlled by varying resistance ultimately slip of the induction generator and power output.

- *Advantages*: does not need costly slip rings. No maintenance of brushes.
- *Disadvantages*: the range of speed control depends on the size of variable rotor resistance. Hence speed variation is limited.

C) Variable speed wind turbine (Doubly Fed Induction Generator - DFIG):

This configuration is equipped with a wound rotor induction generator (WRIG) using Partial Scale Frequency Converter (PSFC); frequency control performs the reactive power compensation with smoother grid connection to reduce losses in the system with wide range of speed variations compared to type (B).

- *Advantages*: wide range of speed available. No need of capacitor bank and soft smoother.
- *Disadvantages*: requires slip rings and protection from grid faults.

D) Variable speed wind turbine (using Full Scale Frequency Convertor):

This configuration is equipped with a wound rotor synchronous generator (WRIG) or with permanent magnet synchronous generator with FSFC used for full scale variable speed wind turbine by connecting generator to grid directly using FSFC performs reactive power compensation as well as smoother grid connection.

- *Advantages*: no need of gear box because power converter acts as an electric gear box. Also does not require capacitor bank and soft smoother. Reduced noise distortions.
- *Disadvantages*: expensive, complexity in design, and requires protection from grid and additional losses due to more electronic components.

2.2 GRIDCODE, NORSOK and IEC standards for wind power:

The Norwegian power grid is divided in three parts, main transmission grid, regional grid and local grid. Norway is part of Nordel system, ruled by the “Nordel Grid Code”. The Nordel Grid Code corresponds to the minimal requirements that must be fulfilled by the participants. Each Transmission System Operator (TSO) has its own code which completes the Nordel code [11, 12].

Today, integration of wind farms has an important role on power transmission systems due to their large power generation and requirements of security of power supply. Hence wind farms

are subjected to specific rules and regulations to transfer and integrate power to exits grid. For the connections of a wind farm in the Norwegian grid, the main requirements are include the following aspects expressed in Table 1.

Table 1: Operation time ranges at varying frequencies for power plants and wind farms

Frequency [Hz]	Maximum operating time	
	Power plants	Wind farms power
45 - 47.5	20 S	20 S
47.5 - 49	30 min	Continuously
49 - 52	Continuously	Continuously
52 - 53	30 min	30 min
53 - 55	20 S	20 S
55 - 57	10 S	10 S

The graphical representation of the above table means operation time, frequency variation and voltage variation are as shown in Figure 2 with different colour bands.

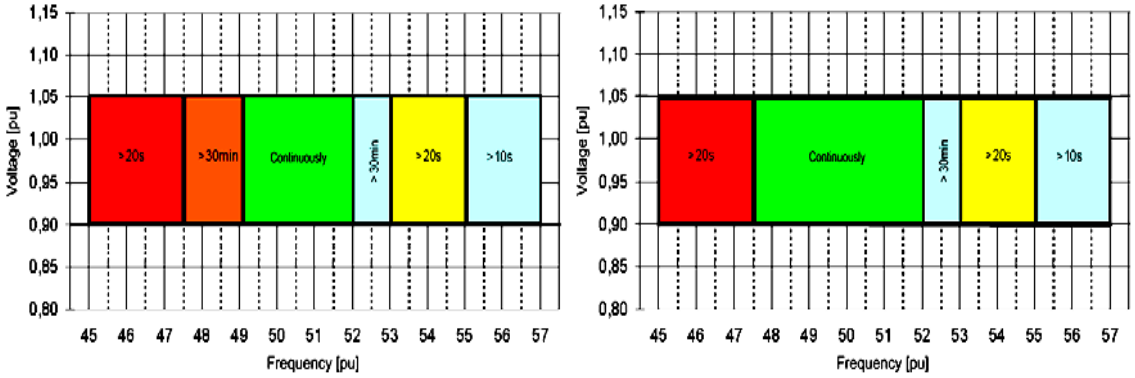

Figure 2: Frequency and voltage requirement for plants (left) and wind farms (right)[11, 12]

Norway has mainly hydro or thermal power generation, the production units have to be able to work at rated power, with a power factor superior to 0.91 inductive or capacitive. While for wind power generation, the requirement is strict with power factor superior to 0.95 inductive or capacitive at rated power as shown in Figure 3:

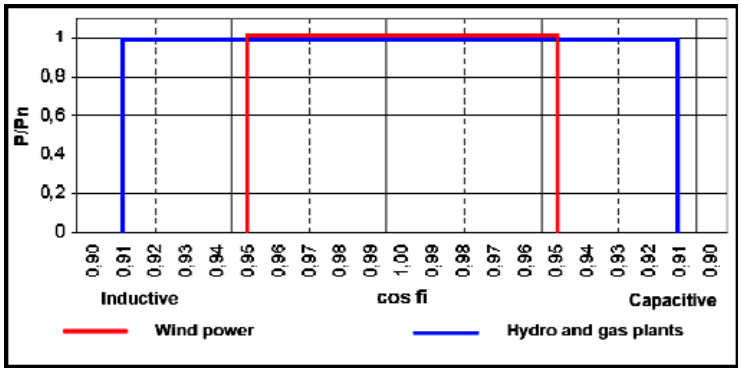

Figure 3: Reactive power capability limitations - wind power and other generation

Other specific requirement for offshore wind power includes:

- Concerning the production, the wind has to be regulated down from the rated power to its stop in the maximum time of 30s.
- The wind farm is also not suppose to limit its active power generation in case of low frequency and then should participate to the frequency regulation.

Wind farm generation unit have also respect to demands in case of fault on the system. The wind power production unites have to be contributes to short-circuit or fault performance for satisfactory operation of the system after the disturbance. These requirements, also called low voltage fault ride through (LVRT) [13]. The fault-ride-through requirements can graphically represent as Figure 4.

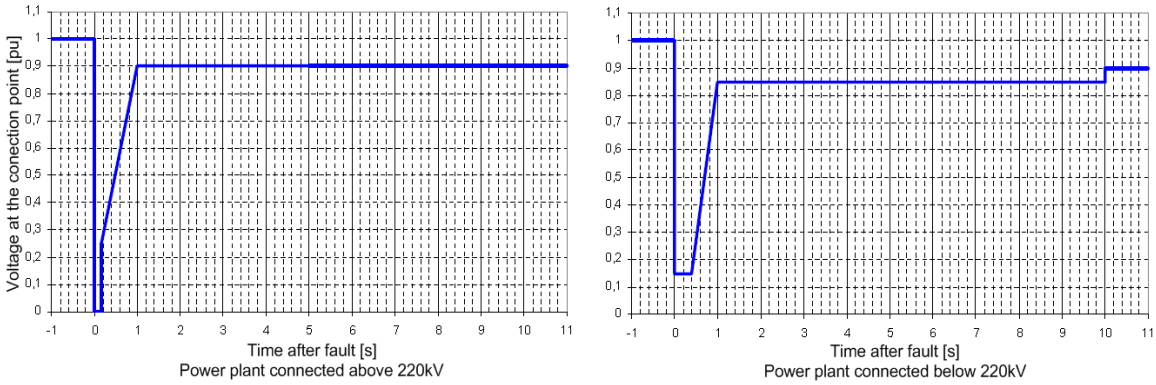

Figure 4: Fault-ride-through requirement for power plant above and below 220kV [13].

NORSOK and IEC Standards:

The NORSOK standard controls provisions for electrical installations at all voltages to provide safety in the design of electrical systems, selection, and use of electrical equipment for generation, storage, distribution, integration and utilization of electrical energy for all purposes in offshore units which are being used for the purpose of exploration or exploitation of petroleum resources. NORSOK standard does not apply for the electrical installations in rooms used for medical purposes or in tankers. This applies to all electrical installations. The installation may be permanent, temporary, transportable or hand-held, to AC installations up to and including 35 000 V and DC installations up to and including 1 500 V. The purpose is to assure, whether frequency and voltage variations are within permissible limits and following NORSOK standards during particular perturbation into system. The limitations as specified in Table 2 are the general requirements according to NORSOK standard E-001[8] which again refers to IEC standard 61892, edition 1[14]. Note be put that the transient frequency deviation limit has changed from ±5 % in Edition 1 to ±10 % in Edition 2 of the IEC 61892-1 standard.

Table 2: NORSOK standards / IEC 61892-1 requirements for maximum voltage and frequency deviations in offshore AC distribution systems

Operation case	Voltage deviation (ΔV)	Frequency deviation (ΔF)
Max continuous deviation	+6 / –10 %	±5 %
Max cyclic deviation	±2 %	±0.5 %
Max transient deviation	±20 %	±10 %
Max transient recovery time	1.5 sec	5 sec

2.3 Challenges for integration of an offshore wind farm to the grid

Due to unevenness and uncontrollability of wind resources, integrating large offshore wind farms into grids has inflicted many challenges on both wind power transmission technologies and transmission grid operation[15] These challenges includes:

1) Requirements of new measurement techniques including new wind climate assessment methodologies and modelling for offshore wind energy and resource assessment.

2) Advanced technical solutions for wind energy transmission from offshore to grid.

3) Grid integration technologies to meet the grid code requirements[12].

4) Operation and management for transmission grid with penetration of large wind power, influence new more challenges regarding to:

- infrastructure requirements
- strategies of managing the intermittency
- grid balancing mechanisms for integration of wind energy,
- proper excessive management for transmitting wind power to the load centers
- the security of supply and stability of transmission grid
- Optimization of transmission investment and O&M cost, etc.

5) Cost reduction of offshore wind energy production and integration.

2.4 Reactive power theory in power system

The active power P and reactive power Q is the main components used in AC system. The active power is transformed in to mechanical and thermal power work. The reactive power is circulating power - not useful for specific work and used to magnetize the magnetic circuits of the equipment. The AC voltage *u(t)* and current *i(t)* can be defined as: $u(t) = U \sin(\omega t)$ & $i(t) = I \sin(\omega t - \varphi)$ as shown in Figure 5 in vector form, where u is the rms value of the voltage, i is the rms value of the current, ω is the pulsation and φ is the phase angle between the voltage and the current.

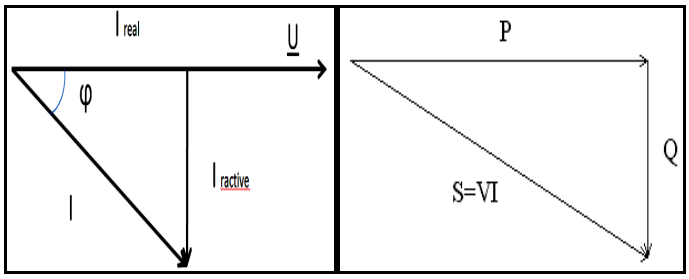

Figure 5: - Vector diagram of voltage, current and relevant power

The real current and the reactive current can be defined as:

$$I_{real} = I * \cos\varphi \quad \& \quad I_{reactive} = I * \sin\varphi$$

So the active power and the reactive power can be measured by multiplying current with voltages as:

$$P_{real} = V * I * \cos\varphi = V * I_{real} \quad \& \quad Q_{reactive} = V * I * \sin\varphi = V * I_{reactive}$$

Hence, apparent power

$$S = V * I$$

Where, S represents apparent power. Diagram shows vector sum of P,Q and apparent power S. The reactive power is negative or positive depends on the φ (the phase angle), if the current lags the voltage, the phase angle is negative and the reactive power is negative and the impedance of the circuit is inductive hence the reactive power is consumed. If φ positive means current lead voltage then reactive power is positive hence the total impedance is capacitive and the circuit produces reactive power.

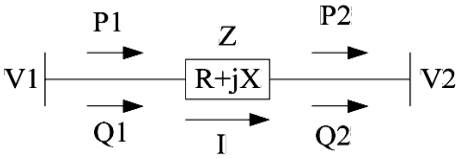

Figure 6: Simple two nodes system

Figure 6 shows simple two node system where the voltage drop between the ends will be:

$$\Delta V = V2 - V1 = Z * I = (R * \cos\varphi + X * \sin\varphi) * I = RI\cos\varphi + XI\sin\varphi$$

By comparing this equation with above active and reactive power equation gives,

$$\Delta V = (RP1 + XQ1) / V1 = (RP2 + XQ2) / V2$$

But $R << X$, gives $\Delta V = XQ1 / V1 = XQ2 / V2$

So the reactive power Q is determined by ΔV. If $V1 > V2$ then the Q flows from the node 1 to node 2 and in the case of $V2 > V1$ the flow is reverse. In other words, if there is a lake of reactive power in one point of the system, the rest of the system should provide the necessary reactive in order to equilibrate the power balance. Otherwise the voltage at the node in deficit can collapse.

The stability of system is linked on flow of reactive power and it is obvious that a good power balance of the system should be made. But flow of reactive power through the grid creates extra losses due to the nature of the transmission lines and the capacities of active power transmission are reduced. The losses on transformers are also increased by the flow of reactive current. In another hand, motors need reactive power to produce the magnetic fields required for their operation. To avoid the circulation of reactive power through the grid even as furnishing it to the consumer, compensation is used. Hence the production is made near the consumer and the consequences of the reactive flow are reduced.

2.5 Power System Stability

A definition of Power System Stability is given by IEEE in [16]

"Power system stability is the ability of an electric power system, for a given initial operating condition, to regain a state of operating equilibrium after being subjected to a physical disturbance, with most system variables bounded so that practically the entire system remains intact."

Stability is the condition of equilibrium between opposite forces. In normal operation, electrical systems operate in such a way that these forces are equilibrated. However if a disturbance happens in the system the state of the forces regarding the equilibrium changes and the system have to react in order to regain the equilibrium. For example if a generator runs temporarily faster, the angular position of its rotor will change and then will influence its output power. Power system stability can be classified according to its nature. There are three main categories of stabilities: rotor angle stability, frequency stability and voltage stability.

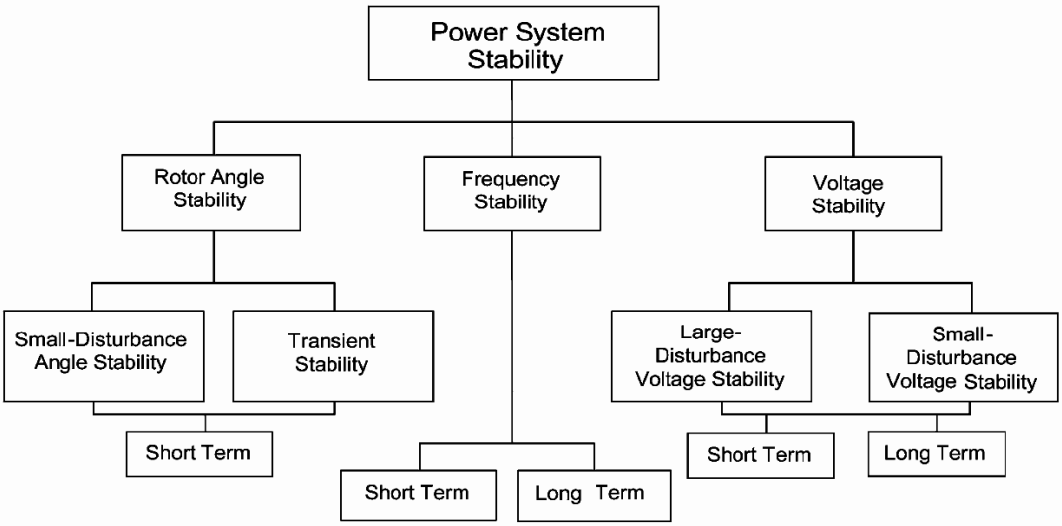

Figure 7: Classification of power system stability [16]

Figure 7 shows detailed classification of power system stability. In this study, the choice was made to focus on the voltage stability and the frequency stability. The reason of this choice is because the strict requirements regarding grid integration system and standards. It would have been not so interested to focus on the rotor angle stability in this study.

The voltage stability is defined like *"the ability of a power system to maintain steady voltages at all busses in the system after being subjected to a disturbance from a given initial operating condition."* and the frequency stability like *"the ability of a power system to maintain steady frequency following a severe system upset resulting in a significant imbalance between generation and load."*[16]

Voltage stability is divided in two categories, the small-disturbance stability and large disturbance stability. The first one is the ability of the system to maintain equilibrium under small disturbance, like small changes in the load or in the generation. Small-signal stability is a problem which is largely influence by the lack of oscillation damping of the system. The second category of stability is the large-disturbance stability. This is the ability of the system to maintain equilibrium under and after transient disturbances like phase-to-ground, phase-to-phase or three-phase short-circuit. These events can occur in lines, transformers or bus bar. The choice was made to studying large-disturbance stability because of the simplified model.

2.6 SVC and STATCOM application - voltage control, system stability enhancement

The voltage level control is achieved by controlling production, absorption and flow of reactive power at all levels in the system. The generating units provide the basic means of voltage control; the automatic voltage regulators control field excitation to maintain a scheduled voltage level at the terminals of the generators. Additional means of control are usually required to control voltage throughout the system. The devices used for this purpose are classified as follows:

- Sources or sinks of reactive power, such as shunt capacitors, shunt reactors,
- Synchronous condensers, static var compensators (SVCs) and STSTCOMs.
- Line reactance compensators, such as series capacitors.
- Regulating transformers, such as tap-changing transformers and boosters.

Shunt capacitors, reactors and series capacitors provide passive compensation. They are either permanently connected to the transmission and distribution system, or switched. They contribute to voltage control by modifying the network characteristics. Synchronous condensers, SVCs and STATCOMs provide active compensation; the reactive power

absorbed/supplied by them is automatically adjusted so that they control/maintain voltages of the buses to which they are connected. Together with the generating units, they establish voltages at specific points in the system. Voltages at other locations in the system are determined by active and reactive power flows through various circuit elements including the passive compensating devices. The functional requirements of SVC and STATCOM, used for transient stability improvements, power oscillation damping and voltage support can be simply stated as follows:

- They must be able to stay in synchronism with the terminal voltage under all conditions, including major disturbances.
- They must be able to regulate (transient stability improvement and voltage support), or control (power oscillation damping) rapidly the terminal voltage by generating reactive power for or absorbing it from system.

2.6.1 Static Var Compensator (SVC)

The Static Var Compensator (SVC), a variable impedance device where the current through a reactor is controlled using back to back connected thyristor valves. SVC has no inertia compared to synchronous condensers and can be extremely fast in response (2-3 cycles) thus the fast control of reactive power. SVC is combination of Thyristor controlled reactor (TCR) and Thyristor switched capacitor (TSC).

2.6.1.1 Thyristor Controlled Reactor (TCR)

The basic elements of a TCR are a reactor in series with a bidirectional thyristor switch and V-I characteristic of TCR also shown in Figure 8, for different firing angles of tyristor switch [17].

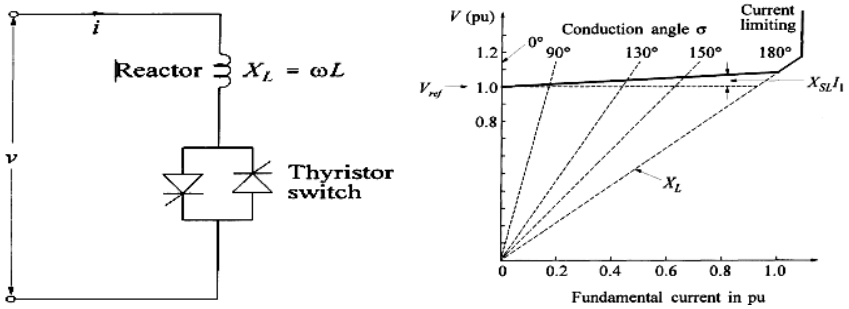

Figure 8: Basic element of TCR and V- I characteristics of TCR

2.6.1.2 Thyristor Switched Capacitor (TSC)

TSC consists of a capacitor bank, each of which is switched on and off by using thyristor switches. Each single-phase unit consists of a capacitor C in series with a bidirectional

thyristor switch and a small inductor L as shown in Figure 9. The inductor is to limit switching transients, to damp inrush currents, and to prevent resonance with the network.

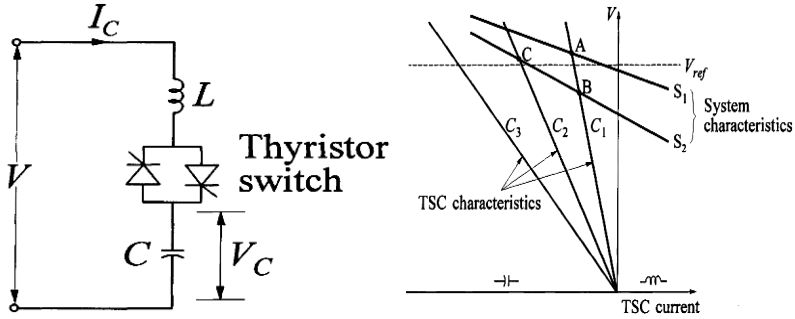

Figure 9: Basic element of TSC and V- I characteristics of TSC

The V-I characteristic of TSC show that the voltage control provided is discontinuous or stepwise. It is determined by the rating and number of parallel connected units [17].

2.6.1.3 Static Var Compensator (SVC)

Figure 10 shows a typical SVS scheme consisting of a TCR, three-unit TSC, and harmonic filters (for filtering TCR-generated harmonics). The typical terminal voltage versus output current characteristic of the SVS together with particular ”load lines” (voltage versus reactive current characteristics) of the ac system is as shown in Figure11.

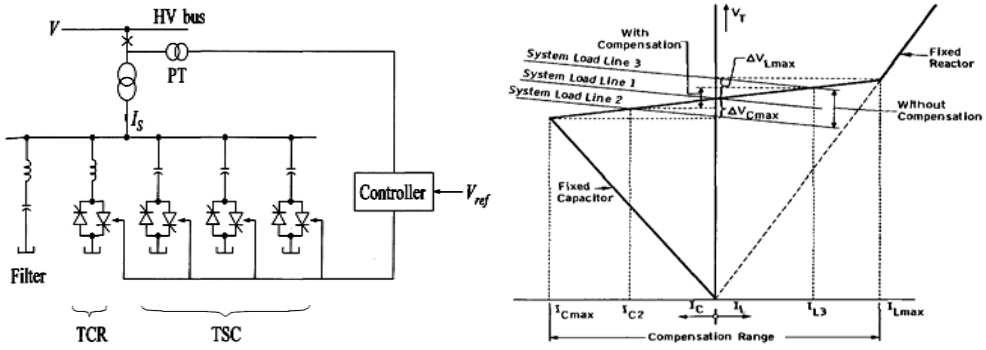

Figure 10: Basic element of SVC and V- I characteristics of SVC

Figure 10 express, Load line 1 intersects the SVC V-l characteristic at the nominal (reference) voltage and hence output current of the compensator is zero. Load line 2 is below load line 1 due to a decrease in the power system voltage (for example, generator outage, starting of big inundation motor). Its intersection with the SVC V-l characteristic calls for capacitive compensating current lC2. Load line 3 is above load line 1 due to an increase in system voltage (for example, load rejection). Intersection with the SVC V-l characteristic defines the inductive compensating current lL3. The intersection points of the load line 2 and 3 with the vertical (voltage) axis define terminal voltage variation without any compensation. The terminal voltage variation with compensation is entirely determined by the regulation slope of

SVC. The linear control range lies within the limits determined by maximum susceptance of reactor and total capacitive susceptance. If the voltage drops below a certain level (typically 0.3 pu) for an extended period, power and thyristor gating energy can be lost, requiring a shutdown of the SVS [18, 19].

Applications: By virtue of SVCs ability to provide continuous and rapid control of reactive power and voltage, SVCs can enhance several aspects of transmission system performance. Application to SVC includes

- Control of temporary (power frequency) overvoltage
- Prevention of voltage collapse
- Enhancement of transient stability and damping of system oscillations

They are also used to minimize fluctuations in system supply voltage caused by repetitive-impact loads such as dragline loads of mining plants, rolling mills, and arc furnaces [17].

2.6.2 Static Synchronous Compensator (STATCOM)

This shunt connected static compensator was developed as an advanced static VAR compensator where a voltage source convertor (VSC) is used instead of the controllable reactors and switched capacitors. Although VSCs require self-commutated power semiconductor devices such as GTO, IGBT, IGCT, MCT, etc. (with higher costs and losses) unlike in the case of variable impedance type SVC which use thyristor devices, there are many technical advantages of a STATCOM over a SVC like:

- Faster response.
- Requires less space as bulky passive components (such as reactors) are eliminated
- Inherently modular and relocatable.
- Can be interfaced with real power sources such as battery, fuel cell or SMES (superconducting magnetic energy storage).
- A STATCOM has superior performance during low voltage condition as the reactive current can be maintained constant.

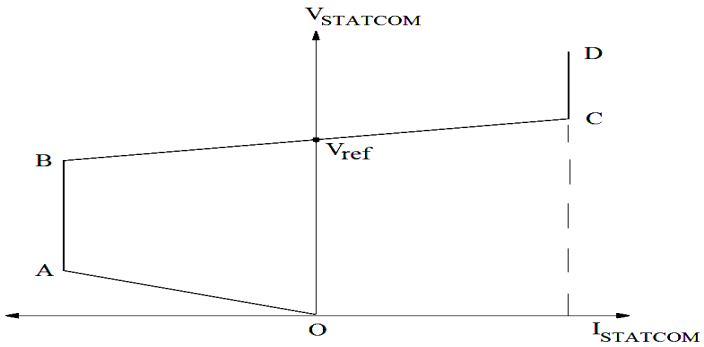

Figure 11: Basic V- I characteristics of STATCOM

Steady state V-I characteristics of a STATCOM shown in Figure 11, losses in the STATCOM are neglected and $I_{STATCOM}$ is assumed to be purely reactive. The negative current indicates capacitive operation and positive current indicates inductive operation as SVC. Limits on the capacitive and inductive currents are symmetric. The positive slope BC provides (i) to prevent the STATCOM hitting the limits often and (ii) to allow parallel operation of two or more units. The reference voltage (Vref.) corresponds to zero current output and generally, the STATCOM is operated close to zero output during normal operating conditions, such that full dynamic range is available during contingencies. This is arranged by controlling the mechanically switched capacitors/reactors connected in parallel with a STATCOM [19].

2.6.3 Comparison of SVC and STATCOM Characteristics

The comparable V-I characteristic of the STATCOM and SVC are shown in Figure 12, the STATCOM can provide both capacitive and inductive compensation and able to control output current over rated maximum capacitive or inductive range independently of the ac system voltage. The STATCOM can provide full capacitive output current at any system voltage, practically down to zero. While SVC, being composed of (thyristor-switched) capacitors and reactors, can supply only diminishing output current with decreasing system voltage as determined by its maximum equivalent capacitive admittance. Thus, STATCOM performs superior then SVC to providing dynamic voltage support.

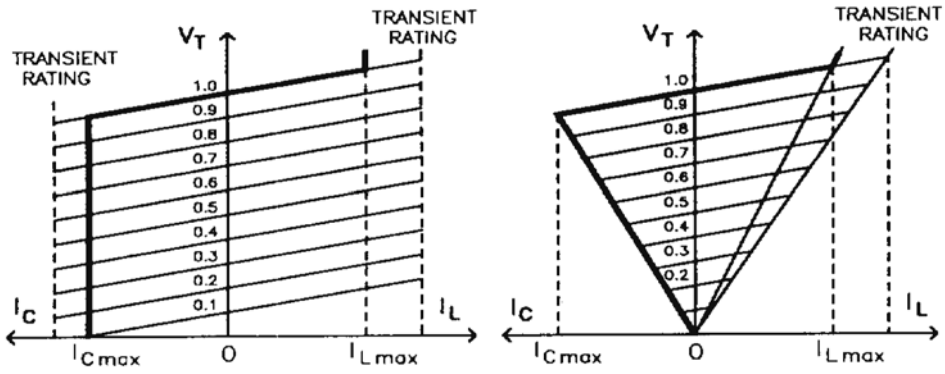

Figure 12: Basic V- I characteristic comparison of SVC and STATCOM

Figure 12 indicates STATCOM has an increased transient rating in both inductive and capacitive operating regions. (In controversial to SVC has no means to increase it since maximum capacitive current it can draw is strictly determined by size of the capacitor and magnitude of the system voltage). Inherently available transient rating of the STATCOM is independent on the characteristics of the power semiconductors used and the junction temperature at which the devices are operated [18, 20].

3 CASE STUDY – PLATFORMS AND SYSTEM TOPOLOGIES

The case study has been designed to analyze reliability, stability and security of an "off grid", system of offshore wind farm integration to offshore oil and gas platforms based on practical platform details and geographical locations of different platforms. The stability of the system is performed based on dynamic voltage and frequency variation in the system. This chapter contains an overview description and basis for selection of power system network, brief about the single line diagram based on different system connection topologies aspect and details about different platforms, their load demand, latest production with power consumption details. The selection of the isolated system is based on real platforms located at Oseberg oilfield in western coast of Norwegian Sea with changed abbreviations due to privacy reasons. In addition, shortly about platform power control strategies and main consideration for voltage and frequency control for the network.

3.1 Platforms detail

The case study includes five individual platforms of different power generations, different voltage and frequency - supply system and load conditions. Due to project confidentiality reasons platforms are referred as Platform1 (PF1), Platform2 (PF2), Platform3 (PF3), Platform4 (PF4) and Platform (PF5). Short summary about platform's electric parameters, operating system voltage and frequency and load details are shown in Table 3. Unique voltage level of 13.8kV and frequency of 60HZ via HVAC system is the main assumption to simulate the whole system to avoid power frequency convertor and HVDC system technology applications at this stage.

Table 3: Platform wise details of generations, operating system and load demand details:

Platforms	Main Power Electric Generation	Main Bus		load
Platform1	3 Gas T. (23MW) + 1 Steam T. (19,4MW)	13,8KV	60HZ	24 MW
Platform2	2 Gas T. (24,8MW)	11KV	50HZ	34 MW
Platform3	2 Gas T. (22MW)	11KV	60HZ	30MW
Platform4	2 Gas T. (24,8MW)	13,8KV	60HZ	34MW
Platform5	1 Gas T. (24,8MW)	11KV	50HZ	25MW

3.1.1 Platform1 (PF1)

Platform1 (PF1) consists of three different structures interconnected as: PF A, PF B and PF C. It is located in the northern part of the North Sea above a sea depth of 100m. The oilfield was discovered in 1979, its development approval dates in 1984 and is on stream since 1988.

PF A contains process and accommodation facility, PF B with drilling and water injection facilities where as PF C with gas processing facility. PF1 is connected to different onshore

pipeline to gas and oil transport and PF2, PF3, PF4 and other platforms that will not be part of this study.

The estimated production during 2010 is 74000 barrels/day of oil, 2.77 billion scm of gas and 0.55 million tonnes of NGL (Natural Gas Liquid). In this estimated production includes the production from PF2 platform because both of them work on the same oilfield.

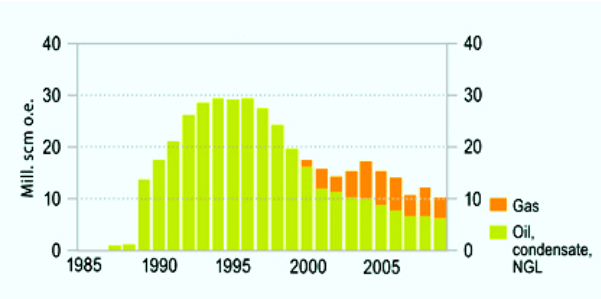

Figure 13: Production at PF1 since 1988 [21]

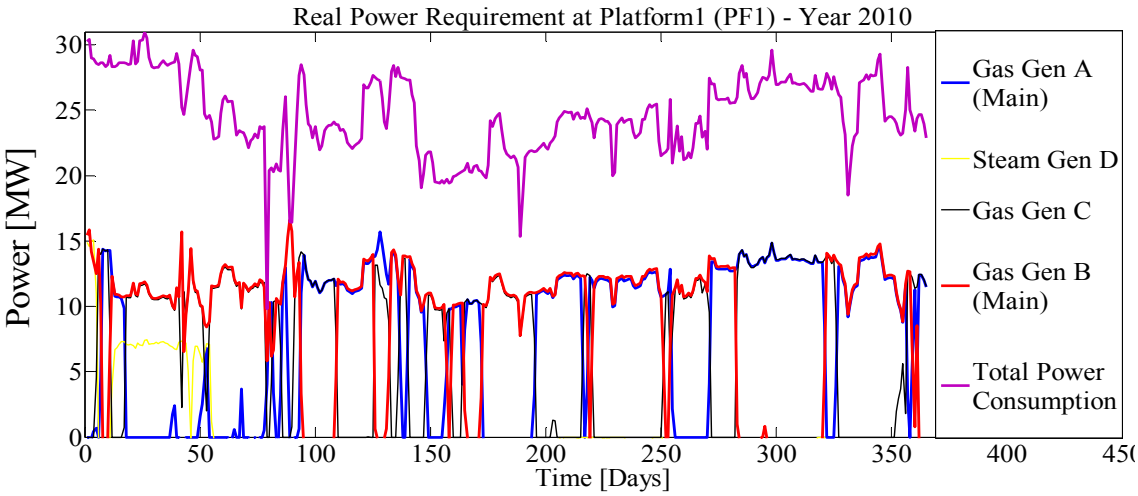

Figure 14: Real power requirement at PF1 – year 2010 [22]

Lifetime estimates made in 2009 show 2031 as PF1's last year of operation and production at PF1 as shown in Figure 13. The generation at PF1 is provided by three gas turbines, Rolls-Royce 211-24G, with a rated power of 23MW in PF A and one steam turbine with a rated power of 19.4MW in PF C. According to the operation mode of the PF1, two turbines always are running simultaneously, one gas turbine and the steam turbine preferably. The load is approximately 24MW in normal operation mode. The daily power consumption details for two running turbines (one Gas + one Steam) separately and average from 01.01.2010 to 31.12.2010, Figure 14 shows average power consumption of about 24MW as described. Single line diagram with detailed network system of platform1 is shown in Figure 15.

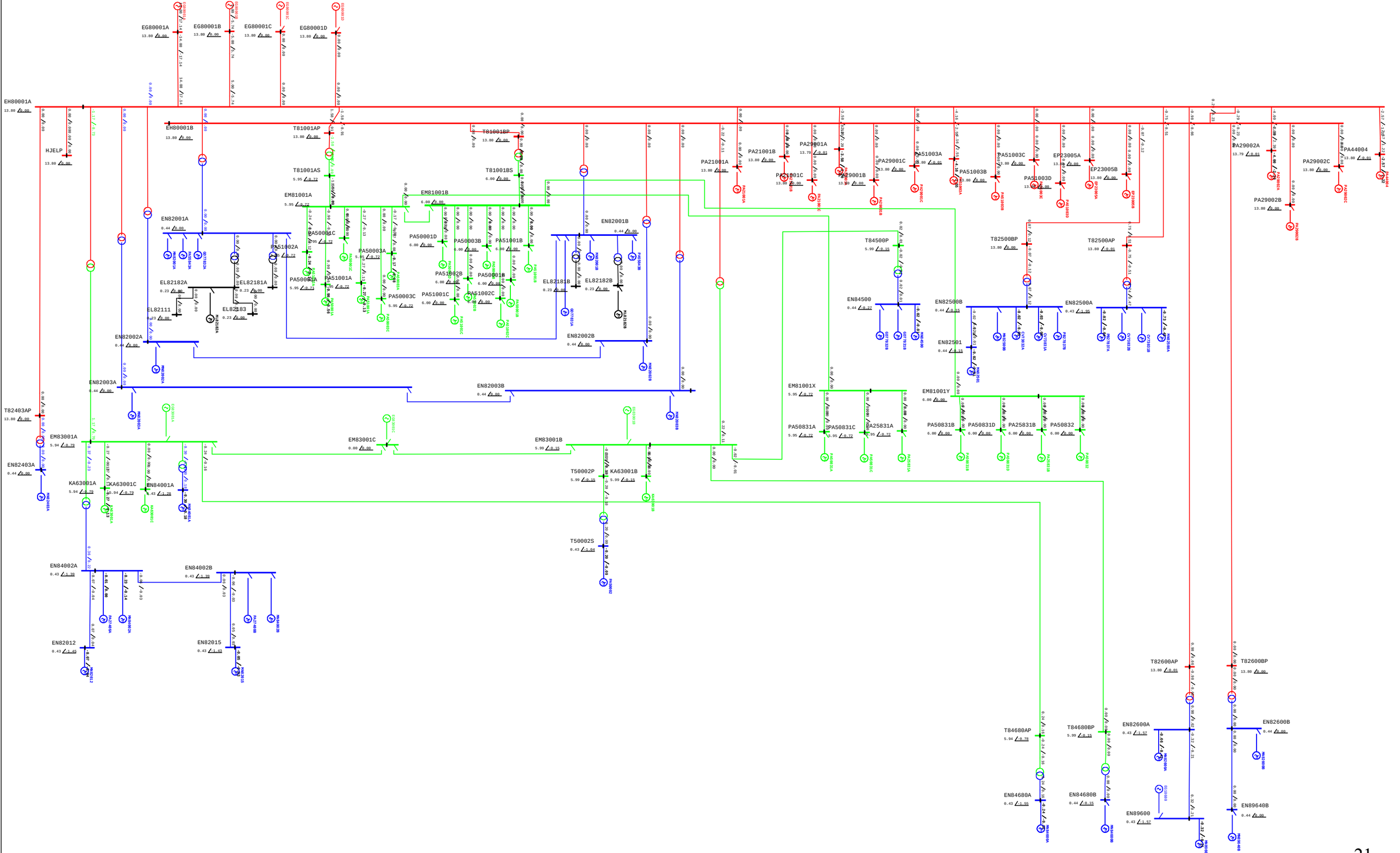

Figure 15: Single line diagram of PF1 with details about voltage level and main components

3.1.2 Platform2 (PF2)

Platform2 is located about 12 km south of PF1 in the northern part of the North Sea - Oseberg oilfield, above a sea depth of approximately 100m. The oilfield was discovered in 1984, its development approval dates in 1997 and is on stream since 2000. PF2 have an integrated steel facility with accommodation, drilling module and first-stage separation of oil and gas. The final processing of oil and gas carry out in PF1, where are sent by pipeline.

Figure 16: Production at PF2 since 2000 [21]

The estimated production in 2010 is 39000 oil barrels/day, 0.37 billion scm of gas and 0.09 million tonnes of NGL as shown in Figure 16. Its license expires in 2031.

Table 4: Recoverable reserves in PF2

Production	Original	Remaining as of 31.12.2009
Oil (million scm)	52.7	15.5
Gas (billion scm)	11.8	5.9
NGL (million tonnes)	1.5	1.5

PF2 has a generation capacity of 44MW provided by two gas turbines LM 2500GE of 22MW each one. The average electric power consumption is going from 16MW in 2008 to 12.2 MW expected in 2020 in normal operation, then only one gas turbine running. The platform load 34MW used as normal operational load for study by future development taking in to account. Figure 17 shows the real power consumption at PF2 with relevant duration and Figure 18 shows the platform details.

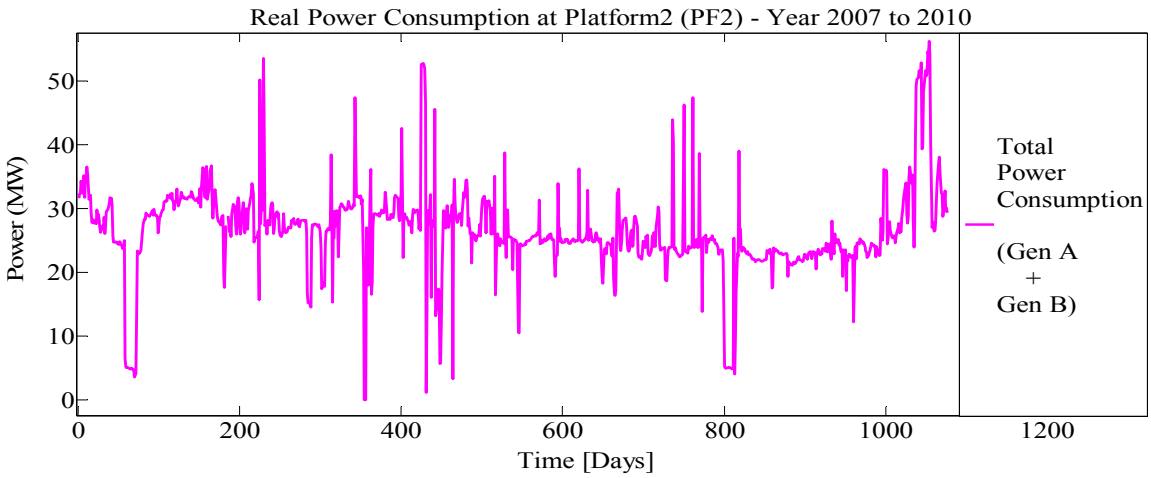

Figure 17: Real power requirement at PF2 – year 2007 to 2010 [22]

Figure 18: Single line diagram of PF2 with details about voltage level and main components

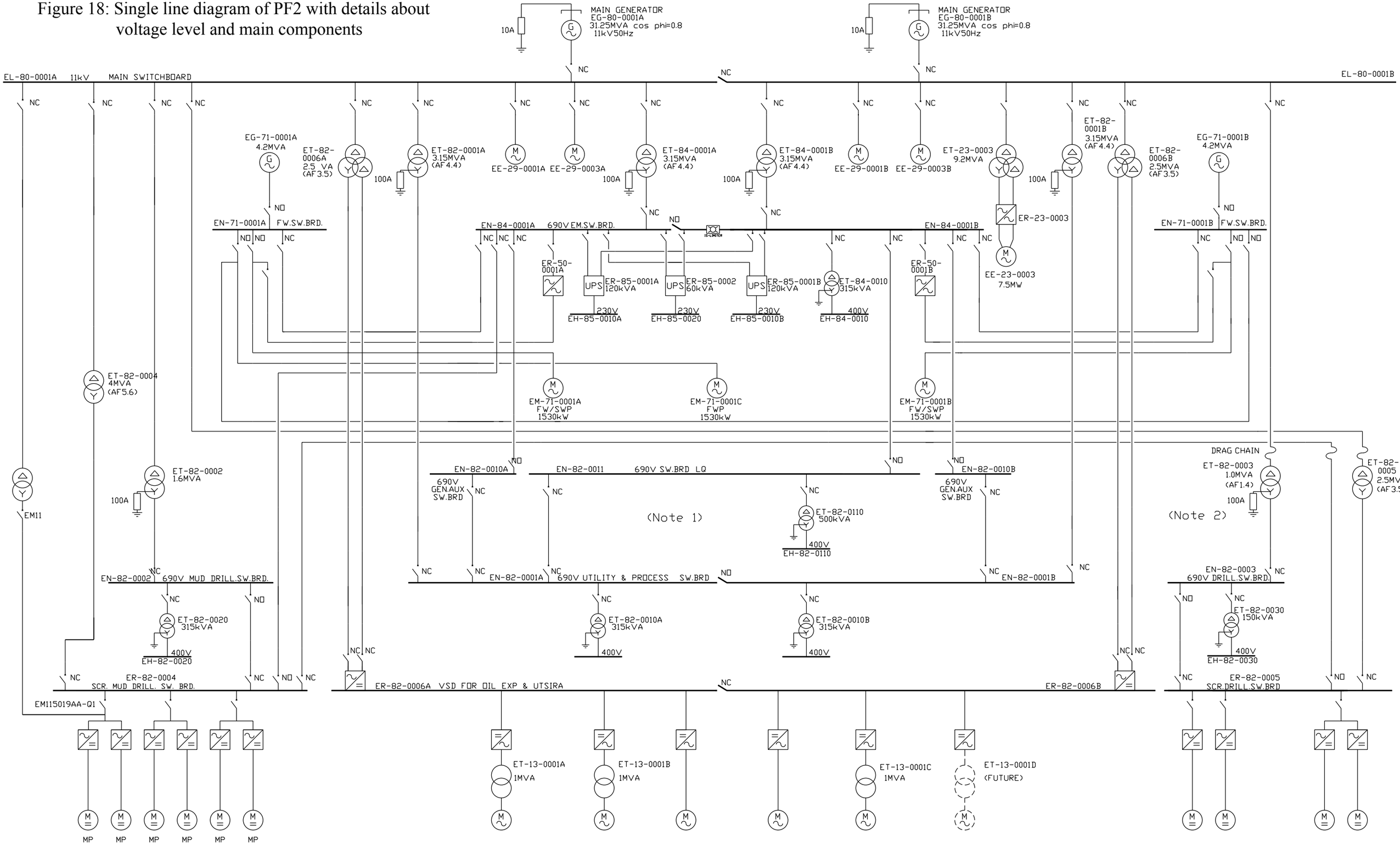

3.1.3 Platform3 (PF3)

Platform3 (PF3) is located about 13 kilometres east of PF1 above a sea depth of approximately 140m. The oilfield was discovered in 1980, its development approval dates in 1990 and is on stream since 1993. This is a bottom fixed platform with accommodation, drilling and integrated production with a steel jacket. The oil is sent to PF1 by pipeline.

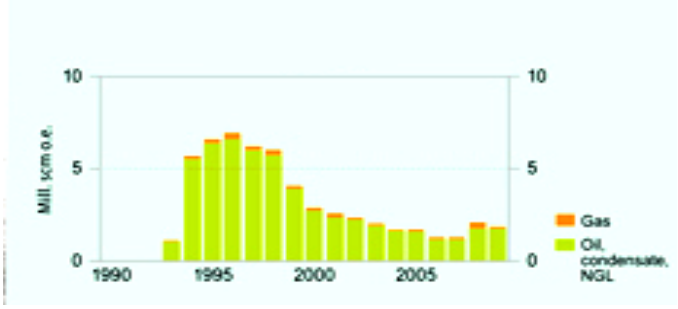

Figure 19: Production at PF3 since 1994 [21]

PF3 is a quite small platform with a daily production of 22000 oil barrels/day, 0.09 billion scm of gas and 0.04 million tonnes of scm as shown in Figure 19. This platform is in tail phase with a lifetime expected of 2013, following estimations made in 2009. However, some studies are in progress to extend the lifetime of Blue until 2020.

Table 5: Recoverable reserves in PF3

	Original	Remaining as of 31.12.2009
Oil (million scm)	56.6	4.8
Gas (billion scm)	3.7	0.8
NGL (million tonnes)	1.2	0.2

PF3 has a generation capacity of 44MW provided by two gas turbines LM 2500GE of 22MW each one. The average electric power consumption is 21.8MW from 2008 to 2013 in normal operation; in this case both gas turbines are running. The maximum platform load supposed to be 30 MW for system analysis matched with real power consumption as in Figure 20.

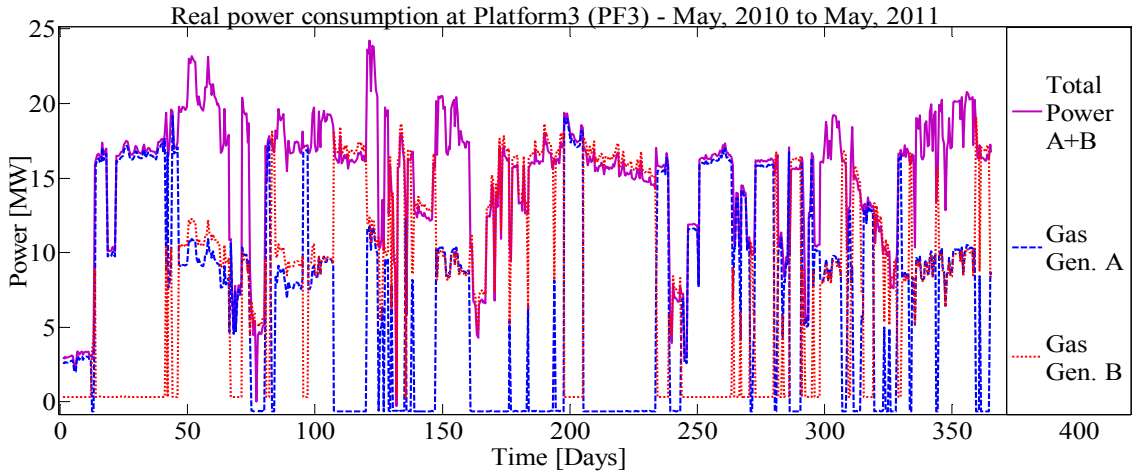

Figure 20: Real power requirement at PF3, year 2010-11 [22]

3.1.4 Platform4 (PF4)

Platform4 (PF4) is located 14.3 Km north of PF1 and it has been producing since 1991 with a license which expires in 2031. It is a drilling, accommodation and production facility with a steel jacket contained platform.

The oil extracted in this platform is sent to PF1 in a multiphase pipeline for processing, whereas one part of the gas extracted is injected in the wells together with water to keep the reservoir pressure. The excess gas is sent to PF1 too.

The electric power supplied to this platform is provided by two Rolls Royce RB211/24G gas turbines with a rated capacity of 24.8MW each one and the load is approximately 34MW in normal operation mode, being the installed load capacity 49MW.

Power consumption by main two gas turbines as an average shows as in Figure 21 indicates load capacity about 34MW in normal operation and hence load capacity of the platform chosen for simulation is also keep same.

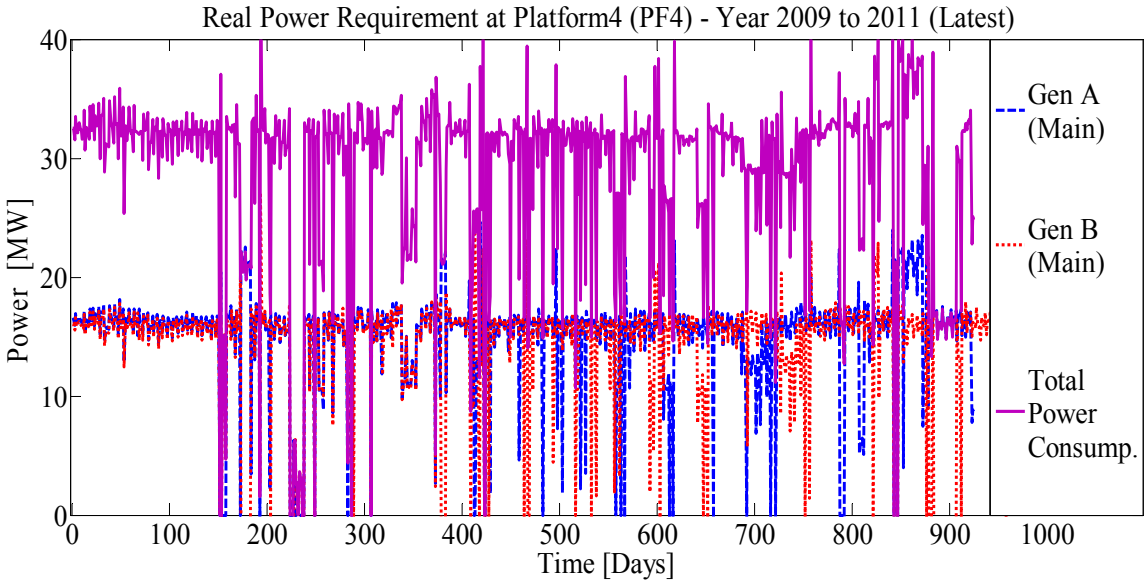

Figure 21: Real power requirement at PF4, year 2009 - 11 [22]

Figure 22: Single line diagram of PF4 with details about voltage level and main components

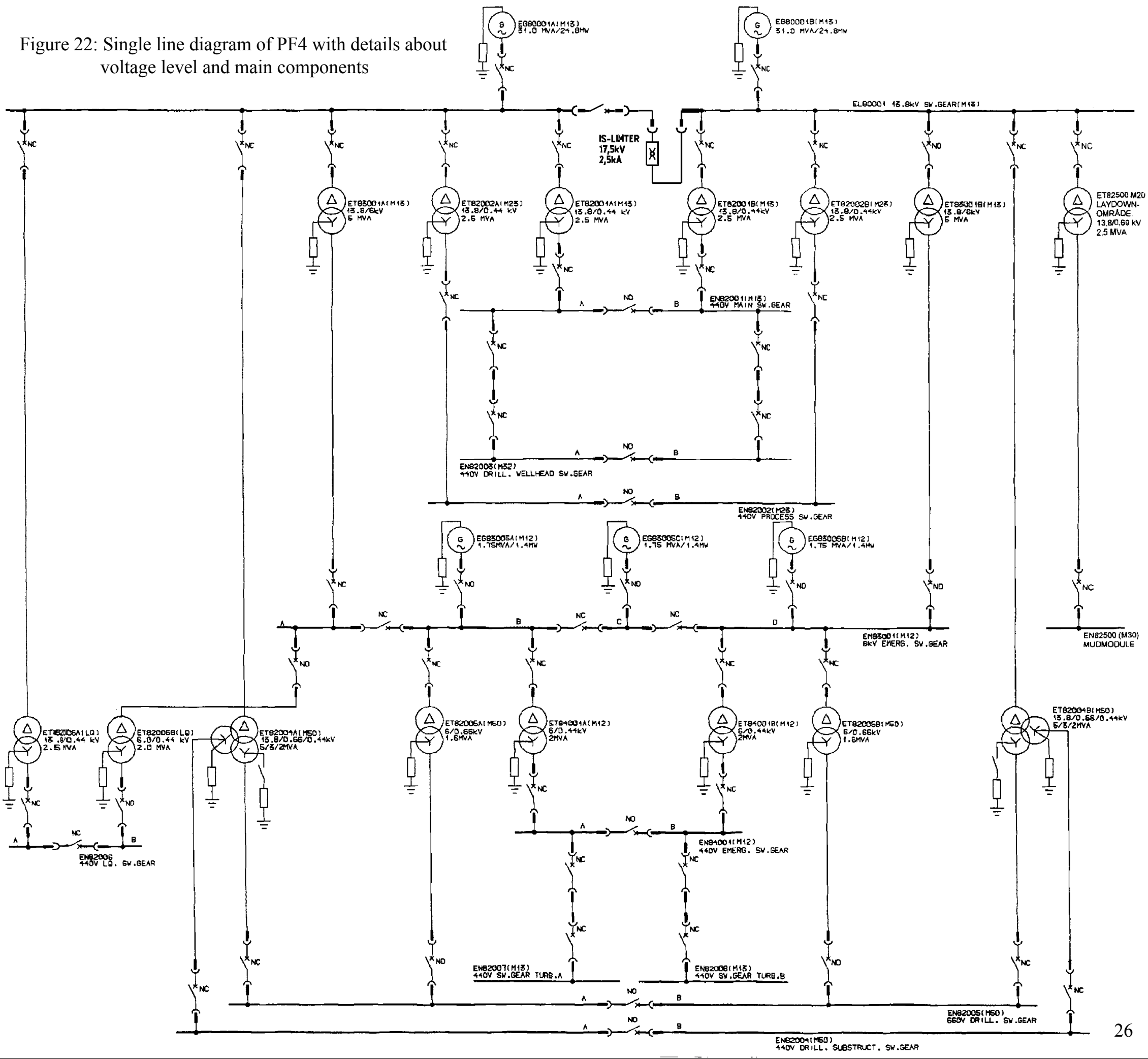

3.1.5 Platform5 (PF5)

Platform5 is located about 25 kilometres north-east of PF1 above a see depth of approximately 160m. The oilfield was discovered in 1981, its development approval dates in 1996 and is on stream since 1999.

This is a bottom fixed platform with accommodation, drilling equipment and first stage processing of gas, water and oil, which is sent to PF1 by a pipeline for further processing. The gas is used in the platform itself for injection in the oilfield and as fuel in the generators.

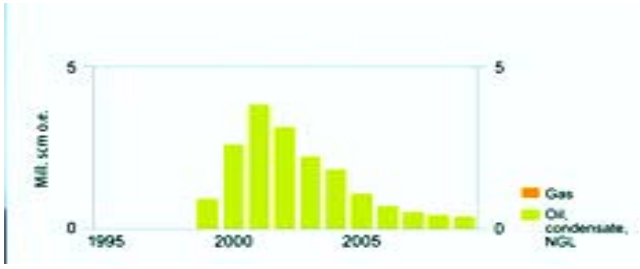

Figure 23: Production at PF5 since 1999 [21]

PF5 is the smallest platform of considered from a production, Figure 23 and electric power consumption point of view. Its expected production to 2010 is about 7000 oil barrels/day. Its license expires in 2031.

Table 6: Recoverable reserves in PF5

	Original	Remaining as of 31.12.2009
Oil (million scm)	28.6	11.1
Gas (billion scm)	0.4	0.1
NGL (million tonnes)	0.1	0.1

It has a generation capacity of 24.8MW provided by only one gas turbine LM 2500GE. The average electric power consumption is going from 18MW in 2009 to 2011 and 5.5 MW expected in 2020 in normal operation. The maximum platform load supposed to be 25MW, which is the power capacity available.

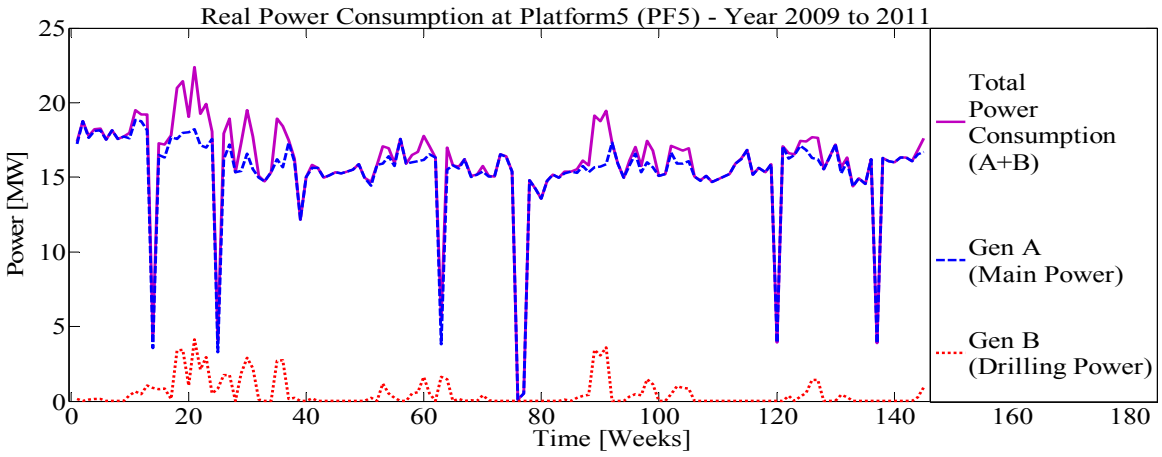

Figure 24: Real power requirement at PF5, year 2009 - 11 [22]

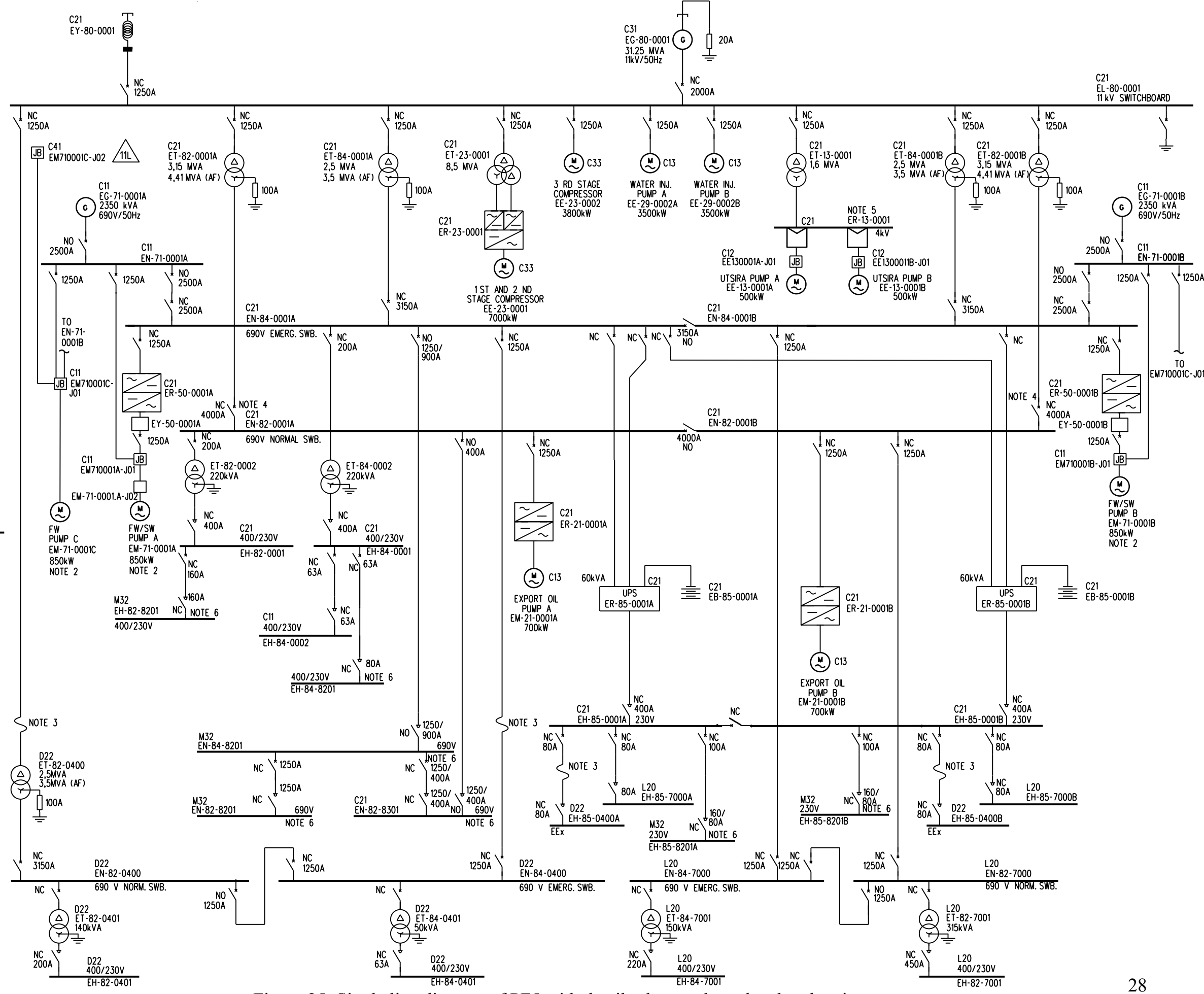

Figure 25: Single line diagram of PF5 with details about voltage level and main components

3.2 Network layout - Topologies

The relative locations of five offshore platforms included in study are founded from Oseberg oilfield in western coast of North Sea as a cluster with different load demands and operating system parameters at each platform. The platforms are located by each other as discussed in section 3.1. The offshore network consists of five platform connected to 100MW (4x5x5MW) radial offshore wind farm as an isolated system shown in Figure 26. The network layout has been studied here is an extension work of previous single platform study [6] to analyze security of power supply and system stability by combining five platforms in different topologies aspects as shown in Figure 26.

To study system security, minimum loss of load and less power fluctuations, three different topology aspects "Star", "Star-F" and "Mesh" are considered according to geographical view. Star topology prefers to separate offshore wind supply owner/consumers, Star-F convenient for minimal offshore cable solution and Mesh for better security of power. The wind farm modelled identical to previous study as Full Power Convertor Wind Turbine (FPCWT) model with four radial feeders consisting five wind turbines in each as cluster of 20WTs as shown in Figure 26. The feeders are connected at common offshore point called "wind farm bus", 36kV level. The total power demand of the five platforms 147 MW, can adjustable by connecting or disconnecting mainly asynchronous motor. The wind turbine each of 5MW gives 100MW of wind farm production to overcome platform demand partially. The load is mainly consists asynchronous motors to run pumps and compression machines on platform covered by gas turbines on each platform, with regulators to ensure satisfactory power quality. The gas turbines are modelled using synchronous generators with full frequency conversion as described in the SIMPOW manual. The proposed interconnection topology, with distances indicated and location of platforms and wind farm are shown in Figure 26.

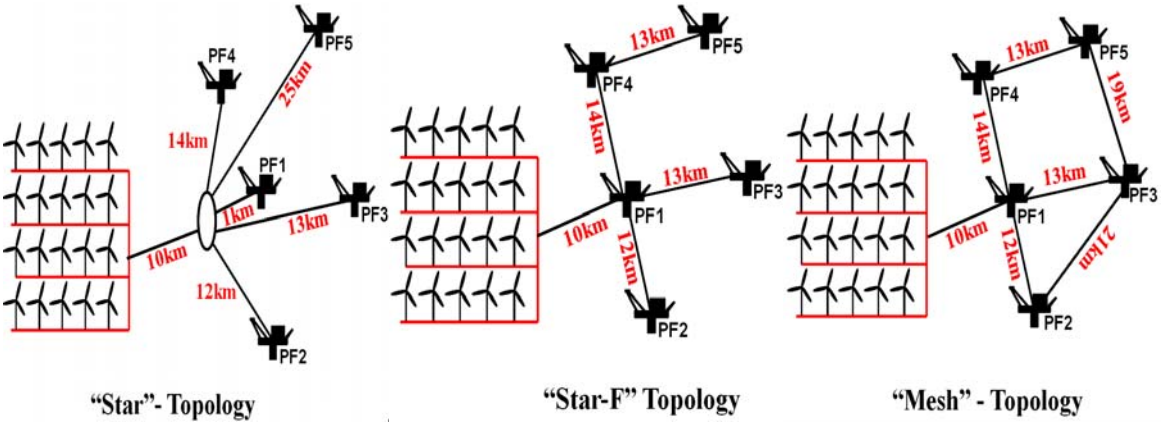

Figure 26: Proposed system network topologies, platform interconnections and distances

3.3 Single line diagram – "Star" topology

A simplified single-line diagram (SLD) of network model for Star topology is shown in Figure 27. This diagram not includes detail for each individual components of platforms but shown as a equivalent single node marked with PF1 so on and shows twenty wind turbines connected as four radial feeders. The feeders are connected at offshore common bus point called wind farm bus. The voltage level for platform main bus bars (load bus) is 13.8 kV, while various voltage levels for interconnection of wind farm with main grid has been considered as part of analysis. Simulations have been performed with two different voltage level of 36 kV and 52 kV as specified in the single line diagram. Which voltage level should be better for system operation mainly depends on distances, power transfer requirements and cost view point. Determining proper voltage level for network case technical point of view is one of the main objectives of the study; however economical aspects are not part of study yet.

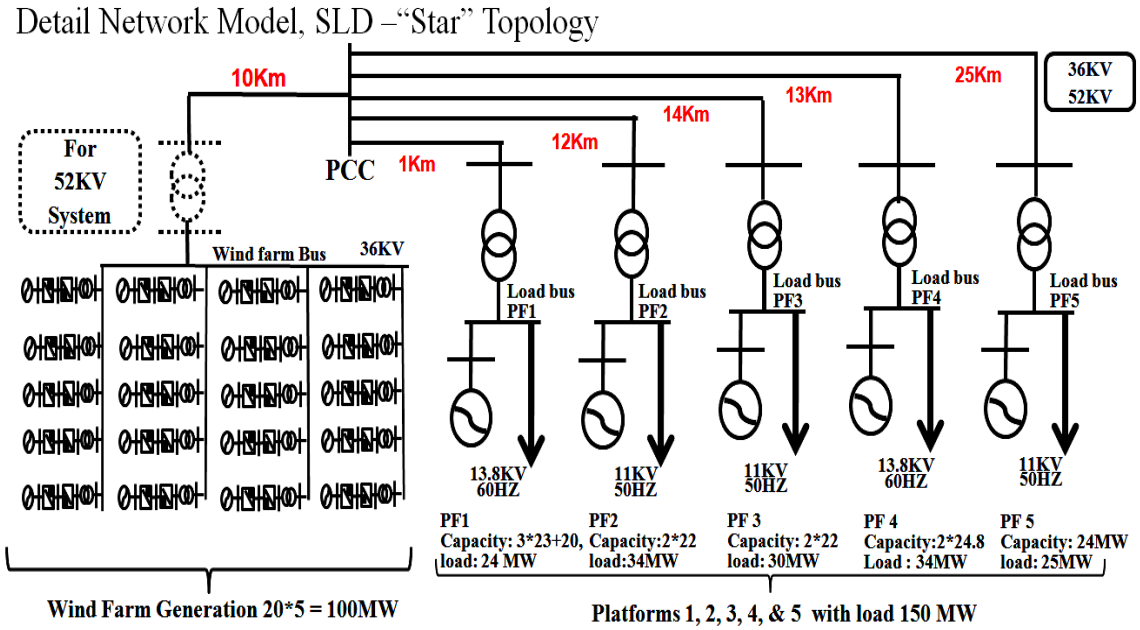

Figure 27: SLD – System network model for "Star" topology. Wind farm - Twenty wind turbines. Platforms – Operational details. Load buses at different PFs marked with names.

As shown SLD for Star – topology, voltage level of 36 kV and 52 kV have transformer voltage ratio of the interconnections are selected accordingly. Direct step up of voltage from wind turbine generation power at 690V to 52kV is not an economically and technically sound solution as requires 20 such transformers [23]. Step up of voltage from 36kV to 52kV done by designing offshore substation system of 52kV transformer as shown in Figure 27. For such a small isolated offshore system 110 kV level is not technically and economical option so not considered as part of study. The node bus connects wind farm and platforms depicted at point

of common coupling (PCC) where the impact of wind penetration, wind loss and FACTS applications based SVC and STATCOM to control dynamic voltage are considered. Load buses at different platforms are depicted with specific name load bus PF1 and so on, during different simulation cases events voltage and frequency deviations at these bases will be measured and compared with NORSOK limitations - Table 2 for different voltage level.

3.4 PF1 - Detailed model

The platform model used in this study for PF1 is identical model as previous study [6], represents one of the platforms of Statoil Oseberg oilfield cluster. Details for other platforms are also partially modelled as SLDs shown in section 3.1. To get overview of common system of all platforms only PF1 is discussed here as shown in Figure 28 with single line diagram representation. Platform1 consists of four on line generators with ratings and detailed parameter as attached in appendix1. For simulation study identical generators with power rating of 28.75 MVA on each platforms are modelled. Different platforms have approx. 80 to 100 node electric system with three main voltage level of 13.8kV, 6.0kV and 0.44kV. But in this study only emphasis is put on 13.8 kV bus (red colour bus) and cosiderd as main load bus since high rating inducation motor are connected at this bus as shown in Figure 28. Platfroms are mainly loaded with asyncronous motors for pumping and pressure compression purpose so draws significant reactive power consumption from the system.This study includes starting of 9MW asynchronous motor directly connected at load bus of 13.8 kV at platform PF4.

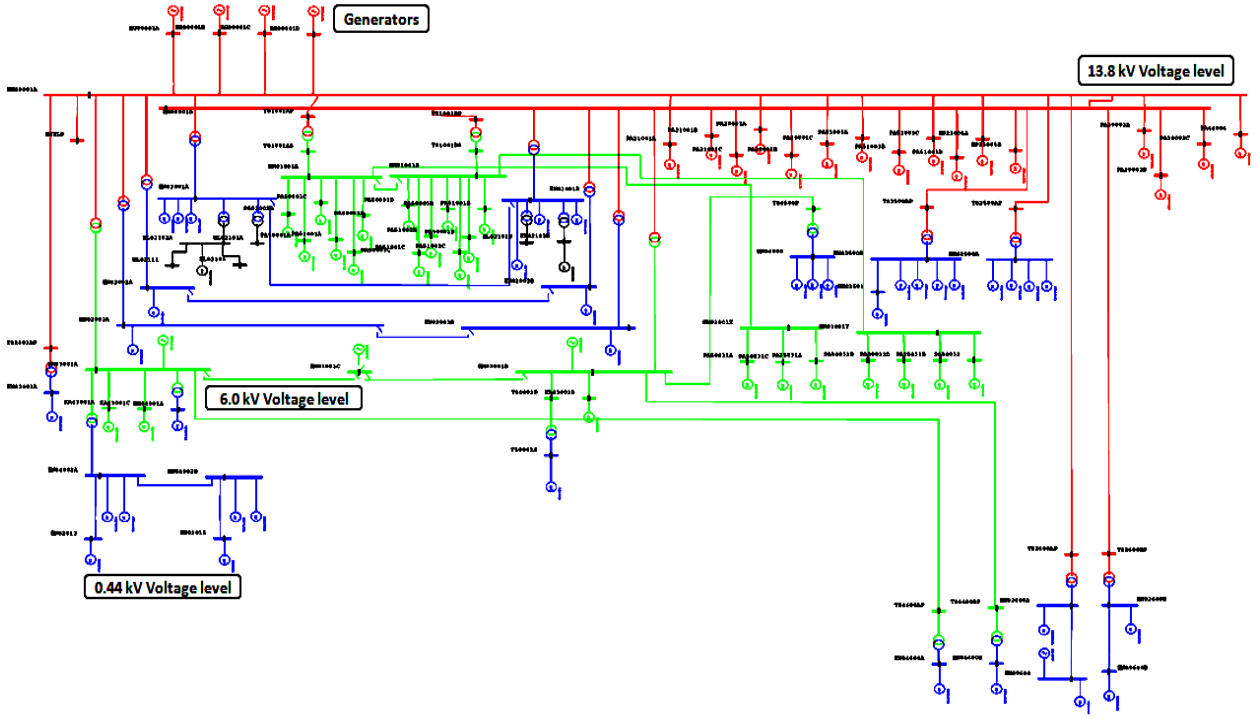

Figure 28: Single line diagram (SLD) – PF1

Details about other network parameters modelling like, transformers, cables, loads, production units, wind turbine units, SVC and STATCOM have been discussed more in details in chapter 4.

3.5 Control strategies and consideration

3.5.1 Basics of power generation

The block diagram of a generating unit considered at platforms is shown in Figure 29 where electrical energy is produced by a synchronous generator driven by a prime mover, usually a turbine or a diesel engine. In this study gas turbine is equipped with a turbine governor which controls either speed or output power according to a preset power–frequency characteristic. The excitation current, and consequently the generator's terminal voltage is controlled by an automatic voltage regulator (AVR). The generating unit is equipped with a main circuit-breaker on the high-voltage side [24].

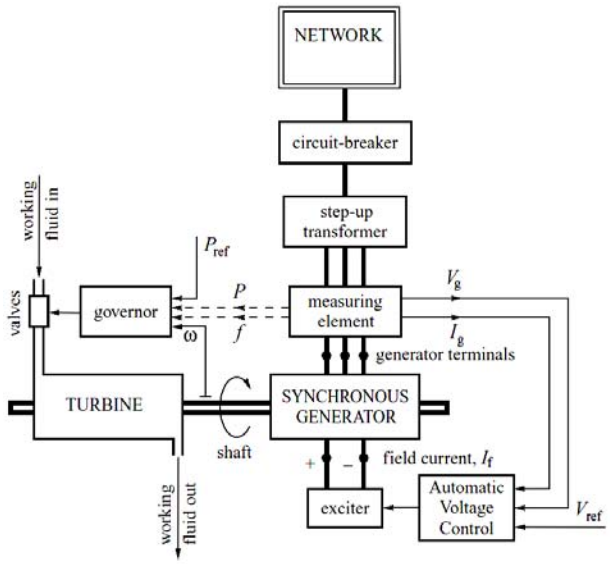

Figure 29: Block diagram of a power generation unit[24]

Since wind farm is a variable source of power the output varies between zero and full capacity gives large variations in power transfer along the interconnecting cables, both in terms of magnitude and direction. This makes the task of keeping stable voltage levels more complicated than in traditional distribution systems. Reasonable voltage levels on the platforms have been ensured in simulations by manually modifying tap positions on the main transformers (between the platforms and the interconnecting grid). Voltage levels are usually regulated via automatic tap changers. However, automatic tap changers typically operate on a longer timescale range (e.g. half a minute) than transient effects studied in the dynamic simulations (seconds), and have therefore no influence on the transient analysis.

3.5.2 Active and reactive power control

According to the theory of transfer of power between two active system [17], the factors influencing in the process of power transfer control between two section / area of interconnected power system are as follows:

- Active power transfer depends mainly on the power angle by which the sending end voltage leads the receiving end voltage.
- Reactive power transfer depends mainly on voltage magnitudes. It is transmitted from the side with higher voltage magnitude to the side with lower voltage magnitude.
- Reactive power cannot be transmitted over long distances since it would require a large voltage gradient to do so.
- An increase in reactive power transfer causes an increase in active as well as reactive power losses.

Active power and frequency control:

For satisfactory operation of a power system, the system frequency should remain nearly constant. The frequency of a system is dependent on active power balance. As frequency is a common factor throughout the system, a change in active power demand at a point is reflected throughout the system by a change in frequency. A speed governor on each generating unit provides the primary speed control, while supplementary control originating at a central control centre allocates generation. The control of generation and frequency is commonly referred to as *load-frequency control* (LFC). When there is a load change, it is reflected instantaneously as a change in the electrical torque output (*Te*) of the generator. This causes a mismatch between the mechanical torque (*Tm*) and the electrical torque (*Te*) which in turn results in speed variations as the equation of motion. In the absence of a speed governor, the system response to a load change is determined by the inertia and the damping of the system. The steady-state speed deviation is such that the change in load is exactly compensated by the variation in load due to frequency sensitivity.

Reactive power and voltage control:

For efficient and reliable operation of power systems, the control of voltage and reactive power should satisfy the following objectives:

- Voltages at terminals of all equipment in the system are within acceptable limits. Both utility and customer equipment are designed to operate at a certain voltage rating.
- System stability is enhanced to maximize utilization of the transmission system. Since voltage and reactive power control have a significant impact of system stability
- The reactive power flow is minimized so as to reduce active power losses and reactive power losses to a practical minimum.

4 REAL OPERATION MEASURMENT DATA – STARTING OF 9MW MOTOR AT PF4 BY UNITECH AS, 2003

4.1 Introduction

The measurements presented in this report were ordered by Hydro (now Statoil) in 17th July 2003. The objective of the measurement was to check system condition after installation of new module at oil platform4. The motor was initially rotation tested with 3MW power generation from each two generators connected to ensure it was rotating correct way. After rotation test, start of complete compressor train was performed at pressure of 17 bar with initial load of 10MW at each generator.

4.2 Background

The simulations and measurements performed in January 2003 by Unitech Power Systems AS showed that it is possible to start the 9 MW asynchronous motor (EE-26-004C) if both (two) generators are in operation [25]. However, it became clear that the exciter current in the generators would be close to its thermal limits during start-up due to a long run up time of motor about 13 seconds. The gas turbine power will also be high if the 9 MW motor are to be started in high load situations. This could lead to high turbine exhaust temperature, which will trigger the temperature limiter; this will lead to escalated frequency drop and should be avoided.

The measurements included in this study were performed start up of 9MW asynchronous motor rotation test at 9th July 2003 and start of the complete compressor train in August 9th 2003. The most likely results for this project study are start of complete train hence results related to these events are considered and included. This report summarizes the measurements of start of 9MW asynchronous motor based complete compressor train. The data for technical proposals from the pertinent compressor motor manufactures were used in the motor star up event as specified below:

- Rated shaft power: 9.0MW
- Rated voltage: 13.8kV
- Rated frequency: 60Hz
- Maximum pu staring current: 4.2
- Construction: 4 pole, 1800 rpm at 60Hz
- Ex classification: Eex p
- Temp. Group: T3
- Cooling method: Seawater

4.3 Measurements – Star up of compressor train Test, 9MW motor

After installation of the new module in the existed system, the motor was first rotation tested on 9th July 2003. On August 9th 2003, start of whole compressor train was performed. The starup was performed with starting pressure of 17 bar on the compressor and prior load of 10MW on each generator connected. Previously for these measurements there was no production on the platform4 due to gas leakage on platform.

To measure the bus voltage and the generator current instruments like; 4-channel transient recorder, 3 current probes and 1 voltage probe were used. Meanwhile to measure the motor current, 2-channel transient recorder and 2 current probes of different types were used as an instrument. The instruments were connected via an intertrig cable in order to make them start logging exactly at the same time. The Wv (wave viewer version 1.17), Flukeview verson 3.0 and Microsoft Excel 2000 software programs were used to download data and to create comma separated data files, which were processed in Excel [26, 27].

4.4 Results and Analysis

Before start of the 9MW electrical motor, no gas injection or oil export was taking place due to gas leakage on Platform4. Generator A and B were loaded with approximately 10MW and 5.5MVAr each prior to the start. During the start, with the help of different measuring instruments voltage and current from different terminals were measured correctly and the relevant curves of voltage and frequency are shown as in Figure 30 and 31. The frequency is calculated from the measurements of the voltage. Maximum voltage drop is measured to –11.6 % ref. to 13.8 kV, voltage overshoot after motor run-up is measured to +6.5 % ref. to 13.8 kV. Minimum frequency during run-up is calculated to 59.6 Hz, maximum frequency after run-up is calculated to 60.7 Hz. The run up time measured for the test was 8.5 second.

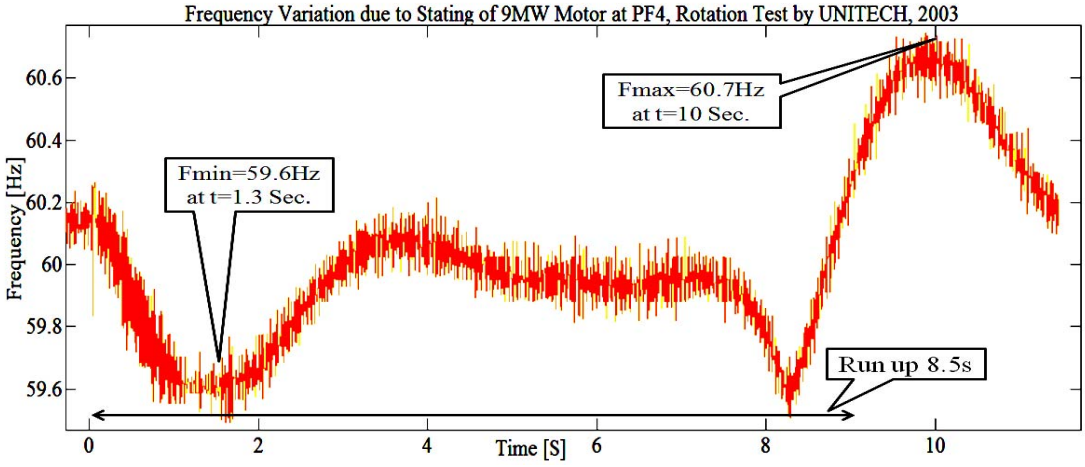

Figure 30: Real frequency variation due to starting of 9MW motor at PF4 (as a single platform) with specific details [25]

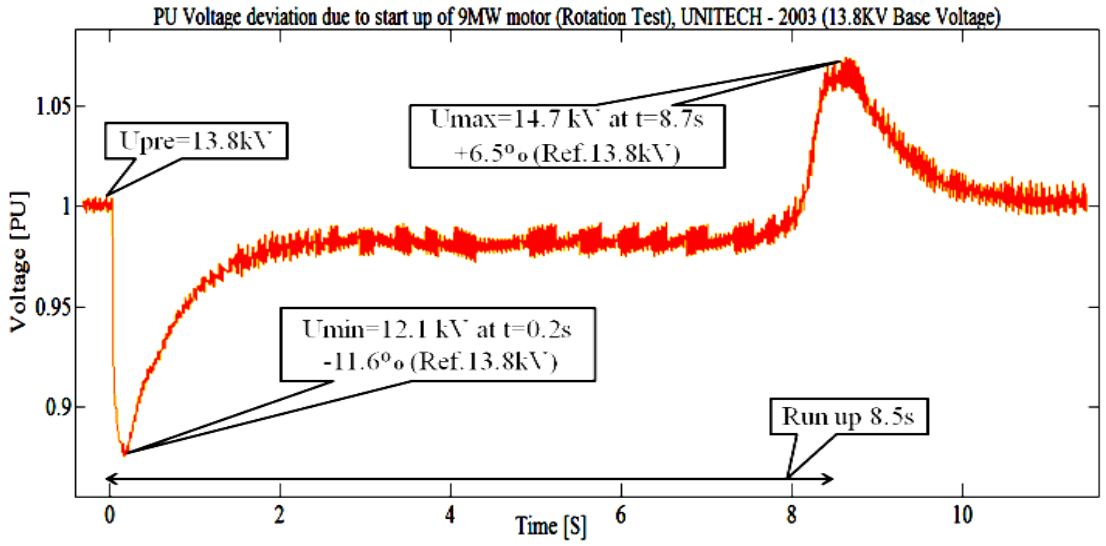

Figure 31: Real voltage variation due to starting of 9MW motor at PF4 (as a single platform) with specific details [25]

4.5 Conclusions and Recommendations

The measurements show that both the frequency and the voltage response are within NORSOK acceptable limits. When the motor is started the measurements shows that the oscillations are well damped. The measured starting time (8.5s) of the compressor is lower than calculated (13.8s) in the simulations. This is most likely caused by either the moment of inertia on the compressor train being lower or the electrical motor develops a higher torque than expected. Both these cases will shorter the motor run-up time in relation to the calculations. A shorter run-up time is regarded advantageous for the electrical system on the platform. According to IEC and NORSOK, the transient voltage dip on the main 13.8 kV switchboard shall not exceed 20% as mentioned in Table 2. Hence the measured values are considered acceptable in all cases.

5 MODELLING OF NETWORK SYSTEM

5.1 Detailed wind farm model - Full Power Convertor Wind Turbine Model (FPCWT)

The wind farm has been modelled as radial connected, four feeders of five wind turbines in each feeder. Each wind turbine has been modelled using the Full Power Converter Wind Turbine (FPCWT) model described in the SIMPOW manual [28]. An illustration of the turbine model is given in Figure 32. The control strategy of the FPCWT model is to control voltage on the AC side of the frequency converter such that the power factor is unity (i.e. minimal reactive power output) and to control the AC voltage at terminal (using its nominal value as target).

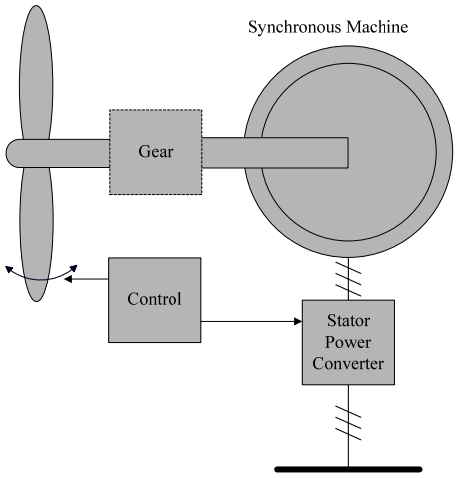

Figure 32: SIMPOW's Full Power Converter Wind Turbine model [28]

Modelling overview: - The FPCWT model consists of seven different modules are as shown in Figure 33.

- Wind turbine model
- Synchronous generator model (Simpow standard model)
- PWM converter model (rectifier and inverter)
- Shunt capacitor (Simpow standard model)
- Speed control system model
- Pitch control system
- AC voltage control system

The model of the frequency converter is represented as voltage source converters (PWM converters) including intermediate dc voltage system; where as a transfer of real power from the generator occurs.

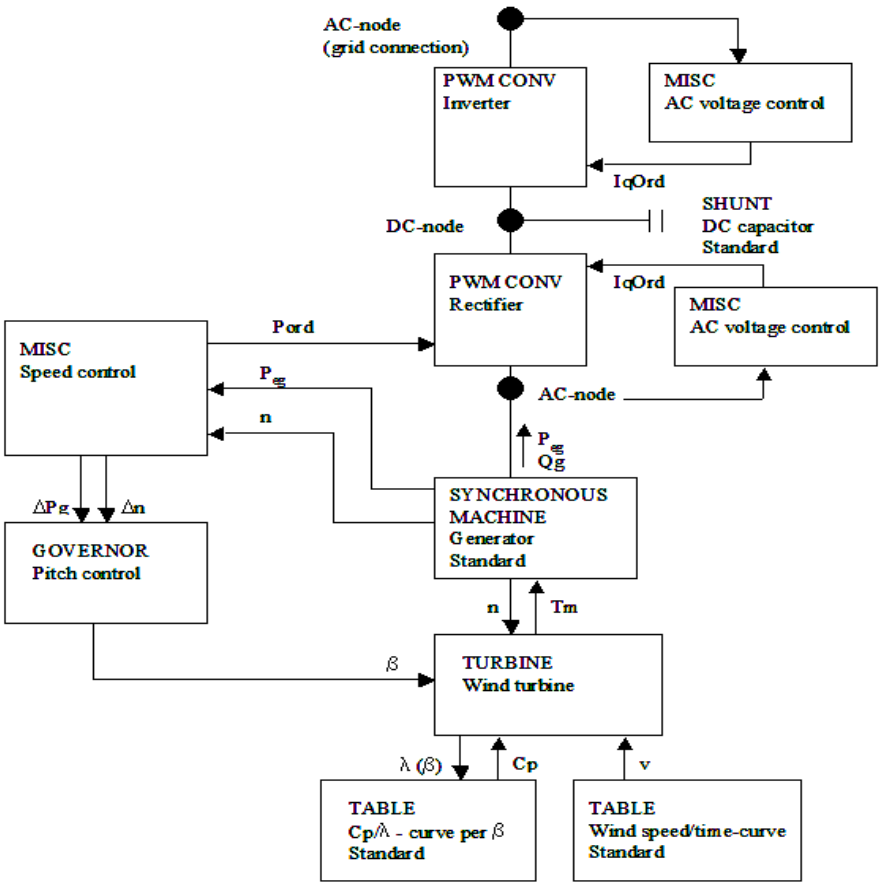

Figure 33: Block diagram of the FPCWT model [28]

One of the standard synchronous machine models is used for the generator. The rated power of the generator is chosen higher than the nominal active power in MW of the FPCWT. The generator is modelled without an exciter, having constant field voltage.

The PWM converter model shown in Figure 34, where choice of the DC voltage level is made so that the modulation index, MI, is within the range of 0-1.The amplitude of the fundamental frequency component of the output voltage varies linearly with MI so range of 0-1 is referred to as linear range [29]. The PWM converter is controlling the internal ac voltage bus, UI so that the real and imaginary current parts through the series reactor are according to orders from controllers. The real current controls the active and imaginary current control the reactive power or the ac voltage comes from the external controller.

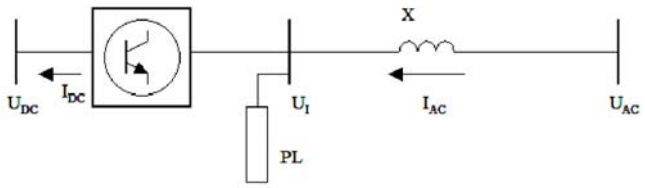

Figure 34: PWM converter model [28]

The speed control system gives the power order to the FPCWT and the pitch control. A block diagram describing the speed control regulator is shown in Figure 35.

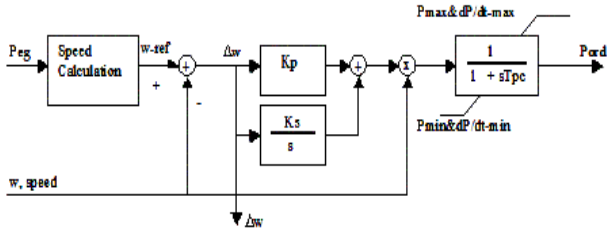

Figure 35: Speed control block diagram [28]

The real power generation and the speed are the input values for the regulator. From the actual real power generation a speed reference is calculated. The difference between this calculated speed and the speed reference goes into the PI-type regulator. The output is then multiplied with the speed and this gives the power order. The power order response is filtered. The pitch control calculates the blade angle. This angle controls the captured wind power or the mechanical torque of the wind turbine. The block diagram for this regulator is shown in Figure 36.

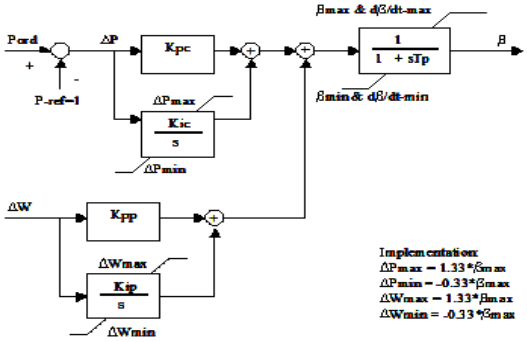

Figure 36: Pitch control block diagram [28]

The input power order and the speed deviation obtained from the speed control, compared with a power reference thus the power difference and the speed deviation go into two separate PI-type regulators as shown in Figure 36. The outputs are added and the sum is the blade angle. Before the angle response is sent to the wind turbine it is filtered with limitations in both size and derivatives.

A block diagram for the AC voltage control regulator is given in Figure 37.

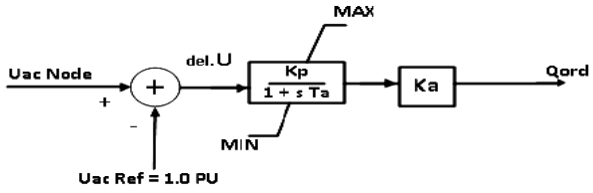

Figure 37: AC voltage control regulator [28]

The input for the regulator is the voltage of the connected bus. The voltage is compared with a specified reference. The voltage deviation goes through a PI-type regulator with maximum and minimum limits. Further details regarding the calculations done in these regulators during simulations are described in [28].

5.2 Modelled Static VAR compensator (SVC)

The regulator controlling the SVCs is a symmetrical static VAR compensator regulator (SVS). The regulator is equipped with a lead RTYPE - 1 network. Figure 38 and 39 shows the SVS regulator with lead network.

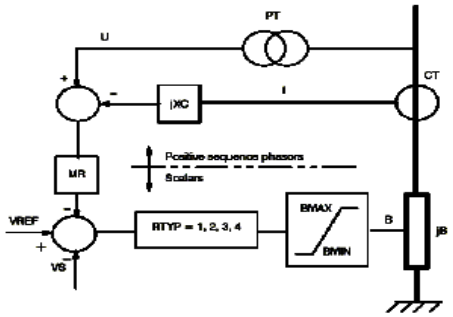

Figure 38: SVS regulator [28]

PT is a potential transformer. CT is a current transformer. MR represents a measuring rectifier. The parameters U, I, and B represent terminal voltage, current output and the susceptance of the SVC.

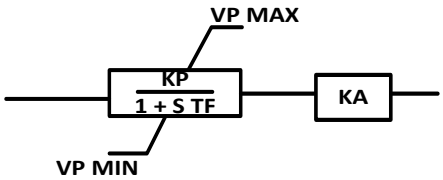

Figure 39: Lead network RTYPE - 1 for SVS regulator [28]

The jXC block gives the reactive compensation degree. A negative value means that a droop in the bus voltage is created, proportional to the lagging current of the SVC. A positive value means a voltage rise. If the current is leading it will give the opposite sign. [19].The regulator monitors the reactive power flow in the transmission line. If this difference is negative, reactive power is drawn from the main grid.

5.3 Modelled STATCOM

A STATCOM makes use of a voltage source converter (VSC), which interconnects an AC network with a capacitor connected to its DC terminals. The valves of a VSC consist of GTO-thyristors and diodes connected in antiparallel. Basically, an AC voltage is generated by

switching the DC voltage to the AC terminals by proper turn on and off the GTO-thyristors, pulse- width-modulation. The frequency, magnitude and phase angle of the AC voltage can be varied by proper control hence VSC can be considered to be a controllable AC voltage source. The VSC is connected to an AC grid by means of a transformer to provide normal voltage transformation. Regulators are used to vary the magnitude and phase of its AC voltage for control of an AC voltage magnitude in the AC network, and for control of the DC voltage of the VSC [28].

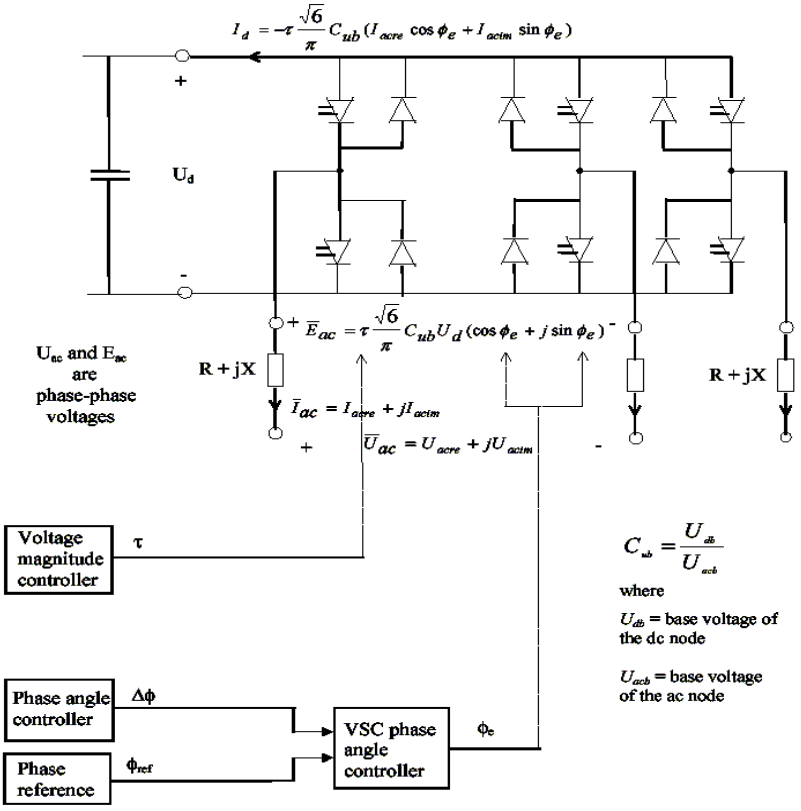

Figure 40: Voltage Source Converter (VSC) circuit [28]

VSC shown in Figure 40 is connected to an electrical system at three terminals: the AC-terminal, at which it interfaces with an AC network the DC-terminal, at which it interfaces with a DC network and the gates of the valves, at which it interfaces with controllers [28].

Assumptions for VSC: Harmonics are neglected, hence, the electrical state in the AC system is assumed to be sinusoidal. In 3-phase application; the model is valid for symmetrical system conditions, means VSC is represented by a positive sequence model per phase.

The DC network normally consists of a capacitor, which acts as an energy storage. Energy can be supplied to it by another converter, or by the voltage source converter itself by control of the phase angle of its AC voltage, which affects the active power to the converter.

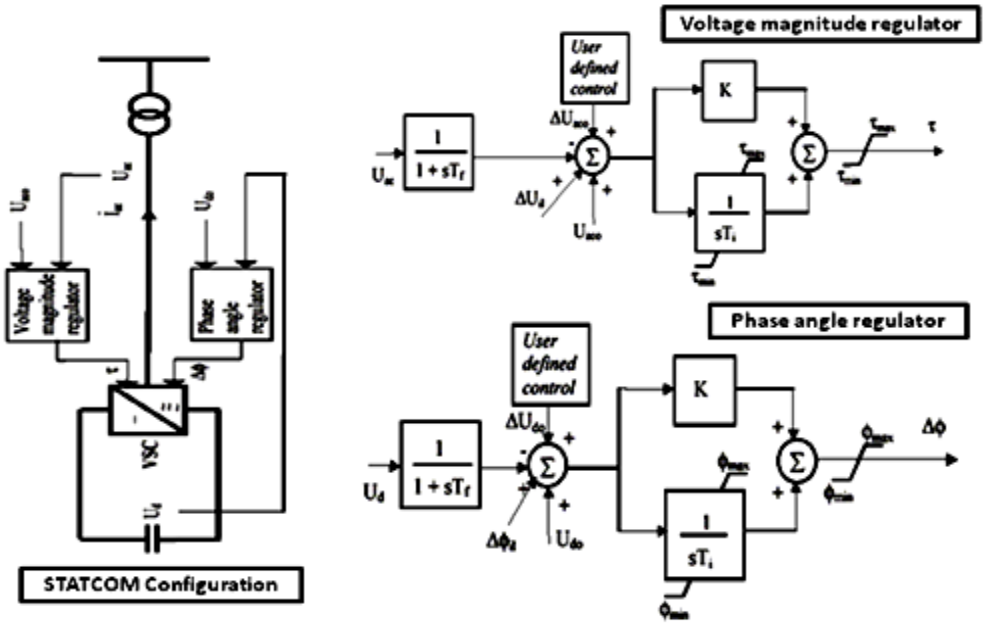

Figure 41: STATCOM config. - Voltage magnitude regulator and Phase angle regulator [28]

Figure 41 shows STATCOM configuration [20] with its voltage magnitude regulator (VMR) and phase angle regulator (PAR) for control of an AC voltage and active power of VSC. The output of VMR is the amplitude factor, by which the magnitude of the AC voltage is varied. The input is the difference between a voltage order and the actual voltage, including a measuring filter and the transfer function is proportional- integrating type. The active power of the voltage source converter can be controlled by varying the phase angle by PAR, relative the phase angle of the voltage on the network side of the converter transformer. It is exploited to keep the average value of the DC voltage on a constant value [28].

5.4 Modelled production units (Generators)

The platform synchronous generators as production unit get control through twin shaft gas turbines (aero-derivatives) including speed governors. In addition Synchronous generators are equipped with cylindrical rotors and brushless excitation systems.

In power flow calculations (optpow case), generators are represented as a simply production sources. While in the dynamic simulation of SIMPOW (dynpow case), generators have to be modelled with more specific detailed.

The synchronous generators are modelled as Type 2, where they are represented with one field winding, one damper winding in d-axis and one damper winding in q-axis with magnetic saturation [28].

The Appendix 1 contains the parameters used for each synchronous generator and excitation system parameters with relevant turbine, governor data. Each plat form contains generators as mentioned in Table 3. There are emergency generators are also at each platforms and they are modeled with same parameters. The generators' data were collected from previous case study and literature that used similar voltage and power rated generators [6, 30, 31].

5.5 Modelled Lines, cables, transformers and loads

The cables should at least have a conductor cross section adequate to meet the system requirements for power transmission capacity. The cost of energy losses can be reduced by using larger conductor. The 100 MW wind farm system required two parallel power cables to transfer adequate power from the wind farm side to platforms cluster system. Production from wind power is high enough at full wind condition requires copper conductor power cables with cross section area of 3 X 1000 mm2 for 36kV voltage system to transfer power securely with lower losses. The design data for the cables are chosen based on rated system voltage, operating frequency, required power transfer capacity in MVA and capacitive charging current with capacitance . All cables and lines for the electrical installation are modelled as impedances with pi – equivalent network, data collected from previous study and ABB catalogs [6, 32, 33]. The parameters for the cables and lines are given in Appendix 1.

The main transformers and wind turbine transformer are modelled as ideal 2-winding transformers with tap changing voltage control and possible phase shift given by the primary and secondary winding connections. The data for the transformers are taken from previous study work. Data relevant to transformer is given in Appendix 1.

The loads contains mostly asynchronous motors are modelled according to the park-transformed two axis theory with the stator flux dynamics neglected. The models allow varying rotor resistance according to slip and saturation characteristics. The data for the motors taken from previous study work [6] as attached in Appendix1. No passive loads are included in the power system model.

6 SIMULATION CASES AND ANALYSIS

6.1 Background

The simulations have been performed to analyse, initial power flow of the network by static analysis and system stability behavior by dynamic analysis. The simulations for the system investigated mainly for percentage of wind power penetration or disconnection events. Cases have been selected to represent a broad variation of combinations of initial conditions and critical perturbation events. In general, the worst case scenarios occur when the system is already stressed in the initial stage and an event occurs that exaggerates system further.

The critical events of perturbations with different initial conditions are broadly classified in four class as A, B, C and D. Where class A, starting of 9MW motor at PF4 is performed to compare simulated results with real data obtained from UNITECH Power System AS. Further, application of power electronics components SVC and Statcom on system dynamics has been studied and compared. Class A also includes impact of system voltage level of 36kV and 52kV on the system transient behavior and stability. Class B, C and D are performed to signify system stability, security of power system, criticality of perturbation events and importance of different topology aspects comparison.

As mentioned four classes of events are:

- A: Starting of 9MW induction motor at PF4
- B: Loss of gas turbine at PF4
- C: Loss of wind power
- D: Loss of interconnection between PF1 and PF4

Class A, starting of 9MW motor at PF4 has sub cases A0, A1 and A2. Case A0 represent single platform case without wind penetration. Case A1 and A2 performed with and without penetration of wind production but with five platform system for different topology aspects. In addition to that, application of FACTS devisees and two different voltage systems of 36kV and 52kV has been also performed.

Class B, C and D as perturbation events of loss of GT at PF4, loss of wind power and loss of interconnection between PF1 and PF4 respectively performed with different sub cases as mentioned in Table 7.

Table 7 and 8 give brief understanding about the selected simulation cases, perturbation events and load demand condition before and after perturbation of the proposed network system. For the selected classes and cases initially static power flow (initial power flow)

analysis and after based on consistent simulation condition of power flow, dynamic analysis are performed to analyse the system dynamics for different perturbation event cases.

The following abbreviations for:

- WT = Wind Turbine GT = Gas Turbine PF1 – PF5 = Platform 1 to 5

Table 7: Selected critical simulation cases events, description and remarks

Class	Case	Case Description	Remarks
A. Starting of Motor	A0	Single platform system: Starting of 9MW motor at platform4 with one and two GT in online in operation subsequently	Result analysis and comparison: 1) With real operational data taken by UNITECH for single platform system. 2) Impact of power electronics equipments - SVC and Statcom 3) 36 and 52 kV voltage level comparison
	A1	Starting of 9MW motor at PF4, 8 GTs online with equal power sharing at different platforms, no wind penetration	
	A2	Starting of 9MW motor at PF4, 8 GTs online with equal power sharing at different platforms, 100MW wind penetration	
B. Loss of Gas Turbine Power	B1	Loss of a GT at PF4, No wind and initially 9GTs online at different platforms	System stability aspects: By dynamic analysis of frequency and voltage variations at different network busses, For 1)Topology : • Star • Star-F • Mesh 2) Wind Power in network system: • No wind • 50MW - loss / insert • 100MW - loss / insert
	B2	Loss of a GT at PF4, 100MW wind and initially 9GTs online at different platforms	
C. Loss of Wind power	C1	Loss of 25% (25MW) wind power, 8GT online with equal power sharing	
	C2	Loss of 50% (50MW) wind power, 8GT online with equal power sharing	
	C3	Loss of 100% (100MW) wind power, 8GT online with equal power sharing	
D. Loss of Interconnection between platform PF1 and PF4	D1	Loss of interconnection - PF1 and PF4, 8 GTs online with equal power sharing at different platforms, with 50MW wind	
	D2	Loss of interconnection - PF1 and PF4, 8 GTs online with equal power sharing at different platforms, with 100MW wind	

Table 8: -Detailed power flow view for critical events at different platforms and wind farm.

Case	Voltage Level (kV)	Prod Load	Wind (MW)	P1 (MW)	P2 (MW)	P3 (MW)	P4 (MW)	P5 (MW)
A: Starting of 9MW induction motor at PF4								
A1	36KV / 52KV	Prod Load	0	20 24	20+20 34	20+20 30	20+20 **25 → 34**	20 25
A2	36KV / 52KV	Prod Load	100	6 24	6 34	6+6 30	6+6 **25 → 34**	6 25
B: Loss of Generator Turbine at PF4								
B1	36KV	Prod Load	0	17+17 24	17+17 34	17+17 30	**17+17→17+0** 34	17 25
B1	36KV	Prod Load	100	12 24	12 34	12 30	**10→ 0** 34	12 25
C: Loss of wind power production								
C1	36KV	Prod Load	**25 → 0**	16 24	16+16 34	16+16 30	16+16 34	16 25
C2	36KV	Load Load	**50 → 0**	12 24	12+12 34	12+12 30	12+12 34	12 25
C3	36KV	Prod Load	**100→ 0**	6 24	6+6 34	6+6 30	6+6 34	6 25
D: Loss of Interconnection between PF1 and PF4								
D1	36KV	Prod Load	50	10 24	10+10 34	10 30	10+10 34	10 25
D1	36KV	Prod Load	100	8 24	8 34	8 30	8+8 34	8 25

6.2 Static Power Flow Analysis

Static power flow analysis (initial load flow) has been performed to assess power losses, voltage drop, reactive power flow situation, generation of power from different production units and to examine whether different system parameters are within permissible limitation or not. The static power flow has been performed for three different topology aspects Star, Star-F and Mesh connected platform system. Wind power penetration of 100MW gives more power flow from wind farm side to platform side shows variation in reactive power flow, more power losses in cables and voltage drops at different busses as specified in Tables. With increased voltage level on the interconnected grid, the currents are reduced and therefore the losses are reduced. In fact, for transfer of 100 MW wind penetration power at 36 kV, two parallel cables are required [34] since current flow is too high for a single cable to carry compared to 52kV system voltage. In addition as the voltage level increases reactive power generation in the network also consequently increases owing to square relation with voltage level.

Initial power flow performed for two tasks A, starting of motor with different wind penetrations and B, loss of generator at PF4 also with and without wind penetration performed

for Star, Star-F and Mesh topology. Power flow for A and B results are almost similar as initial conditions remain unchanged and more detailed results from the initial power flow analyses, comparison of three different topologies and different class could be getting in appendix 2.

Table 9, 10, 11 and 12 expressed summary of power flow results for case A1, A2, B1 and B2 respectively. The tables shows, total power production, total load situation, network losses, transmission losses, network generation, power electronics effect due to integration of wind power and power situation at different generating units.

Table 9: - Initial power flow results case A1 - no wind penetration

Case A1: Staring of 9MW motor at PF4, no wind									
TOPOPLOGY	**STAR**			**STAR-F**			**MESH**		
TOTAL PROD.	**MW**	**Mvar**		**MW**	**Mvar**		**MW**	**Mvar**	
PRODUCTIONS	143.638	79.5021		143.584	80.2937		143.560	76.2438	
PWM CONVERTORS	-0.135E-02	-3.42862		-0.575E-03	-2.21431		-0.307E-02	-5.17840	
NETWORK GEN.		9.09579			6.88067			13.8699	
TOTAL	**143.636**	**85.1693**		**143.584**	**84.9600**		**143.557**	**84.9353**	
TOTAL LOAD	**MW**	**Mvar**		**MW**	**Mvar**		**MW**	**Mvar**	
SHUNT REACTORS	0.250E-04	0.00000		0.250E-04	0.00000		0.250E-04	0.00000	
ASYNCHRON. LOAD	143.394	83.6520		143.394	83.6520		143.394	83.6522	
NETWORK LOSSES	0.242217	1.51728		0.189826	1.30804		0.162759	1.28312	
TOTAL	**143.636**	**85.1693**		**143.584**	**84.9600**		**143.557**	**84.9353**	
PARAMETERS	MW	Mvar		MW	Mvar		MW	Mvar	
SW P1_EG80001A	17.6376	14.8242		17.5844	14.8265		17.5598	14.8276	
TRANS. LOSSES	**0.168492**	**0.438997**		**0.116920**	**0.246440**		**0.08690**	**0.161421**	
PRODUCTION UNIT	**MW**	**Mvar**	**Mva**	**MW**	**Mvar**	**Mva**	**MW**	**Mvar**	**Mva**
PROD P1_EG80001A	**17.6376**	**14.8242**	**23.0399**	**17.5844**	**14.8265**	**23.0008**	**17.5598**	**14.8276**	**22.9827**
PROD P2_EG80001A	18.0000	9.76997	20.4805	18.0000	10.2325	20.7052	18.0000	9.24595	20.2358
PROD P3_EG80001A	18.0000	7.47733	19.4913	18.0000	7.83352	19.6307	18.0000	6.63203	19.1829
PROD P4_EG80001A	18.0000	6.82020	19.2488	18.0000	6.70664	19.2088	18.0000	6.56517	19.1599
PROD P5_EG80001A	18.0000	14.6105	23.1833	18.0000	14.6945	23.2363	18.0000	12.9730	22.1878
PROD P2_EG80001B	18.0000	9.00000	20.1246	18.0000	9.00000	20.1246	18.0000	9.00000	20.1246
PROD P3_EG80001B	18.0000	8.00000	19.6977	18.0000	8.00000	19.6977	18.0000	8.00000	19.6977
PROD P4_EG80001B	18.0000	9.00000	20.1246	18.0000	9.00000	20.1246	18.0000	9.00000	20.1246

Single line diagrams (SLDs) for three different topologies Star, Star-F and Mesh for case A1 are shown in Figures 42, 43 and 44 respectively. The name of the relevant buses is given in the first row, followed by per-unit value of the voltage and phase angle in degrees. Closed to the lines, active and reactive powers are given respectively in MW and MVar. A positive sign stands for production and a negative sign for exportation. Thus, on one line two power pair values appear and are opposite to each other, regardless of the transmission losses, depending on which side they are taken into account.

Case A1: Starting of 9MW asynchronous motor at PF4, No wind penetration for "Star" Topology with 36kV voltage system. Power Load flow - Single Line Diagram representation shows load bus voltages 13.8kV (blue colour), main platform voltages (red colour), power generation at GTs (purple colour) and power flow situation of whole network.

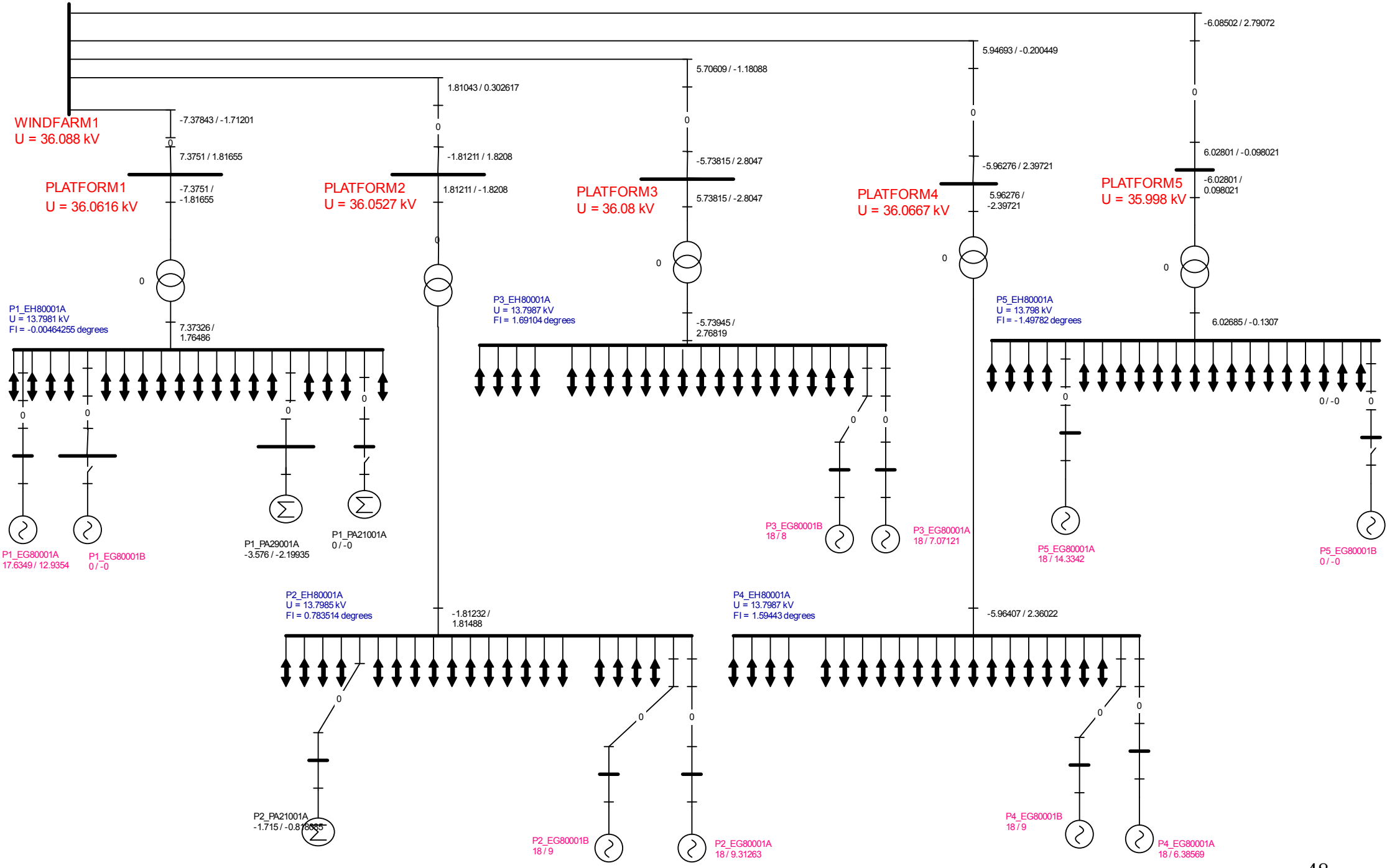

Figure 42: “Star topology” single line diagram – initial power flow, Case A1 (no wind)

Case A1: Starting of 9MW asynchronous motor at PF4, No wind penetration for "Star-F" Topology with 36kV voltage system. Power Load flow - Single Line Diagram representation shows load bus voltages 13.8kV (blue colour), platforms voltage (red colour), generation at different platforms (purple colour) and power flow situation of whole network.

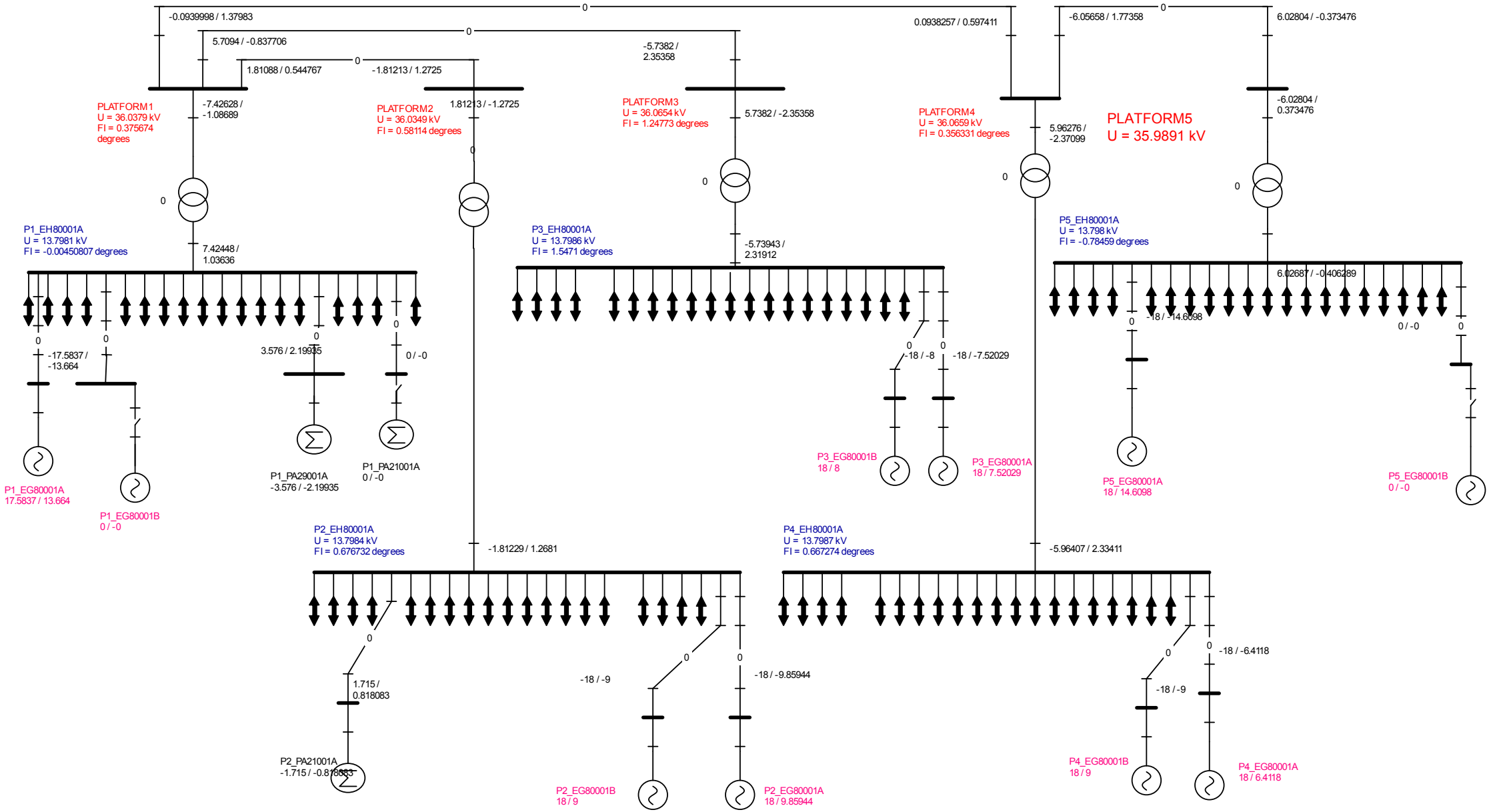

Figure 43: “Star-F topology” single line diagram – initial power flow, Case A1 (no wind)

Case A1: Starting of 9MW asynchronous motor at PF4, No wind penetration for "Mesh" Topology with 36kV voltage system. Power Load flow - Single Line Diagram representation shows load bus voltages 13.8kV (blue colour), platforms voltage (red colour), generation at different platforms (purple colour) and power flow situation of whole network.

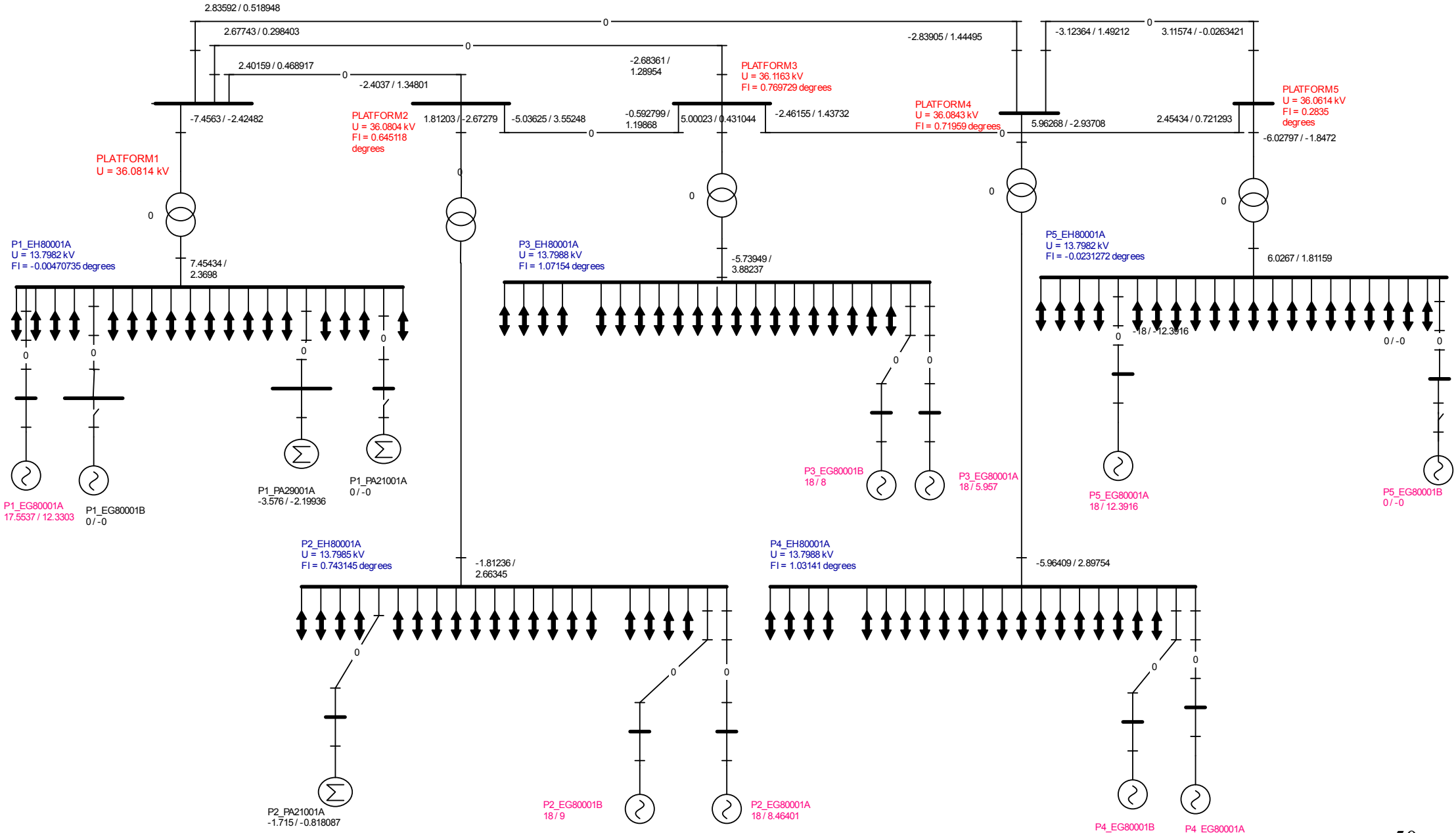

Figure 44: “Mesh topology” single line diagram – initial power flow, Case A1 (no wind)

Power flow - SLD gives broad understanding about power flow at different system busses and cables, voltage drop, main platform buses and load buses voltages, current flow situation, reactive power flow from different generating units and number of generating units involved online in operation. It can be seen from different SLDs that voltages at different buses are within permissible limit of standards in steady state condition. More initial power flow result SLDs for different perturbation events are attached in Appendix 2 to get detailed view about wind penetration effect on network system. Appendix 2 also includes SLDs with effect of SVC and STATCO application at PF1. Table 10, express summary of different parameters results for case A2 with 100 MW wind penetration. It can be seen easily as 100MW wind power penetration in the system gives significant reduction of power production from different 8 generating units at different platforms.

Table 10:- Initial power flow results case A2 – 100MW wind penetration

Case A2: Staring of 9MW motor at PF4, 100MW wind									
	STAR			**STAR-F**			**MESH**		
TOTAL PROD.	**MW**	**Mvar**		**MW**	**Mvar**		**MW**	**Mvar**	
PRODUCTIONS	151.755	101.665		151.804	104.003		151.471	96.0209	
PWM CONVERTORS	-4.24050	-7.21147		-4.24049	-6.27263		-4.24049	-7.14873	
NETWORK GEN.		**13.7067**			**11.4836**			**18.4515**	
TOTAL	**147.515**	**108.160**		**147.563**	**109.214**		**147.230**	**107.324**	
TOTAL LOAD	MW	Mvar		MW	Mvar		MW	Mvar	
SHUNT REACTORS	0.500E-03	0.00000		0.500E-03	0.00000		0.500E-03	0.00000	
ASYNCH. LOAD	143.394	83.6524		143.394	83.6523		143.394	83.6527	
NETWORK LOSSES	**4.12043**	**24.5076**		**4.16889**	**25.5620**		**3.83601**	**23.6709**	
OTAL	**147.515**	**108.160**		**147.563**	**109.214**		**147.230**	**107.324**	
PARAMETERS	**MW**	**Mvar**		**MW**	**Mvar**		**MW**	**Mvar**	
SW P1_EG80001A	9.75539	16.3932		9.80385	17.6886		9.47097	15.8514	
SW WTG1 to WTG20	100.000	0.00000		100.000	0.00000		100.000	0.00000	
SWING BUS TOTAL	109.755	16.3932		109.804	17.6886		109.471	15.8514	
RANSMISS. LOSSES	**3.53580**	**12.7865**		**3.58444**	**13.8413**		**3.25237**	**11.9775**	
	MW	**Mva**	**Mva**	**MW**	**Mvar**	**Mva**	**MW**	**Mvar**	**Mva**
PROD P1_EG80001A	9.75539	16.3932	19.0763	9.80385	17.6886	20.2238	9.47097	15.8514	18.4653
PROD P2_EG80001A	6.00000	12.3141	13.6981	6.00000	12.9230	14.2480	6.00000	11.5246	12.9930
ROD P3_EG80001A	6.00000	11.6811	13.1319	6.00000	12.1787	13.5765	6.00000	9.83205	11.5182
PROD P4_EG80001A	6.00000	10.0832	11.7333	6.00000	10.0470	11.7023	6.00000	9.67605	11.3853
PROD P5_EG80001A	6.00000	19.1933	20.1092	6.00000	19.1659	20.0832	6.00000	17.1368	18.1568
PROD P2_EG80001B	6.00000	11.0000	12.5300	6.00000	11.0000	12.5300	6.00000	11.0000	12.5300
PROD P3_EG80001B	6.00000	11.0000	12.5300	6.00000	11.0000	12.5300	6.00000	11.0000	12.5300
PROD P4_EG80001B	6.00000	10.0000	11.6619	6.00000	10.0000	11.6619	6.00000	10.0000	11.6619

Table 11: - Initial power flow results case B1 – no wind penetration

Case B1: Loss of GT at PF4, no wind penetration, topology Analysis									
TOPOLOGY	STAR			STAR-F			MESH		
TOTAL PROD.	**MW**	**Mvar**		**MW**	**Mvar**		**MW**	**Mvar**	
PRODUCTIONS	143.634	75.9689		143.592	78.0941		143.549	70.9323	
NETWORK GEN.		9.11704			6.89222			13.9021	
TOTAL	**143.634**	**85.0860**		**143.592**	**84.9864**		**143.549**	**84.8343**	
TOTAL LOAD	**MW**	**Mvar**		**MW**	**Mvar**		**MW**	**Mvar**	
ASYNCH. LOAD	143.394	83.6527		143.394	83.6526		143.394	83.6530	
NETWORK LOSSES	0.24047	1.43326		0.19843	1.33376		0.15515	1.18133	
TOTAL	**143.634**	**85.0860**		**143.592**	**84.9863**		**143.549**	**84.8343**	
	MW	**Mvar**		**MW**	**Mvar**		**MW**	**Mvar**	
SW P1_EG80001A	15.6344	2.08491		15.5924	3.15736		15.5491	1.86572	
SW BUS TOTAL	15.6344	2.08491		15.5924	3.15736		15.5491	1.86572	
TRANS. LOSSES	**0.16899**	**0.40797**		**0.12722**	**0.31633**		**0.08318**	**0.142363**	
	MW	**Mvar**	**Mva**	**MW**	**Mvar**	**Mva**	**MW**	**Mvar**	**Mva**
PROD P1_EG80001A	15.6344	2.08491	15.7728	15.5924	3.15736	15.9088	15.5491	1.86572	15.6606
PROD P2_EG80001A	16.0000	9.60448	18.6614	16.0000	10.0416	18.8900	16.0000	8.69203	18.2086
PROD P3_EG80001A	16.0000	8.80961	18.2650	16.0000	9.18219	18.4476	16.0000	7.54654	17.6904
PROD P4_EG80001A	16.0000	7.63981	17.7304	16.0000	7.55156	17.6925	16.0000	7.08136	17.4970
ROD P5_EG80001A	16.0000	14.8301	21.8159	16.0000	15.1614	22.0424	16.0000	12.7466	20.4567
PROD P1_EG80001B	16.0000	9.00000	18.3576	16.0000	9.00000	18.3576	16.0000	9.00000	18.3576
PROD P2_EG80001B	16.0000	9.00000	18.3576	16.0000	9.00000	18.3576	16.0000	9.00000	18.3576
PROD P3_EG80001B	16.0000	7.00000	17.4642	16.0000	7.00000	17.4642	16.0000	7.00000	17.4643
PROD P4_EG80001B	16.0000	8.00000	17.8885	16.0000	8.00000	17.8885	16.0000	8.00000	17.8885

Table 12: - Initial power flow results case B2 – 100MW wind penetration

Case B2: Loss of GT at PF4, 100MW wind penetration, topology Analysis									
	STAR			STAR-F			MESH		
TOTAL PRODUCTION	**MW**	**Mvar**		**MW**	**Mvar**		**MW**	**Mvar**	
PRODUCTIONS	151.851	102.131		151.913	104.590		151.555	96.4750	
PWM CONVERTORS	-4.24049	-7.25942		-4.24049	-6.33639		-4.24049	-7.22390	
NETWORK GEN.		**13.7069**			**11.484**			**18.4511**	
TOTAL	**147.610**	**108.578**		**147.672**	**109.738**		**147.314**	**107.702**	
TOTAL LOAD	**MW**	**Mvar**		**MW**	**Mvar**		**MW**	**Mvar**	
SHUNT REACTORS	0.500E-03	0.00000		0.500E-03	0.00000		0.500E-03	0.00000	
ASYNCH. LOAD	143.394	83.6530		143.394	83.6529		143.394	83.6533	
NETWORK LOSSES	**4.21590**	**24.9254**		**4.27779**	**26.0851**		**3.91994**	**24.0489**	
TOTAL	**147.610**	**108.578**		**147.672**	**109.738**		**147.314**	**107.702**	
	MW	**Mvar**		**MW**	**Mvar**		**MW**	**Mvar**	
SW P1_EG80001A	7.05085	8.00993		7.11274	9.44785		6.75489	7.58710	
SW WTG1 to WTG20	100.000	0.00000		100.000	0.00000		100.000	0.00000	
TRANSMISS. LOSSES	**3.62971**	**13.1611**		**3.69178**	**14.3210**		**3.33487**	**12.3157**	
	MW	**Mvar**	**Mva**	**MW**	**Mvar**	**Mva**	**MW**	**Mvar**	**Mva**
PROD P1_EG80001A	**7.05085**	**8.00993**	**10.6711**	**7.11274**	**9.44785**	**11.8259**	**6.75489**	**7.58710**	**10.1584**
PROD P2_EG80001A	5.50000	11.4978	12.7455	5.50000	12.0807	13.2737	5.50000	10.6858	12.0182
PROD P3_EG80001A	5.50000	10.9905	12.2899	5.50000	11.4701	12.7206	5.50000	9.08223	10.6178
PROD P4_EG80001A	5.50000	10.2576	11.6391	5.50000	10.2300	11.6147	5.50000	9.83074	11.2647
PROD P5_EG80001A	5.50000	19.3751	20.1406	5.50000	19.3618	20.1278	5.50000	17.2891	18.1428
PROD P1_EG80001B	6.30000	8.00000	10.1828	6.30000	8.00000	10.1828	6.30000	8.00000	10.1828
PROD P2_EG80001B	5.50000	12.0000	13.2004	5.50000	12.0000	13.2004	5.50000	12.0000	13.2004
PROD P3_EG80001B	5.50000	12.0000	13.2004	5.50000	12.0000	13.2004	5.50000	12.0000	13.2004
PROD P4_EG80001B	5.50000	10.0000	11.4127	5.50000	10.0000	11.4127	5.50000	10.0000	11.4127

6.3 Static Power Flow - Results and Discussion

Table 13: Summary of Results - Static Power flow for different topologies

STATIC POWER FLOW ANALYSIS- Losses Comparison				
CATEGORY	TOPOLOGY	STAR	STAR-F	MESH
	CASES	MVAR	MVAR	MVAR
NETWORK GENERATION (REACTIVE PRODUCATION)	A1	9.09579	6.88067	13.8699
	A2	13.7067	11.4836	18.4515
	B1	9.11704	6.89222	13.9021
	B2	13.7069	11.4843	18.4511
	CASES	MW	*MW*	MW
NETWORK LOSSES [MW]	A1	0.24221	0.18982	**0.16275**
	A2	4.12043	4.16889	**3.83601**
	B1	0.24047	0.19843	**0.15515**
	B2	4.21590	4.27779	**3.91994**

Table 14: Summary of Results - Static Power flow for voltage level

CATEGORY	TOPOLOGY	36kV	52kV
	STAR	MVAR	MVAR
NETWORK GENERATION (REACTIVE PRODUCATION)	A1	9.1123	***18.0939***
	A2	13.706	***22.8206***
	B1	9.1234	***19.2351***
	B2	12.567	***22.9435***
	CASES	MW	*MW*
NETWORK LOSSES (MW)	A1	0.24221	*0.19071*
	A2	**4.12043**	***3.13567***
	B1	0.24047	*0.18071*
	B2	**4.21590**	***3.25677***

Discussion:

Summary Tables 13 and 14 shows, reactive power generation and active power losses for the integrated isolated network system according to different topology and voltage level aspects. Table 13 indicates, mesh topology gives less active power losses compared to two others; however mesh topology have more reactive power generation owing to more interconnecting cables in the system results into more lengths of cable consequently more capacitive charging current as discussed in section 5. Star and Star-F topology have similar network losses and less reactive power generation during full wind penetration due to more active power flow and almost similar length of subsea cables for network system. Table 14 expresses that 52kV voltage system gives less network losses but more reactive power production according to direct proportionate relation of reactive power generation to square of voltage. It can also been seen that as wind penetration increases more power flow in integrated system of wind farm and platforms results in to more losses in network.

6.4 Dynamic Simulation Study

The objective of the dynamic simulation study is to assess magnitude (peak) of the largest transients of frequency and voltage variations of network load buses and hence to analyse whether the system is stable or not by following offshore NORSOK standards as referred in Table 2. The dynamic simulation study also gives understanding about the criticality of system for different contingency perturbation case events. Simulations are made with DYNPOW, which is the tool available in SIMPOW for dynamic simulations of electric power systems. New files have to be created in order to complete initial conditions given by the load flow achieved with OPTPOW based on given practical data. Dynamic simulation study has main approach to examine the system stability and reliability due to different percentage of wind penetrations or wind loss by judging frequency and voltage variation ranges following NORSOK standards. Study also yields understanding of system behavior based on major oscillations and damping when different perturbations/disturbance accurse since damping of is an important part for system to be stabilized.

To get overview of dynamic simulations cases events classification in this chapter, Table 7 and 8 is an important tool to understand. Based on Table 7, the dynamic study is divided in four main class as A, B, C and D, according to different kind of perturbations implemented in the system. Class A, B, C and D are further subdivided in to different cases according to wind power applications and network topologies aspects. At the end of each class, summary of results, relevant analysis, primary examination and discussion have been performed.

Details of different classes as below (following Table 4),

A) Online starting of large 9MW induction motor at PF4
B) Loss of Gas turbine at PF4
C) Loss of wind power by 25%, 50% and 100% respectively
D) Loss of interconnection between PF1 and PF4 with 50% and 100% wind power.

Class A, starting of 9MW motor at PF4 is performed to access mainly frequency and voltage deviations at load bus PF1, common bus of coupling with wind farm and load bus PF4, bus at 9MW motor connected directly. Detailed motor parameter and modelling are follows previous study and specified in Appendix 1. The dynamic results obtained in term of voltage and frequency variations are compared with real operation data (referred as reference data for this study) taken by UNITECH AS since discussed in chapter 4. By comparison, would like to examine system behavior, criticality of perturbation and significance and consequences of wind insight in system. In addition Case A includes dynamic comparison study of, application

of SVC and STATCOM during transients how it improves voltage control capability of network system and voltage system comparison of 36kV with 52kV for different topologies aspects.

Class B, C and D, for loss of GT, loss of wind power and loss of interconnection respectively are also performed on different topologies aspects, to analyze dynamics of voltage and frequency, criticality of perturbations, system behavior due to perturbations and importance and consequences of wind power loss or wind power penetration in the system. At the end of each class, comparison made for different topology according to percentage of wind penetration and loss. At the last of all class study final summary of results, relevant analysis and discussion have been done.

6.4.1 Class A: Online Starting of 9MW Induction motor at PF4, 8 GTs online with equal power sharing.

6.4.1.1 Real operational data and topology comparison aspects:

A0: Dynamic simulation - Single platform system, startup of 9MW motor at PF4

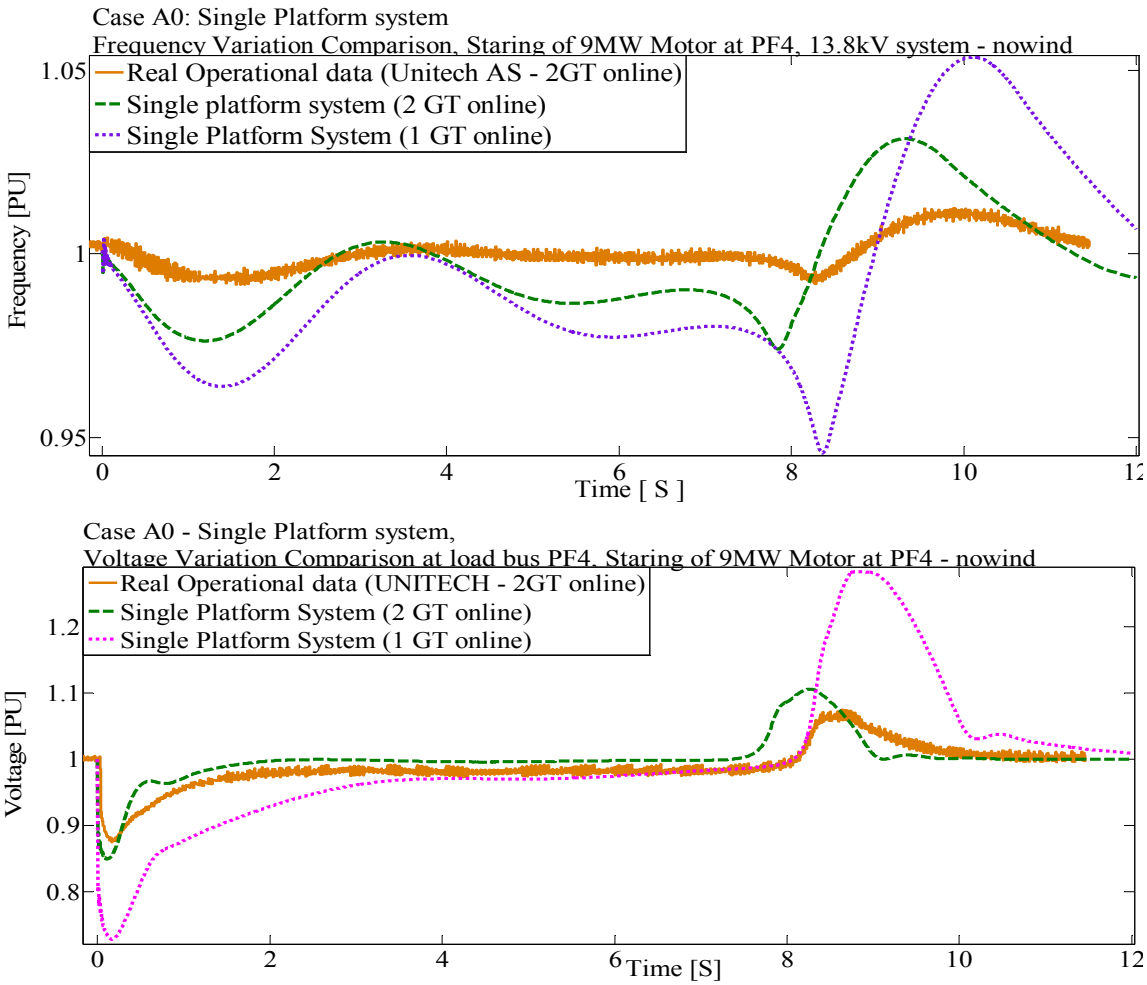

Figure 45: Frequency and voltage variation comparison with reference real data

A1: Dynamic simulation – Five platform system, startup of 9MW motor at PF4, 8 GTs online at different platforms with equal power sharing, no wind penetration

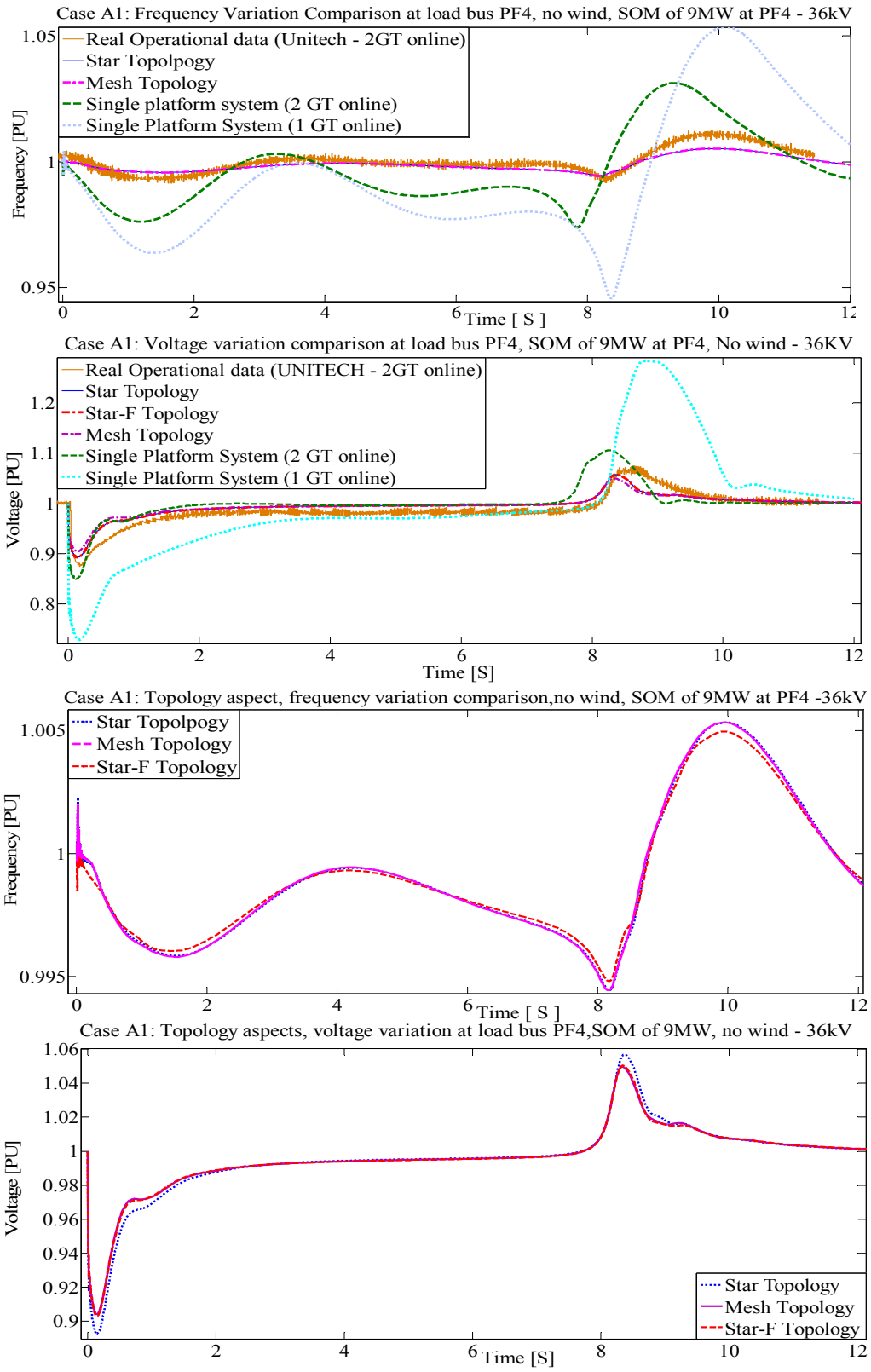

Figure 46: Topology aspets - voltage and frequency variation, SOM of 9MW at PF4, no wind

A2: Dynamic simulation – Five platform system, startup of 9MW motor at PF4, 8 GTs running at different platforms with equal power sharing, 100MW wind penetration

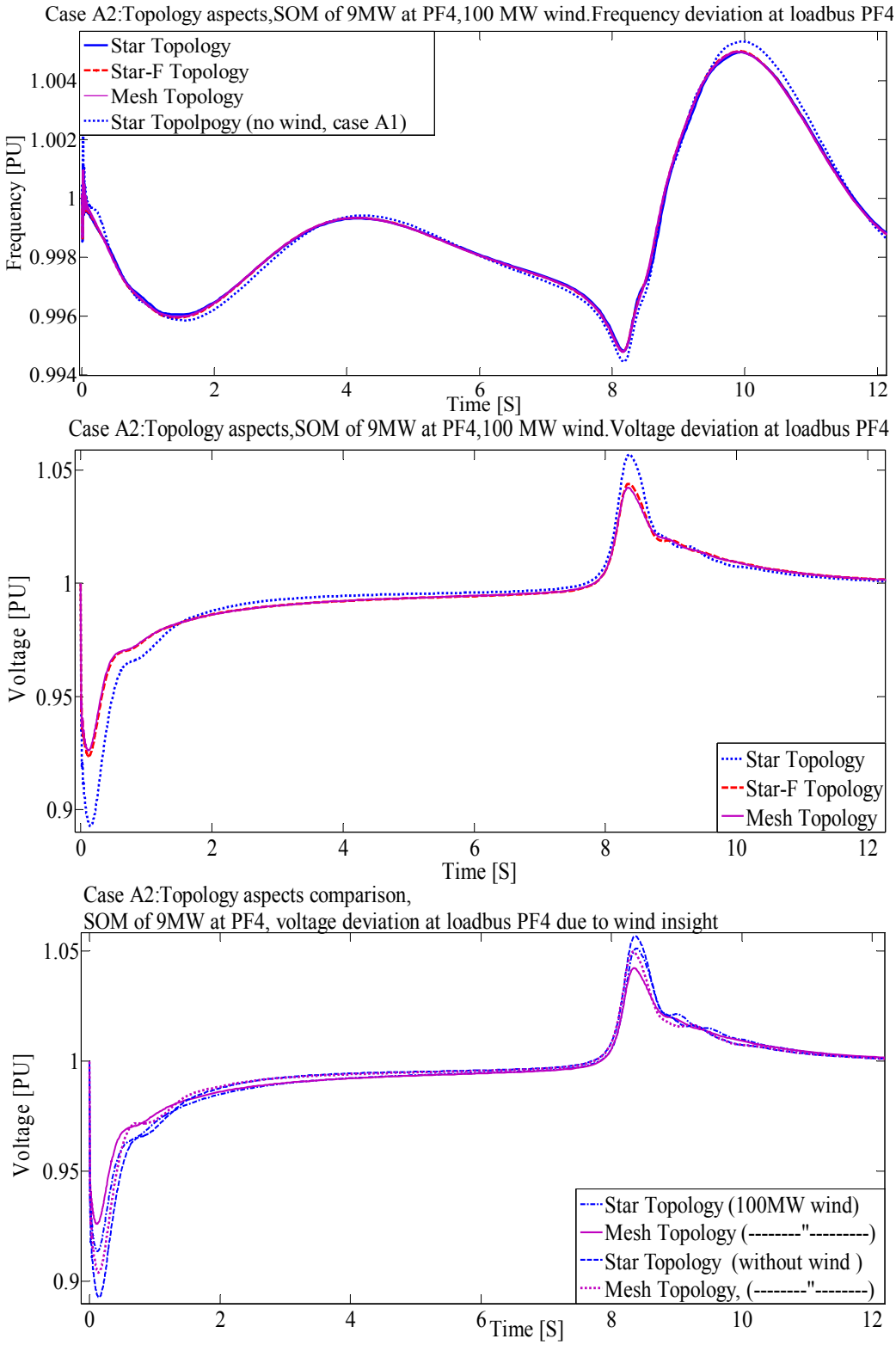

Figure 47: Topology aspets - voltage and frequency variation, SOM of 9MW at PF4, 100MW wind penetration

6.4.1.2 SVC and STATCOM application aspects for STAR topology:

A1: Dynamic simulation – Start up of 9MW motor at PF4, 8 GTs running at different platforms with equal power sharing, no wind penetration with SVC/Statcom at PF1.

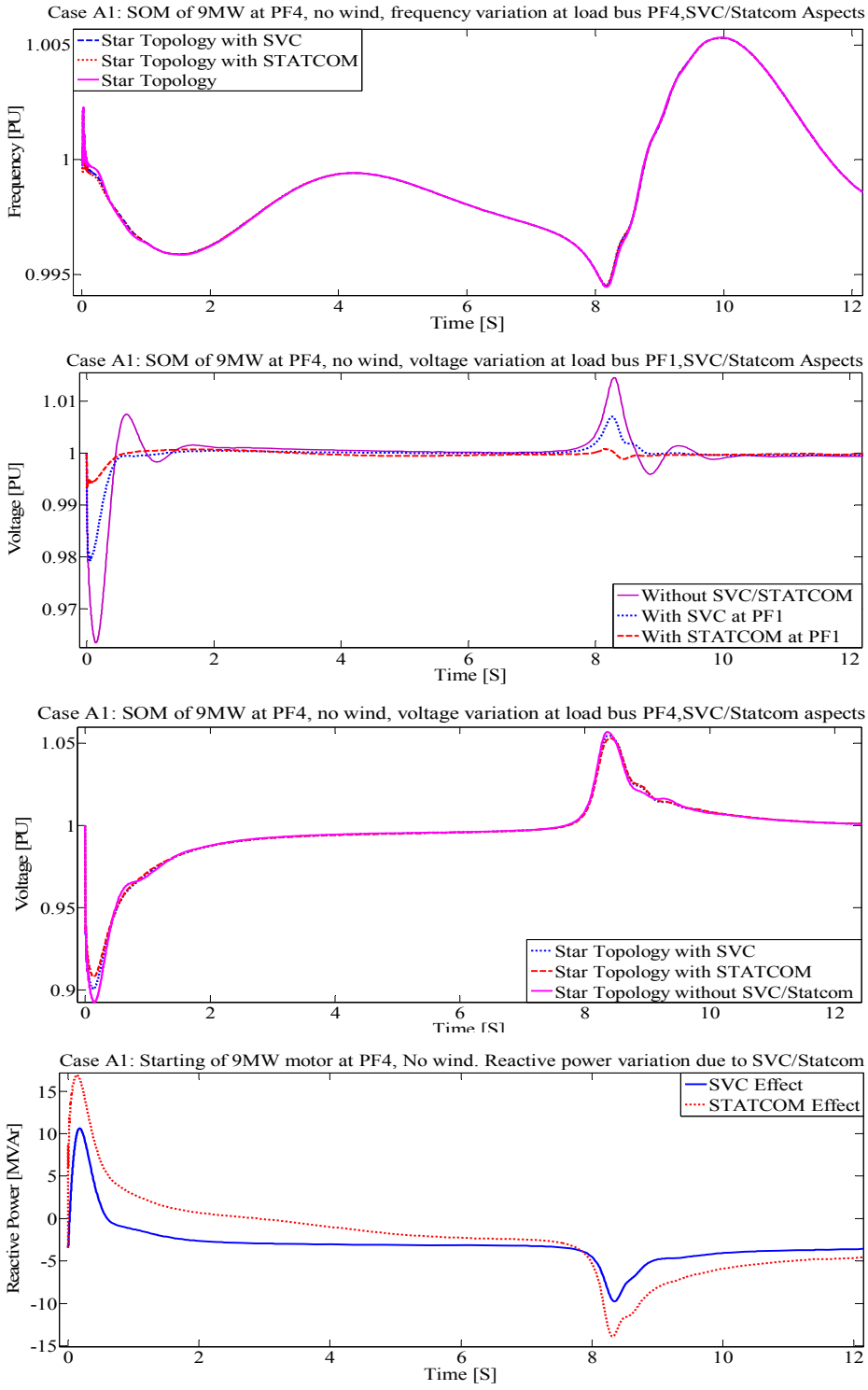

Figure 48: SVC/Statcom aspects : Voltage deviation, frequency variation and generator reactive power genenation variation due to statting of 9MW induaction motor, no wind

A2: Dynamic simulation – Start up of 9MW motor at PF4, 8 GTs online at different platforms with equal power sharing, 100MW wind with SVC/Statcom at PF1.

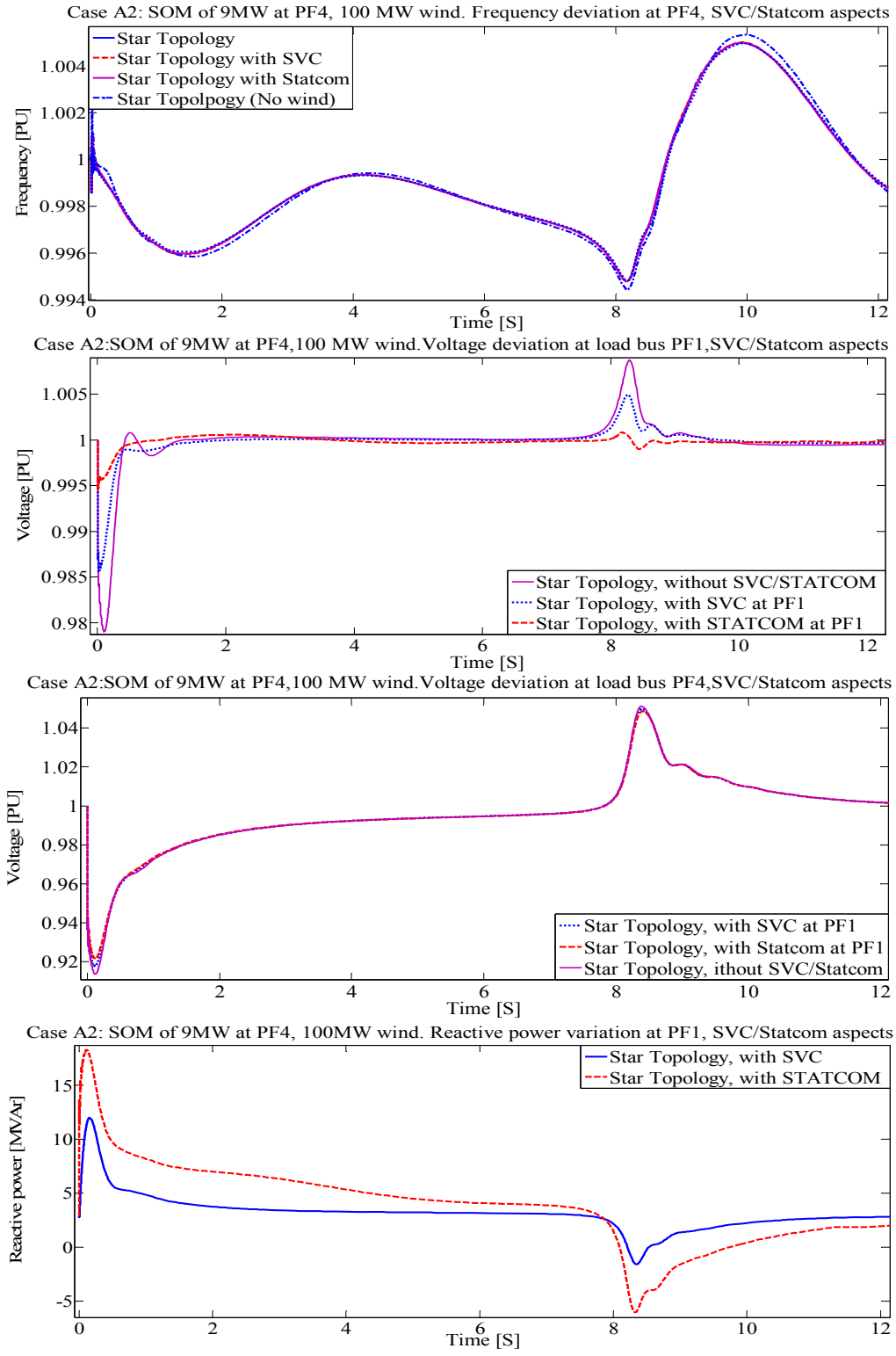

Figure 49: SVC/Statcom aspects : Voltage deviation, frequency variation and generator reactive power genenation variation due to statting of 9MW induaction motor, 100MW wind

6.4.1.3 36kV and 52kV voltage level comparison aspects for STAR topology

A1: Dynamic simulation – Start up of 9MW motor at PF4, 8 GTs running at different platforms with equal power sharing, no wind penetration with 36kV and 52kV system.

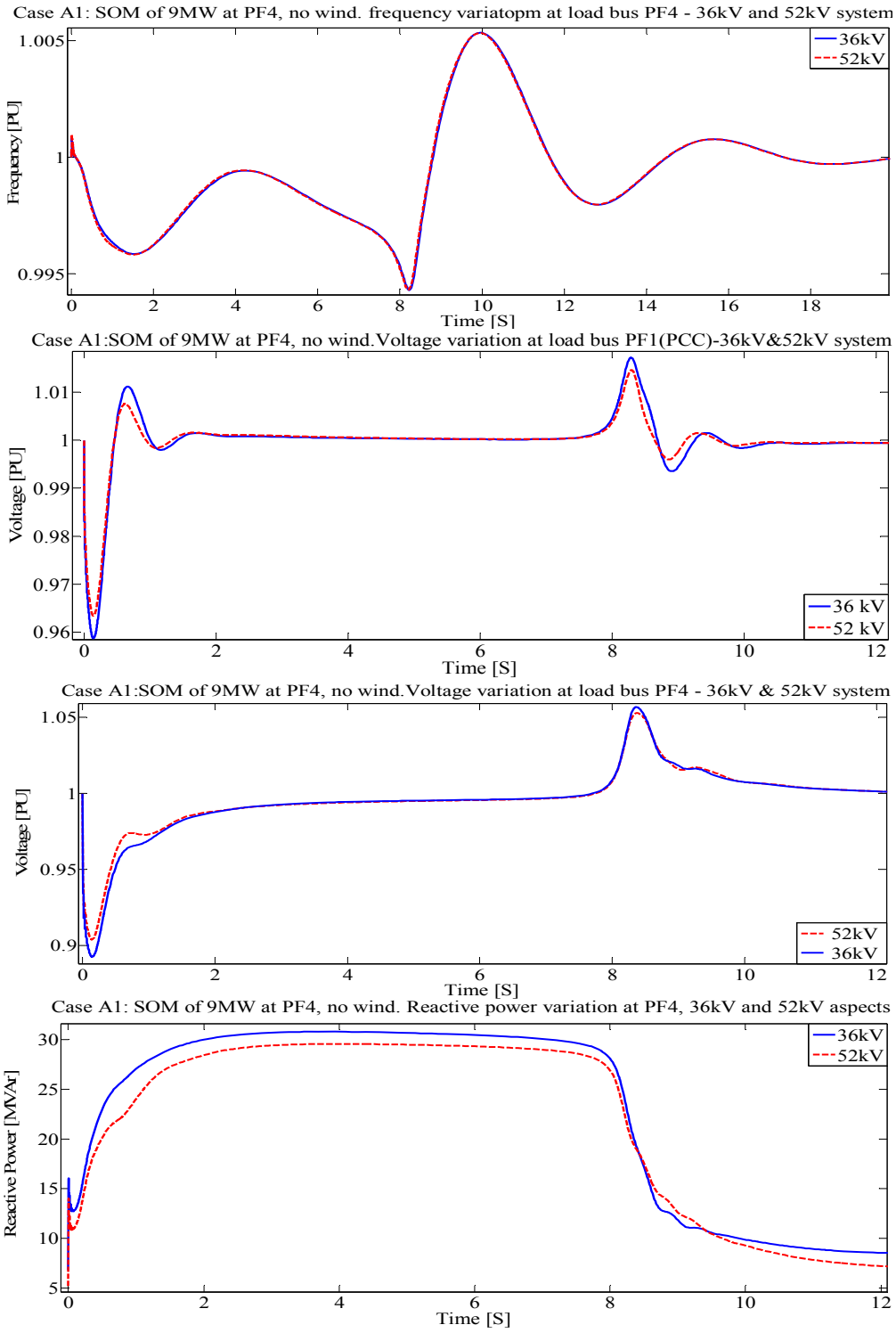

Figure 50: Voltage level aspects : Voltage deviation, frequency variation and generator reactive power genenation variation due to statting of 9MW induaction motor, no wind

A2: Dynamic simulation – Start up of 9MW motor at PF4, 8 GTs online at different platforms with equal power sharing, 100MW wind with 36kV and 52kV system aspects.

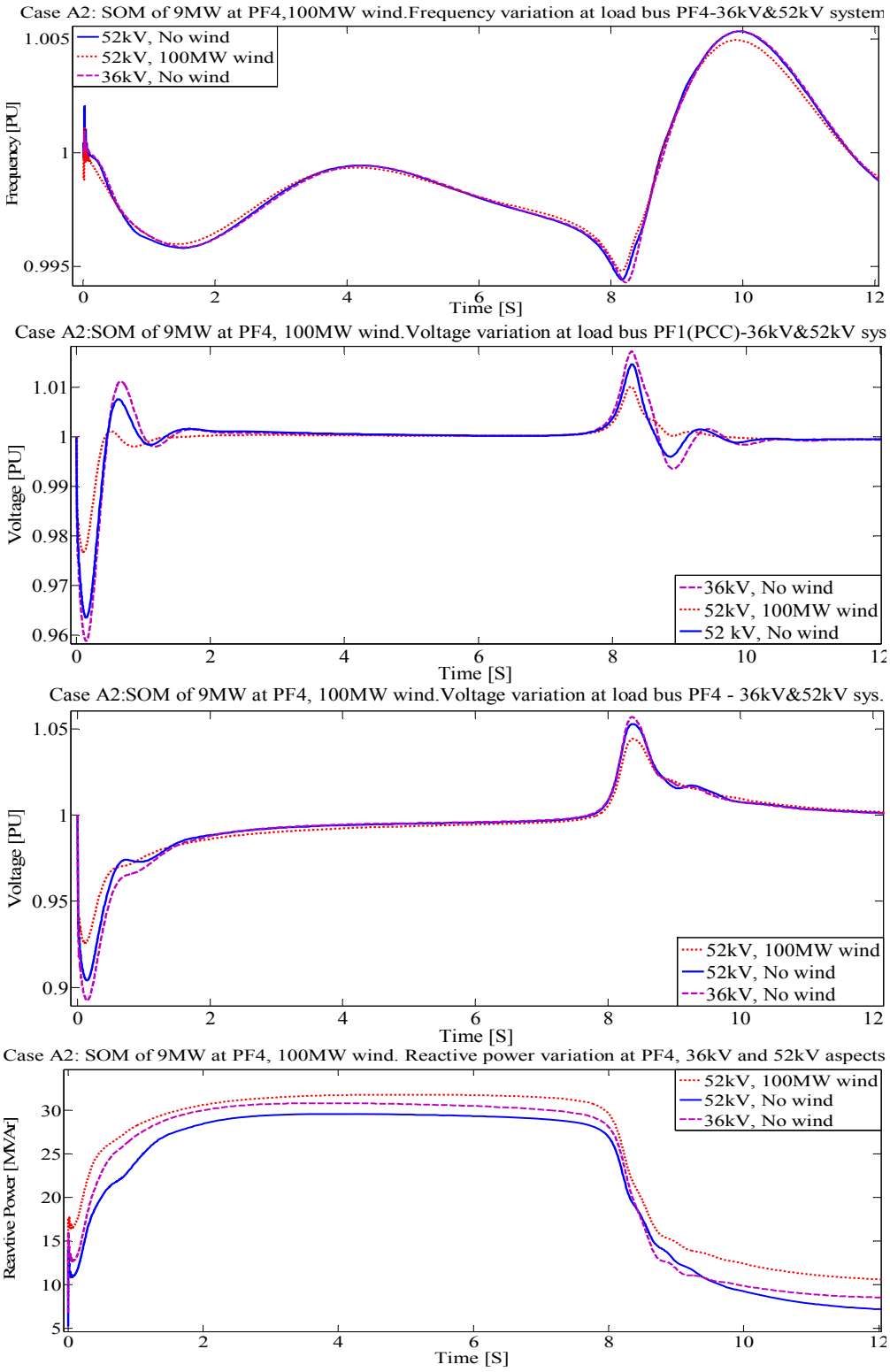

Figure 51: Voltage level aspects : Voltage deviation, frequency variation and generator reactive power genenation variation due to statting of 9MW induaction motor, 100MW wind

Dynamic analysis: Class A - Result summary and Discussion

Table 15:- Result summary table - Voltage and frequency deviation comparison, Class A

Aspects	Topologies		Frequency Variation at load bus PF4 Δf (%)		Voltage Deviation at load bus PF4 ΔV (%)	
			No Wind (A1)	Full Wind (A2)	No Wind (A1)	Full Wind (A2)
Single platform system (13.8kV) and Topology aspects comparison	Real Operational data (UNITECH, 2GT)		**0.83**	**-**	**13.1**	-
	Single Platform System (One GT online)		**5.5**	**3.20**	**24.0**	**16.0**
	Single Platform System (Two GT online)		2.5	1.25	15.0	10.0
	Star Topology		**0.54**	**0.54**	11.0	9.2
	Star-F Topology		**0.54**	**0.54**	9.5	7.5
	Mesh Topology		**0.54**	**0.54**	8.0	7.0
SVC and Statcom application aspects at PF1	Star Topology	Without	0.54	0.54	11.0	9.2
		With SVC	0.54	0.54	10.0	8.0
		With Statcom	0.54	0.54	**9.0**	**7.8**
36kV and 52kV level aspects	Star Topology	36kV level	0.54	0.54	11.0	9.2
		52kV level	0.54	0.54	**9.3**	**7.0**

Discussion and analysis:

Table 14 express importance of an integrated system of five platforms compared to single platform system of previous study [6] on starting of big induction motor. Frequency deviation (Δf) and voltage deviations (ΔV) are within permissible limit and following NORSOK standards - Table 2 even better way for integrated system. Single platform system, simulation results shows one GT online gives unstable operation of starting of 9MW motor with 24% of ΔV and 5.5% of Δf which are out of limits specified in Table 2. Thus at least two generators must be needed online to start-up such a big motor as also proven by UNITECH AS in chapter 4 for stable start-up of motor. As wind penetration gains, Δf remains stable but ΔV reduces implies more wind power penetration help to stabilize system. According to topology point of view mesh topology has lowest voltage deviation compared to two other. For star topology, STATCOM have better dynamic voltage control and dynamic system enhancement capability compared to SVC for same power ratings. Finally 52 kV system gives less ΔV effect then 36kV voltage level with more even transient behavior of voltage and power generated by different GTs on different platforms as shown in Figures 50 and 51. Hence 52kV could be better option for offshore power transmission system. Importance of wind penetration results in reduction of offshore platform online generation hence optimizes power balance through extra spinning reserve is the synergic aspects of integrated system.

6.4.2 Class B: Loss of a Gas Turbine (GT) at PF4, 9 GTs online with equal power sharing

B1: Loss of a GT at PF4, no wind

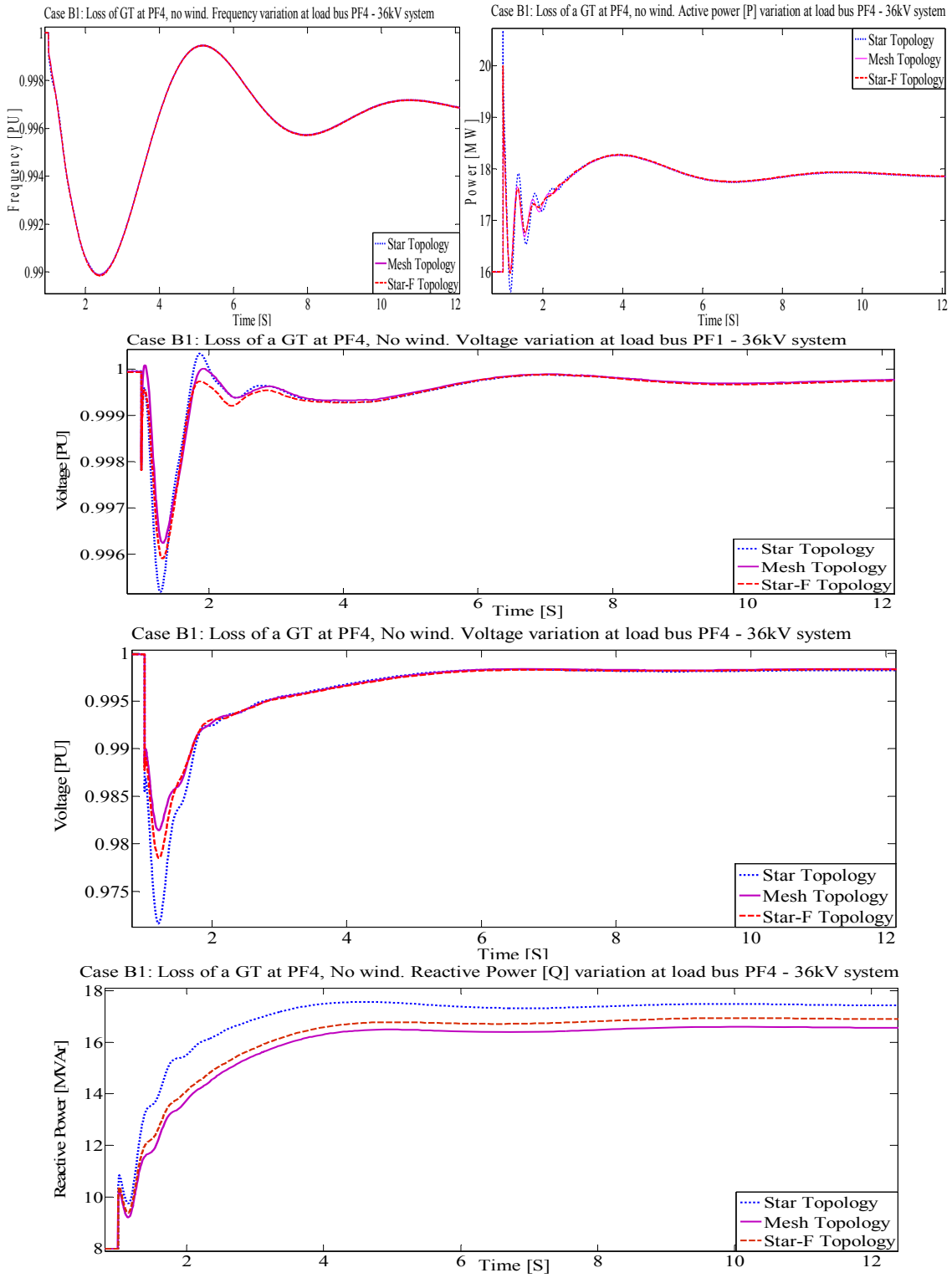

Figure 52: Topology aspets: Voltage deviation, frequency variation and effect on GTs active and reactive power genenation due loss of a GT, no wind

B2: Loss of a GT at PF4, 100MW wind

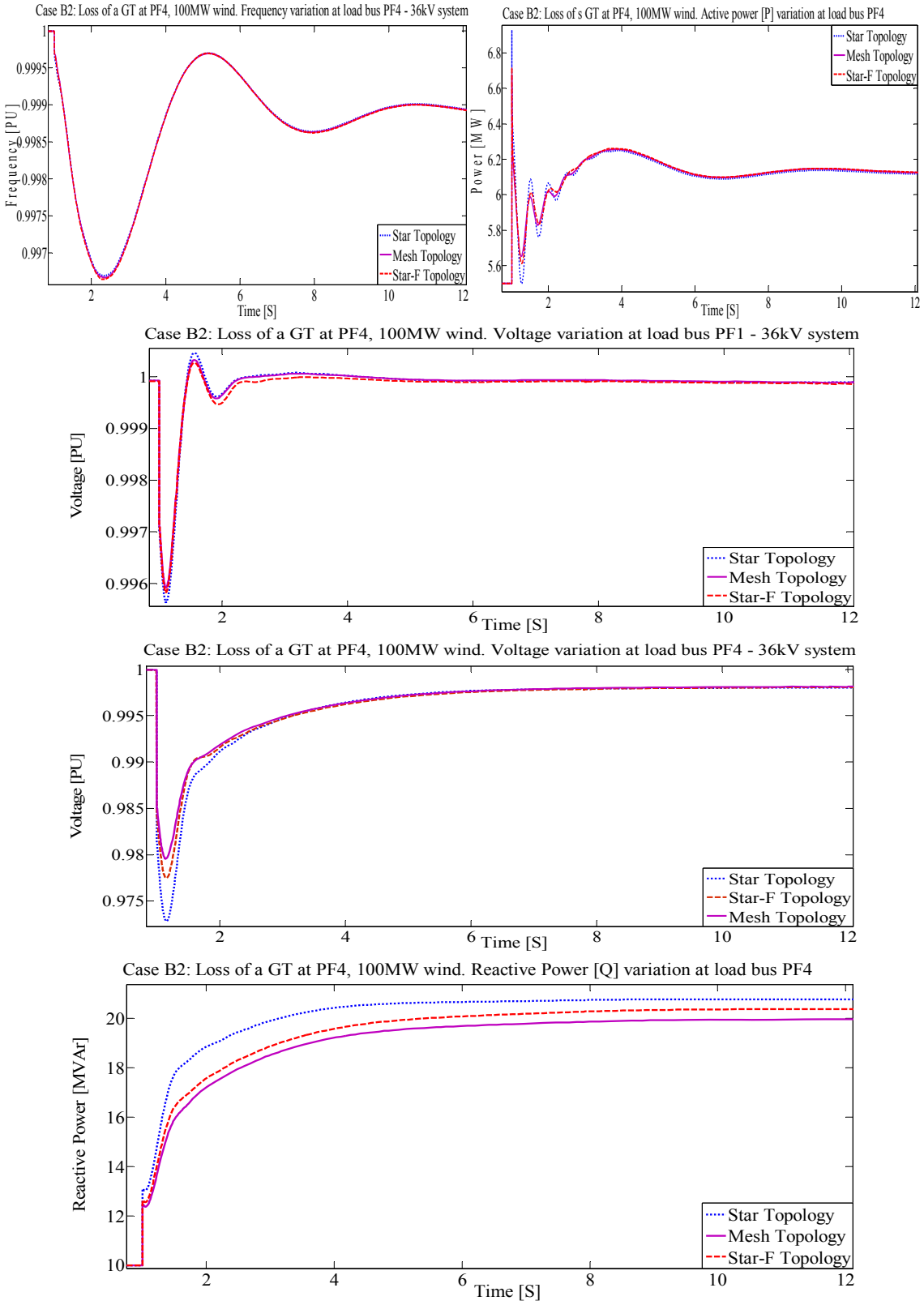

Figure 53: Topology aspets: Voltage deviation, frequency variation and effect on GTs active and reactive power genenation due loss of a GT, 100MW wind

Dynamic analysis: Class B - Result comparison

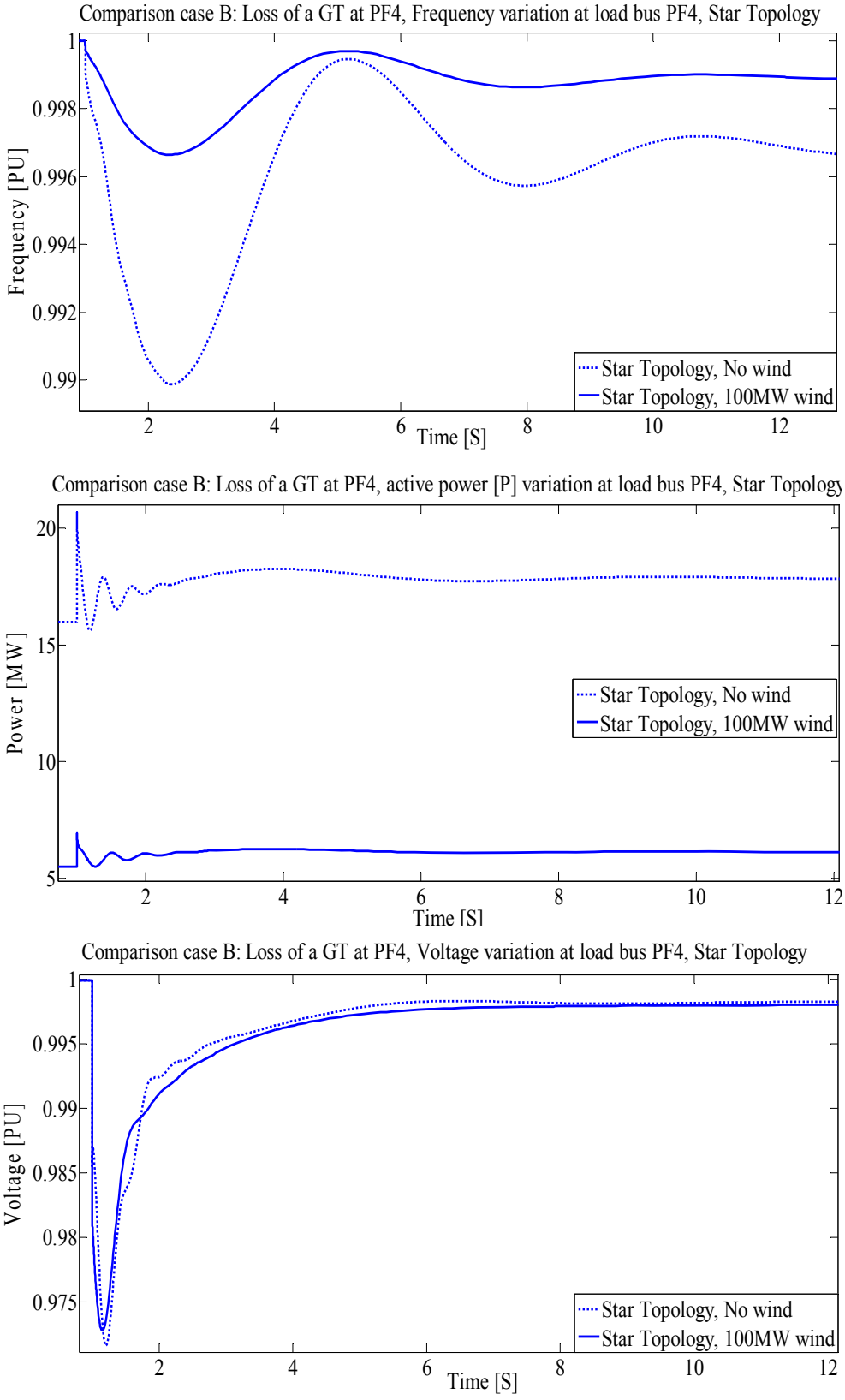

Figure 54: Frequency variation and voltage deviation due to loss of a GT at PF4

6.4.3 Class C: Loss of a wind power at PCC, 8 GTs online with equal power sharing

C1: Loss of 25% (25MW) wind power, 8 GTs in operation

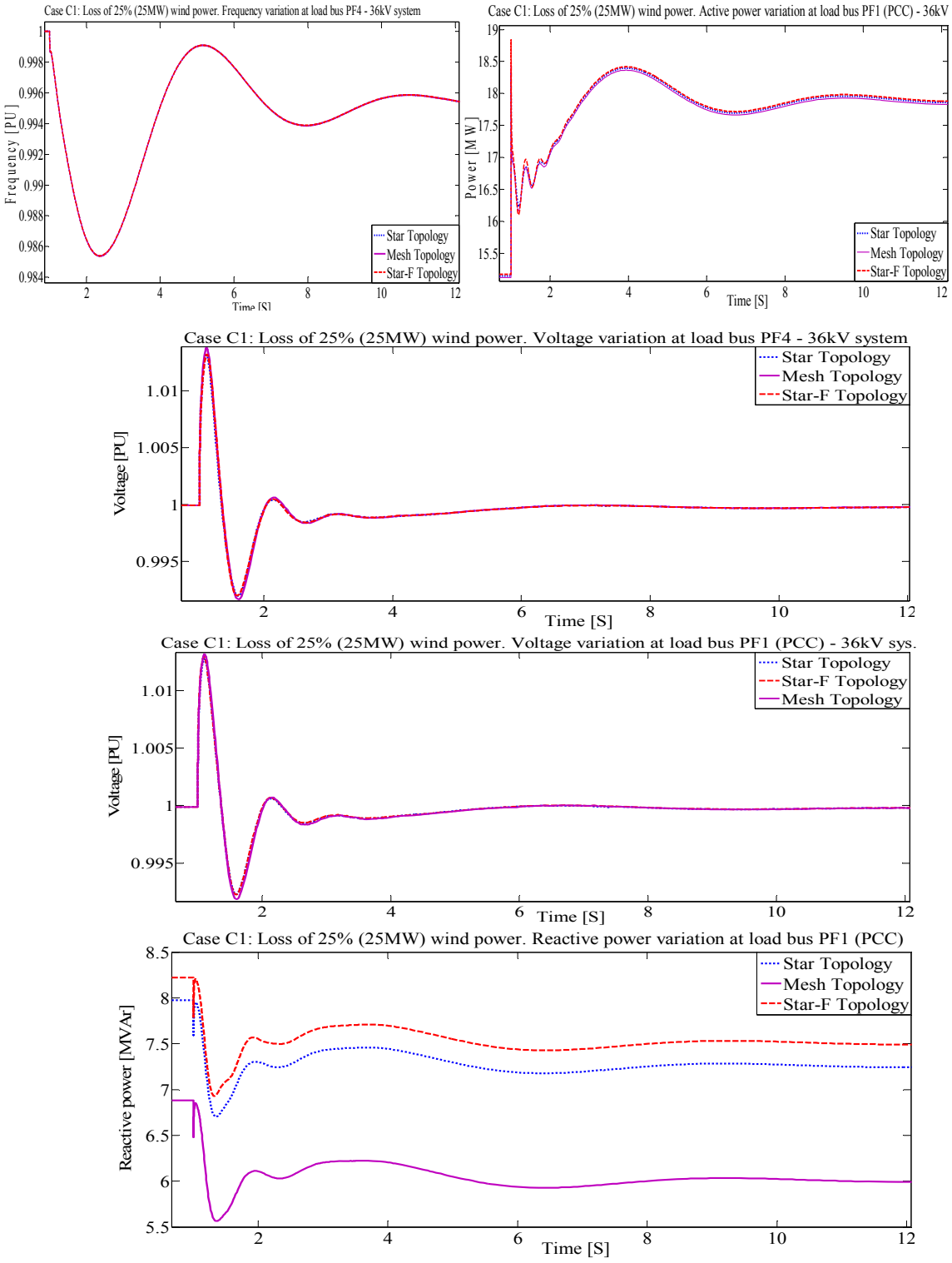

Figure 55: Topology aspets: Voltage deviation, frequency variation and effect on Gen's active and reactive power genenation due loss of a 25% wind power

C2: Loss of 50% (50MW) wind power, 8 GTs in operation

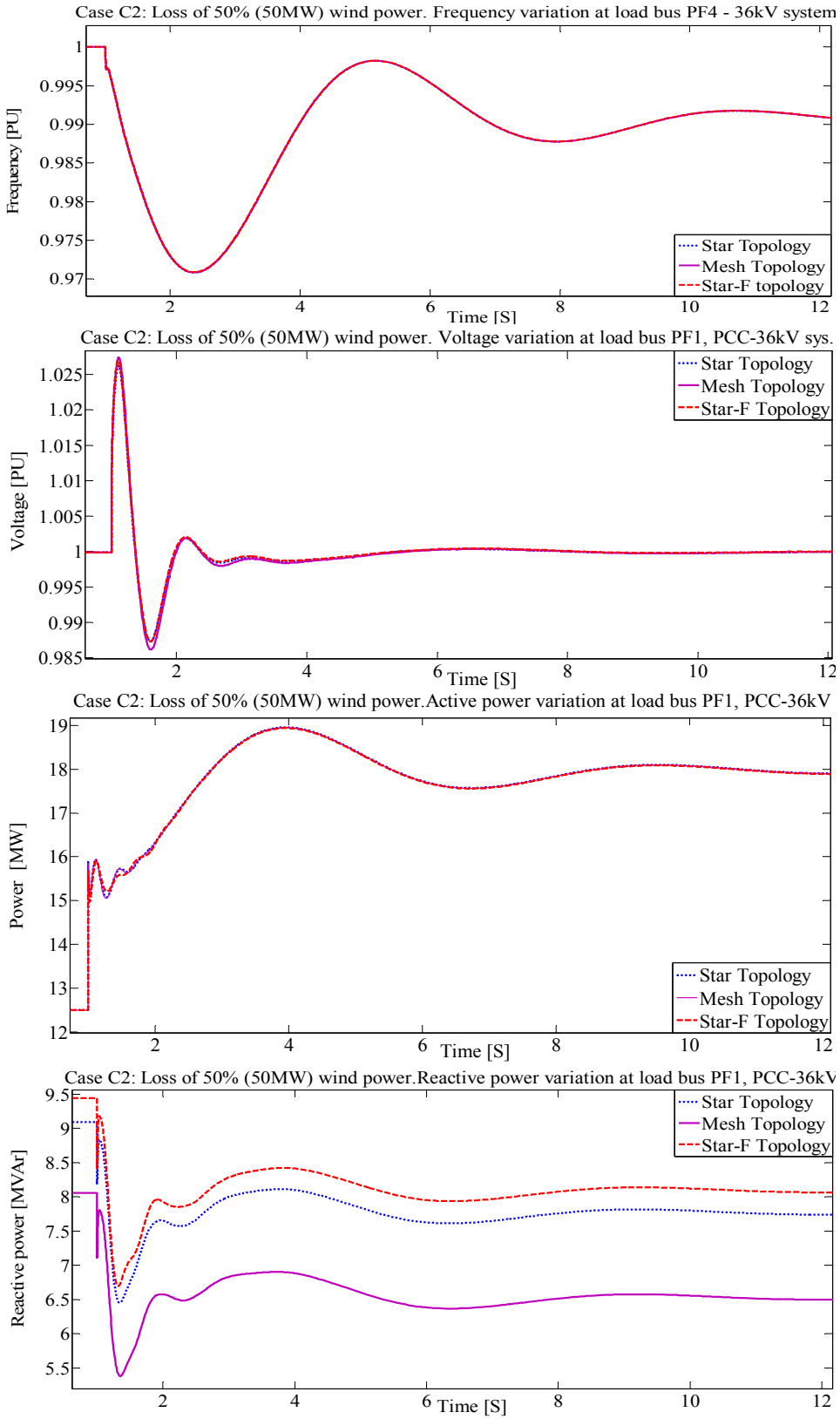

Figure 56: Topology aspets: Voltage deviation, frequency variation and effect on Gen's active and reactive power genenation due loss of a 50% wind power

C3: Loss of 100% (100MW) wind power, 8 GTs in operation

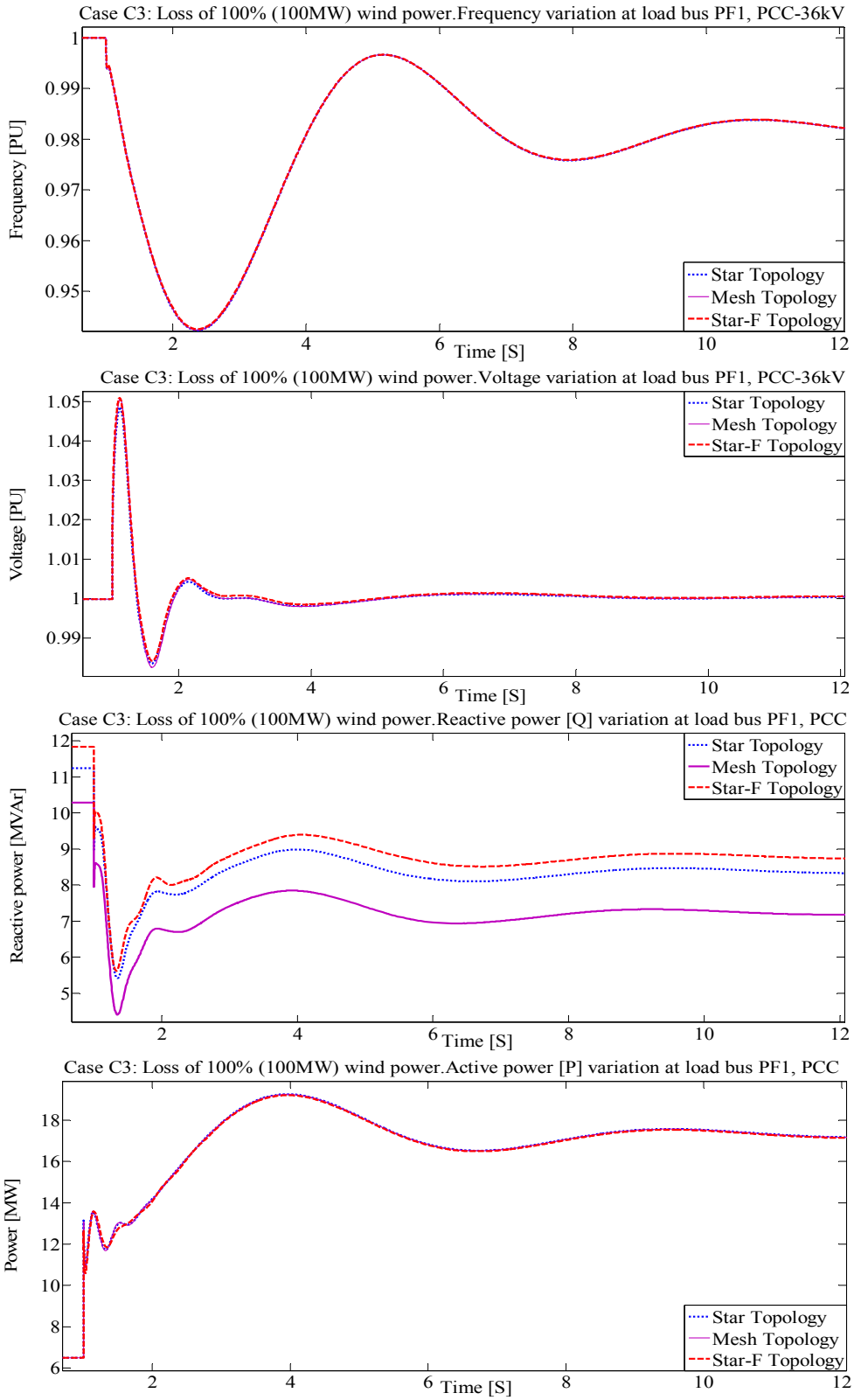

Figure 57: Topology aspets: Voltage deviation, frequency variation and effect on Gen's active and reactive power genenation due loss of a 100 % wind power

Dynamic analysis: Class C - Result comparison

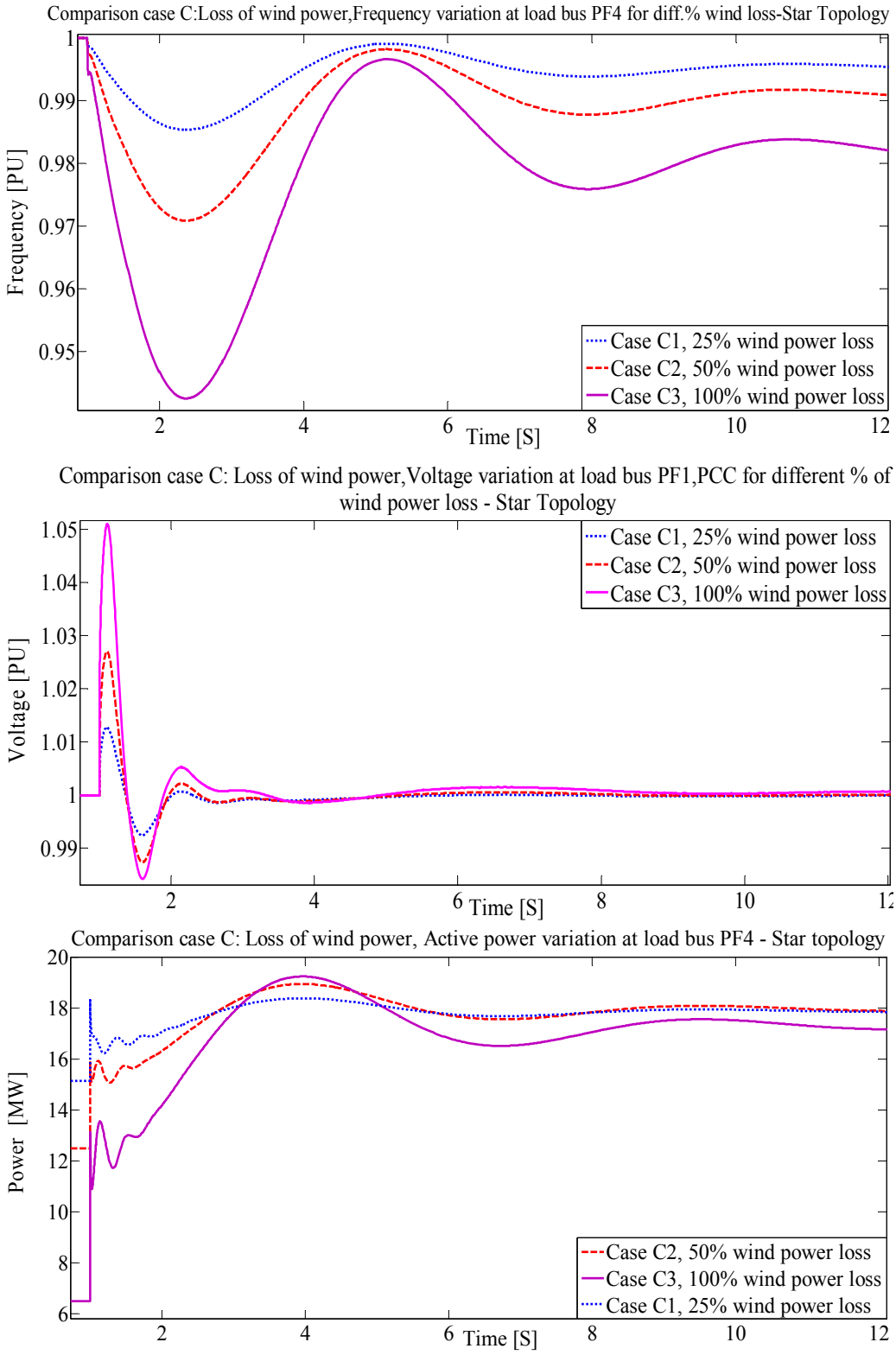

Figure 58: Frequency variation, voltage deviation and power contribution due to loss of different % of wind power at PCC

6.4.4 Class D: Loss of interconnection cable between PF1 (PCC) and PF4, topology aspects with different % wind power penetration

D1: Loss of interconnection cable between PF1 (PCC) and PF4, 50MW wind penetration

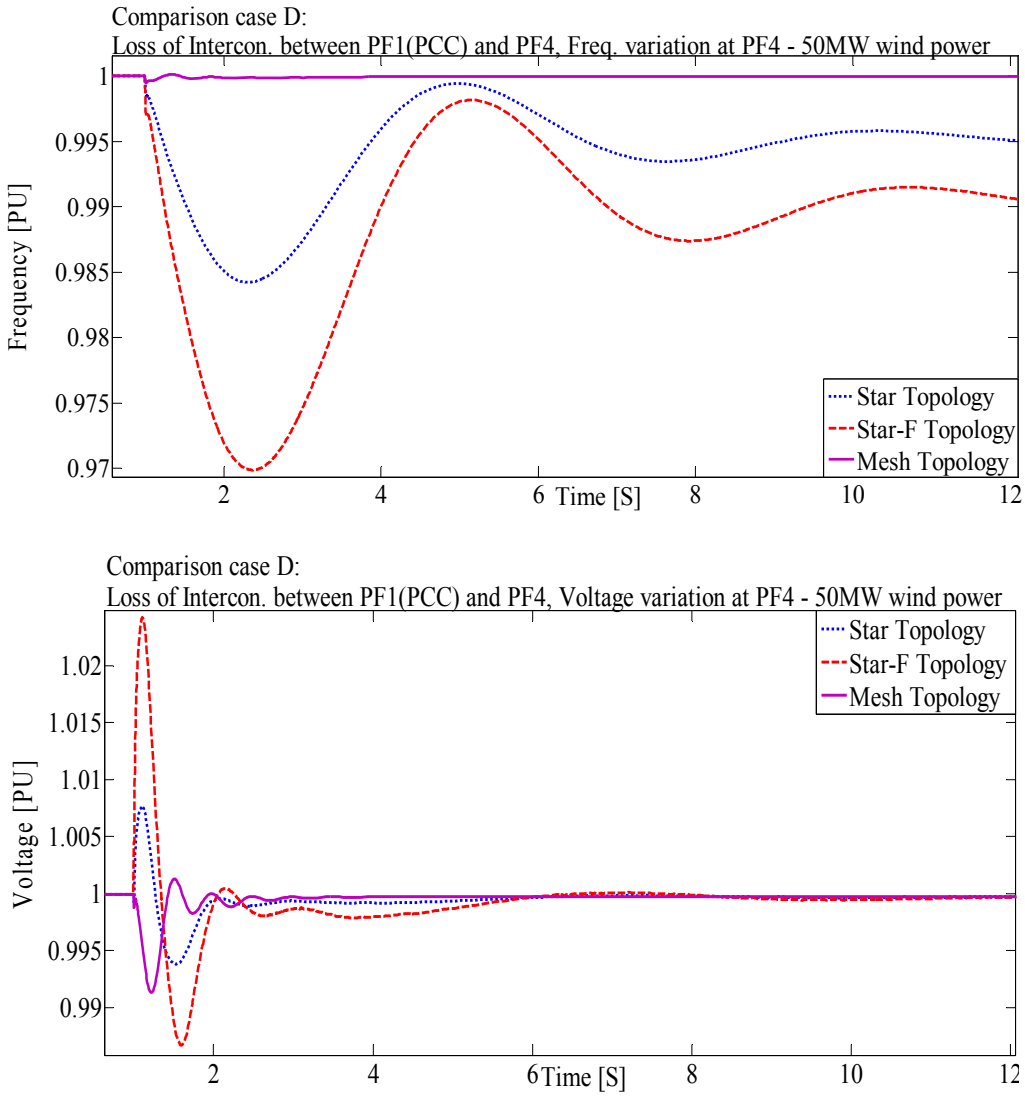

Figure 59: Topology aspets: Frequency deviation and voltage variation due loss of interconnecting cable between PF1 (PCC) and PF4, 50MW wind penetration

D2: Loss of interconnection between PF1 (PCC) and PF4, 100MW wind penetration

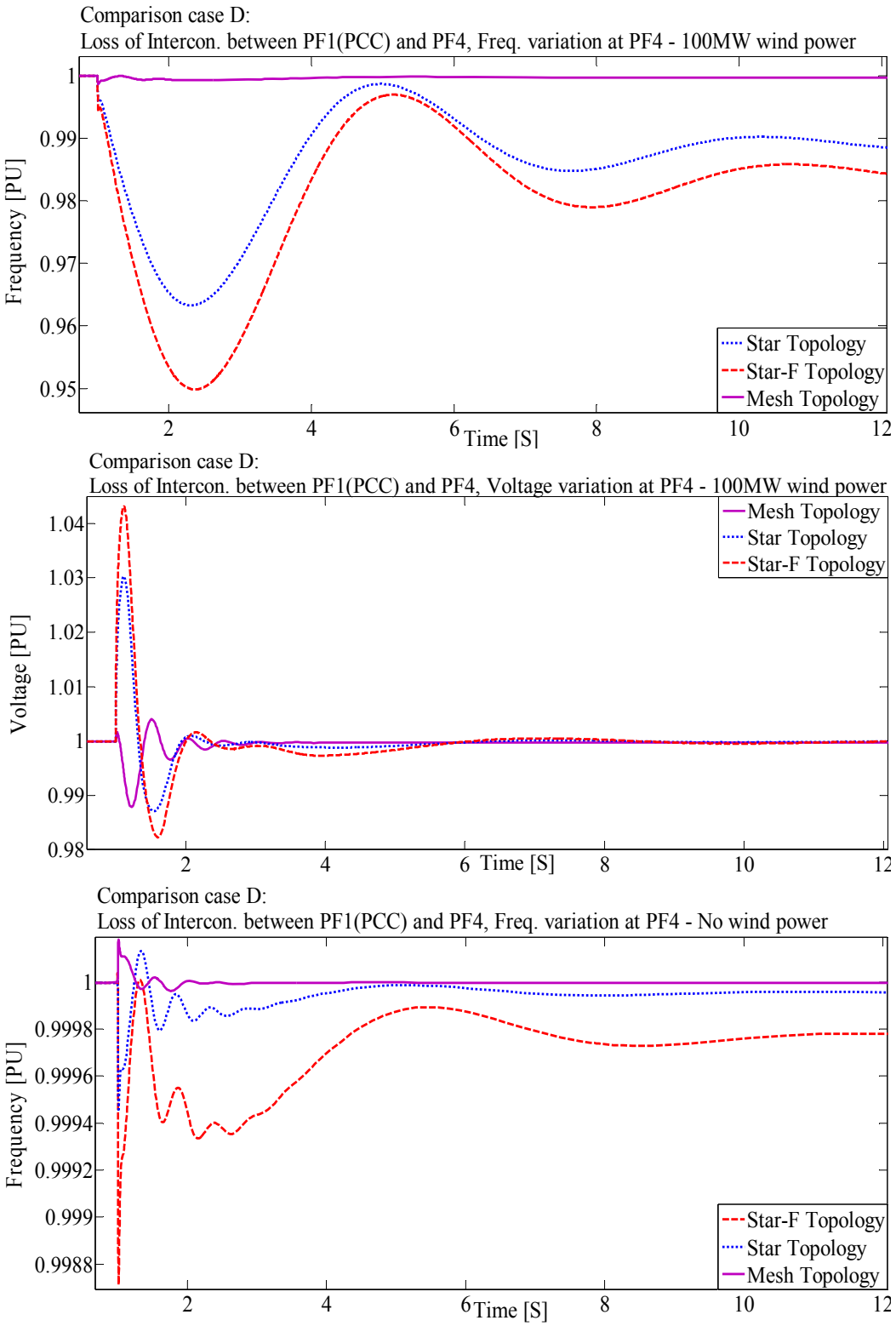

Figure 60: Topology aspets: Frequency deviation and voltage variation due loss of interconnecting cable between PF1 (PCC) and PF4, 50MW wind penetration

Dynamic analysis: Class D - Result comparison

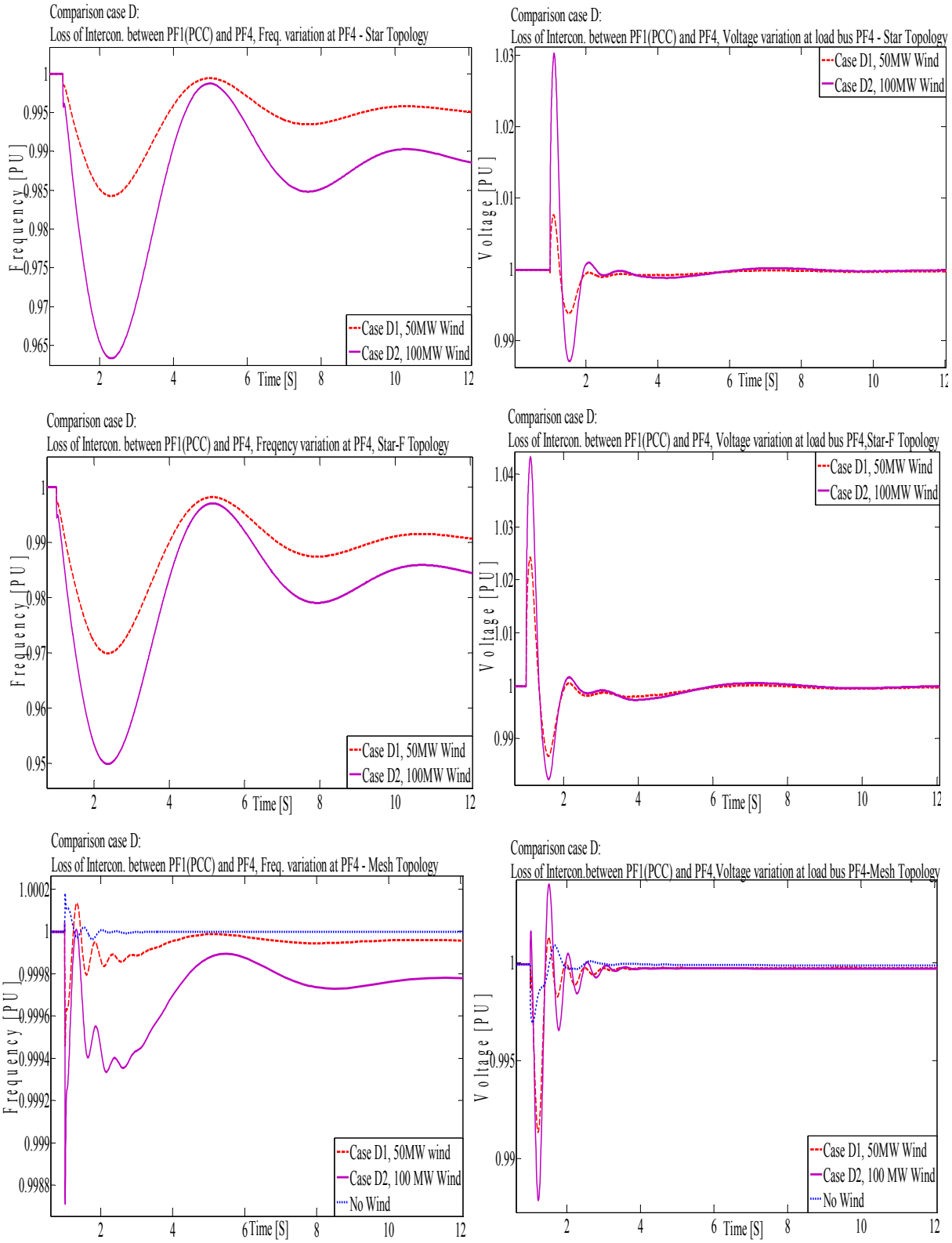

Figure 61: Frequency variation and voltage deviation at load bus PF4 due to loss of interconecation for different topology aspects

Dynamic analysis: Class B, C and D - Result summary and Discussion

Table 16:- Summary table - Voltage and frequency deviation comparison, Class B, C and D

Case and Type		Frequency Deviation at load bus PF4 ΔF (%)			Voltage Deviation at load bus PF4 ΔV (%)		
		No wind	Full Wind		No wind	Full Wind	
Case B (Loss of GT)	Star	1.0	0.35		2.9	2.7	
	Star-F	1.0	0.35		2.4	2.4	
	Mesh	1.0	0.35		**2.0**	**1.5**	
		25MW Wind	50MW Wind	100MW Wind	25MW Wind*	50MW Wind*	100MW Wind*
Case C (Loss of Wind)	Star	1.5	2.9	**5.7**	1.25	2.0	5.0
	Star-F	1.5	2.9	**5.7**	1.25	2.0	5.0
	Mesh	1.5	2.9	**5.7**	1.25	2.0	5.0
		50MW wind	100MW Wind		50MW Wind	100MW Wind	
Case D (Loss of Intercon.)	Star	1.5	3.7		0.75	3.0	
	Star-F	3.0	5.0		2.5	4.5	
	Mesh	**0.04**	**0.13**		**0.07**	**1.0**	

- * Voltage deviation at load bus PF1 (PCC) is considered since wind loss at that bus.

Discussion and analysis:

Table 16 shows, loss of large amount of wind power is most critical case compared to fewer amounts of wind power. Loss of 100MW wind power at a time gives unstable system with frequency deviation of 5.7% which is not acceptable as specified in Table 2 and gives indication regarding how much max. Wind power possible to integrate in the system. Meanwhile increases of percentage loss of wind power also increases voltage deviation but within permissible limit. High wind penetration has a diminishing effect in frequency and voltage deviation in case of loss of Gas turbine compared to no wind penetration. It can also be seen that loss of a GT from system is not so critical event as loss of wind power hence depends on how much amount of power loss occurs for particular events. One important point to notice for different topology aspects, wind power penetration or loss has no effect on frequency deviation and a fewer effect on voltage deviation for particular topology. Loss of interconnection between two platforms PF1 and PF4 is most critical event when large amount of power from wind farm is in operation. Overall Mesh topology have a best performance compared to other two topologies in case of wind power loss, generation loss at platform or loss of interconnection due to higher possibility of power transfer capability. Mesh topology gives better power supply security and less loss of load in case of loss of cables by stabilizing system more efficiently owing to rapid flow of power from adjacent generating source.

7 CONCLUSION AND FURTHER WORK

This thesis work investigates the electric grid stability, reliability and security of an offshore isolated system integration of radial wind farm of 100MW to five offshore platforms as an "off grid" system with the help of static power flow and dynamic simulation analysis for different perturbation events. Main aspects of study include different system topologies, different percentage of wind power penetration and wind power loss in the system.

7.1 Conclusions

The importance of an interconnecting grid system is seen from cases A1, A2 and as specified in Table 15, where starting of a big induction motor is found not to give large frequency or voltage deviations compared to a previous study of a single platform system. The system copes well with the platform's power demand being met by increased output from gas turbines on neighboring platforms. This is an important and significant contribution of the integrated grid system. Voltage deviation is the most critical in the case of staring of big motor events compared to other perturbation events. It can also be concluded that the meshed network topology provides the overall best performace.

As expected, the loss of wind power was found to be more critical when more wind power was initially present in the system. This means that the most critical loss-of-production scenarios are the ones with sudden loss of large amount of wind power. An increasing amount of loss of wind power were analysed in the cases C1, C2 and C3. The most critical case C3 with 100% sudden loss of wind power gave unacceptable frequency deviation.

From the assessment of two different voltage levels at 36kV and 52kV, including analyses of perturbation events such as starting of a big induction motor, it can be concluded that the 52 kV network system gives better dynamic stability behaviour compared to the other one. The study showed that with 52kV the network losses was lower than with 36kV and it gives less voltage and frequency deviations at transient events. For the same study it can also be concluded that FACTS devices like SVC and STATCOM provide better voltage controllability and hence improved power transfer capability of the system. In addition STATCOM is more efficient than SVC due to its better reactive power compensation capability at lower voltages. The STATCOM is thus able to improve the power transmission capability for the same power rating.

Finaly, it can also be concluded that a meshed network topology have better performance and show less volage and frequency deviations compared to the other two (radial) topologies and

gives better power supply security and less loss of load for all kind of perturbation events included in this study.

7.2 Further work

The system could be connected to the onshore existed grid through either HVAC or HVDC cables transmission system. This opens for a broad range of new simulation cases, where the gas turbine has reduced size or can be removed. The land-connection system will further decrease CO2- emissions and getting toward commitment.

The different system topology, different voltage level study included in this work is based on technical aspects only. It is also important and interesting to consider economical as well as compactness-space volume relevant aspects for offshore applciations. Frequency control and spinning reserve on wind farm side are also important aspects need to be investigated. Based on wind power NORSOK standards, maximum wind power penetarion possible to integrate in the system is also important point to be considered for further study.

The simulation model SIMPOW is less detailed; it would be more realistic to run system with detailed parameter control software which has higher range of system control and so no need for the extensive use of aggregation model and basic limitations. A laboratory setup can also be developed to verify the simulations and make the results more reliable.

REFERENCES

1. UNFCCC. *Kyoto - Protocol, Japan* 1997; Available from: http://en.wikipedia.org/wiki/Kyoto_Protocol#cite_note-unfccc2005-0.
2. *Klimakur 2020 - sektoriell tiltaksanalyse petroleumssektoren*. 2010, Klima og forurensingsdirektoratet, Oljedirektoratet, NVE & Petroleumstilsynet.
3. Bartels, M., et al., *Planning of the grid integration of wind energy in Germany onshore and offshore up to the year 2020.* International Journal of Global Energy Issues, 2006. **25**(Copyright 2006, The Institution of Engineering and Technology): p. 257-75.
4. Oljedirektoratet, et al., *Kraft fra land til norsk sokkel*. Januar 2008: Oslo.
5. Norway, *Floating Wind Turbine - Hywind*. 2009.
6. He, W., et al., *The potential of integrating wind power with offshore oil and gas platforms.* Wind Engineering, 2010. **34**(Compendex): p. 125-137.
7. Xu, L. and S. Islam. *Reliability Issues of Offshore Wind Farm Topology*. in *Probabilistic Methods Applied to Power Systems, 2008. PMAPS '08. Proceedings of the 10th International Conference on*. 2008.
8. NORSOK, *NORSOK Standard E-001 Electrical systems, 5th ed. Standards Norway,July 2007.*
9. Manwell, J.F., ed. *Wind Energy Explained Theory Design and Application*. 2002, John Wiley & Sons Ltd.
10. Ackermann, T. and R.I.o. Technology, eds. *Wind Power in Power Systems*. 2005, John Wiley & Sons, Ltd,: Stockholm, Sweden.
11. Nordel. *Code* Available from: www.nordel.org.
12. CODE, G. *Nordic grid code 2007* Available from: www.nordel.org.
13. Statnett, *Statnett, FIKS – "Funksjonskrav i kraftsystemet",*.
14. *IEC 61892-1 , Mobile and fixed offshore units – Electrical installations – Part 1: General requirements and conditions, Edition 2.0*. 2010, IEC.
15. Yao, L. (CIGRE 2008) *Large Offshore Wind Farm Grid Integration - Challenges & Solutions*.
16. IEEE/CIGRE Work Group on Stability Terms and Definitions, D.a.C.o. and M. Power System Stability".
17. Kundur, P., *Power System Stability and Control*. 1994, McGraw-Hill, Inc.

18. Gyugyi, L., *Power electronics in electric utilities: static VAR compensators.* Proceedings of the IEEE, 1988. **76**(Copyright 1988, IEE): p. 483-94.
19. Padiyar, K.R., ed. *FACTS Controllers In Power Transmission and Distribution*. 2007, New Age International (P) Ltd., Publishers: New Delhi.
20. Gyugyi, L., *Dynamic compensation of AC transmission lines by solid-state synchronous voltage sources.* IEEE Transactions on Power Delivery, 1994. **9**(Compendex): p. 904-911.
21. Energy, M.o.P.a., *"Ministry of Petroleum and Energy" - FACTS: The Norwegian Petroleum Sector. 2010.* . 2010.
22. Statoil, *Information, Platform Producation & Power consumption - Statoil*. 2011.
23. Bresesti, P., et al., *HVDC Connection of Offshore Wind Farms to the Transmission System.* Energy Conversion, IEEE Transactions on, 2007. **22**(1): p. 37-43.
24. Machowski, J., ed. *J. Machowski, J. W. Bialek, J. R. Bumby, Power System Dynamics and Stability, John Wiley & Sons Ltd, 1997*. 1997.
25. UNITECH, *Power System Measurements at Oseberg C - Star up of 9MW Gas Injecation Compressor EE-26004-C*. Aug - 2003: UNITECH-Stavanger.
26. UNITECH, *Why, When and How to Perform Industrial Power System (IPS) Dynamic Studies*. 1999.
27. UNITECH, *Unitech Power System, "Overall System Design", Industrial Power System design course - as if operation really matteted.* December 1999.
28. SIMPOW, *STRI AB, SIMPOW User Manual 11.0. 2008.* .
29. Robbins, M.U.a., ed. *Power Electronics Converters, Applications and Design.* Third ed., ed. T. Edition. 2007, John Wiley & Sons, New York.
30. Bystøl, T.B., *"Stabilitetsporblemer i distribusjonsnett med lokal kraftproduksjon." NTNU, 2007*. 2007.
31. T. Toftevaag, E.J., and A. Petterteig, *"The influence of impedance values andexcitation system tuning on synchronous generators' stability in distribution grids," Norway: 2008.* 2008.
32. ABB, *ABB - XLPE User's guide Rev.02*. 2010.
33. ABB, *XLPE Submarine Cable Systems - Attachment to XLPE Cable Systems - User´s guide.* 2010.
34. *Planleggingsbok for kraftnett, bind III, kapittel 5*. (Updated 2003) ed. 1993: SINTEF.

PAPER:

Integration of offshore wind farm with multiple oil and gas platforms

Harald G Svendsen*, Eirik Veirød Øyslebø*, Maheshkumar Hadiya†, and Kjetil Uhlen†
*SINTEF Energy Research, Trondheim, Norway
†Norwegian University of Science and Technology, Trondheim, Norway

***Abstract*—This paper discusses power stability and control issues for an isolated offshore system consisting of a wind farm and five oil and gas platforms.**

I. Introduction

In response to global warming and as part of international commitments, Norway has defined targets for reduction of CO_2 emissions in the coming years. Although Norwegian electric power supply is dominated by hydro power, the offshore petroleum installations largely rely on fossil fuels for their power demand. Hence, an electrification of oil and gas platforms has been identified as a priority.

An alternative to electrification via cables from land [1], [2], [3] is to connect offshore petroleum installations directly to offshore power production [4], [5], [6], [7] with or without connection to land. The most realistic candidate for offshore renewable power production is currently an offshore wind farm. Such an offshore platform/wind farm combination represents a potential good match for the offshore petroleum sector's desire for renewable energy with the offshore wind power industry's desire for an early market.

This is the motivation for the current study, which investigates the platform/wind farm alternative through a case study analysis. The goal of the study is to address control and stability issues in broad terms.

The work presented has been done within the Norwegian Research Centre for Offshore Wind Technology (NOWITECH).

II. The case study

The study focuses on power control and stability for an isolated offshore system consisting of five platforms interconnected with each other and with an offshore wind farm, see figure 1. The wind farm capacity is taken to be 100 MW, and the active power demand on the platforms adds up to 147 MW, i.e. the wind farm capacity is less, but of comparable size to the total load.

Frequency and voltage variations are in this study assessed based on the maximum allowable limits defined by the NORSOK E-001 [8] and IEC 61892-1 [9] standards for offshore AC distribution systems. (NORSOK refers to edition 1 of the IEC standard, but a second edition has recently been published.) It should be emphasised that the NORSOK limits are guidelines and that platform operators may impose stricter power stability requirements.

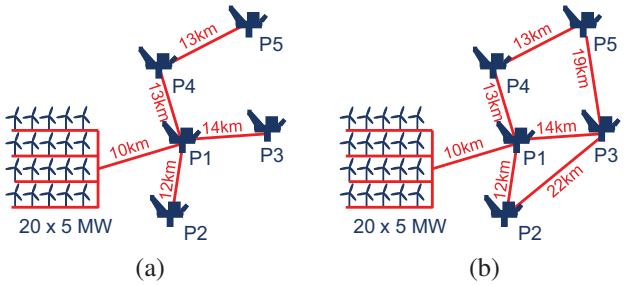

Figure 1. Layout of case study model: a) star topology, b) meshed topology.

A. Single platform

A previous study [5] has investigated the integration of a smaller wind farm (4×5 MW) connected to a single platform, with emphasis on power stability and fuel and emission reductions on the platform.

In terms of transient stability, that study found the largest voltage deviations for direct online start-up of the largest motor ($\Delta U = 18\%$, $\Delta f = 5.1\%$) and the largest frequency deviations for loss of wind farm (producing at 50% of capacity) combined with load shedding ($\Delta U = 2\%$, $\Delta f = 7.3\%$). The inclusion of wind power was observed to give reduced voltage deviations during motor start-up, due to the connected conventional generator being de-loaded by the amount of wind power produced. Compared with limits for transient deviations set by NORSOK standards, see table II, it is evident that the voltage deviations are within the allowable range, but frequency deviations are not. Sudden fall-out of the wind farm as a worst case scenario was then simulated for different operating conditions to identify the maximum permissible wind power penetration that would give transient deviations within the NORSOK limits.

The study also investigated reduction of fuel use and CO_2/NO_x emissions as a result of the wind power integration, and found an overall reduction of about 40%. In the present multi-platform case, we expect similar reductions, although this has not been explicitly investigated.

B. Multiple platforms

The interconnection of multiple platforms with a wind farm as a an isolatated system introduces new challenges related to topology of interconnecting grid and control strategy, that have hitherto not been analysed. Two central questions are addressed by this study:

Table I
POWER DEMAND AND GENERATION CAPACITY ON PLATFORMS

Platform	Demand	Generation capacity
P1	25 MW	28.75 MVA $\times 2$
P2	34 MW	28.75 MVA $\times 2$
P3	30 MW	28.75 MVA $\times 2$
P4	34 MW	28.75 MVA $\times 2$
P5	24 MW	28.75 MVA $\times 2$

- What is the best way to interconnect such a system?
- How does the interconnecting grid affect voltage and frequency stability?

The present case study investigates these questions from a technical point of view through steady state power flow analysis for a number of operational states, and through analysis of transient behaviour via dynamic simulations of a number of disturbances.

An important motivation for considering interconnection of oil and gas platforms is that it enables a more flexible and fuel efficient operation of the gas turbines, whilst maintaining the same (or better) power supply security level. Moreover, for integration of a large wind farm it is a pre-requisite that multiple platforms are interconnected in order to get a good match between power demand and wind farm capacity.

The interconnected platforms are thought of as existing platforms that today rely on gas turbines for their power supply and control. It is therefore assumed that multiple gas turbines are present at each platforms also in the interconnected system.

The system is illustrated in figure 1, with the two different grid topologies considered in this paper. The power demand and generation capacity on each platform is indicated in table I.

C. Operational benefits of interconnected system

Due to severe consequence in case of power failure, oil and gas platforms tend to have high power security requirements. This typically involves having an online backup gas turbine large enough to provide power supply if another gas turbine fails. For five isolated platforms, therefore, five online backup gas turbines are required. Since the efficiency of gas turbines drops when the output is reduced, this necessarily gives sub-optimal operation from a narrow fuel and emissions point of view.

By interconnecting the system the overall efficiency can be increased since the same power security can be maintained with less backup generation capacity. This has both economic and environmental benefits. The integration of a large wind farm in the system gives additional benefits as fuel is further reduced, as mentioned in section II-A. However, due to the variability of wind power and the increased system complexity, this comes with added challenges regarding security of supply and power stability.

What determines how many gas turbines must be online, is the requirement that at any time, the online gas turbine capacity must be large enough that the system can cope with natural variations in demand and supply and with single (designed-for) contingencies ($N-1$ criterion), i.e. operate satisfactory during

- Failure of a gas turbine generator
- Fall-out of a cable or transformer
- Wind power variations (rapid drop of wind speed)
- Demand variations (e.g. motor start-up)

The worst case scenario with loss of power is the fall-out of the connection to the wind farm in situations when it produces at full power, i.e. 100 MW. For comparison, failure of a single gas turbine represents loss of maximum about 25 MW. If the wind farm is connected via a single transformer/cable, this implies an online backup power requirement of 100 MW. If, on the other hand, the wind farm is connected with with dual transformer/cable, the worst case sudden loss of wind power is significantly less dramatic. Typically, the worst case would now be the loss of a wind farm feeder, with a maximum power loss depending on the internal wind farm layout. In this study the wind farm is modelled as four feeders with 25 MW capacity on each.

These security considerations have been kept in mind in the simulations presented in this paper, but a thorough reliability analysis is part of planned future work. A further investigation of the economic benefits of such an interconnected system with wind integration is also left for future work, as this paper focusses on technical aspects only.

Two different grid topologies for the interconnecting grid have been considered in this study. These are referred to as the star topology and the meshed topology, as illustrated in figure 1. The star topology represents the *minimum cable* alternative, whilst the meshed topology is an alternative with increased security where all platforms have at least two connections to other platforms.

D. Simulation model

A simulation model that represents the system shown in figure 1 has been established using SIMPOW [10]. It includes a detailed model for the platforms based on previous work [5], and a detailed wind farm model based on the standard full power converter wind turbine (FPCWT) model included in SIMPOW. A high voltage AC grid interconnects the platforms and the wind farm. A simplified single-line diagram of the model (for the star topology) is shown in figure 2.

The five platforms are all represented using the same 100 bus model. This model is based on an actual platform that is today in operation as an isolated system, with main power supply voltage at 13.8 kV and frequency of 60 Hz. Each platform has multiple gas turbines that may or may not be in operation. The power demand is mainly due to pumps driven by induction motors. Although the five platforms are represented with the same model, they can be assigned different demand and generation by adjusting parameters or connecting/disconnecting components. As mentioned previously, it is assumed in this study that the wind farm and the interconnecting grid is connected to existing platforms, such that each platform has sufficient gas power generation capacity to be self reliant (including backup capacity).

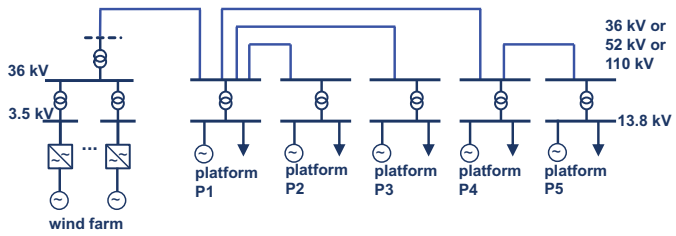

Figure 2. Simplified single line diagram for the interconnecting grid.

Table II
NORSOK LIMITS FOR OFFSHORE AC DISTRIBUTION SYSTEMS. MAXIMUM ALLOWABLE DEVIATIONS FROM NOMINAL VALUES.

	Voltage (ΔU)	Frequency (Δf)
Constant	$+6/-10\%$	$\pm 5\%$
Transient	$\pm 20\%$	$\pm 5\%$
Cyclic	$\pm 2\%$	$\pm 0.5\%$
Recovery time	1.5 sec	5 sec

Parameters for the cables and transformers in the interconnecting grid are based on refs. [11], [12] and otherwise generic values suitable for the specific voltage level and power rating.

Voltage control on the platforms is mainly achieved through the gas turbine governors. The wind farm frequency converter also includes voltage control with a specified set value on the grid side.

The gas turbines are modelled with the standard GAST model which is included in SIMPOW This model is preferred due to its simplicity and due to difficulties in obtaining representative parameters for more detailed gas turbine models.

E. Dynamic simulation cases

The dynamic simulation cases considered here can be defined as a combination of an initial state of operation, and a disturbance. Since this is a hypothetical system, there is a large number of potential configurations that could be studied. The initial state is specified by fixing several variables:

- Interconnecting grid voltage level (36/52/110 kV)
- Interconnecting grid topology (star/meshed)
- Wind penetration (0 – 100 MW)
- Number and initial power output of online gas turbines

The three different voltage levels are chosen to represent quite different options, but the exact values are more or less arbitrary.

The disturbances considered in this study can be grouped in three categories:

- Start-up of large induction motor
- Loss of interconnection
- Loss of production (wind turbines or gas generators)

Of course, a complete scan of all possible combinations of initial states and disturbances is neither feasible nor particularly enlightening. Instead, a few of the most interesting combinations are presented here in order to cast light on the specific issues being addressed.

It should be noted that maximum peaks for frequency and voltage deviations depend on the number of online gas turbines in the model. More online gas turbines implies better stability, but also increased fuel use since efficiency is reduced when they operate at lower power output. The problem of optimising the operation of the gas turbines is an interesting question that has only been discussed superficially in this paper, see section II-C.

III. SIMULATION RESULTS

This section contains the main results from the case study investigations. First, results from steady-state simulations are presented, giving a comparison of losses for different voltage levels and wind penetration situations. Then, results from dynamic simulations investigating system stability are presented in the subsequent subsections. The results from these simulations indicate:

- Transient frequency deviations may exceed the 5% NORSOK limit in cases with sudden loss of large amounts of wind power (loss of wind farm, or loss of interconnector)
- Transient voltage deviations are less than 8% in all cases, well within the NORSOK limit of 20%. The largest deviations are found for motor start-up.

A. Power transmission losses

The voltage levels considered for the interconnecting grid are 36 kV, 52 kV, and 110 kV. Table III shows the computed losses for different values for grid voltage and wind power penetration. With low wind penetration there is little power flow between the platforms (each being supplied by its own gas turbines), and the transmission losses are therefore low independently of grid voltage, as expected. With increased wind penetration, there is increased power flow in the grid and therefore increased losses. As the table shows, there is only a small difference in the power losses for the 36 kV and 52 kV grid voltages, but significantly reduced losses for the 110 kV grid voltage level.

From the perspective of power losses, it is clear that higher grid voltage is an advantage. But losses is only part of the consideration, availability and proven reliability of equipment are very important, as is the economics of the choice. The different grid voltages considered in this study represent a range of realistic choices. See ref. [13] for further discussion of voltage levels in the context of electrification of oil and gas platforms.

The dynamic behaviour of the system is affected by the grid voltage level. Figures 4 and 6 show the dependence on grid voltage level for voltage deviations during disturbances. As is clear from the figures, grid voltage is not a critical factor for voltage stability in the present case, as voltage deviations in all cases are anyway well within allowable limits. Dynamic behaviour is further explored in the next sections.

B. Start-up of large induction motor

Direct online start of the largest induction motor in the system represents the largest disturbance during normal operation. The resulting voltage variations can therefore be considered as the largest normal variations, and as such set a benchmark for

Table III
TRANSMISSION LOSSES FOR DIFFERENT VOLTAGE LEVELS AND WIND FARM POWER OUTPUT.

Case	36 kV grid (MW)	52 kV grid (MW)	110 kV grid (MW)
No wind	0.002	0.005	0.010
50 MW wind	0.65	0.63	0.15
100 MW wind	2.34	2.30	0.55

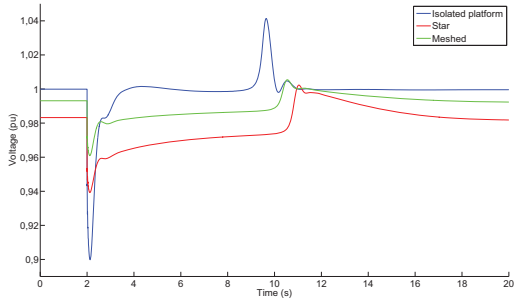

Figure 3. Voltage deviation at platform P3 during start-up of large induction motor on P3, with 100 MW wind power penetration for star and meshed topology, compared to single platform case

other simulations. The largest induction motor in this system has a rating of 5.78 MVA.

Voltage deviations on P3 during start-up of a motor on the same platform are shown in figure 3 for a situation with 100 MW wind production and 6 online gas turbines in total. The single platform case is included for reference, and indicates deviations during start-up of a motor on an isolated single platform with load 24 MW, no wind and two online gas turbines. The maximum voltage dip for the single platform case is 10%. If the load is reduced to 19 MW and only one gas turbine is online, the voltage dip is 18%, which reproduces the result from the previous single platform study [5].

For the interconnected system with star topology, the voltage dip is reduced to 6%, and with meshed topology it is futher reduced to 4%. This confirms the expectation that voltage stability generally improves with better interconnection.

A comparison of voltage deviations for different grid voltage levels is shown in figure 4. As mentioned above, this figure indicates improved behaviour for higher grid voltage, but as the deviations are small, this is not a crucial issue. The largest voltage dip is 7.5% for the 36 kV case.

C. Loss of interconnector

The improved power stability with the meshed topology compared to the star topology is even clearer when considering loss of a platform–to–platform interconnector. Figure 5 compares frequency deviations on P4 during loss of the P1–P4 interconnector in situations with 100 MW wind power. With a star topology this splits the system into two separate synchronous parts, with the largest impact seen on the P4/P5 subsystem. The maximum frequency dip in this case is -5%,

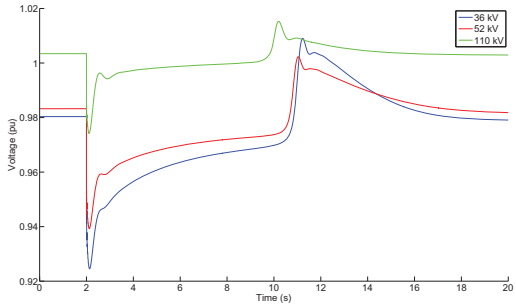

Figure 4. Voltage deviation dependence on grid voltage level. Deviations at platform P3 during start-up of large induction motor on P3, with 100 MW wind power penetration and star topology.

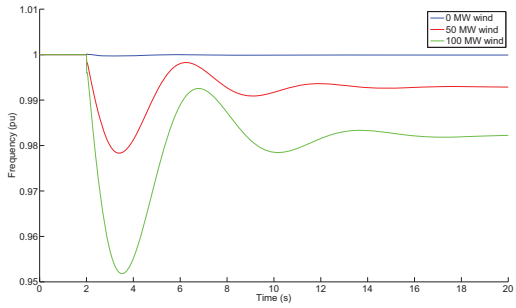

Figure 5. Frequency deviation at platform P4 during sudden loss of the P1–P4 interconnector for different wind penetration levels.

whereas with a meshed topology, there is virtually no impact on frequency.

The allowable transient frequency deviation limit according to NORSOK (table II) is 5%, so this disturbance is potentially critical in the case with star topology. One consequence of this result is that 100 MW of wind power is about the maximum which can be integrated in this platform system. Alternatively, it can be interpreted as an indication that there is need for improved frequency control, or that the system requires a meshed topology.

D. Loss of production

For sudden loss of wind power, there is no significant difference between the two topologies.

Voltage deviations during sudden loss of the entire wind farm at maximum production is shown in figure 6 for different voltage levels. The maximum voltage deviation is $+6\%$, which is again well within the NORSOK limits. The wind farm initially draws reactive power due to reactive power demand in the cables and transformers, resulting in a sudden voltage rise when the connection is lost.

Frequency deviations for the same disturbance, and also for the less dramatic event of loosing only a wind farm feeder are shown in figure 7. Frequency response is the same regardless of grid voltage, so only one curve for each disturbance is plotted. For loss of 100 MW wind, the maximum frequency

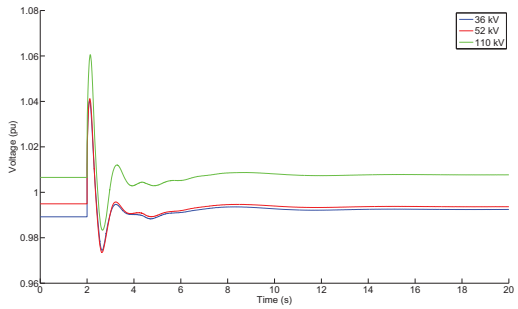

Figure 6. Voltage deviation at platform P4's main bus bar during sudden loss of wind power (from 100 MW to zero).

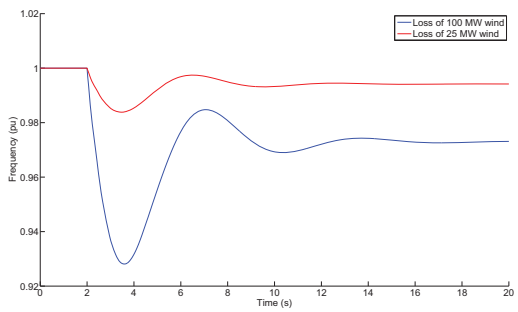

Figure 7. Frequency deviation during sudden loss of a wind power

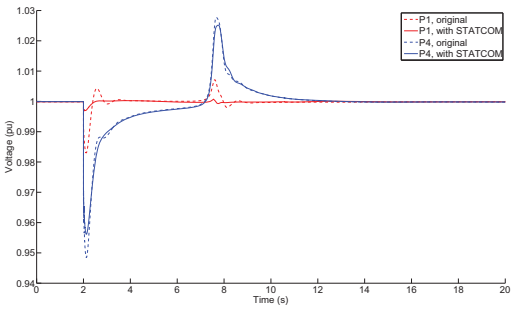

Figure 8. Voltage deviations during start-up of motor on P4 with and without STATCOM connected to P1.

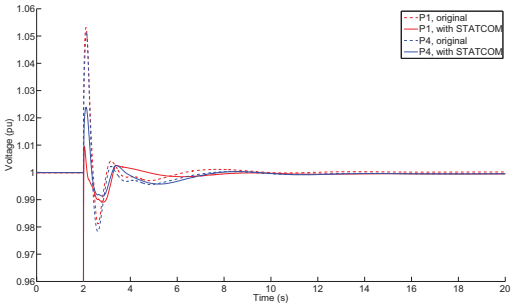

Figure 9. Voltage deviations during loss of 100 MW wind with and without STATCOM connected to P1.

deviation is -7%, which exceeds the NORSOK limit. To ensure that this could never happen, one alternative, as mentioned above, would be to limit the wind power penetration such that the potential deviations were reduced to within acceptable limits. Another alternative would be to use two cables and transformers for the wind farm connection. In that case, the worst (single contingency) loss of production would be the loss of a wind farm feeder. Since the wind power capacity on each feeder in our model is 25 MW, which is similar to the gas turbine power rating, the system impact of loss of a feeder is similar to the loss of a gas turbine. As expected, the impact of the loss of a single wind farm feeder is much less, with a maximum frequency deviation of less than 2%.

E. Reactive compensation

An interesting question is how the addition of a reactive power compensating device affects the voltage stability in this isolated system. To illustrate this, simulations have been done for the 36 kV star topology case with a 45 MVA STATCOM connected to P1 on 36 kV level. Comparisons of voltage deviations during during motor start-up, and during loss of 100 MW wind power are shown in figure 8 and figure 9 respectively.

Voltage deviations even in the original system without any compensating device are in fact not very large, but it is nonetheless interesting to observe that for loss of wind (figure 9), the STATCOM more than halves the maximum deviation. The effect is seen on both P1 and P4 platforms, although the improvement is most significant on P1 where the STATCOM is connected. The sharp dip at 2s is only due to model inaccuracy, and does not represent any realistic behaviour. For the motor start-up case (figure 8), the STATCOM has relatively little influence on the voltage variation on the platform where the motor is started (P4), but a significant influence on the platform where the STATCOM is placed (P1). In other words, a STATCOM on P1 is not suitable to stabilise voltage deviations on P4 which are due to a local P4 disturbance.

As noted in section II-B, the present model assumes an interconnection of existing platforms, each with multiple gas turbines present. Power stability in this model is therefore achieved by the gas turbine controls, and as we have seen, there is no indication of a need for extra reactive compensation devices. The inclusion of a STATCOM in the system would be more relevant for the interconnection of *new* platforms without gas turbines. With this in mind, the figures above have been included to illustrate what voltage stability improvements may typically be achieved by including a STATCOM in this type of system.

F. Gas turbine model parameters

It is interesting to probe how sensitive the results are to the modelling of the platform gas turbines. This study has used the standard GAST model, with parameters tuned such that the behaviour resembles behaviour of a more detailed commercial model obtained under confidentiality. Figure 10

Table IV
DSLS/GAST GAS TURBINE MODEL PARAMETERS

Parameter	Description	original	modified
R	Speed droop	0.05	0.05
T1	Governor time const (s)	3.0	0.4
T2	Combustion chamber time const (s)	0.01	0.1
T3	Exhaust measuring time const (s)	1.7	3.0
AT	Ambient temperature load limit	0.95	0.95
KT	Gain adj. of load-limited feedback	2.0	2.0
VMAX	Maximum turbine output	1.0	1.0
VMIN	Minimum turbine output	0.0	-0.05
DTURB	Speed damping const	1.0	0.0

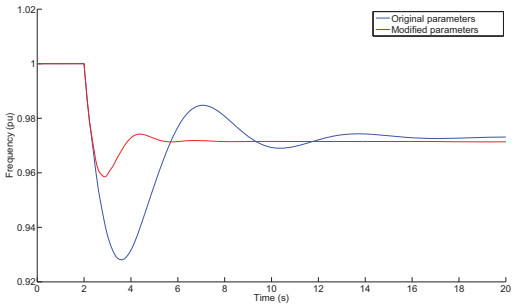

Figure 10. Comparison of frequency response during loss of 100 MW wind for different GAST model parameters.

shows a comparison of frequency response during sudden loss of 100 MW wind in the star topology with 52 kV grid for GAST model parameters used in this study (original parameters), and parameters indicated in the PSSE manual [14] as representing "typical" gas turbines (modified parameters), see table IV for the values used. As we can see, the choice of parameters influence the frequency response significantly, with only half as large deviation with the modified parameters suggested in the PSS/E manual.

Modelling of gas turbines has been discussed in more detail in refs. [15], [16].

IV. Conclusions

This study has explored a case study with the integration of an offshore wind farm and five oil and gas platforms as an isolated system. Topology and voltage level for the interconnecting grid has been discussed, and dynamic simulations have exposed power stability properties of the system in various configurations.

Compared to a single stand-alone platform, it has been demonstrated that the interconnected system has improved voltage stability, with the largest improvement observed for the meshed grid topology. I.e. more interconnection gives better voltage stability. The meshed topology also allows more flexible operation of gas turbines whilst maintaining the same (or higher) level of security. The main disadvantage of the meshed topology is the extra cable costs.

This study shows that the system operates satisfactory regarding voltage stability. Whether frequency stability is acceptable or not depends on the configuration. Important factors that have been identified in this regard are the grid topology, single or dual cables/transformers for the wind farm connection, and gas turbine control parameters.

The requirement of satisfactory frequency stability during sudden loss of wind power or an interconnector indicates that a wind farm capacity of 100 MW is about the maximum which can be integrated with the interconnected platform system. However, the number depends on choice of topology and may be increased with an improved control strategy.

This study has been concerned with a hypothetical case study. For the assessment of concrete cases, more detailed data and simulations are required to give firm conclusions about the level of power system stability. However, the present study has given important insights about generic behaviour, and indicates that the solutions required for making such interconnected systems operationally secure and beneficial are easily within the reach of current technology.

Acknowledgement

We would like to thank Wei He at Statoil for suggesting the case study and for valuable input and discussions.

References

[1] S. Gilje and L. Carlsson, "Valhall re-development project, power from shore," in *ENERGEX 2006*, 2006.
[2] T. F. Nestli, L. Stendius, M. J. Johansson, A. Abrahamsson, and P. C. Kjaer, "Powering troll," *ABB Review*, no. 2, pp. 15–20, 2003.
[3] T. M. Haileselassie and K. Uhlen, "Primary frequency control of remote grids connected by multi-terminal hvdc," 2010, pp. 1–6.
[4] D. Hu, X. Zhao, X. Cai, and J. Wang, "Impact of wind power on stability of offshore platform power systems," in *Electric Utility Deregulation and Restructuring and Power Technologies, DRPT 2008, Nanjing China*, 2008, pp. 1688–1692.
[5] W. He, G. Jacobsen, T. Anderson, F. Olsen, T. D. Hanson, M. Korpås, T. Toftevaag, J. Eek, K. Uhlen, and E. Johansson, "The potential of integrating wind power with offshore oil and gas platforms," *Wind Engineering*, vol. 34, no. 2, pp. 125–137, 2010.
[6] "Beatrice wind farm demonstrator project scoping report," www.beatricewind.co.uk, Talisman Energy, Tech. Rep.
[7] R. Maclean, "Electrical system design for the proposed one gigawatt beatrice offshore wind farm," 2004.
[8] *NORSOK Standard E-001 Electrical systems*, Standards Norway Std., Rev. 5, July 2007.
[9] *IEC 61892–1 Mobile and fixed offshore units – Electrical installations – Part 1: General requirements and conditions*, IEC Std., Rev. 1, 2001.
[10] *SIMPOW User manual v11.0*, STRI AB.
[11] *XLPE Cable Systems – User's guide rev.2*, ABB, www.abb.com/cables.
[12] *XLPE Submarine Cable Systems – Attachment to XLPE User's guide*, www.abb.com/cables.
[13] "Elektrifisering av norsk sokkel – transmisjonssystem fra land og distribusjon til plattformer," Unitech, Tech. Rep., 2007.
[14] Power Technologies Inc., *PSS/E Volume II: Program Application Guide, Chapter 16 – Speed Governor SystemModeling*, 2004.
[15] M. Nagpal, A. Moshref, G. K. Morison, and P. Kundur, "Experience with testing and modeling of gas turbines," in *Power Engineering Society Winter Meeting, IEEE*, vol. 2, 2001, pp. 652–656.
[16] S. K. Yee, J. V. Milanović, and F. M. Hughes, "Overview and comparative analysis of gs turbine models for system stability studies," *IEEE Transactions on Power Systems*, vol. 23, no. 1, 2008.

ABSTRACT FOR OFFSHORE WIND - 2011

29 November – 1 December *2011*, Amsterdam at Netherlands

A case study of integrating a wind farm with offshore oil and gas platforms grid and with an onshore electrical grid

Wei He
(Statoil, Norway)

Zhe Chen, Gang Shi and Emilio del Rio
(Aalborg University, Denmark)

Kjetil Uhlen, Harald Svendsen, Maheshkumar Hadiya
(SINTEF Energy Research & NTNU, Norway)

Summary (max. 100 words)

This research project explored the technical feasibility of utilizing wind farms as a supplementary power source to an electrical grid of offshore oil / gas platform and providing surplus power to an onshore grid. Three case studies comprising wind farms rated at 20 MW, 100 MW and 1000 MW have focused on: i) the operation benefits of CO_2 / NO_x emission reduction and electrical grid stability ii) the control strategy and the interconnecting grid topology, iii) the technical implementation feasibility. The proposed 20 MW, 100 MW and 1000 MW wind farm cases are theoretically feasible, although further studies are needed.

Full description (max. 400 words)

The successful pilot operation of Statoil's floating Hywind 2.3 MW wind turbine unit has demonstrated the potential to utilize the wind energy nearby offshore oil and gas platforms where the water depth is from a hundred to several hundreds of meters.

Firstly, integration of four 5MW wind power generators to an offshore platform for electricity generation could achieve significant reductions of fuel gas and CO_2 / NO_x emissions. One yearly case based on the real load data gave an annual reduction of 40 % CO_2 / NO_x emissions. The electrical grid stability after integration of 20 MW wind power was tested under various dynamic situations, including: motor starts, loss of one gas turbine, loss of all wind turbines and wind speed fluctuations.

Secondly, to utilize more wind power the 20 MW case was extended to include a 100 MW wind farm which will be connected to five nearby oil and gas platforms by sub-sea power cables. The 100 MW case was focused on the identifying maximum amount of wind power which that can be integrated into the stand-alone electrical grid on each platform with regard to the governing standards concerning acceptable frequency and voltage variations. The challenges in terms of control strategy and interconnecting grid topology were also addressed.

Thirdly, in order to achieve an economically feasible offshore wind farm, a 1000 MW wind farm was proposed for supplying wind power to both the oil & gas platforms and to the onshore electrical grid. The studied 1000 MW case focused on the technical implementation as follows.

- Evaluate the wind farm size and design the wind farm layout.
- Design the wind farm connecting electrical grid.
- Configuration of the main components and the voltage levels.
- Analyze the electrical grid stability.

The dynamic simulation models of the 20 MW and 100 MW cases have been implemented in EMTDC/PSCAD and in SIMPOW, respectively. The models include both the platform electrical grids models and the wind farm models. The 1000 MW model in EMTDC/PSCAD also includes the MTDC (multi-terminal direct current) system to transport the surplus electricity to the onshore electrical grid.

In conclusion, this study shows that utilizing offshore wind farm for offshore oil and gas platforms and for supplying the power to onshore be a promising theoretical alternative to reduce CO_2 / NO_x emissions, although further studies are required to overcome many other operational and economic hurdles.

APPENDICES

APPENDIX 1 – PARAMETER DATA

APPENDIX 2 – STATIC POWER FOLW AND DYNAMIC RESULTS – CLASS A, B, C AND D.

Appendix 1 - Parameter Data

Appendix 1.1: Main synchronous generators data

PARAMETERS	UNIT	EG80001 A, B & C	EG 80001D
Rated power	S_N [MVA]	28.75	22.82
Rated voltage	U_N [kV]	13.8	13.8
Rated frequency	f_N [Hz]	60	60
Rated power factor	$\cos\varphi_N$	0.8	0.85
Speed	n [rpm]	3600	
Direct axis synchronous reactance	X_d [p.u.]	1.88	2.18
Direct axis transient reactance	X_d' [p.u.]	0.217	0.25
Direct axis subtransient reactance	X_d'' [p.u.]	0.16	0.172
Quadrature axis synchronous reactance	X_q [p.u.]	1.76	1.76
Quadrature axis transient reactance	X_q' [p.u.]	0.406	-
Quadrature axis subtransient reactance	X_q'' [p.u.]	0.203	0.203
Armature resistance (^oC)	r_a [p.u.]	0.0022	0.0022
Zero sequence reactance	X_0 [p.u.]	0.073	
Leakage reactance	X_l [p.u.]	0.117	0.117
Direct axis open-circuit transient time constant	T_{d0}' [s]	3.2	3.2
Direct axis open-circuit subtransient time constant	T_{d0}'' [s]	0.05	0.05
Direct axis short-circuit transient time constant	T_d' [s]		
Direct axis short-circuit subtransient time constant	T_d'' [s]	0.02	
Quadrature axis open-circuit subtransient time constant	T_{q0}'' [s]	0.05	0.05
Quadrature axis short-circuit subtransient time constant	T_q'' [s]		
Inertia constant	H [s]	1.2853	1.2853
Moment of inertia	J [kgm^2]	520	

Appendix 1.2: Extra synchronous generator data.

PARAMETERS	UNIT	EG83001 A, B & C	EG18680
Rated power	S_N [MVA]	1.75	3.0
Rated voltage	U_N [kV]	6.0	0.44
Rated frequency	f_N [Hz]	60	60
Rated power factor	$\cos\varphi_N$	0.8	0.72
Direct axis synchronous reactance	X_d [p.u.]	1.4	1.25
Direct axis transient reactance	X_d' [p.u.]	0.23	0.162
Direct axis subtransient reactance	X_d'' [p.u.]	0.14	0.104
Quadrature axis synchronous reactance	X_q [p.u.]	1.26	1.25
Quadrature axis transient reactance	X_q' [p.u.]	-	-
Quadrature axis subtransient reactance	X_q'' [p.u.]	0.2	0.17
Armature resistance (^oC)	r_a [p.u.]	0.0031	0.0031
Zero sequence resistance	R_0 [p.u.]	-	-
Zero sequence reactance	X_0 [p.u.]	-	-
Leakage reactance	X_l [p.u.]	0.135	0.095
Direct axis open-circuit transient time constant	T_{d0}' [s]	2.9	1.78
Direct axis open-circuit subtransient time constant	T_{d0}'' [s]	0.025	0.042
Direct axis short-circuit transient time constant	T_d' [s]	-	-
Direct axis short-circuit subtransient time constant	T_d'' [s]	-	-
Quadrature axis open-circuit subtransient time constant	T_{q0}'' [s]	0.139	0.221
Quadrature axis short-circuit subtransient time constant	T_q'' [s]	-	-
Inertia constant	H [s]	1.0	1.0
Moment of inertia	J [kgm^2]		

Appendix 1.3: Wind turbine Synchronous generator data from SIMPOW manual

PARAMETERS	UNIT	WTG
Rated power	S_N [MVA]	5.3
Rated voltage	U_N [kV]	3.0
Rated frequency	f_N [Hz]	60
Direct axis synchronous reactance	X_d [p.u.]	1.9
Direct axis transient reactance	X_d' [p.u.]	0.32
Direct axis subtransient reactance	X_d'' [p.u.]	0.2
Quadrature axis synchronous reactance	X_q [p.u.]	1.6
Quadrature axis transient reactance	X_q' [p.u.]	-
Quadrature axis subtransient reactance	X_q'' [p.u.]	0.21
Armature resistance (^oC)	r_a [p.u.]	0.0025
Zero sequence resistance	R_0 [p.u.]	-
Zero sequence reactance	X_0 [p.u.]	-
Leakage reactance	X_l [p.u.]	0.14
Direct axis open-circuit transient time constant	T_{d0}' [s]	5.0
Direct axis open-circuit subtransient time constant	T_{d0}'' [s]	0.03
Direct axis short-circuit transient time constant	T_d' [s]	-
Direct axis short-circuit subtransient time constant	T_d'' [s]	-
Quadrature axis open-circuit subtransient time constant	T_{q0}'' [s]	0.07
Quadrature axis short-circuit subtransient time constant	T_q'' [s]	-
Inertia constant	H [s]	5.5
Moment of inertia	J [kgm^2]	-

Appendix 1.4: Data for power electronics rectifier from SIMPOW manual

PARAMETERS	UNIT	RECT_WTG1
Rated power	S_N [MVA]	5.3
Rated voltage	U_N [kV]	3.0
Rated frequency	f_N [Hz]	60
Active power loss	P_L	0.02
Filter reactance	n [p.u]	0.3
DC-voltage	U_{DC} [V]	5000
DC-link capacitance	C_{dc} [F]	0.0024

Appendix 1.5: Data for power electronics inverter form SIMPOW manual

PARAMETERS	UNIT	RECT_WTG1
Rated power	S_N [MVA]	5.3
Rated voltage	U_N [kV]	3.5
Rated frequency	f_N [Hz]	60
Active power loss	P_L	0.02
Filter reactance	n [p.u]	0.3

Appendix 1.6: Data for lines and cables 13.8 and 6 kV system (Lower level not included)

FROM BUS	TO BUS	KV	LENGTH[M]	R	X
EH80001A	PA29002A	13.8	115	0.0938	0.1430
EH80001A	PA44004	13.8	100	0.0938	0.1430
EH80001B	PA29002B	13.8	111	0.0938	0.1430
EH80001B	PA29002C	13.8	72	0.0938	0.1430
EH80001A	T82600AP	13.8	330	0.0938	0.1430
EH80001B	T82600BP	13.8	430	0.0938	0.1430
EH80001A	T81001AP	13.8	30	0.0469	0.0715
EH80001B	T81001BP	13.8	30	0.0469	0.0715
EH80001A	PA51003A	13.8	82	0.0938	0.1430
EH80001B	PA51003B	13.8	58	0.0938	0.1430
EH80001A	PA51003C	13.8	75	0.0938	0.1430
EH80001B	PA51003D	13.8	60	0.0938	0.1430
EH80001A	PA29001A	13.8	115	0.0938	0.1430
EH80001A	PA29001C	13.8	72	0.0938	0.1430
EH80001B	PA29001B	13.8	111	0.0938	0.1430
EH80001A	PA21001A	13.8	180	0.0938	0.1430
EH80001B	PA21001B	13.8	102	0.0938	0.1430
EH80001A	T82403AP	13.8	130	0.0938	0.1430
EH80001B	PA21001C	13.8	104	0.0938	0.1430
EH80001A	EP23005A	13.8	94	0.0938	0.1430
EH80001B	EP23005B	13.8	106	0.0938	0.1430
EH80001A	T82500AP	13.8	350	0.1580	0.1480
EH80001B	T82500BP	13.8	350	0.1580	0.1480
WTG1B	EH80001A	13.8	1.0	0.125	0.132
EM83001B	T84680BP	6	411	0.2520	0.1240
EM83001A	T84680AP	6	345	0.2520	0.1240
EM83001B	T84500P	6	30	0.4910	0.1370
EM83001B	KA63001B	6	98	0.252	0.124
EM83001A	KA63001A	6	86	0.252	0.124
EM83001A	KA63001C	6	86	0.252	0.124
EM81001X	PA25831A	6	350	0.9210	0.1500
EM81001A	PA50001A	6	155	0.252	0.124
EM81001A	PA50001C	6	155	0.252	0.124
EM81001A	PA50003A	6	148	0.252	0.124
EM81001A	PA50003C	6	138	0.252	0.124
EM81001X	PA50831A	6	350	0.2520	0.1240
EM81001X	PA50831C	6	350	0.2520	0.1240

Appendix 1.7: Data for transformers

NO.	FROM BUS	TO BUS	MVA	PKV	SKV	IMP. [PU]	
						ER %	EX %
TR1 (36 kV)	PLATFORM1	P1_EH80001A	200	36	13.8	0.32	5.99
TR2 (36 kV)	PLATFORM2	P1_EH80001A	200	36	13.8	0.32	5.99
TR3 (36 kV)	PLATFORM3	P1_EH80001A	200	36	13.8	0.32	5.99
TR4 (36 kV)	PLATFORM4	P1_EH80001A	200	36	13.8	0.32	5.99
TR5 (36 kV)	PLATFORM5	P1_EH80001A	200	36	13.8	0.32	5.99
TR1 (52 kV)	PLATFORM1	P1_EH80001A	200	52	13.8	0.32	5.99
TR2 (52 kV)	PLATFORM2	P1_EH80001A	200	52	13.8	0.32	5.99
TR3 (52 kV)	PLATFORM3	P1_EH80001A	200	52	13.8	0.32	5.99
TR4 (52 kV)	PLATFORM4	P1_EH80001A	200	52	13.8	0.32	5.99
TR5 (52 kV)	PLATFORM5	P1_EH80001A	200	52	13.8	0.32	5.99
TRANSFOR	WINDFARM	P1_EH80001A	200	36	110	0.42	1.2
TR1 (110kV)	PLATFORM1	P1_EH80001A	200	110	13.8	0.5	10.0
TR2 (110kV)	PLATFORM2	P1_EH80001A	200	110	13.8	0.5	10.0
TR3 (110kV)	PLATFORM3	P1_EH80001A	200	110	13.8	0.5	10.0
TR4 (110kV)	PLATFORM4	P1_EH80001A	200	110	13.8	0.5	10.0
TR5 (110kV)	PLATFORM5	P1_EH80001A	200	110	13.8	0.5	10.0
ET81001A/B	T8100AP	T81001AS	13.0	13.8	0.645	0.36	10.37
ET82001A/B	EH80001A/B	EN82001A	2.5	13.8	0.463	0.64	6.97
ET82002A/B	EH80001A/B	EN82002A	2.5	13.8	0.463	0.64	6.97
ET82003A/B	EH80001A/B	EN82003A/B	2.5	13.8	0.463	0.64	6.97
ET83001A/B	EH80001A/B	EM83001A/B	5.0	13.8	6.3	0.32	5.99
ET82403A	T82403AP	EN82403A	2.0	13.8	0.46	0.64	5.96
ET82600A/B	T82600AP/BP	EN82600A/B	3.15	13.8	0.47	0.63	8.98
ET82500A/B	T82500AP/BP	EN82500A/B	1.6	13.8	0.463	0.85	7.62
-	WTG1A	WTG1B	5.0	13.8	3.5	0.32	5.99
ET84500	T84500P	EN84500	0.63	6.0	0.462	1.04	6.17
ET84680A/B	T84680AP/BP	EN84680A/B	1.0	6.0	0.46	0.78	5.95
ET84001A	EM83001A	EN84001A	2.0	6.0	0.46	0.65	5.96
ET84002A	EM83001	EN84002A	2.0	6.0	0.46	0.65	5.96
ET50002	T5002P	T5002S	0.5	6.0	0.46	1.04	4.378
ET82181A/B	EN82001A/B	EL82181A/B	0.315	0.44	0.23	1.17	7.41
ET82182A/B	EN82001A/B	EL82182A/B	0.315	0.44	0.23	1.17	7.41

Case A1: Starting of 9MW asynchronous motor at PF4, No wind penetration for "Star" Topology with 36kV voltage system. Power Load flow - Single Line Diagram representation shows load bus voltages 13.8kV (blue colour), main platform voltages (red colour), power generation at GTs (purple colour) and power flow situation of whole network.

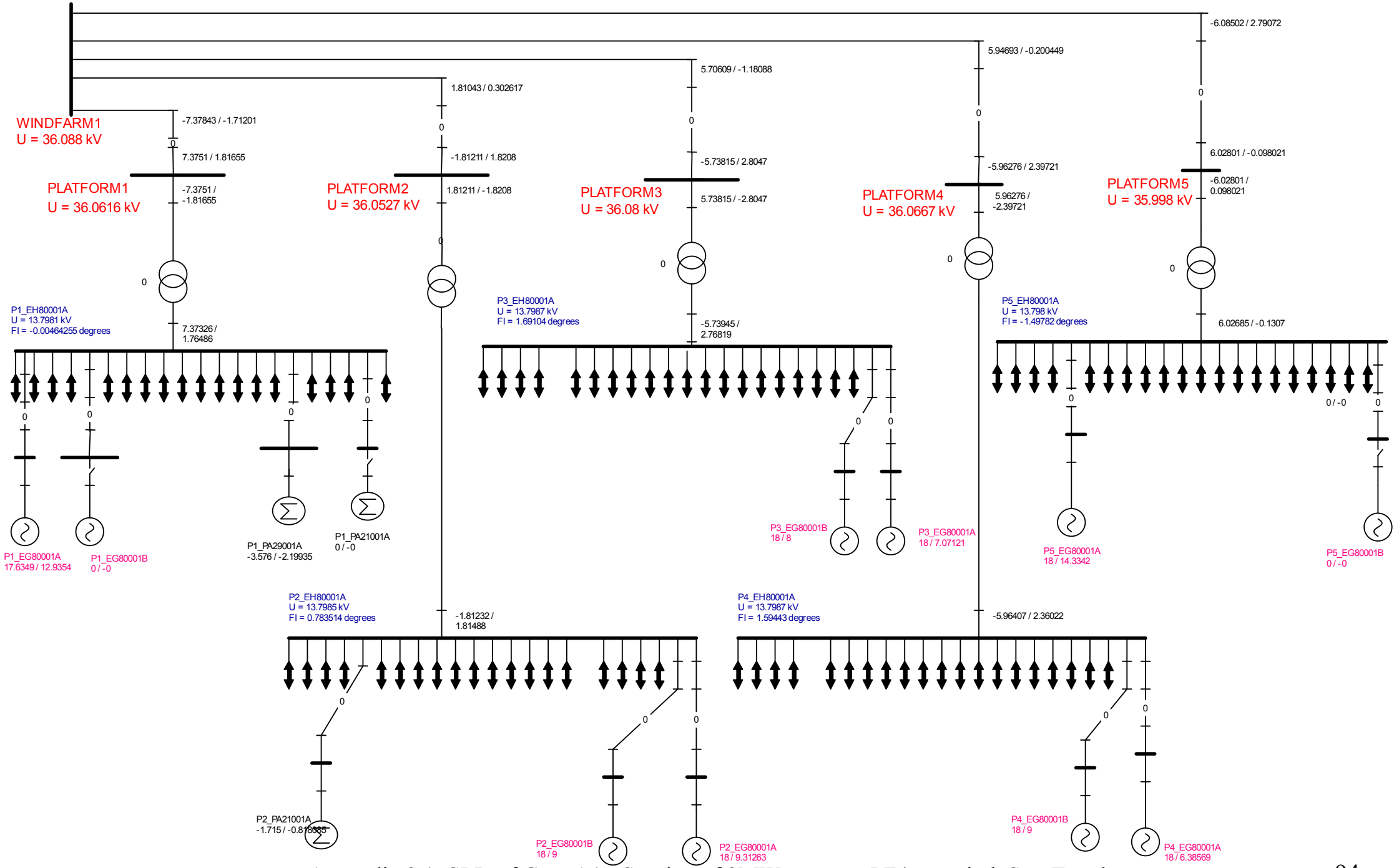

Appendix 2.1: SLD of Case A1 - Starting of 9MW motor at PF4, no wind, Star Topology

Case A1, Starting of 9MW motor at PF4 for "Star - Topology", No wind penetration, 36kV Voltage system. Graphs of Frequency variation at different platform buses, Load Bus Voltage variation ref. to 13.8kV in pu, Active Power and Reactive Power behavior at different online platform GTs.

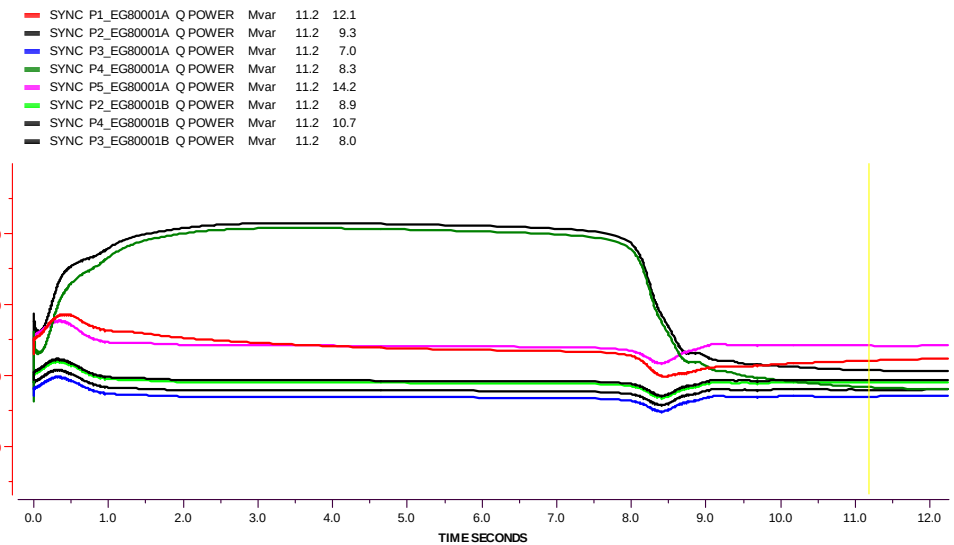

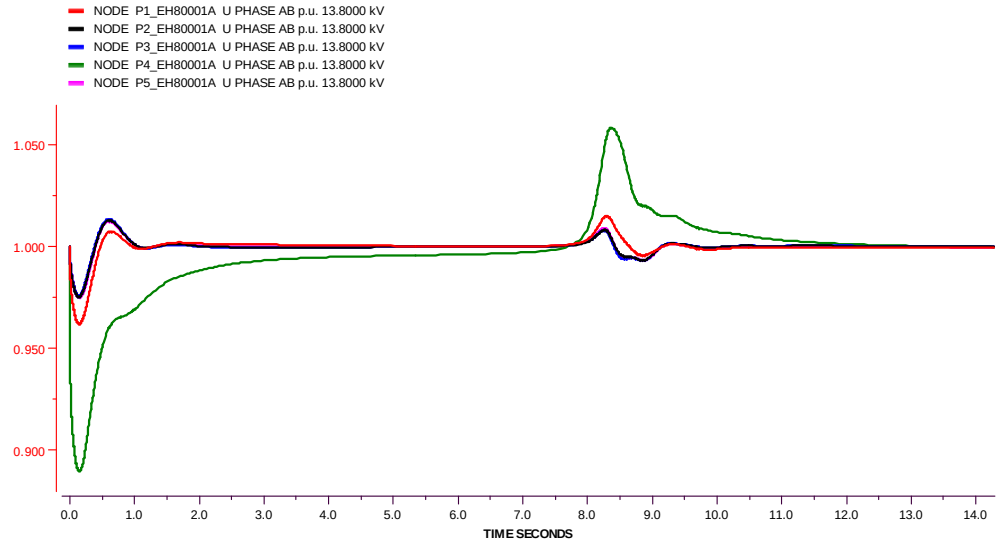

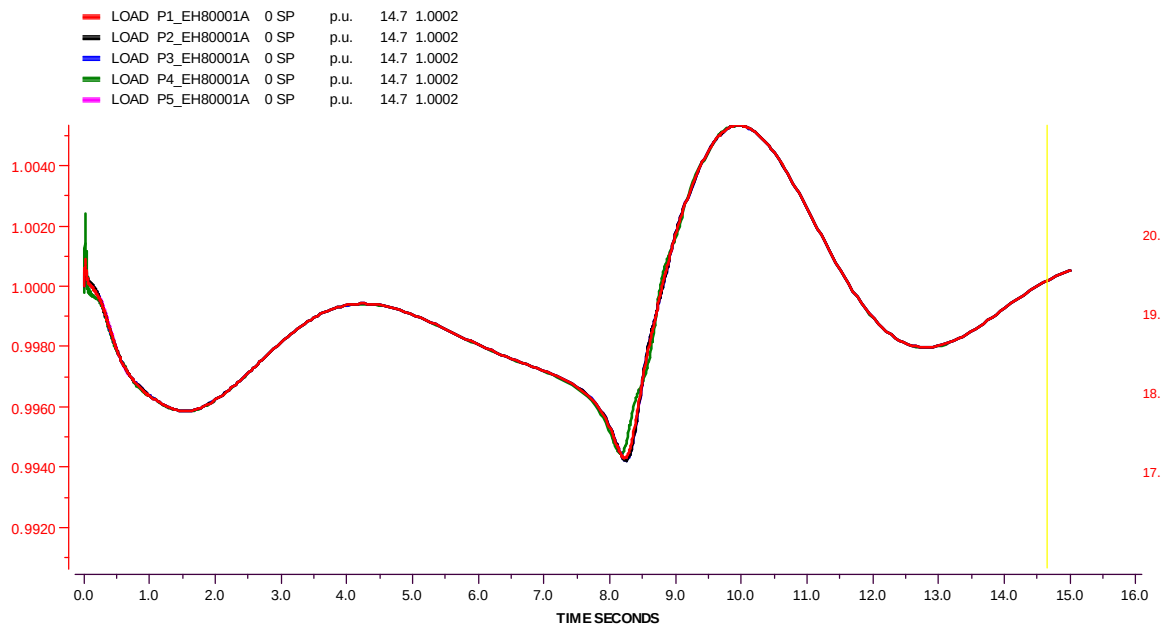

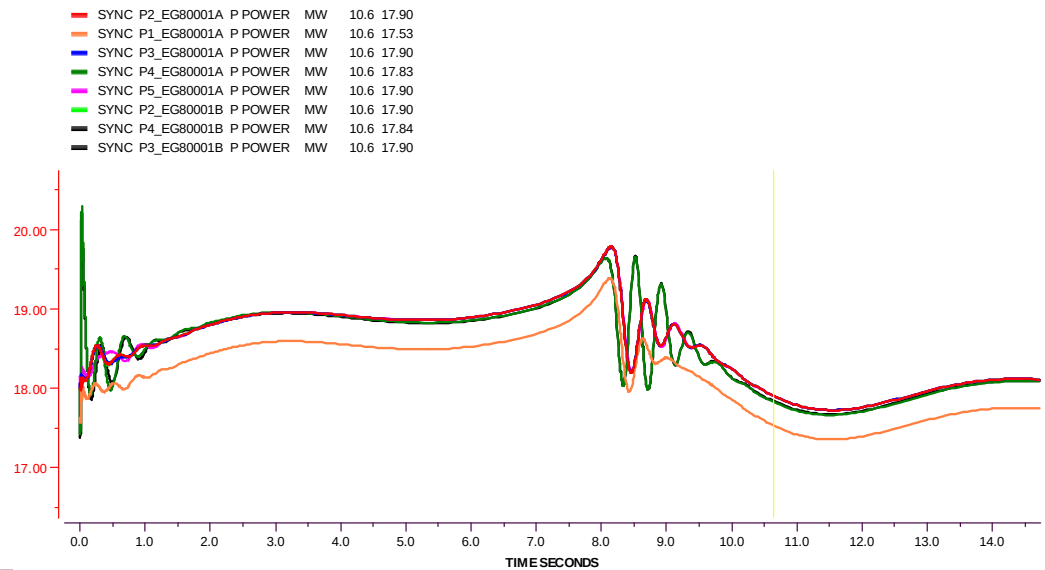

Appendix 2.2: Graphs of Case A1 - Starting of 9MW motor at PF4, no wind, Star Topology

Case A1: Starting of 9MW asynchronous motor at PF4, No wind penetration for "Star" Topology with 36kV voltage system. Power Load flow - Single Line Diagram representation shows load bus voltages ref.13.8kV in pu(blue colour), main platforms voltages 36kV (red colour), power generation at GTs (purple colour) with effect of SVC at PF1

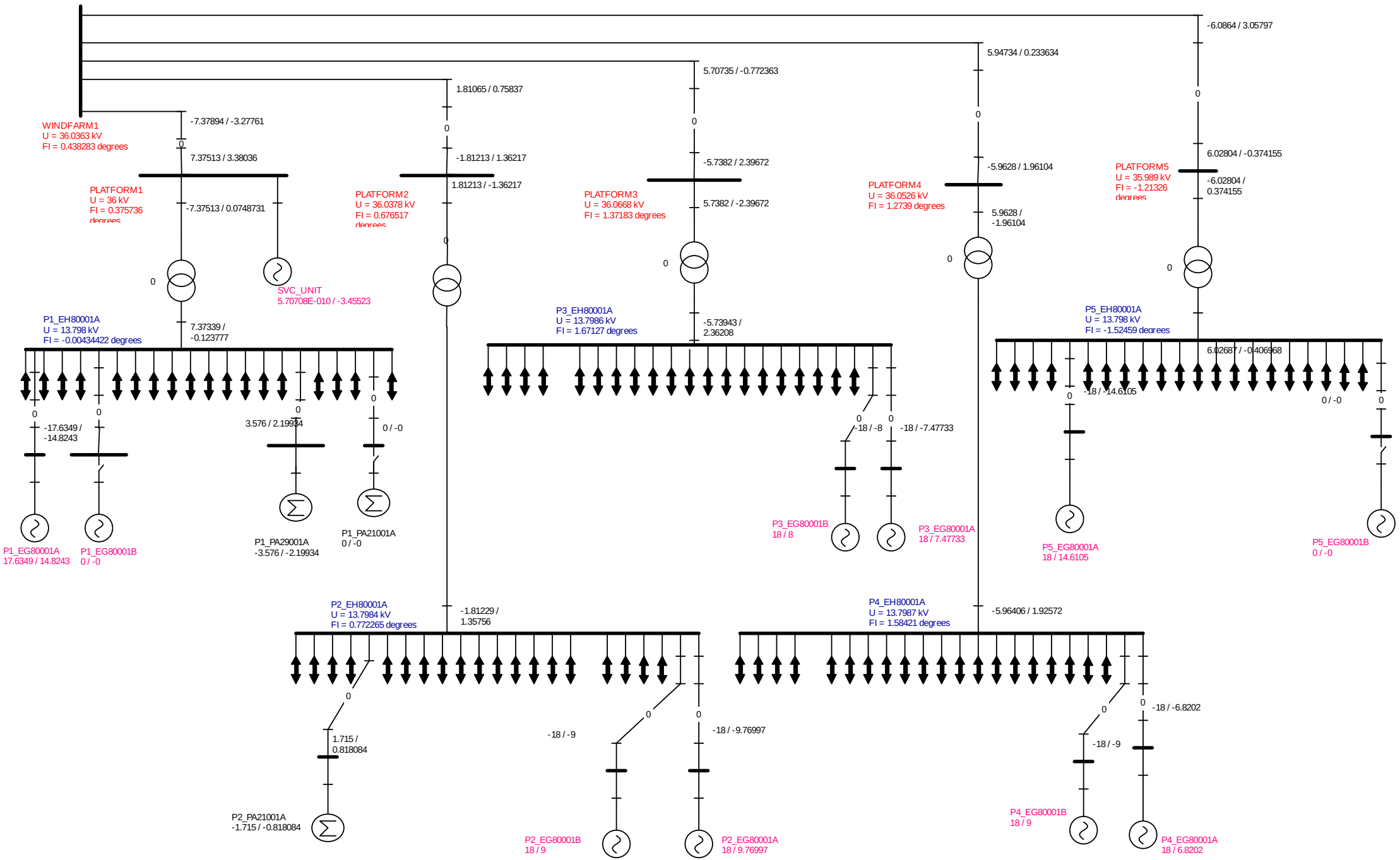

Appendix 2.3: SLD of Case A1 - Starting of 9MW motor at PF4, no wind, Star Topology, SVC effect

Case A1, Starting of 9MW motor at PF4 for "Star Topology", No wind penetration, 36kV Voltage system. Graphs of Frequency variations, Load Bus Voltage ref. to 13.8kV in pu, Active Power and Reactive Power behavior at different GTs with effect of SVC at PF1.

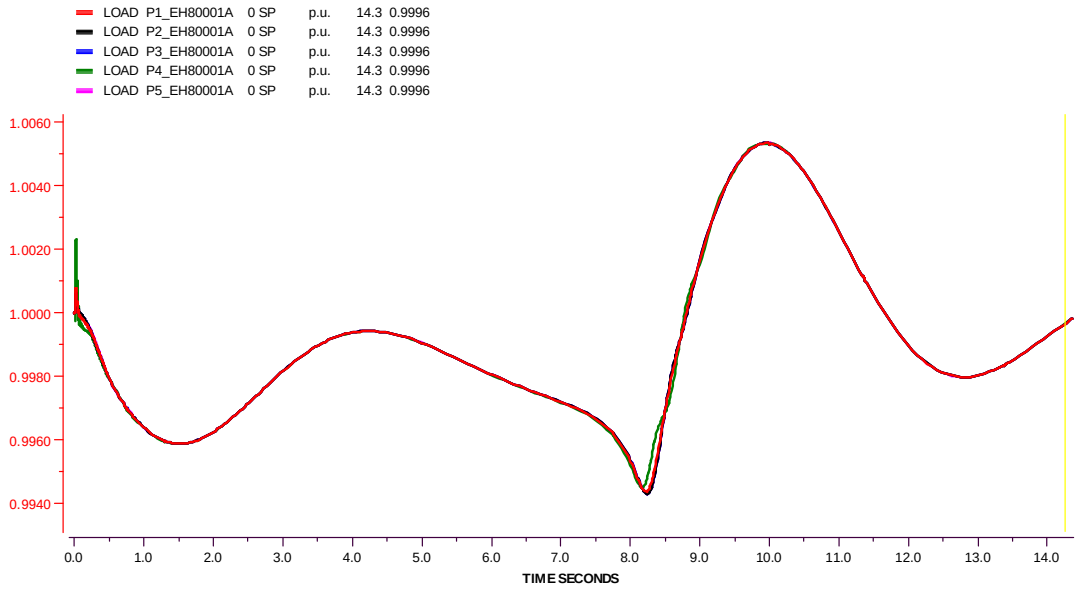

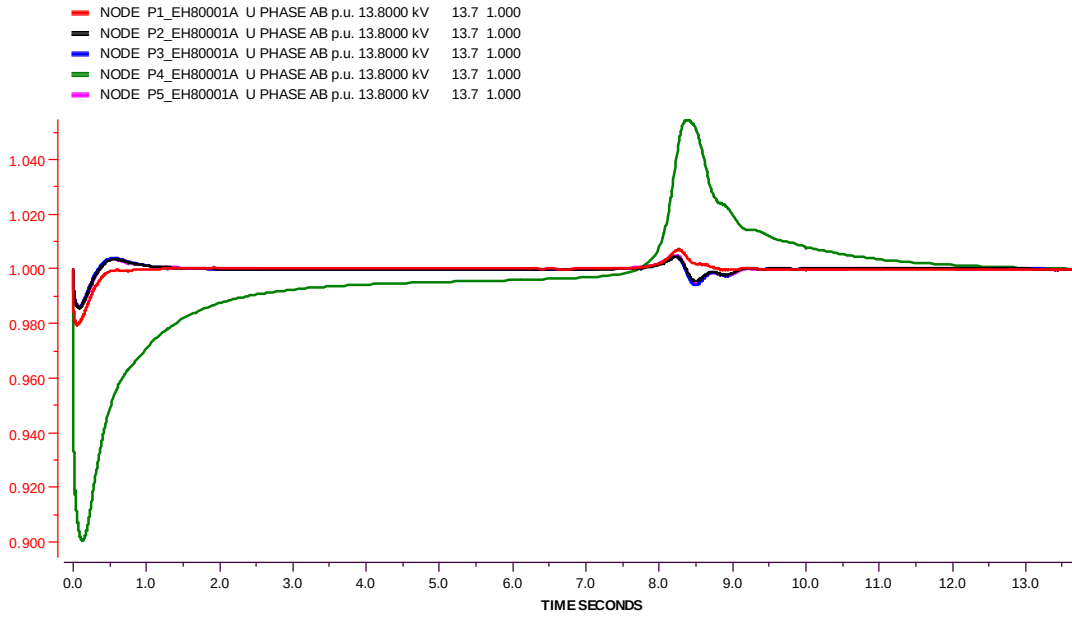

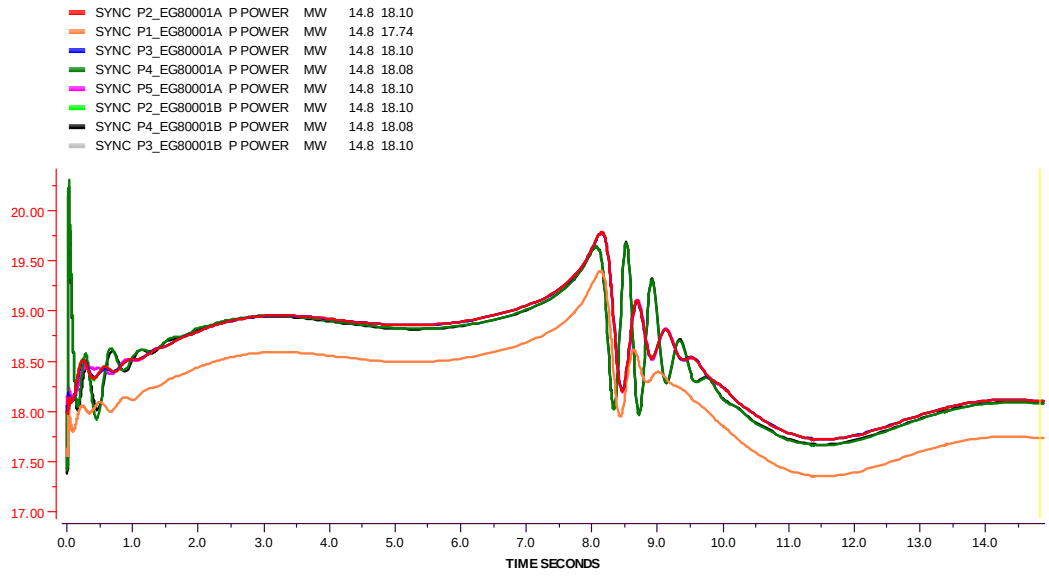

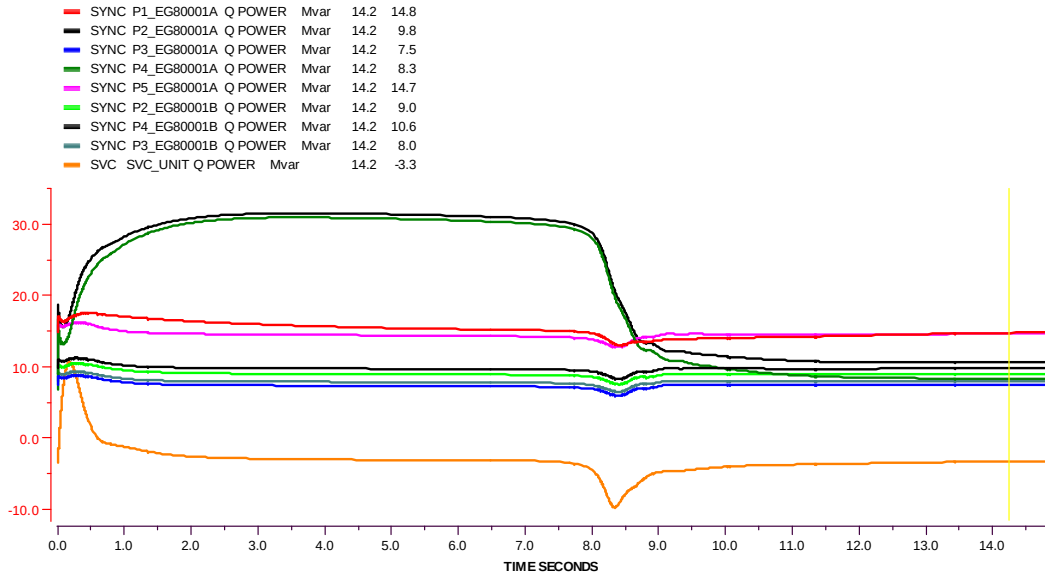

Appendix 2.4: Graphs of Case A1 - Starting of 9MW motor at PF4, no wind, Star Topology, SVC effect

Case A1: Starting of 9MW asynchronous motor at PF4, No wind penetration for "Star" Topology with 36kV voltage system. Power Load flow - Single Line Diagram representation shows load bus voltages ref.13.8kV in pu(blue colour), main platforms voltages 36kV (red colour), power generation at GTs (purple colour) with power flow situation

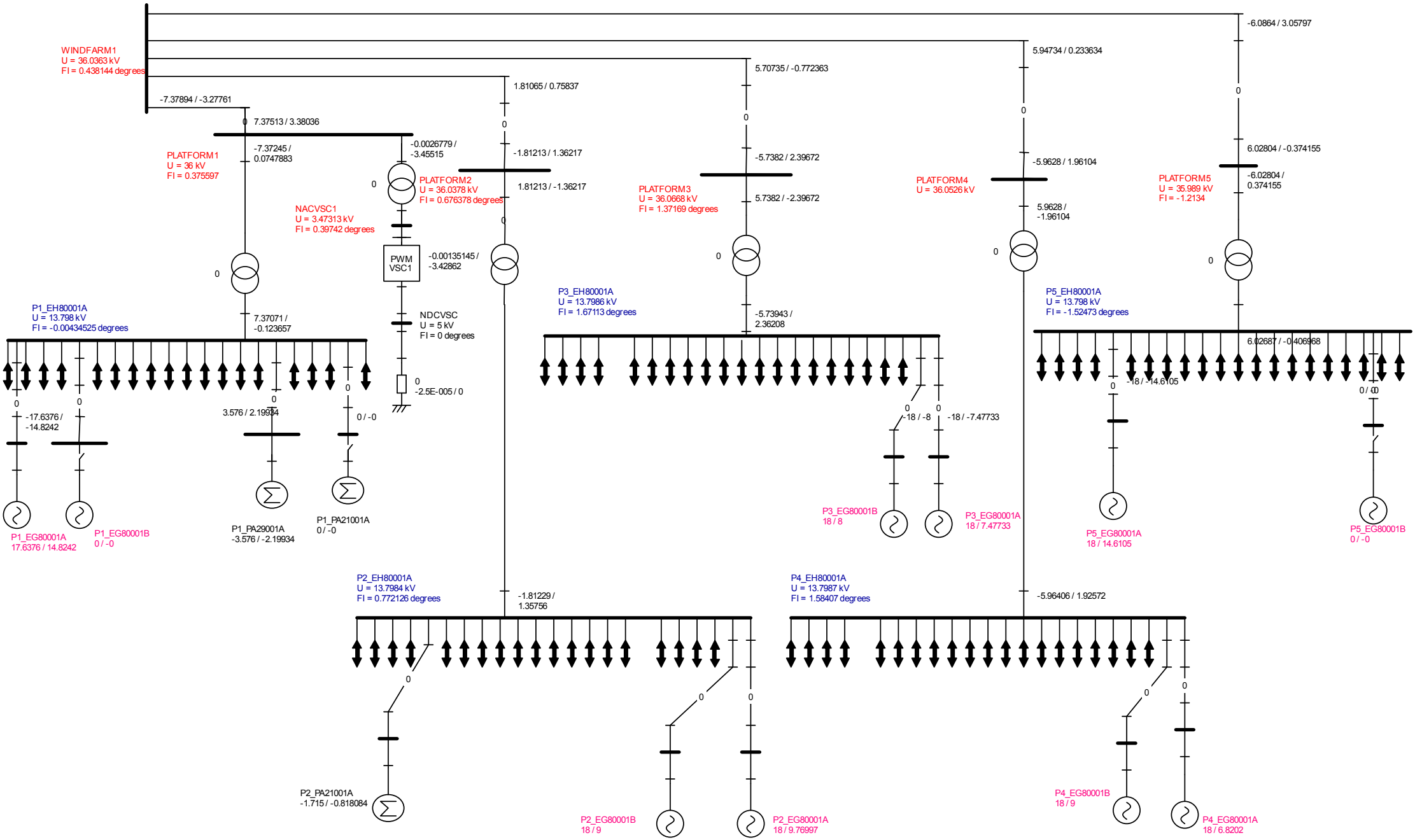

Case A1, Starting of 9MW motor at PF4 for "Star Topology", No wind penetration, 36kV Voltage system. Diagrams of Frequency variation at load buses, Load bus voltage ref. to 13.8kV in pu, Active Power and Reactive Power behavior at different platform GTs with effect of STATCOM at Platform1.

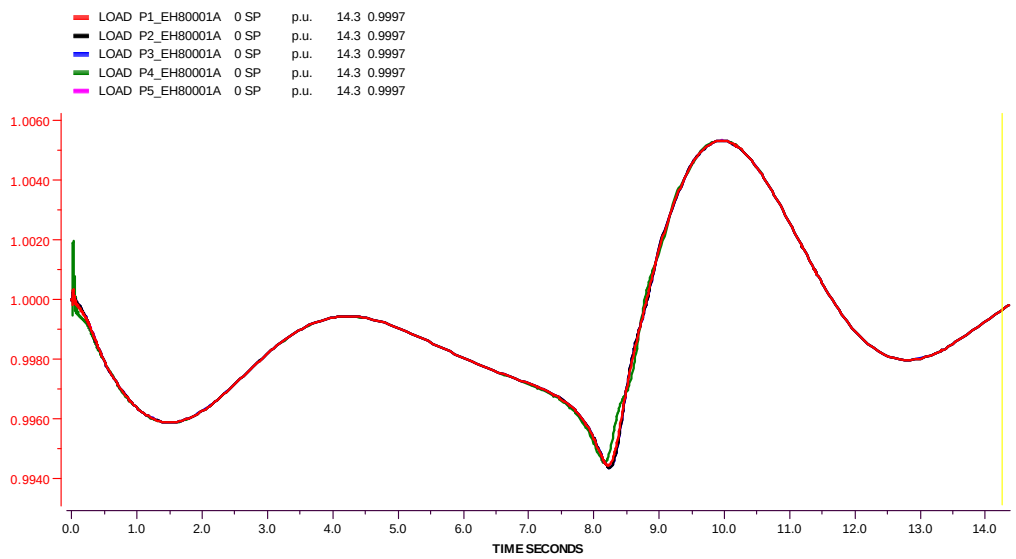

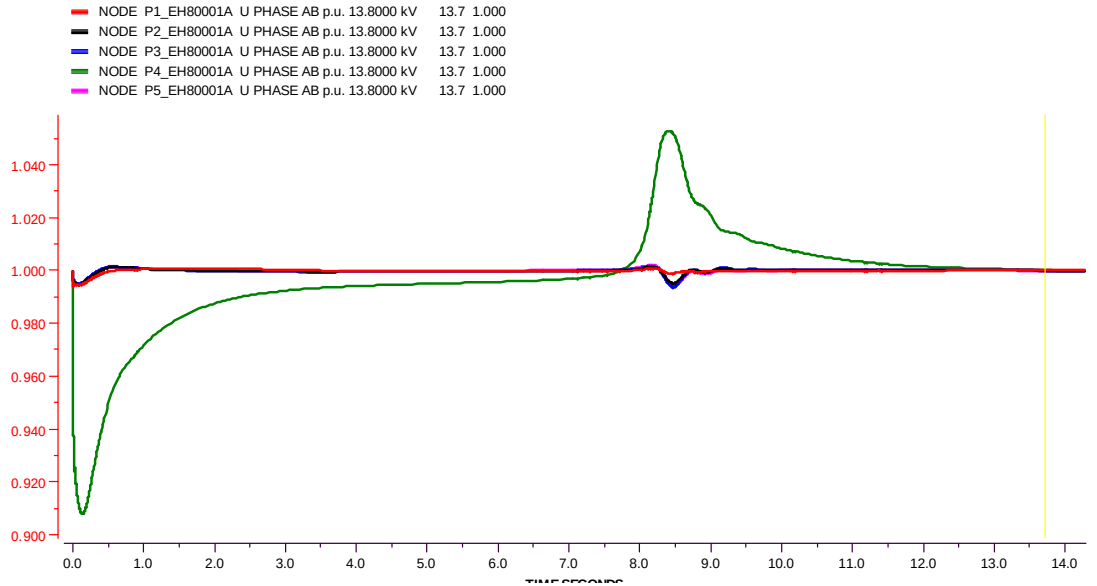

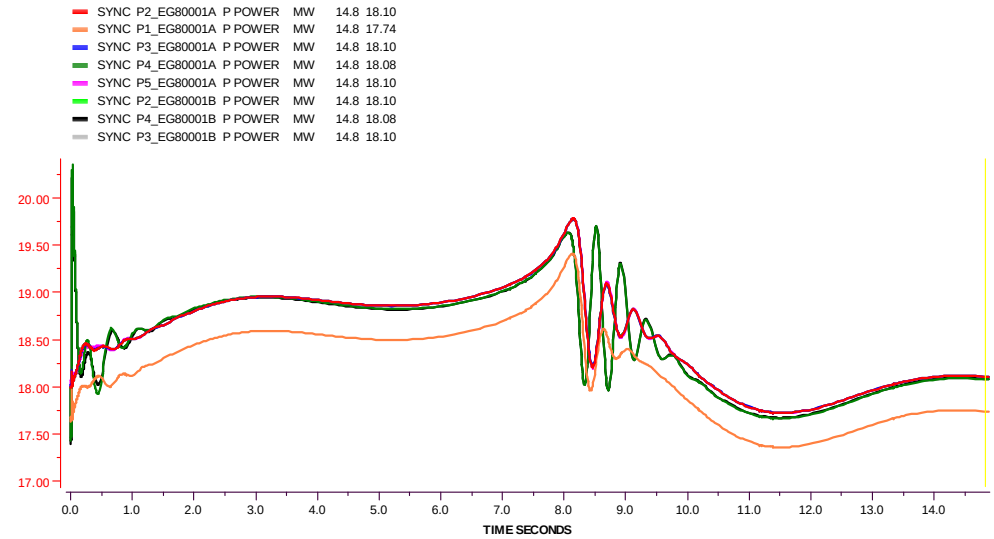

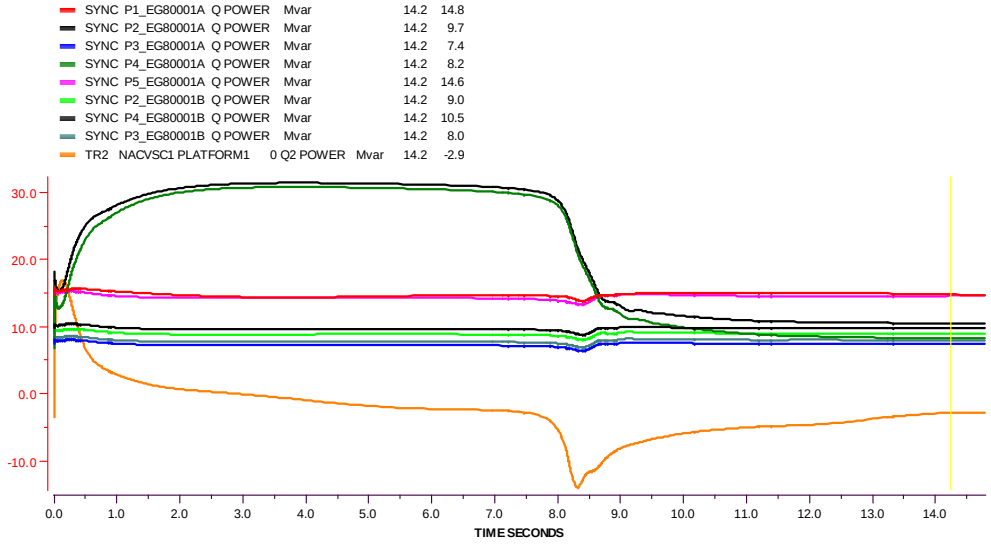

Appendix 2.6: Diagrams of Case A1 - Starting of 9MW motor at PF4, no wind, Star Topology , STATCOM effect

Case A1: Starting of 9MW asynchronous motor at PF4, No wind penetration for "Star-F" Topology with 36kV voltage system. Power Load flow - Single Line Diagram representation shows load bus voltages 13.8kV (blue colour), platforms voltage (red colour), generation at different platforms (purple colour) and power flow situation of whole network.

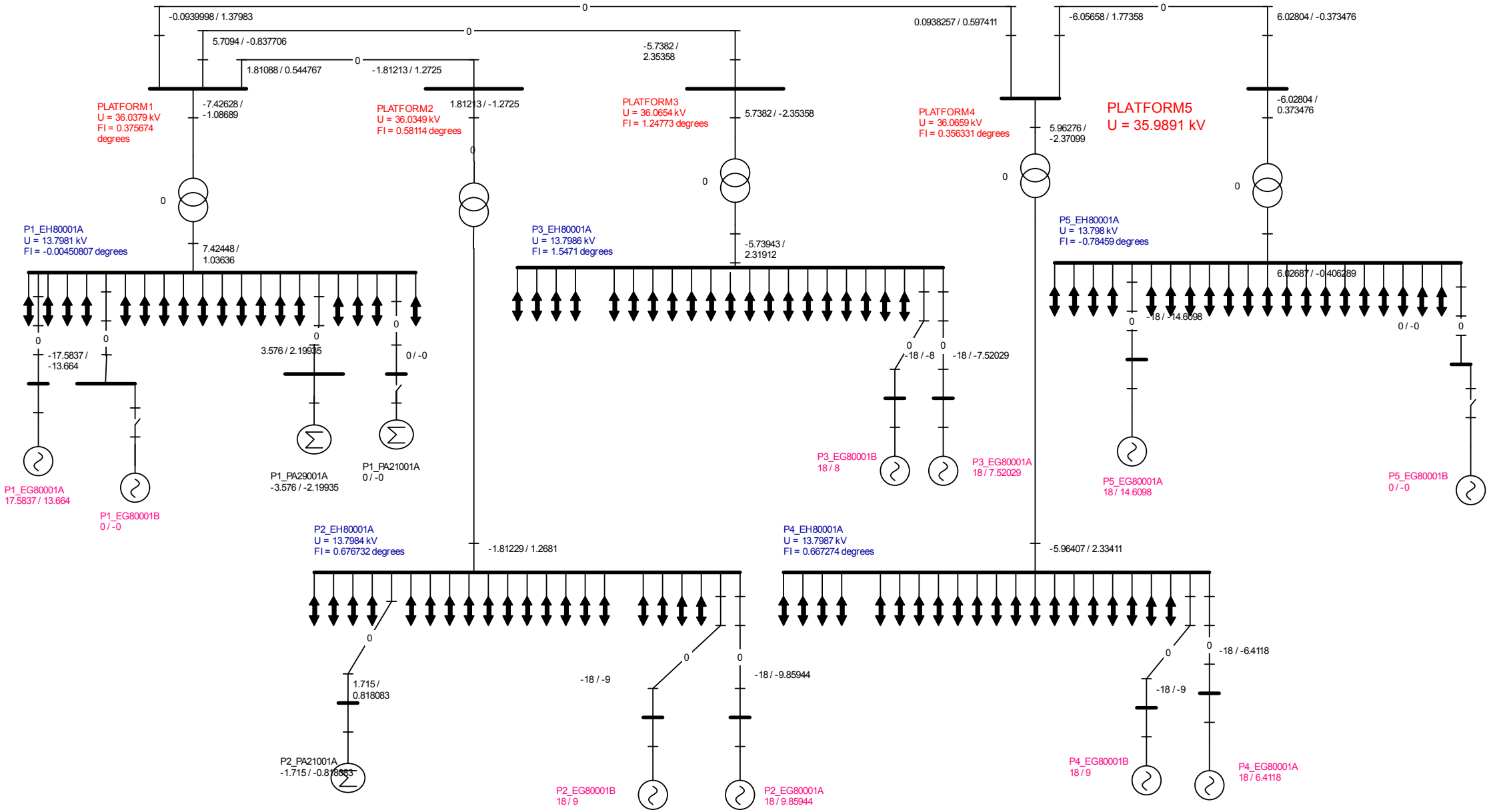

Appendix 2.7: SLD of Case A1 - Starting of 9MW motor at PF4, no wind, Star-F Topology

Case A1, Starting of 9MW motor at PF4 for "Star-F Topology", No wind penetration, 36kV Voltage system. Diagram represents, Frequency variation at different platform buses, Load Bus Voltage variation ref. to 13.8kV in pu, Active Power and Reactive Power behavior at different GTs. No effect of SVC and STATCOM are considered.

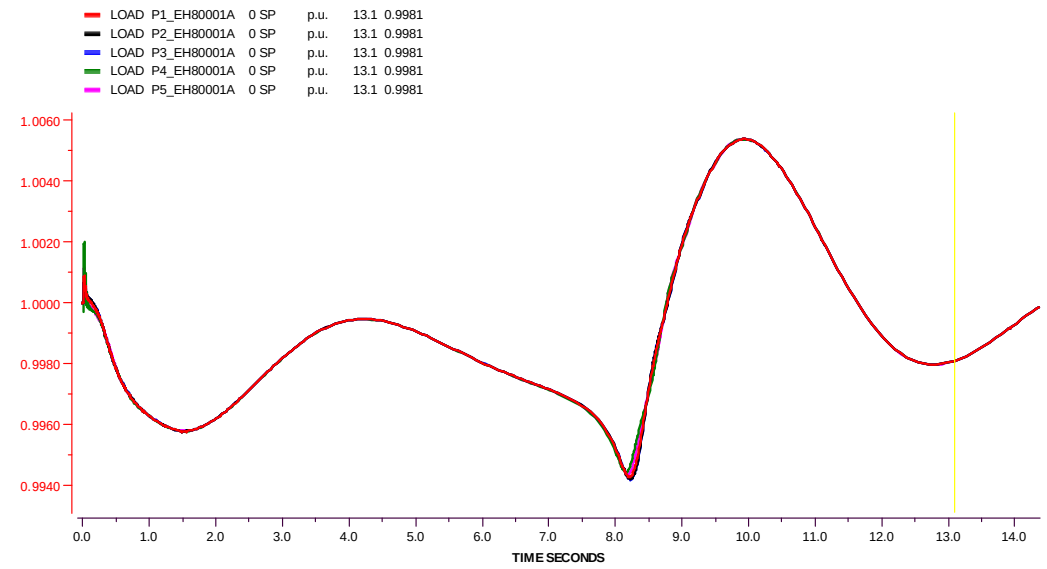

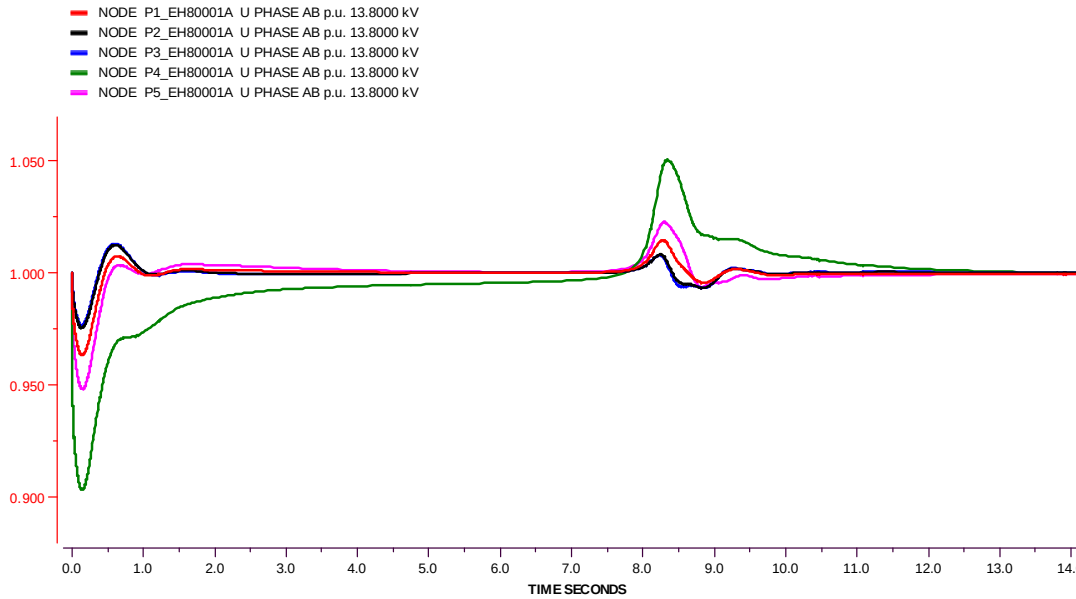

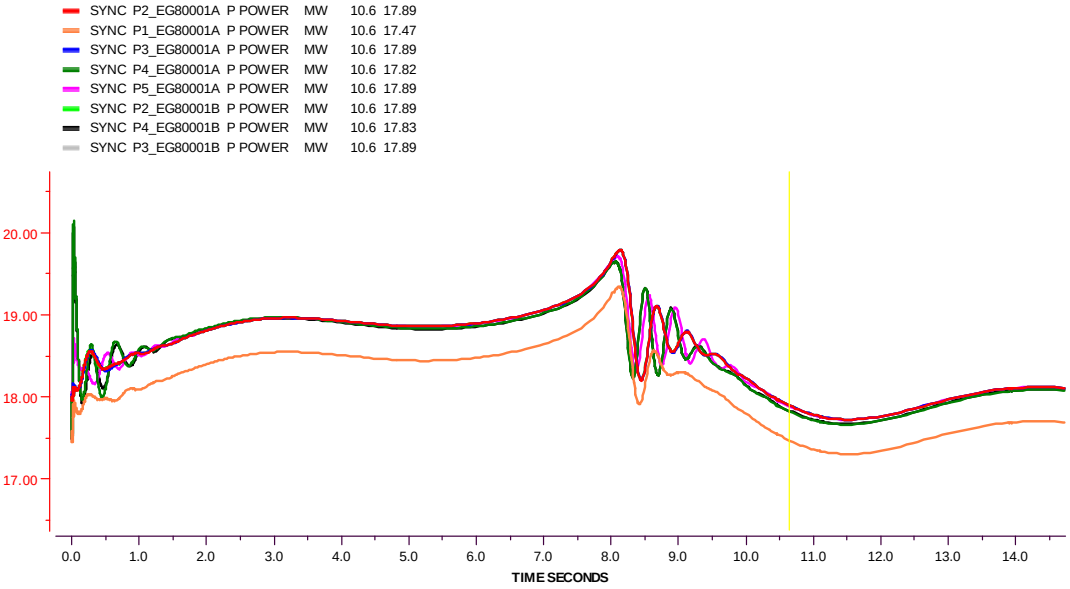

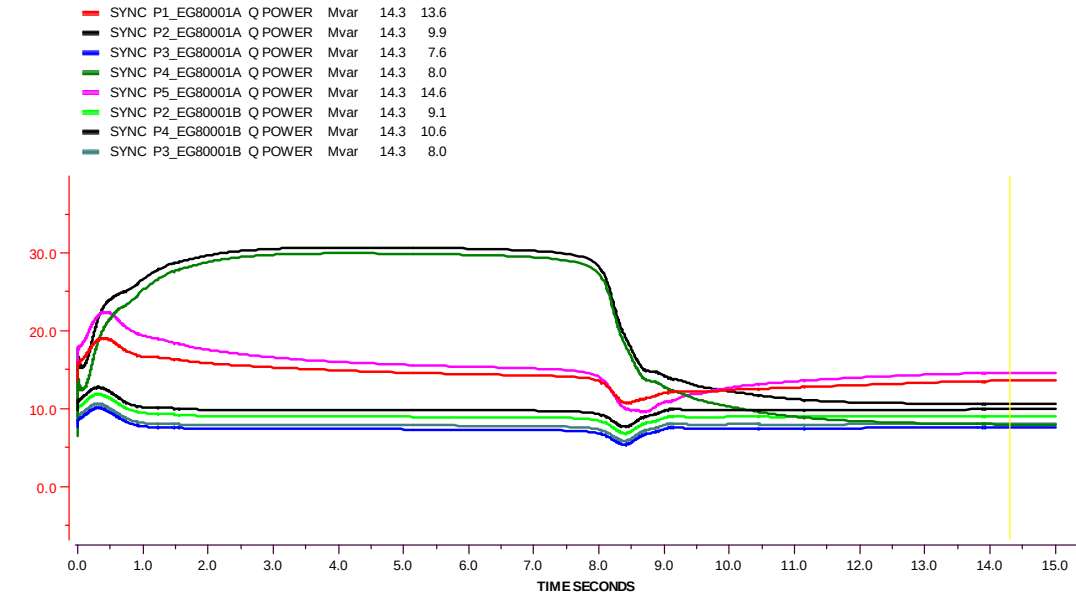

Appendix 2.8: Diagrams of Case A1 - Starting of 9MW motor at PF4, no wind, Star-F Topology

Case A1: Starting of 9MW asynchronous motor at PF4, No wind penetration for "Mesh" Topology with 36kV voltage system. Power Load flow - Single Line Diagram representation shows load bus voltages 13.8kV (blue colour), platforms voltage (red colour), generation at different platforms (purple colour) and power flow situation of whole network.

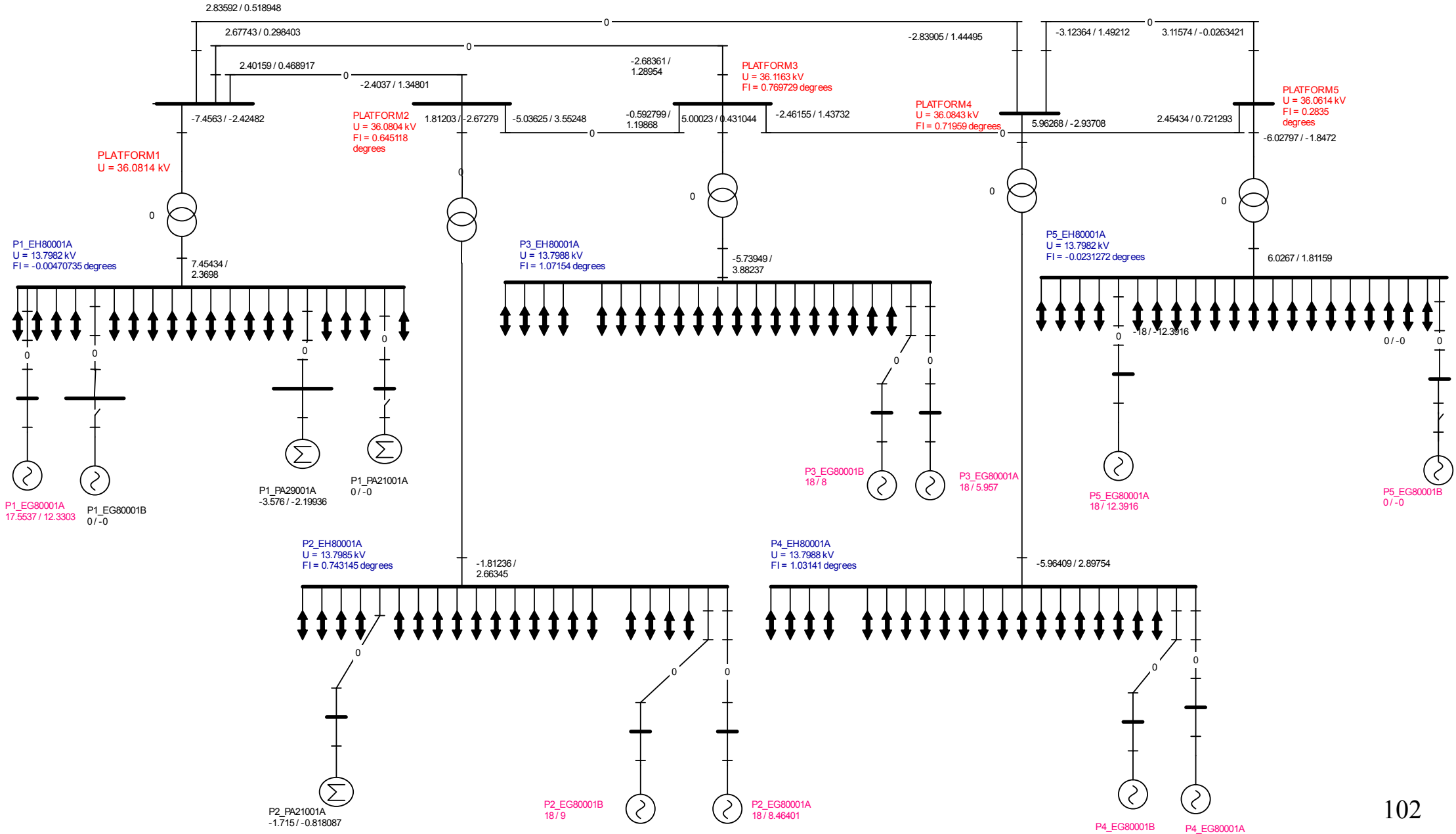

Appendix 2.9: SLD of Case A1 - Starting of 9MW motor at PF4, no wind, Mesh Topology

Case A1: Starting of 9MW motor at PF4 for "Mesh Topology", No wind penetration, 36kV Voltage system. Graphs of Frequency, Load Bus Voltage ref. 13.8kV in pu, Active Power and Reactive Power behavior at different GTs. No effect of SVC and STATCOM considered.

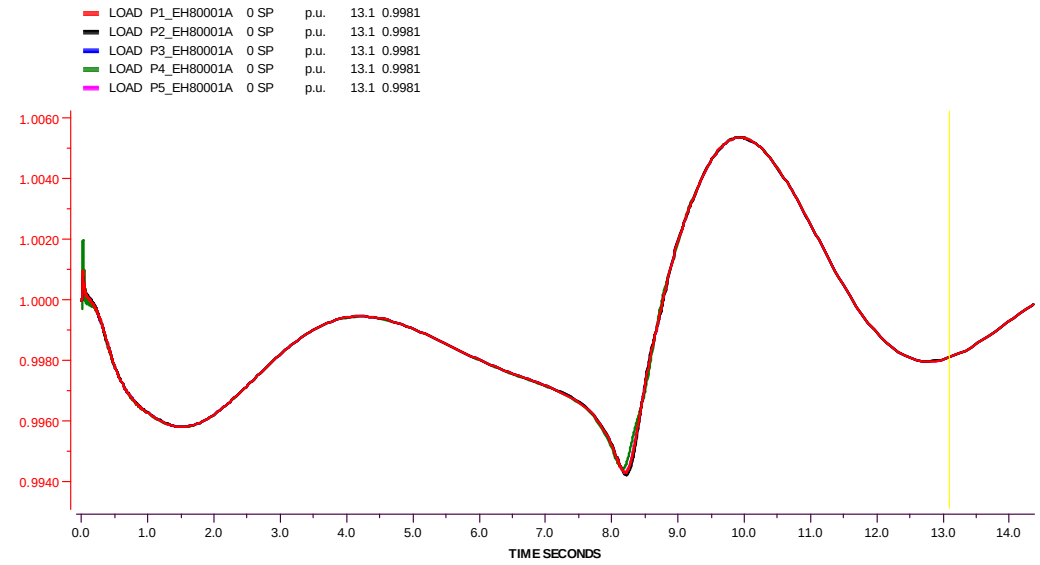

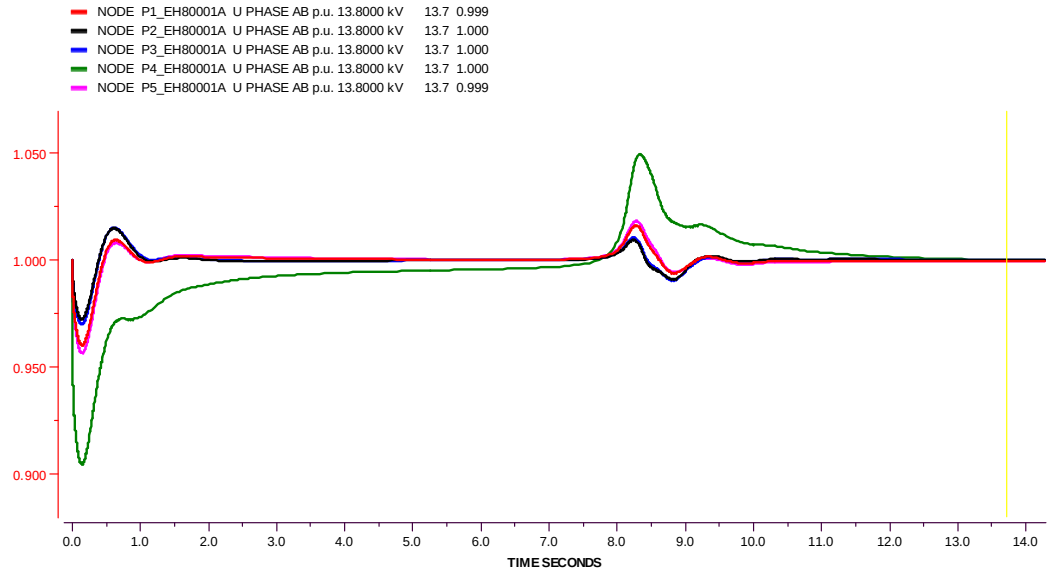

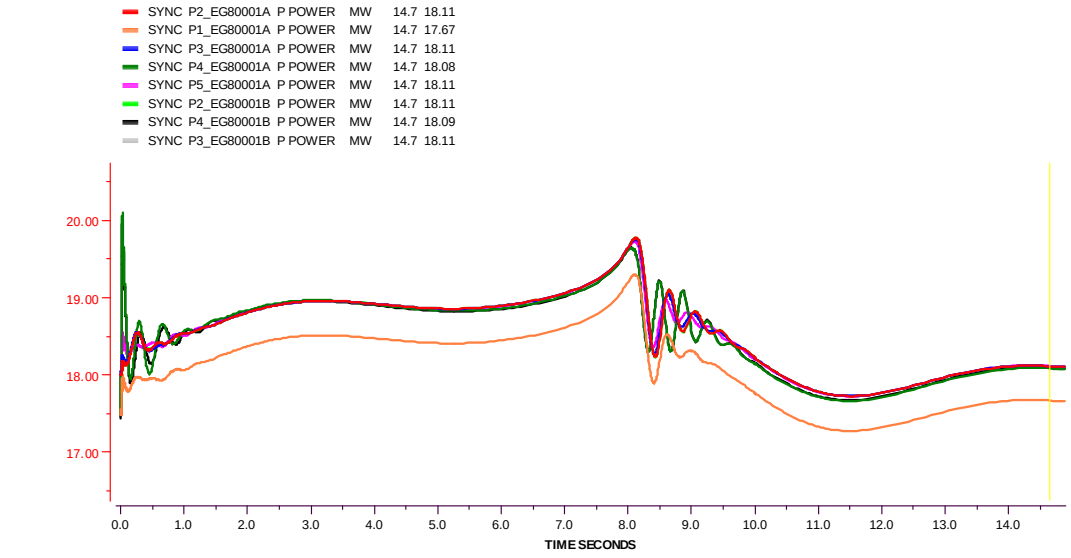

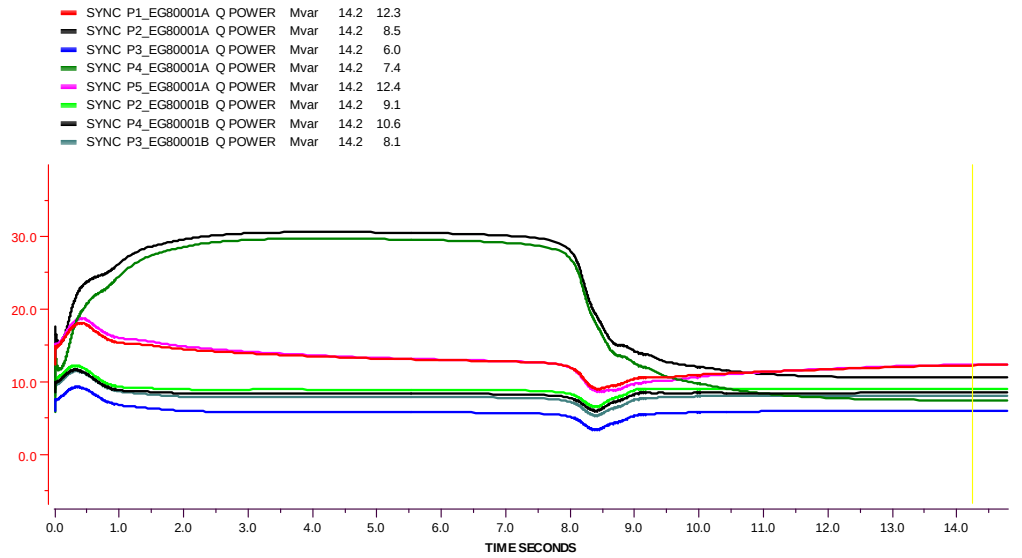

Case A2: Starting of 9MW motor at PF4, 100 MW wind penetration for "Star Topology" - 36kV voltage system. Single line diagram - Power flow analysis, GTs in operation with equal load sharing. No effect of SVC or STATCOM considered. SLD represents platform load bus voltages - 13.8kV (blue colour), main platforms interconnection voltages - 36kV (red colour) and power generation at platforms with wind turbine (purple colour).

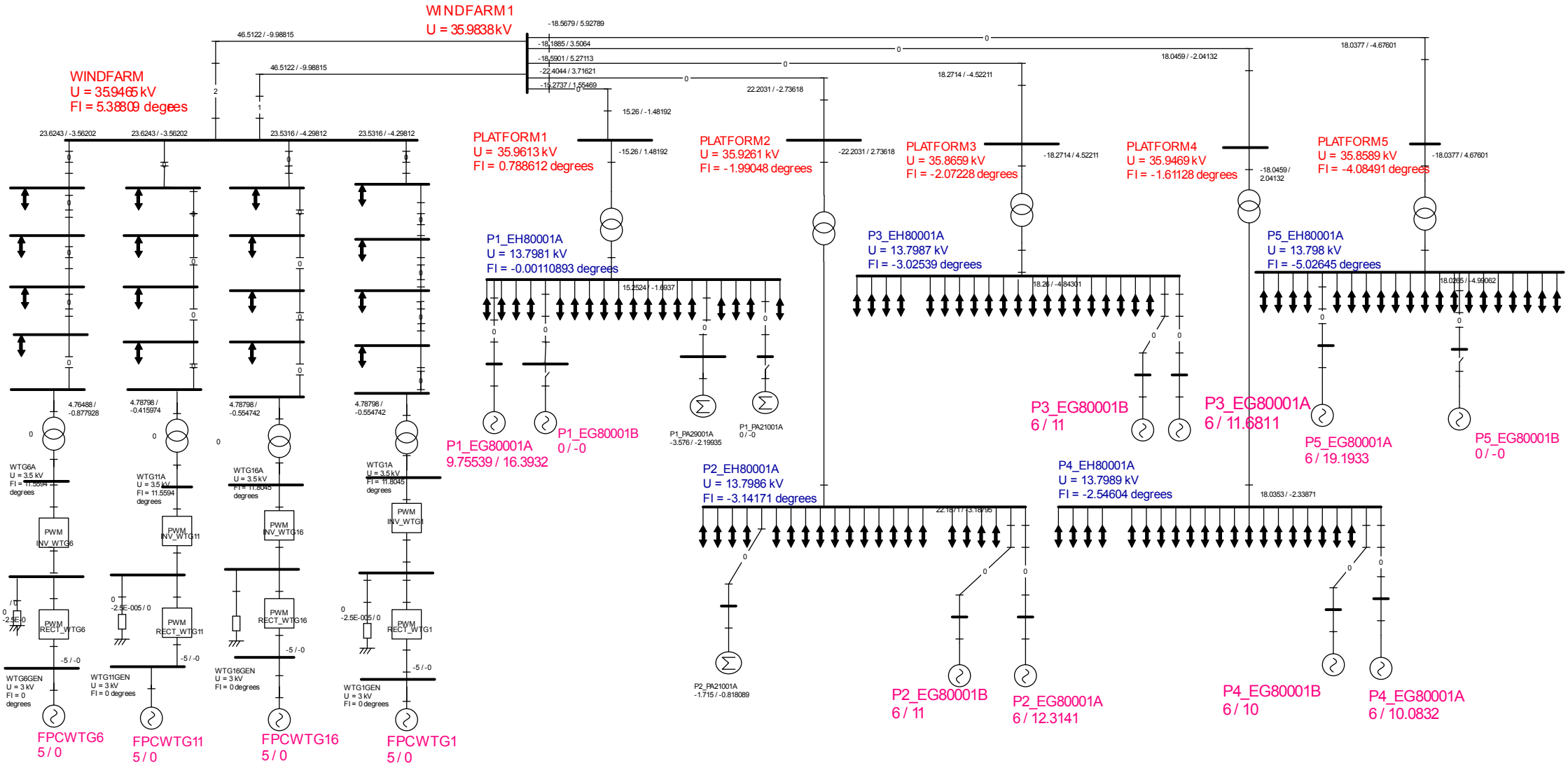

Appendix 2.11: SLD of Case A2 - Starting of 9MW motor at PF4, 100MW wind, Star Topology

Case A2: Starting of 9MW motor at PF4, 100 MW wind penetration for "Star Topology" - 36kV voltage system. Diagram represents frequency variations at different platform buses, 13.8kV load bus voltage variation, power at each online generators in MW and reactive power at each GTs in MVAr. No effect of SVC or STATCOM are considered.

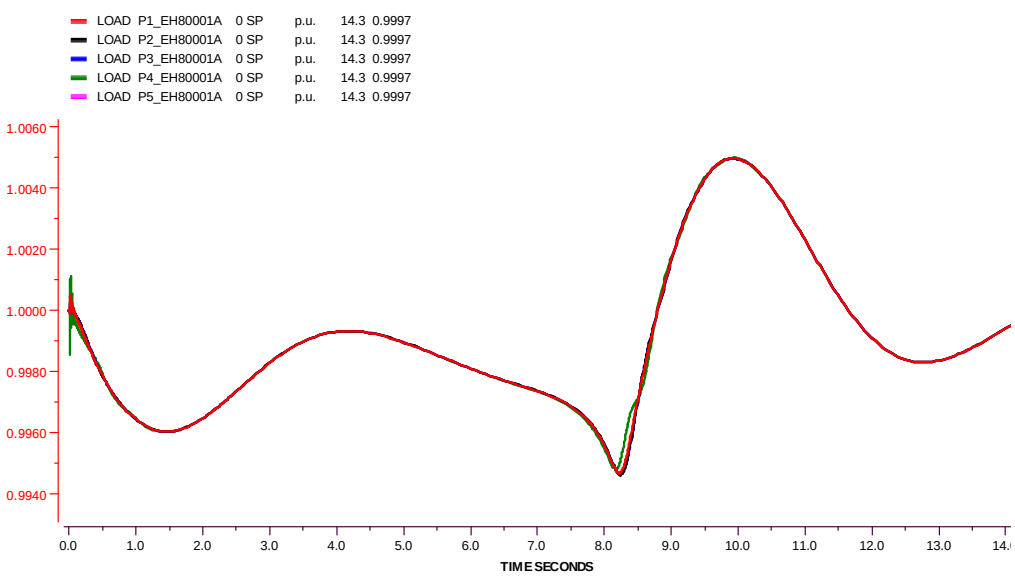

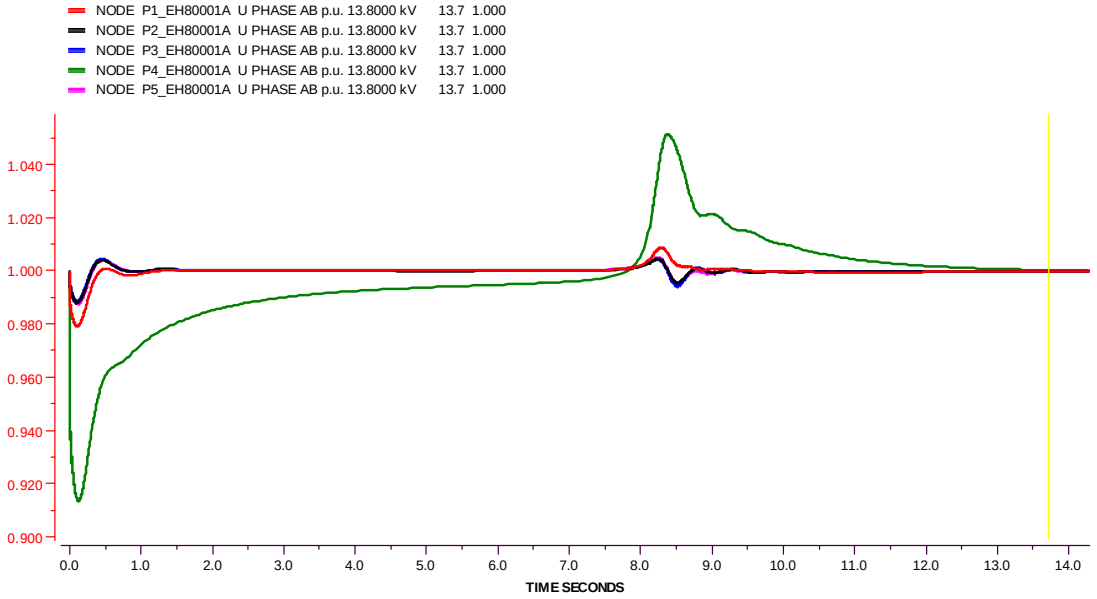

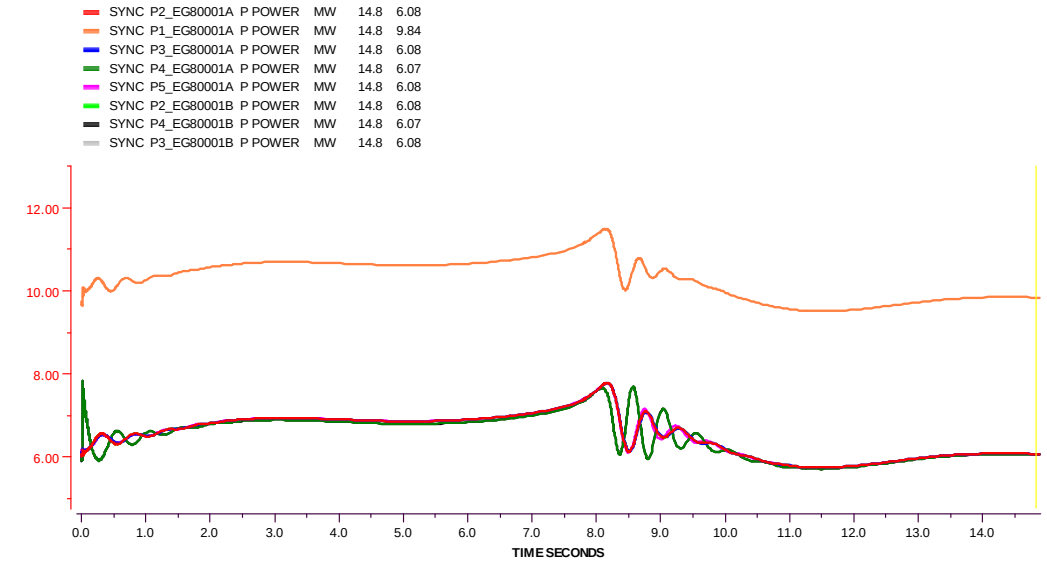

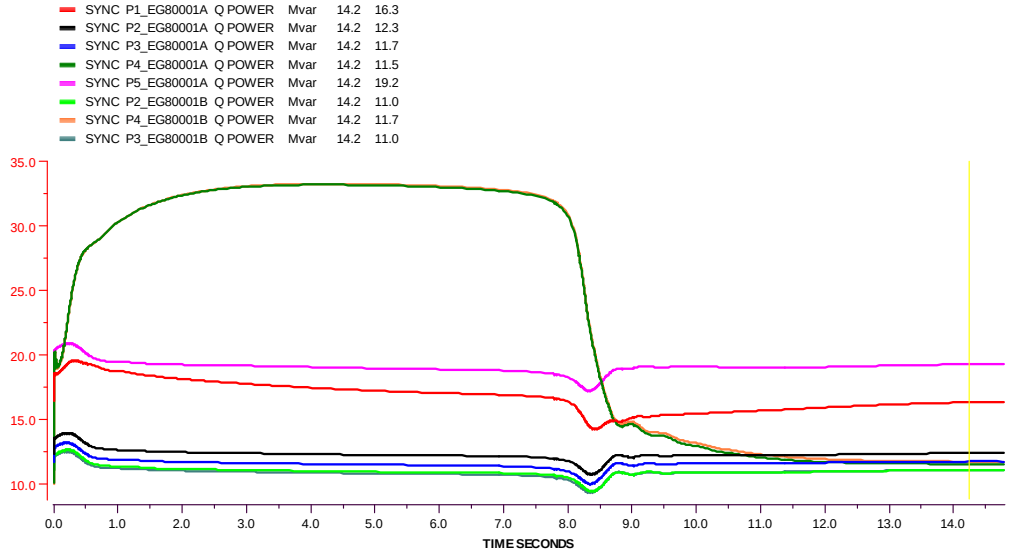

Appendix 2.12: Diagrams of Case A2 - Starting of 9MW motor at PF4, 100MW wind, Star Topology

Case A2: Starting of 9MW motor at PF4, 100 MW wind penetration for "Star-F Topology" - 36kV voltage system. Single line diagram - Power flow analysis, GTs at different PFs in operation with equal load sharing. No effect of SVC or STATCOM considered. SLD represents platform load bus voltages - 13.8kV (blue colour), main platforms interconnection voltages - 36kV (red colour) and power generation at platform GTs with wind turbine WTs (purple colour).

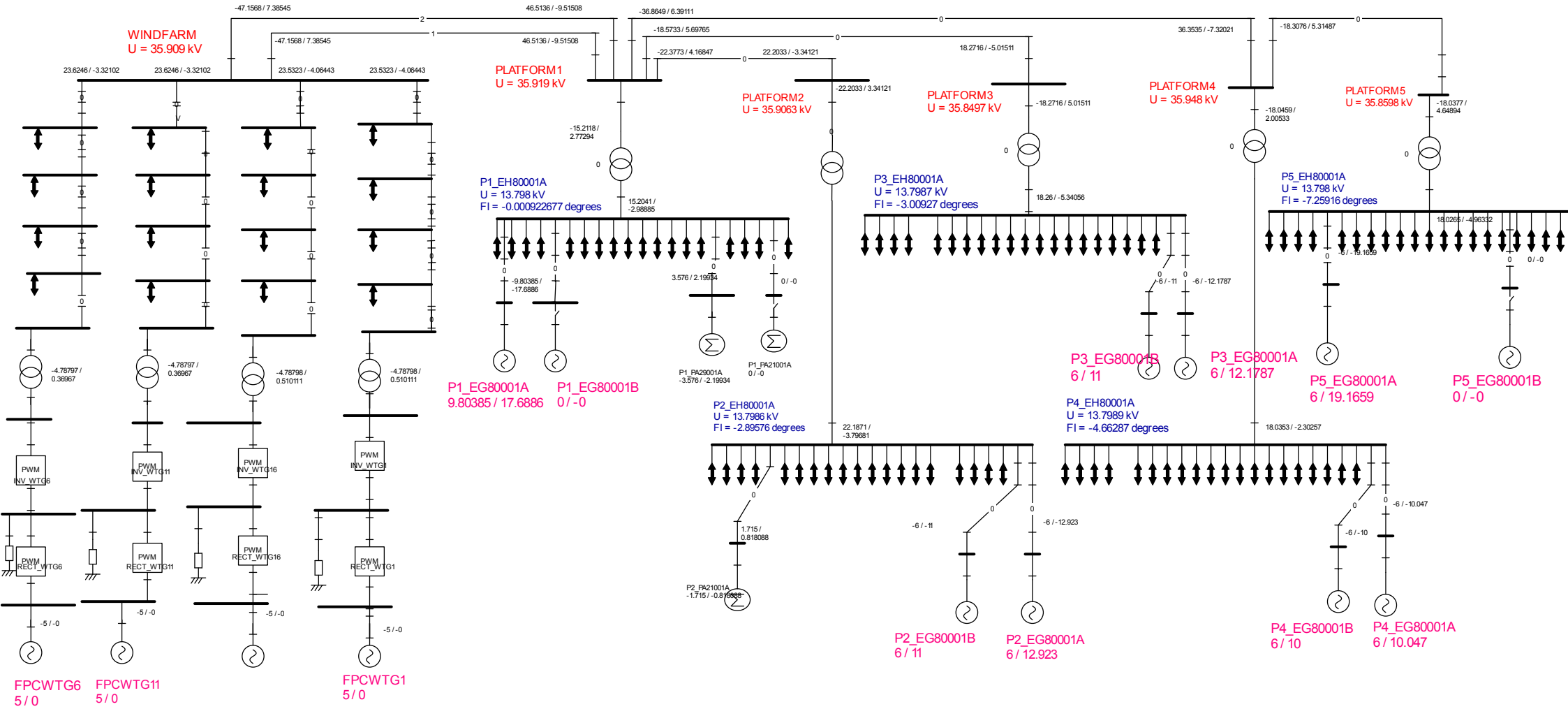

Appendix 2.13: SLD of Case A2 - Starting of 9MW motor at PF4, 100MW wind, Star-F Topology

Case A2: Starting of 9MW motor at PF4, 100 MW wind penetration for "Star-F Topology" - 36kV voltage system. Diagram represents frequency variations at different platform buses, 13.8kV load bus voltage variation, power at each online generators in MW and reactive power at each online GTs in MVAr. No effect of SVC or STATCOM are considered.

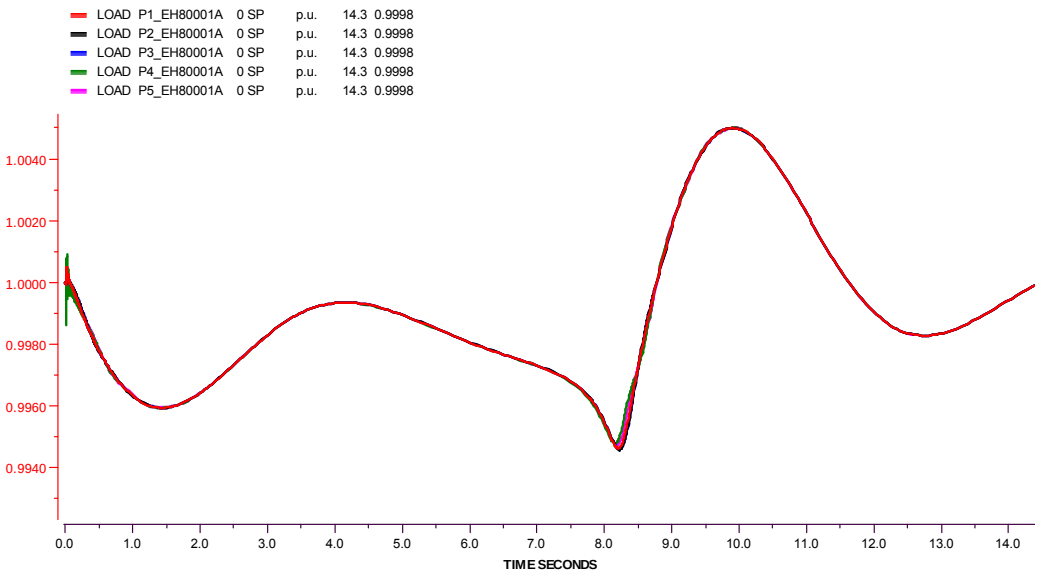

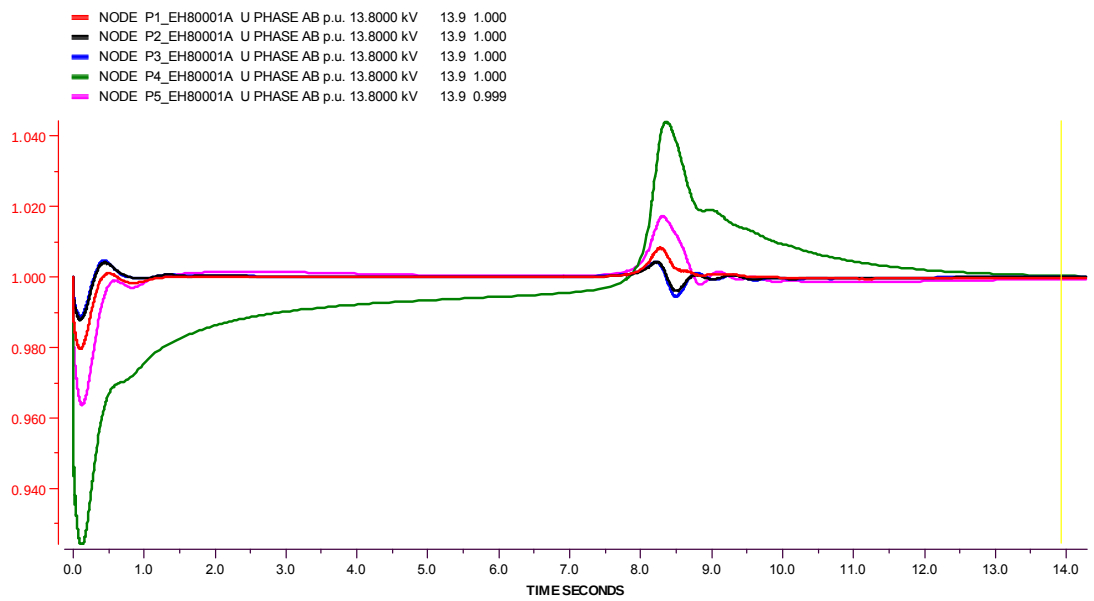

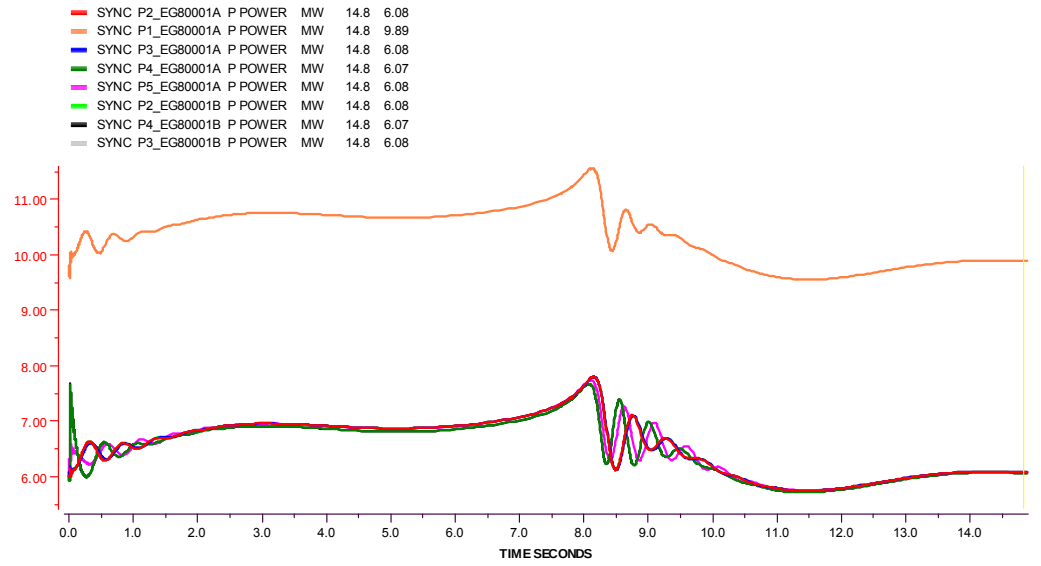

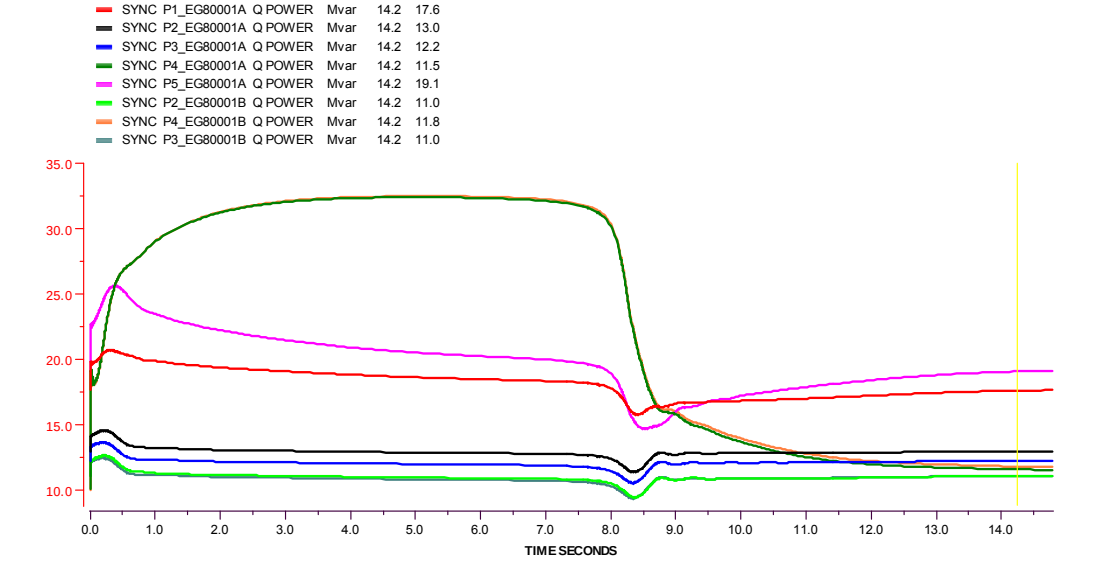

Case A2: Starting of 9MW motor at PF4, 100 MW wind penetration for "Mesh Topology" - 36kV voltage system. Single line diagram - Power flow analysis, GTs at different PFs in operation with equal load sharing. No effect of SVC or STATCOM considered. SLD represents platform load bus voltages - 13.8kV (blue colour), main platforms interconnection voltages - 36kV (red colour) and power generation at platform GTs with wind turbine WTs (purple colour).

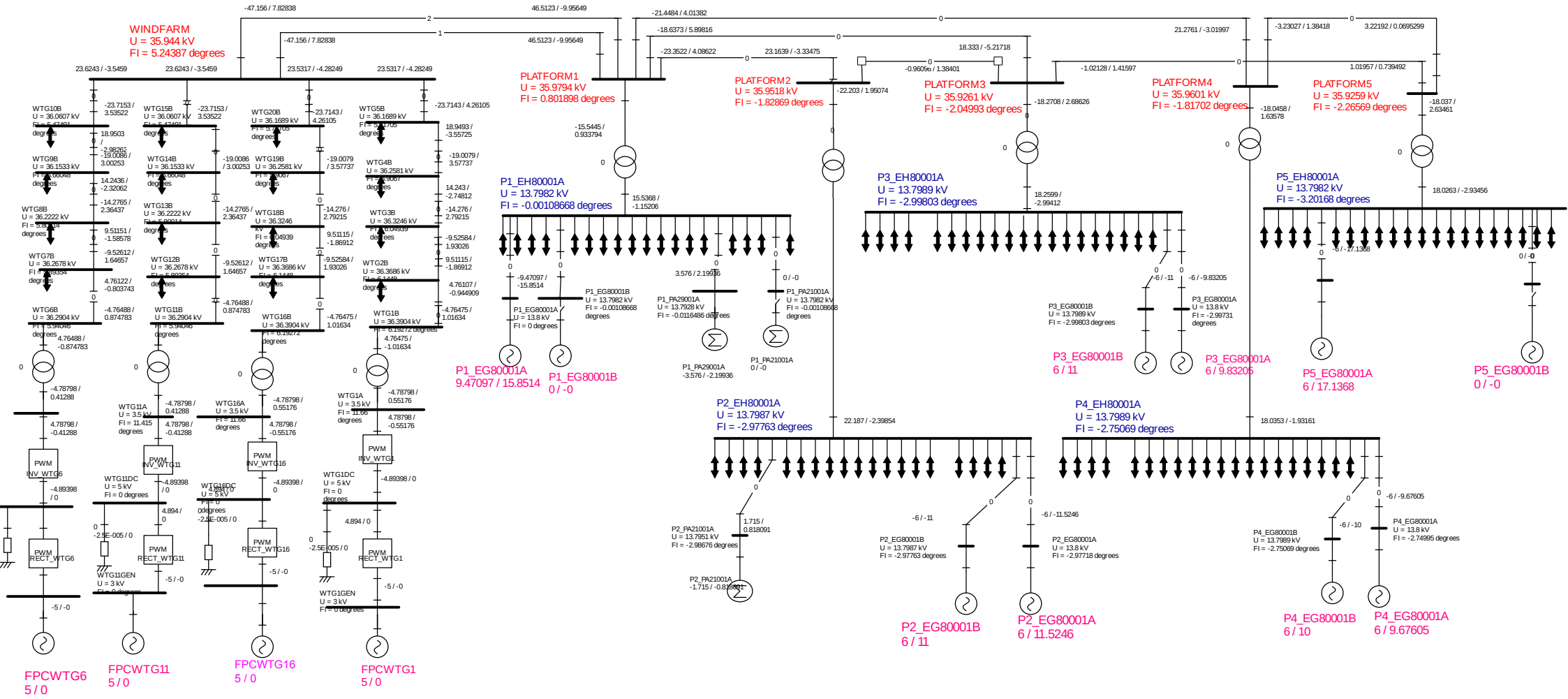

Appendix 2.15: SLD of Case A2 - Starting of 9MW motor at PF4, 100MW wind, Mesh Topology

Case A2: Starting of 9MW motor at PF4, 100 MW wind penetration for "Mesh Topology" - 36kV voltage system. Diagram represents frequency variations at different platform buses, 13.8kV load bus voltage variation, power at each online generators in MW and reactive power at each online GTs in MVAr. No effect of SVC or STATCOM are considered.

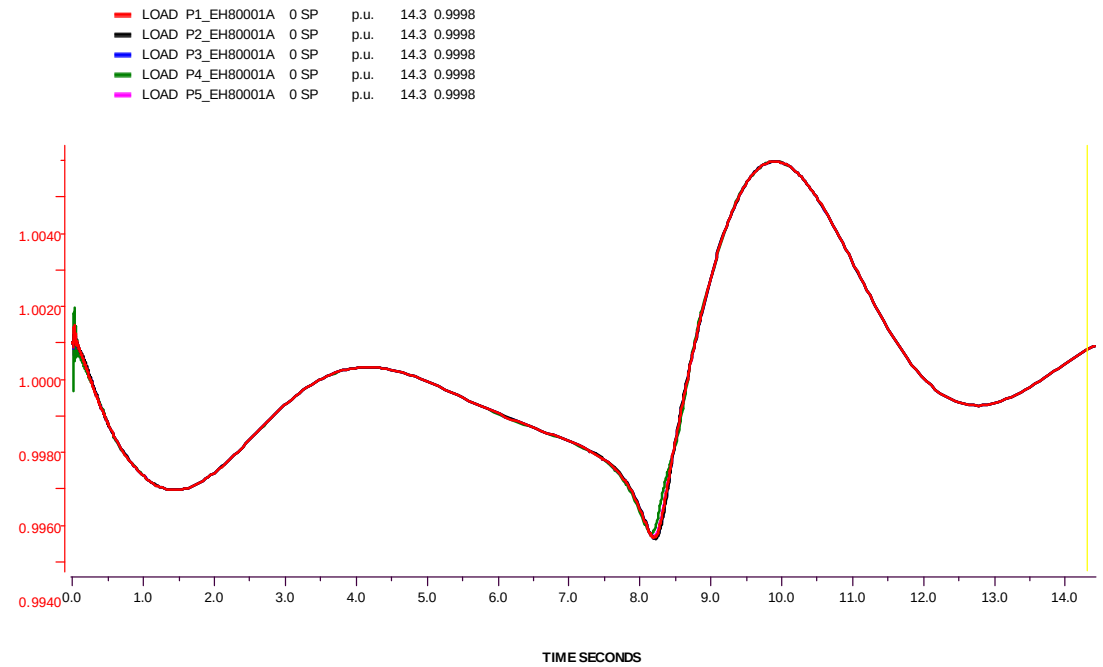

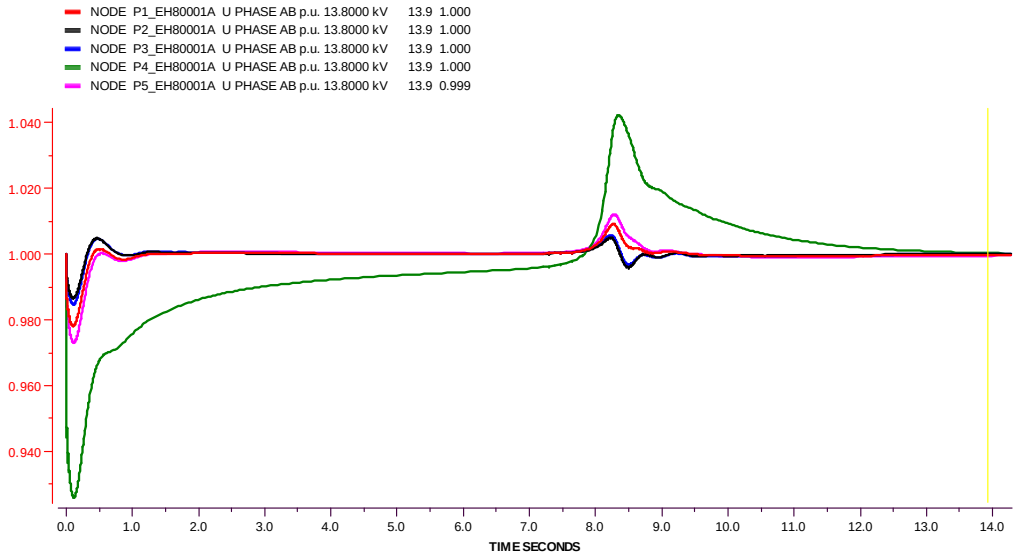

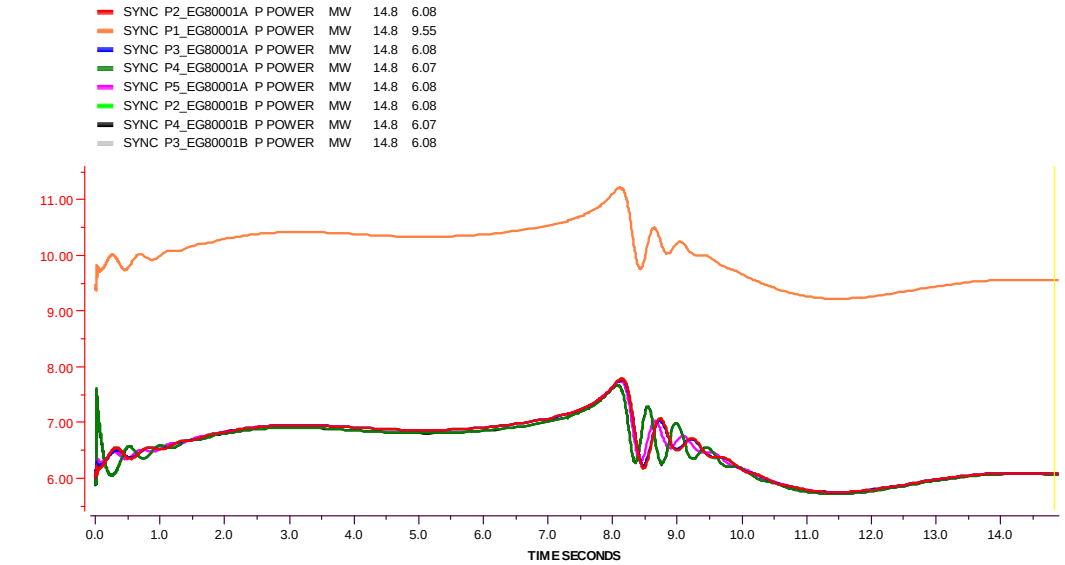

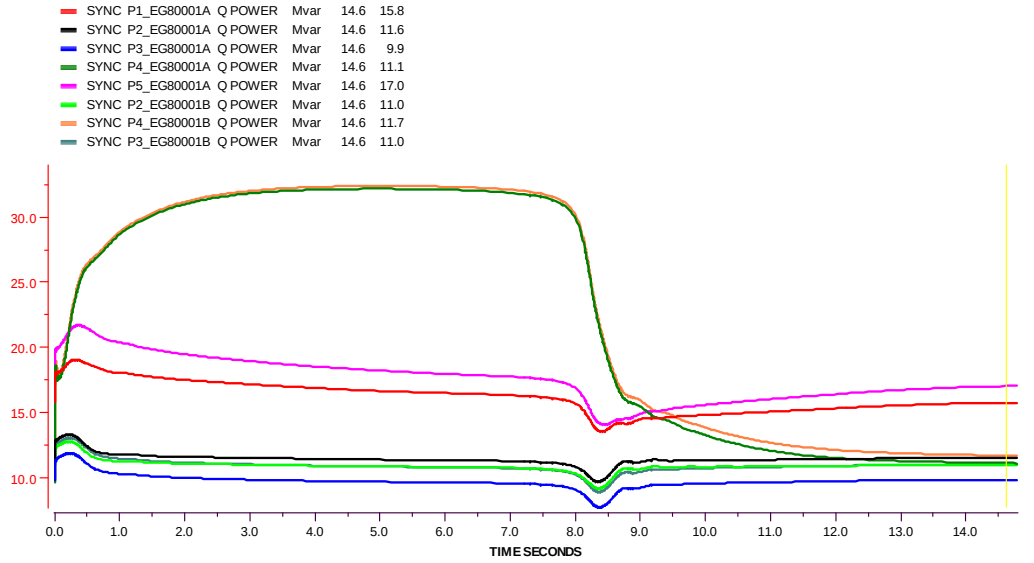

Case B1: Loss of a Gas Turbine at PF4 (Platform4), No wind penetration for "Star" Topology with 36kV voltage system. Power flow - Single Line Diagram indicates Platform load bus voltages of 13.8kV (blue colour), main platform voltages (red colour), power generation at different 9 online GTs (purple colour) and power flow situation of whole network.

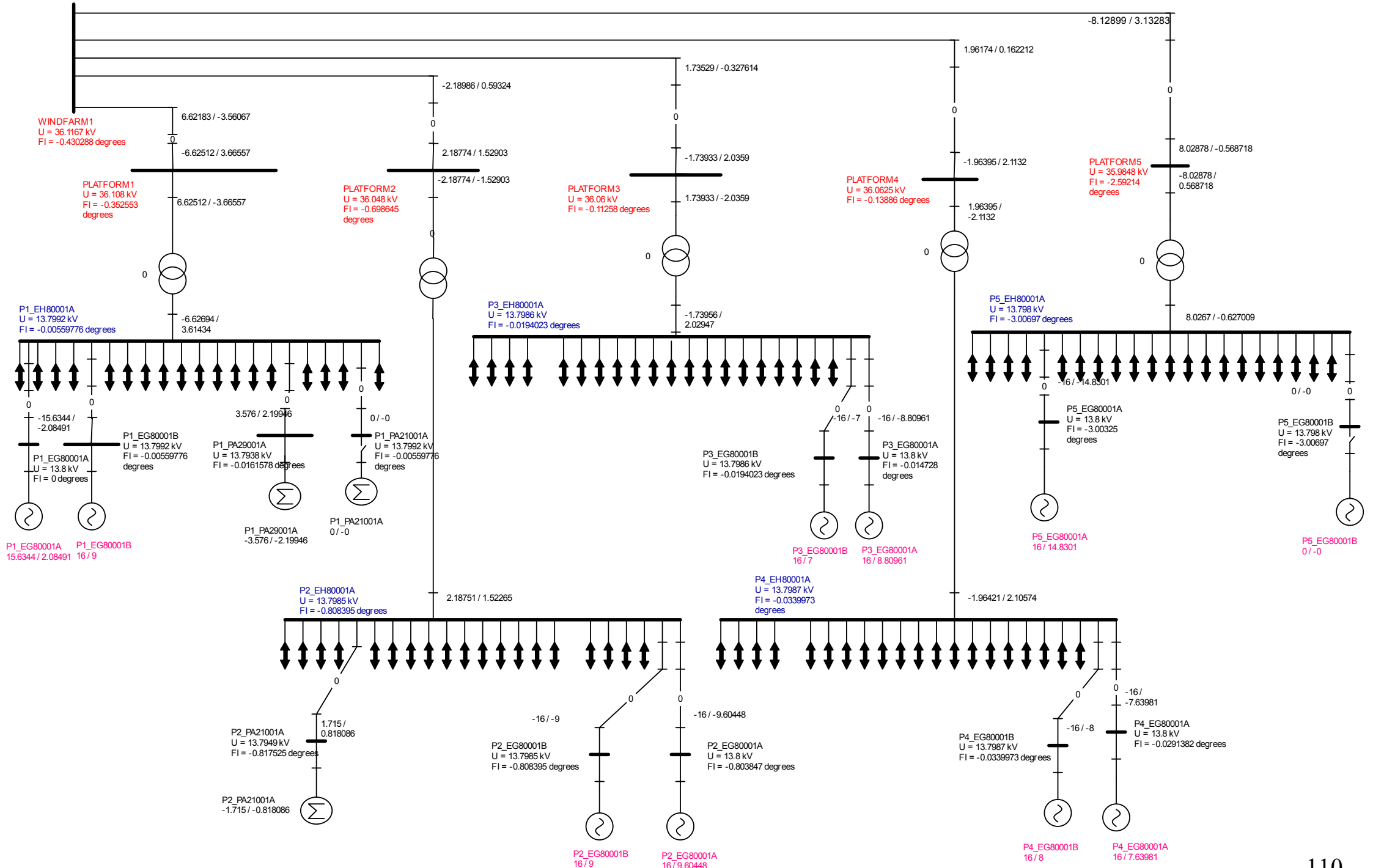

Appendix 2.17: SLD of Case B1 – Loss of a GT at PF4, no wind, Star Topology

Case B1: Loss of Gas Turbine at PF4 for "Star Topology", No wind penetration, with 36kV Voltage system. Graphs of Frequency variation at different platform buses, Load bus voltage variation ref. to 13.8kV in pu, Active power and reactive power behavior at different online platform GTs.

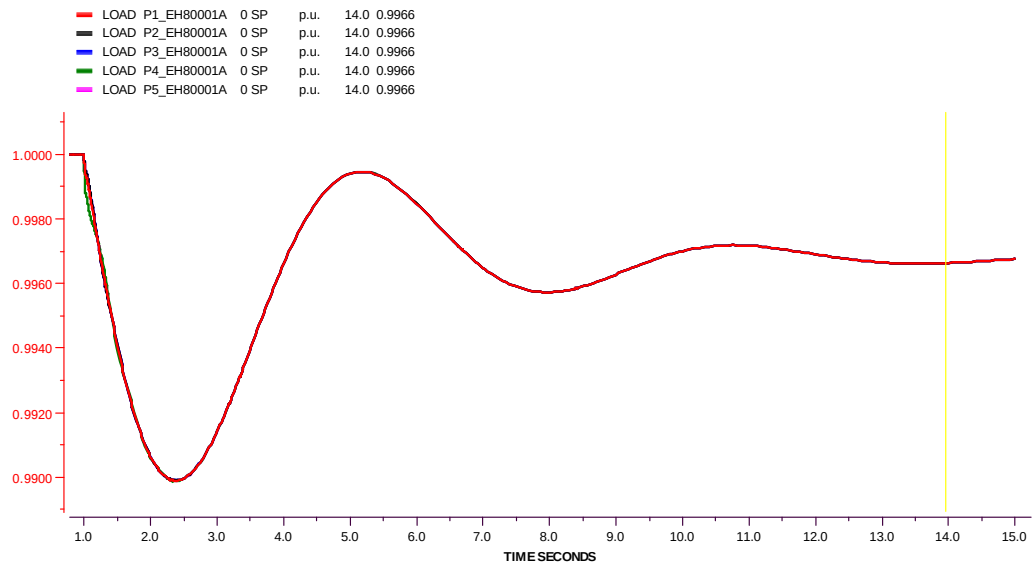

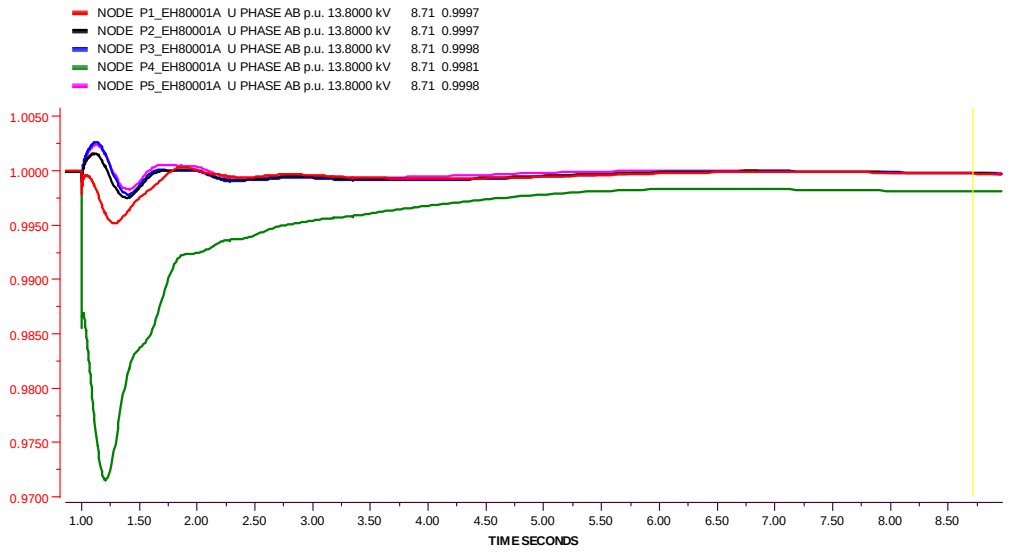

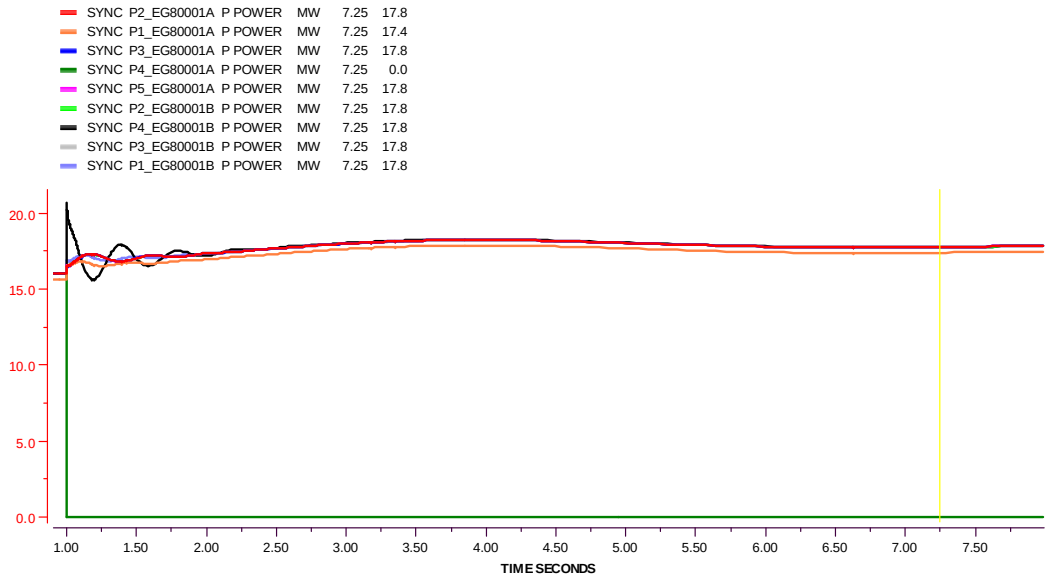

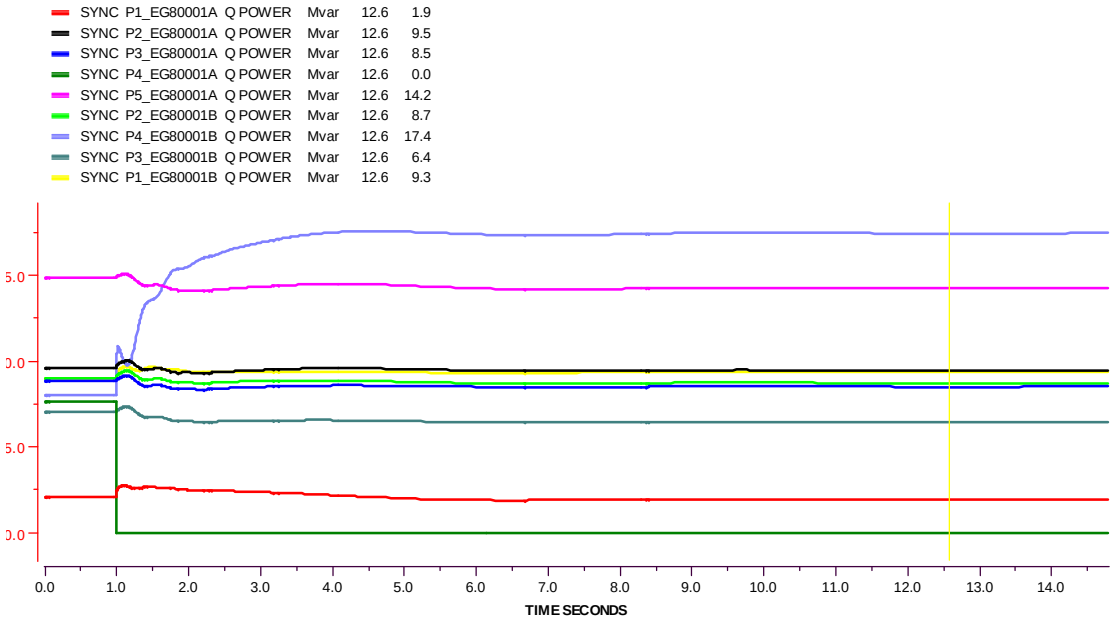

Appendix 2.18: Diagram of Case B1 – Loss of a GT at PF4, no wind, Star Topology

Case B2: Loss of a Gas Turbine at PF4 (Platform4), 100MW wind penetration for "Star" Topology with 36kV voltage system. Power flow - Single Line Diagram indicates different platform load bus voltages of 13.8kV (blue colour), main platform voltages (red colour), power generation at different 9 online GTs (purple colour) and power flow situation of whole network.

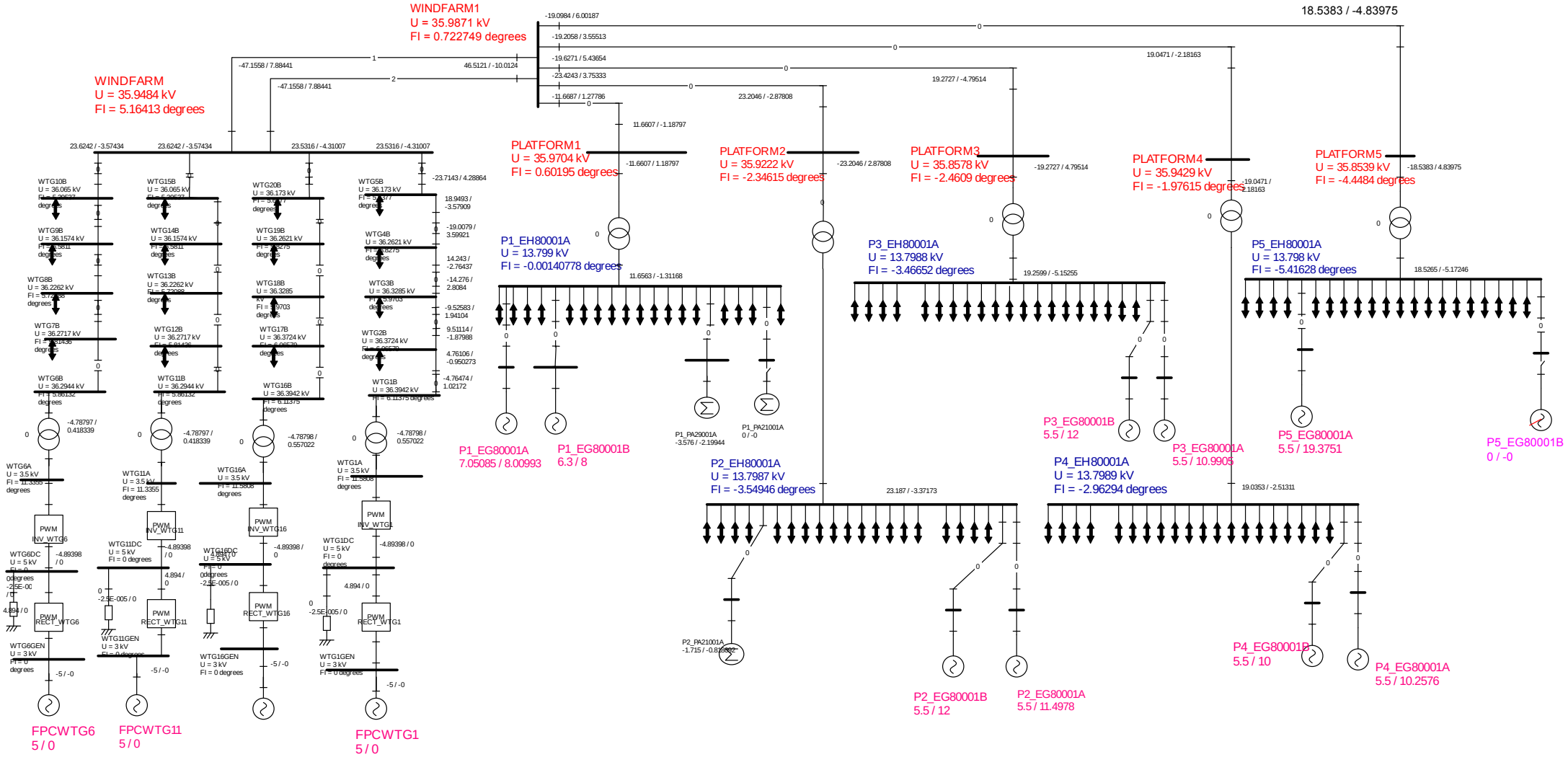

Case B2: Loss of Gas Turbine at PF4 for "Star Topology", 100MW wind penetration, with 36kV Voltage system. Graphs of Frequency variation at different platform buses, Load bus voltage variation ref. to 13.8kV in pu, Active power and reactive power behavior at different online platform GTs at different platforms.

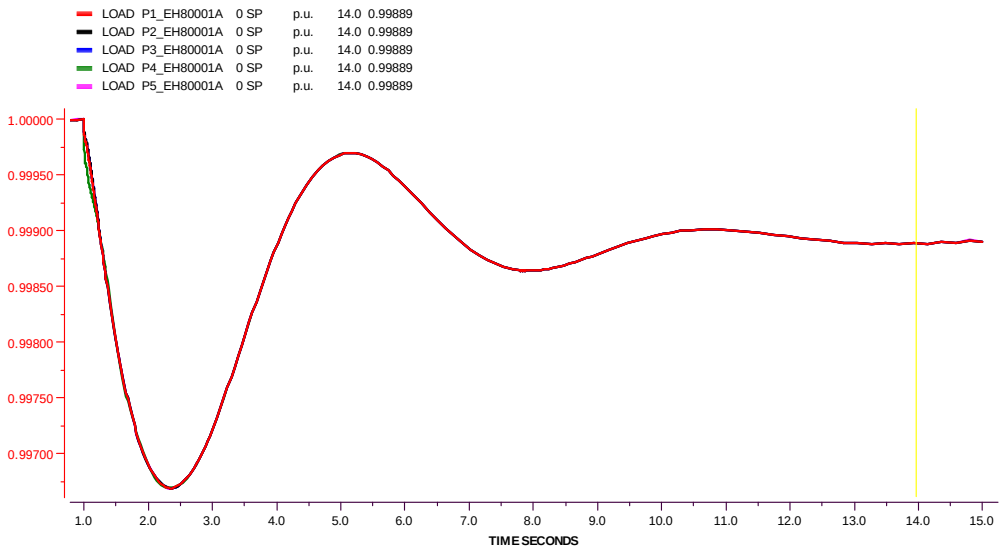

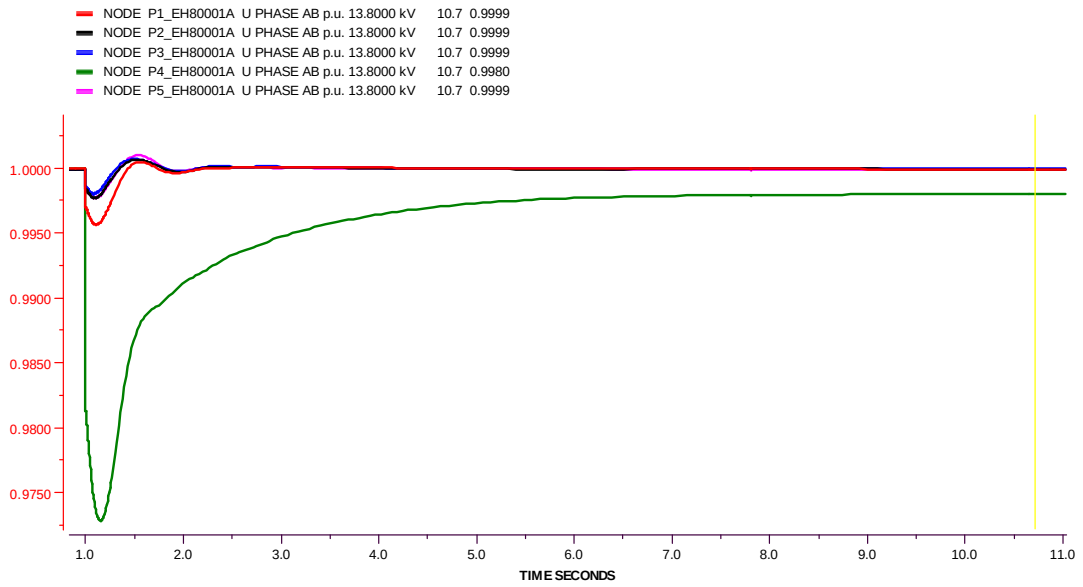

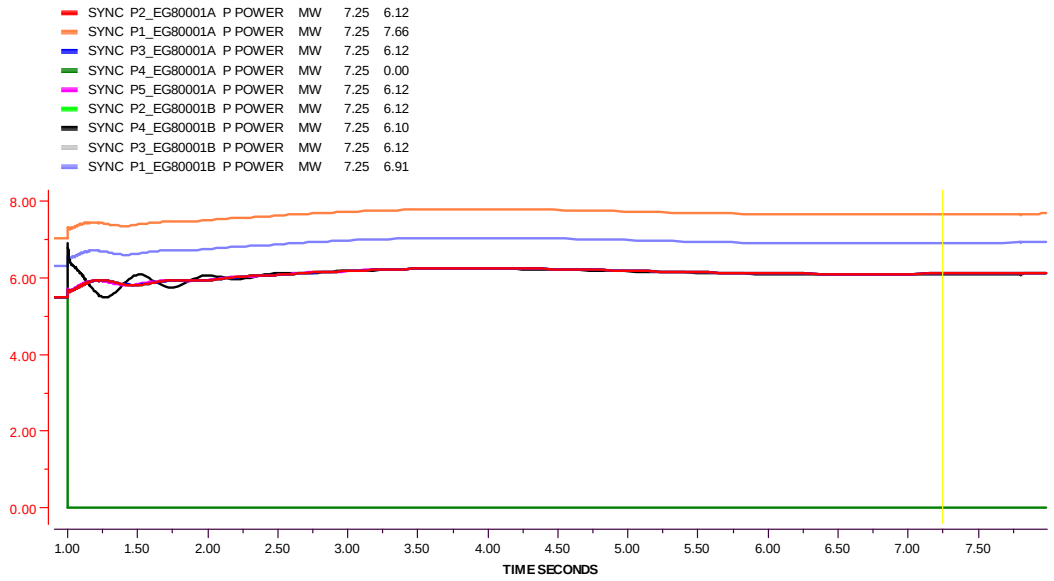

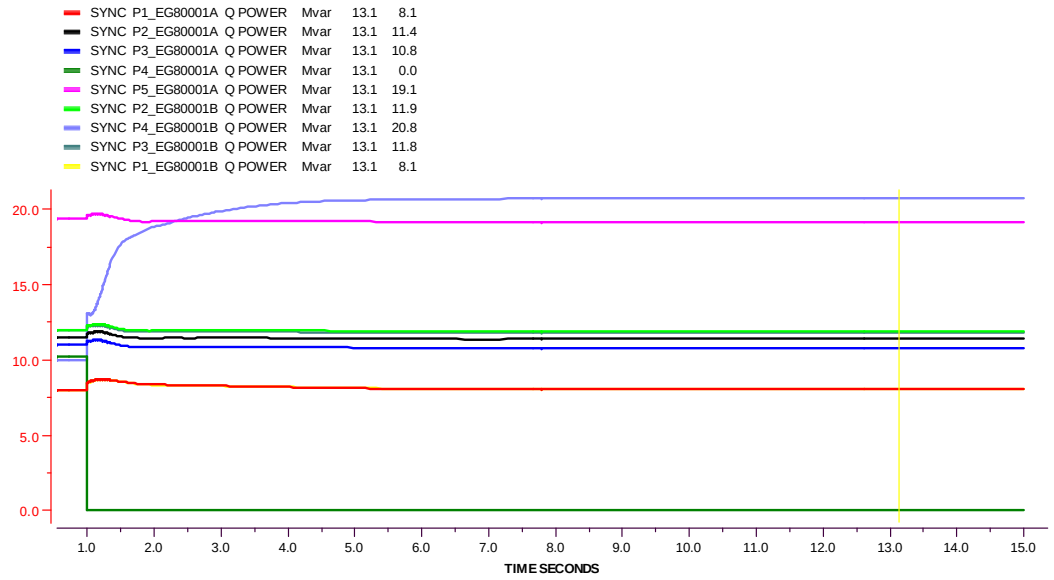

Appendix 2.20: Diagram of Case B2 – Loss of a GT at PF4, 100MW wind, Star Topology

Case C1: Loss of 25% [25MW] wind power for "Star" Topology with 36kV voltage system. Power flow - Single Line Diagram represents, Platform load bus voltages of 13.8kV (blue colour), main platform bus voltages (red colour), power generation at different 8 online GTs (purple colour) and power flow situation at network.
Note: 25% of wind power are represented equivalently by single power production unit owing to SIMPOW tool simplicity.

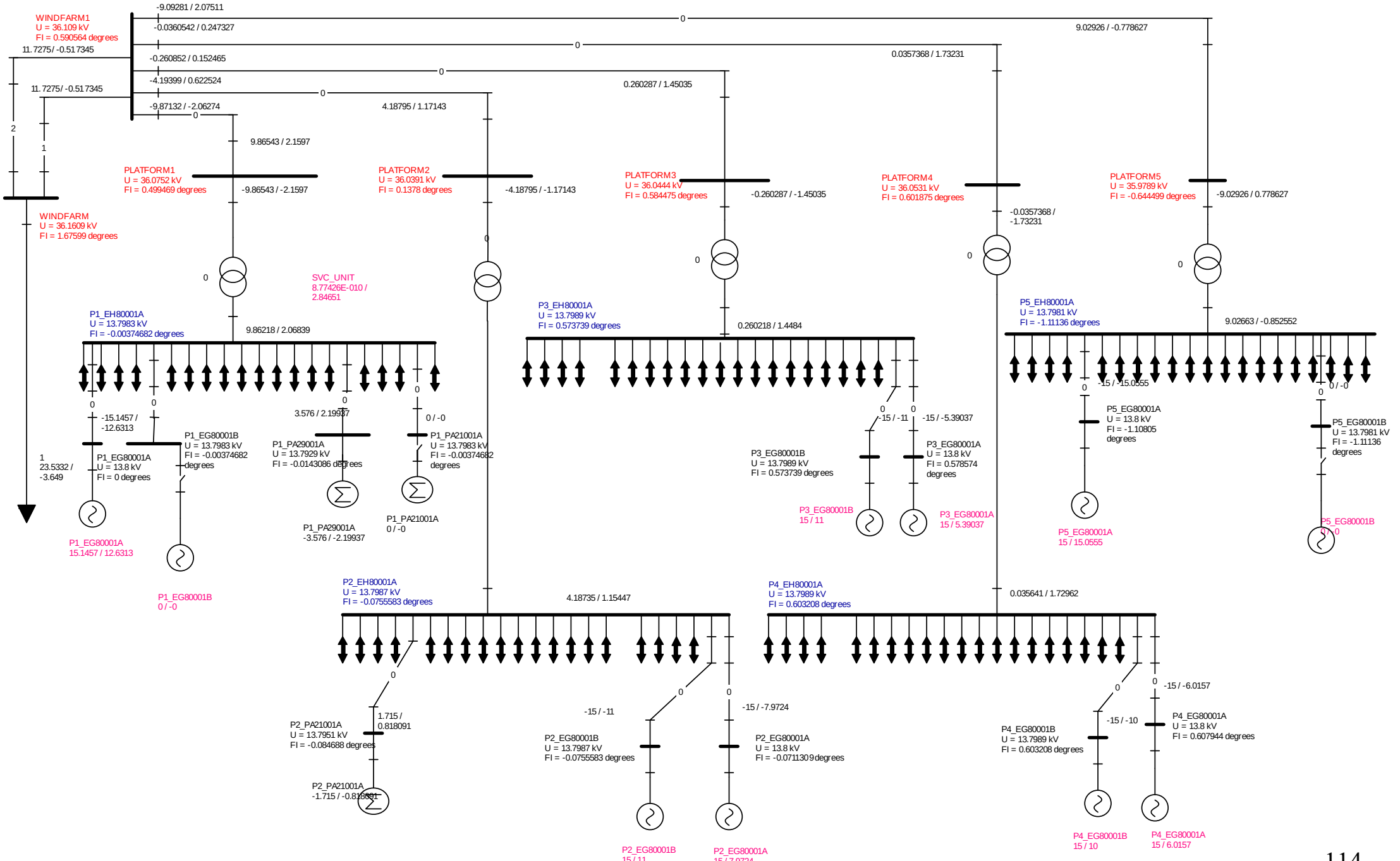

Appendix 2.21: SLD of Case C1 – Loss of a wind power at PCC, 25MW wind loss, Star Topology

Case C1: Loss of 25% [25MW] wind power for "Star" Topology with 36kV Voltage system. Diagram represents, frequency variation at different platform buses, Load bus voltage variation ref. to 13.8kV in pu, Active power and reactive power behavior at different online platform GTs at different platforms.

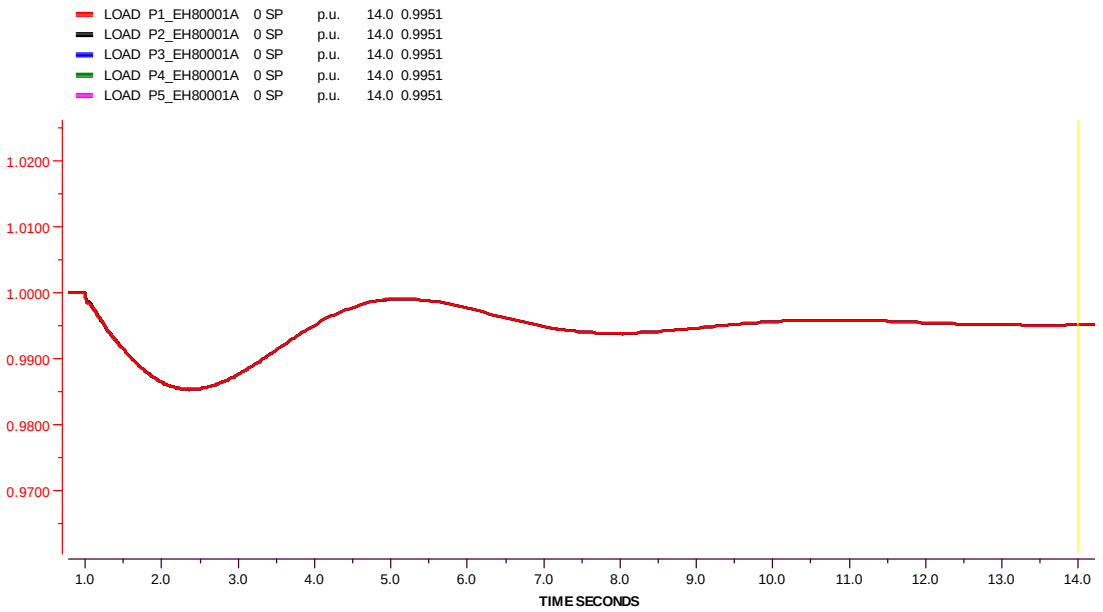

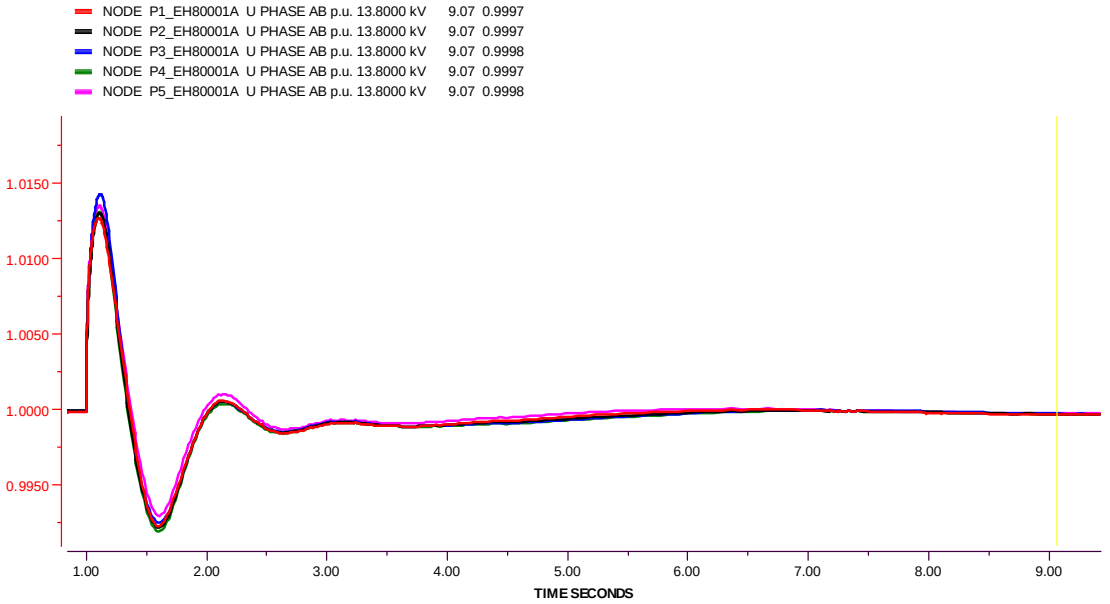

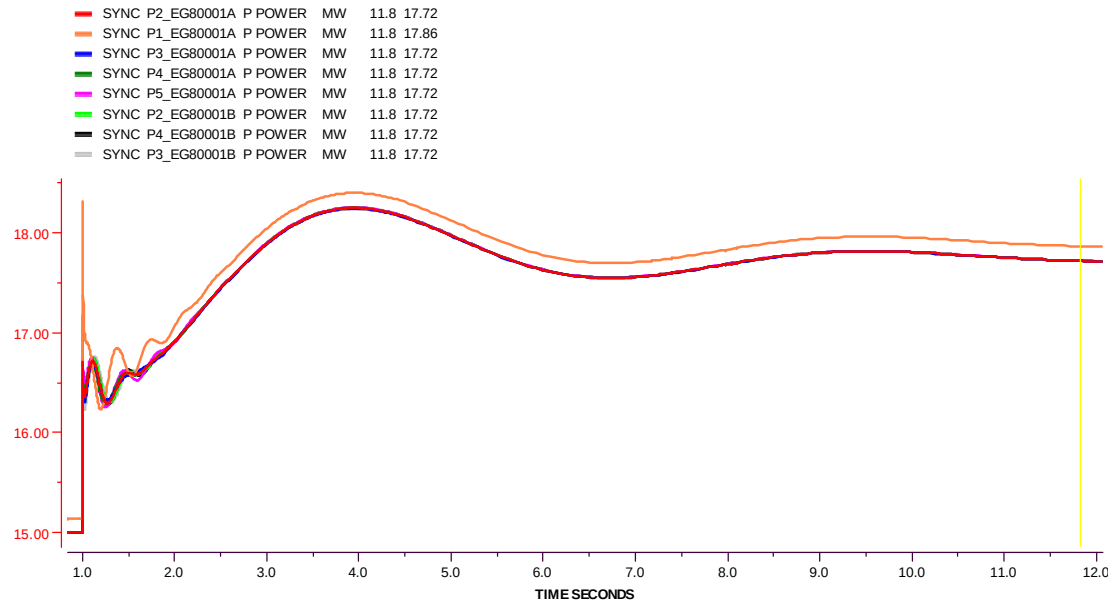

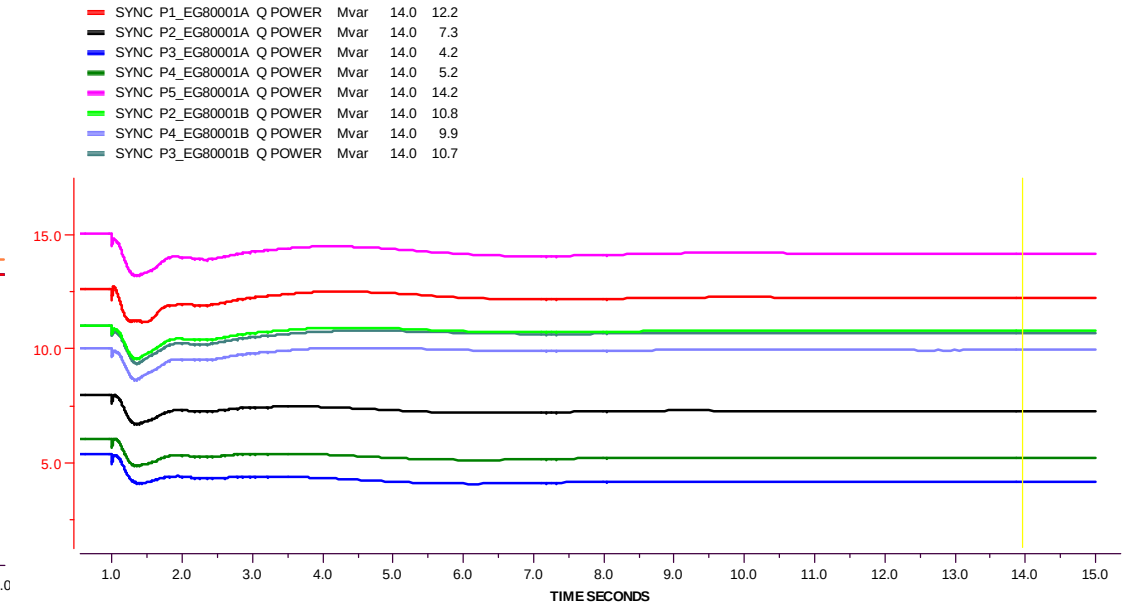

Appendix 2.22: Diagram of Case C1 – Loss of a wind power at PCC, 25MW wind loss, Star Topology

Case C2: Loss of 50% [50MW] wind power for "Star" Topology with 36kV voltage system. Power flow - Single Line Diagram represents, Platform load bus voltages of 13.8kV (blue colour), main platform bus voltages (red colour), power generation at different 8 online GTs (purple colour) and power flow situation at network.
Note: 25% of wind power are represented equivalently by single power production unit owing to SIMPOW tool simplicity.

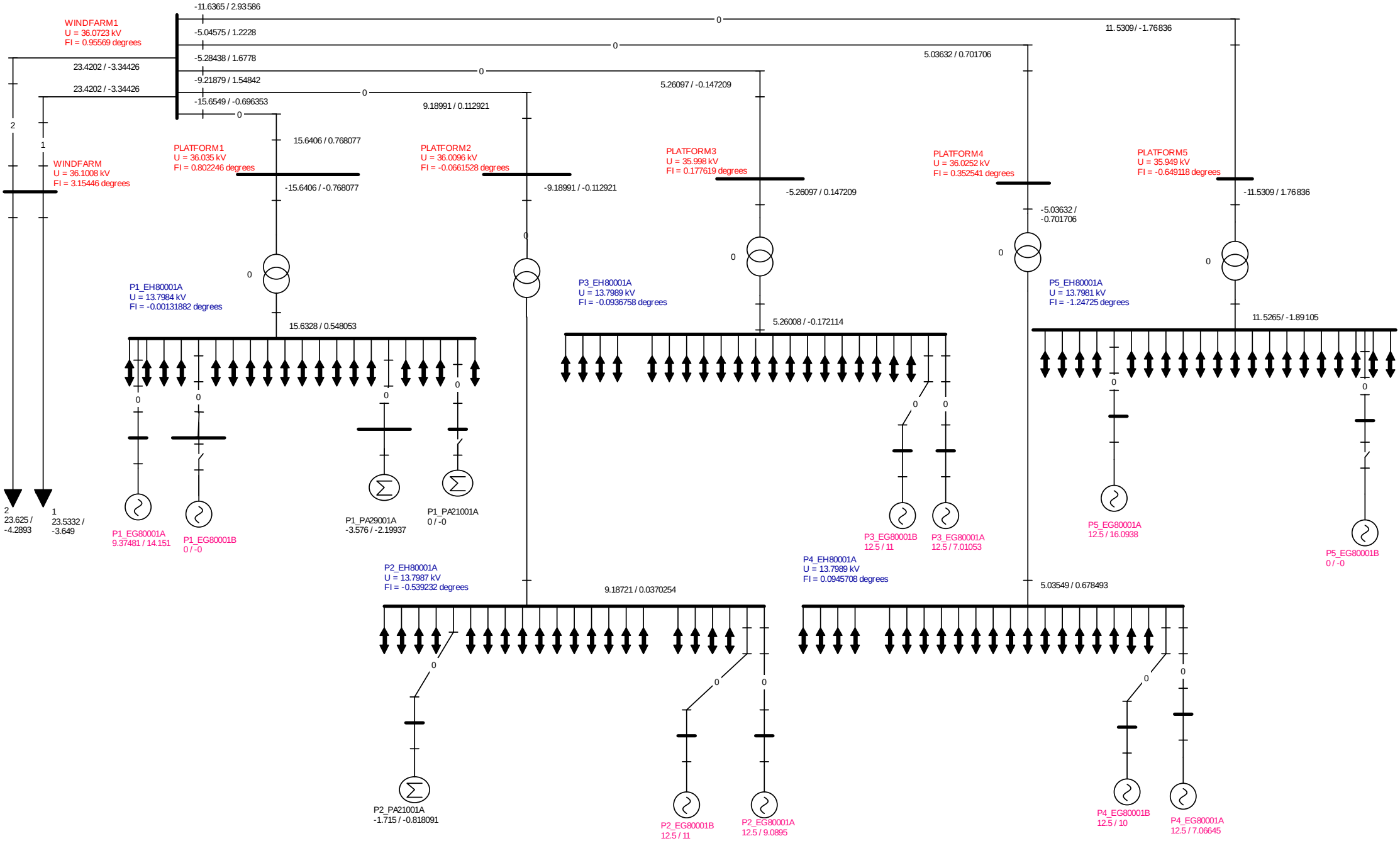

Appendix 2.23: SLD of Case C2 – Loss of a wind power at PCC, 50 MW wind loss, Star Topology

Case C2: Loss of 50% [50MW] wind power for "Star" Topology with 36kV Voltage system. Diagram represents, frequency variation at different platform buses, Load bus voltage variation ref. to 13.8kV in pu, Active power and reactive power behavior at different online platform GTs at different platforms.

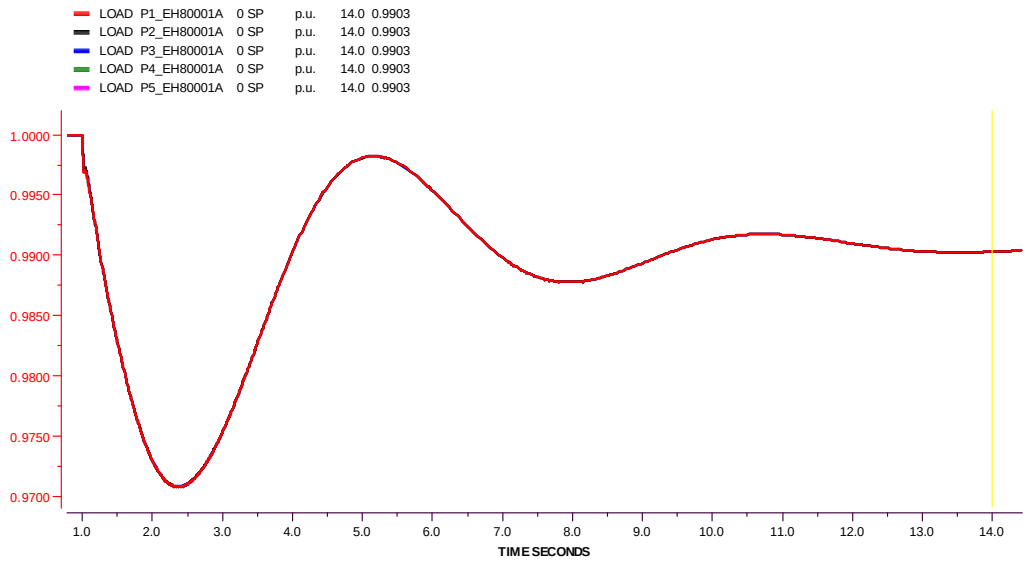

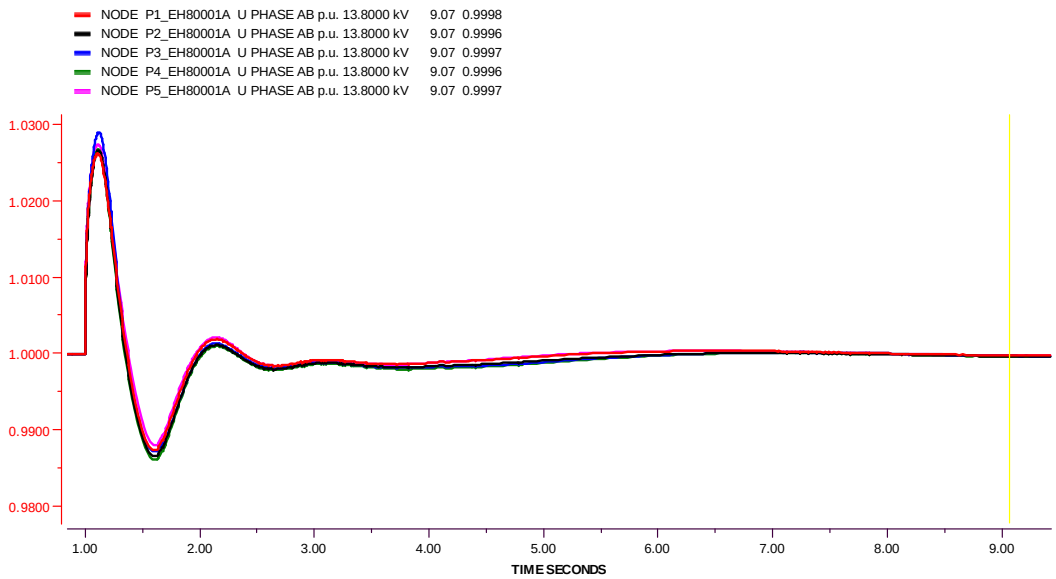

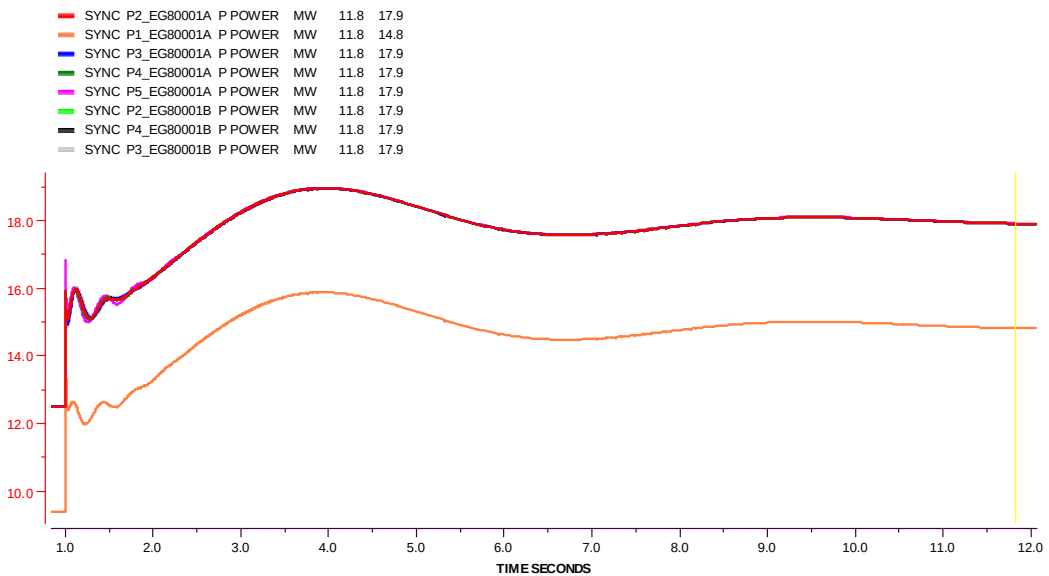

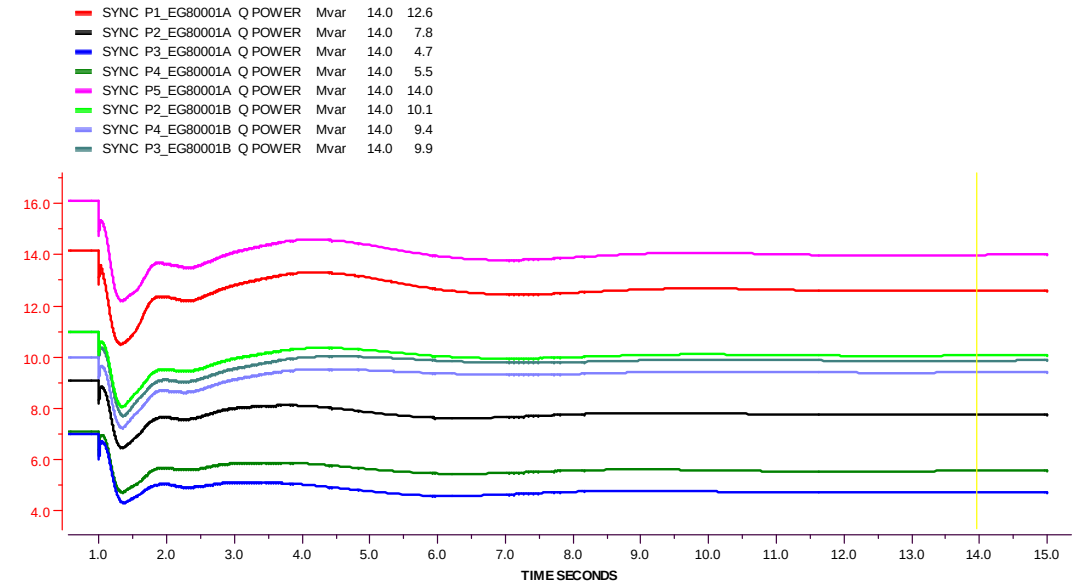

Appendix 2.24: Diagram of Case C2 – Loss of a wind power at PCC, 50 MW wind loss, Star Topology

Case C3: Loss of 100% [100MW] wind power for "Star" Topology with 36kV voltage system. Power flow - Single Line Diagram represents, Platform load bus voltages of 13.8kV (blue colour), main platform bus voltages (red colour), power generation at different 8 online GTs (purple colour) and power flow situation at network.
Note: 25% of wind power are represented equivalently by single power production unit owing to SIMPOW tool simplicity.

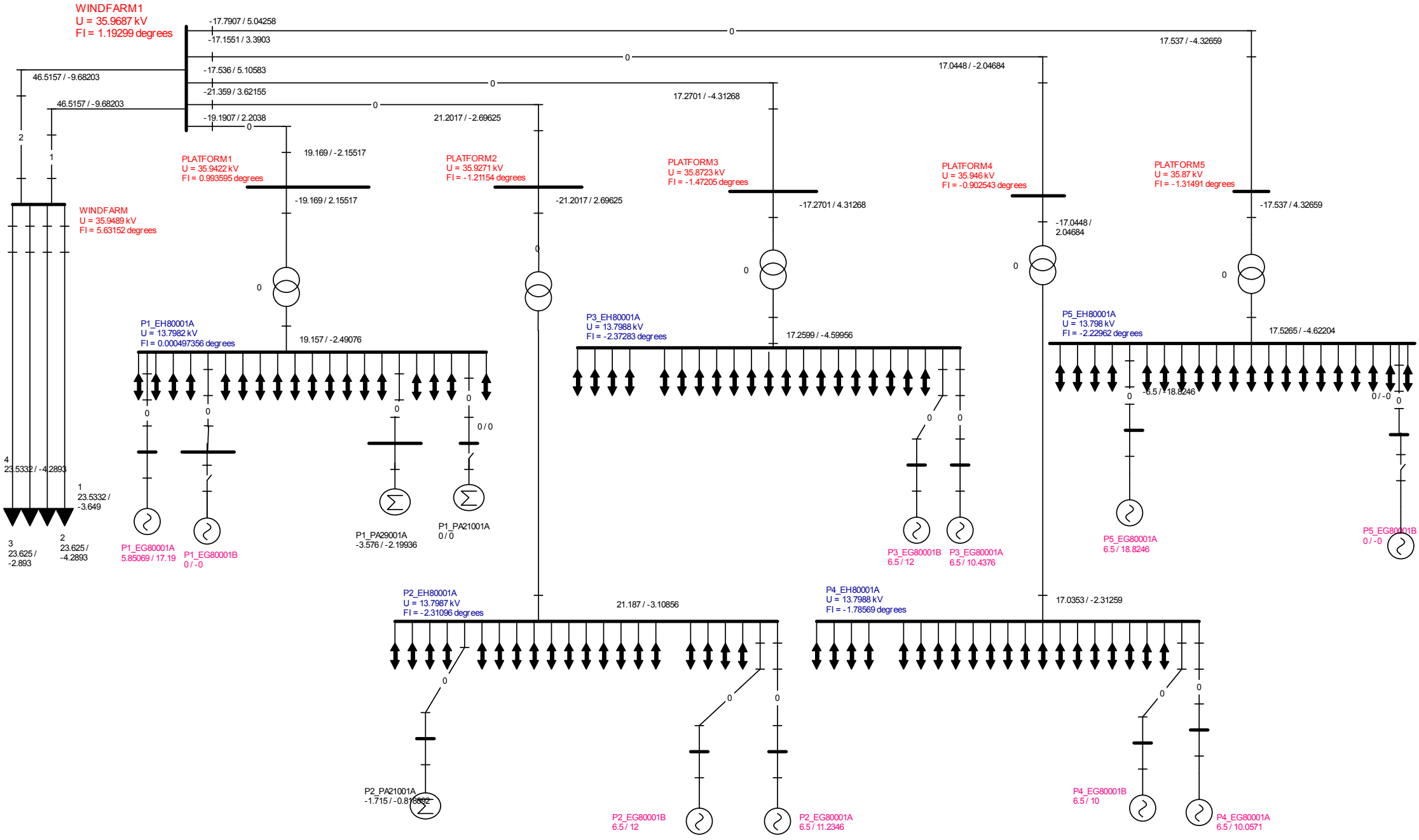

Appendix 2.25: SLD of Case C3 – Loss of a wind power at PCC, 100 MW wind loss, Star Topology

Case C3: Loss of 100% [100MW] wind power for "Star" Topology with 36kV Voltage system. Diagram represents, frequency variation at different platform buses, Load bus voltage variation ref. to 13.8kV in pu, Active power and reactive power behavior at different online platform GTs at different platforms.

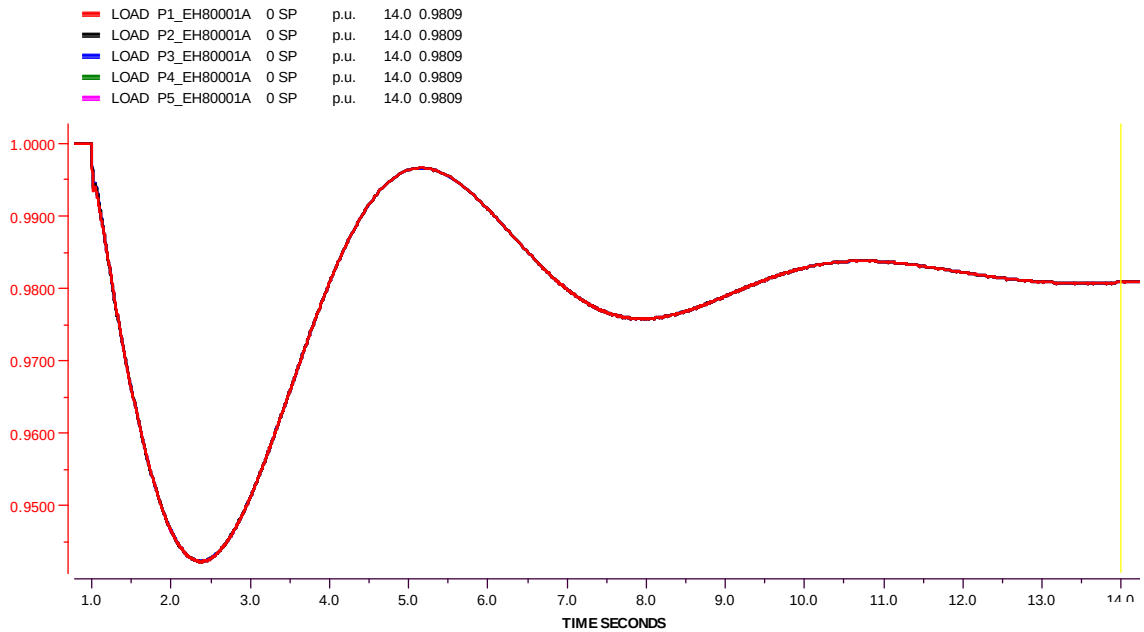

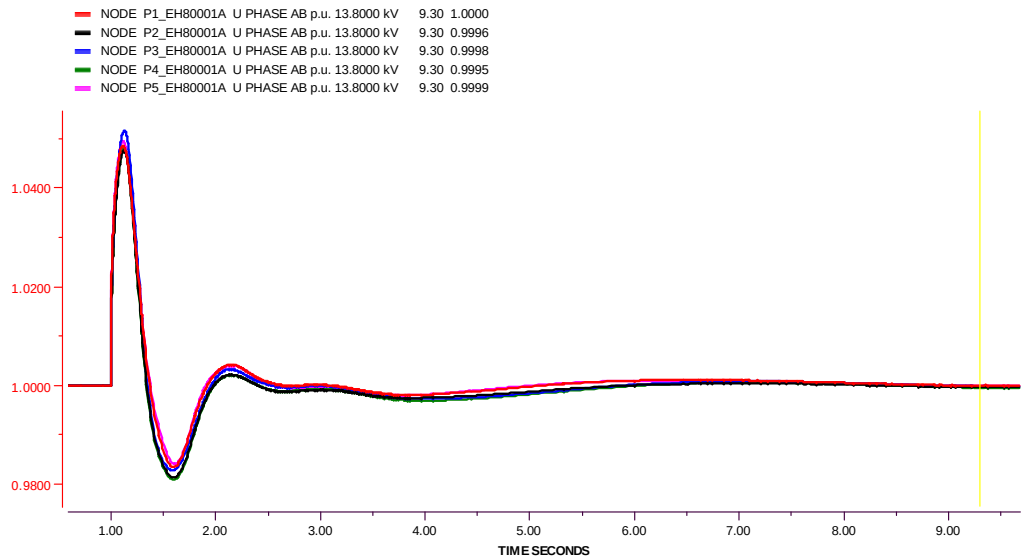

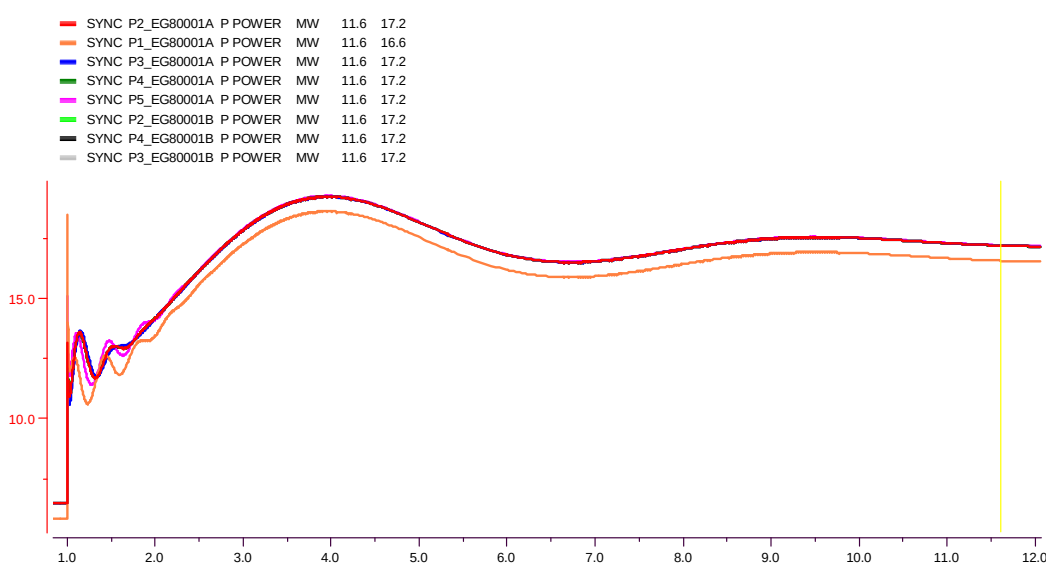

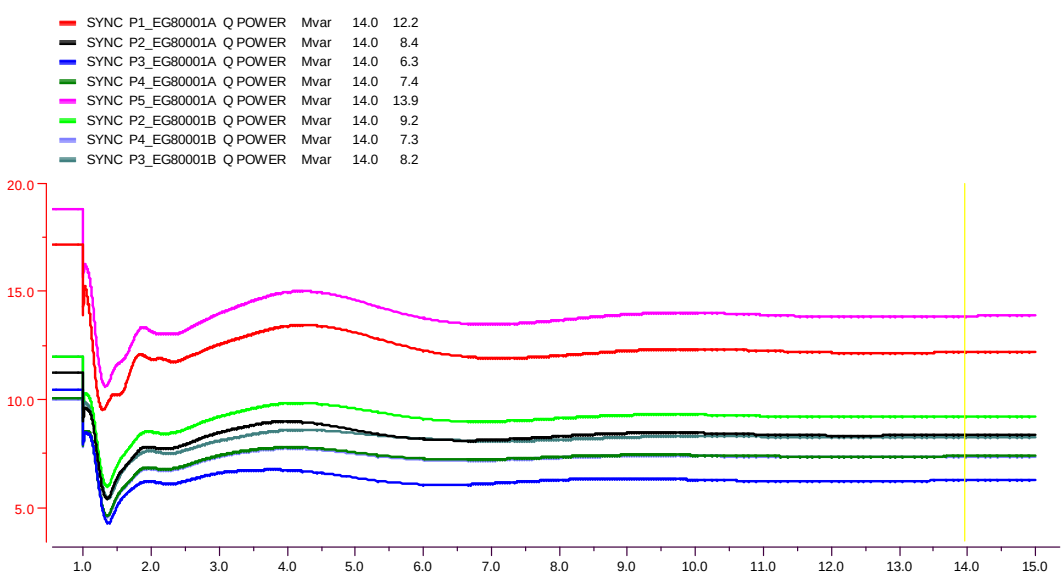

Appendix 2.26: Diagram of Case C3 – Loss of a wind power at PCC, 100 MW wind loss, Star Topology

Case D0: Loss of interconnection cable between PF1 (PCC) and PF4 for "Star" Topology, 36kV voltage system with no wind power included. Single Line Diagram represents, platform load bus voltages of 13.8kV (blue colour), main platform bus voltages (red colour), power generation at different 8 online GTs (purple colour) and power flow situation at network. Note: For simplicity disconnecting cable marked with red arrows in SLD.

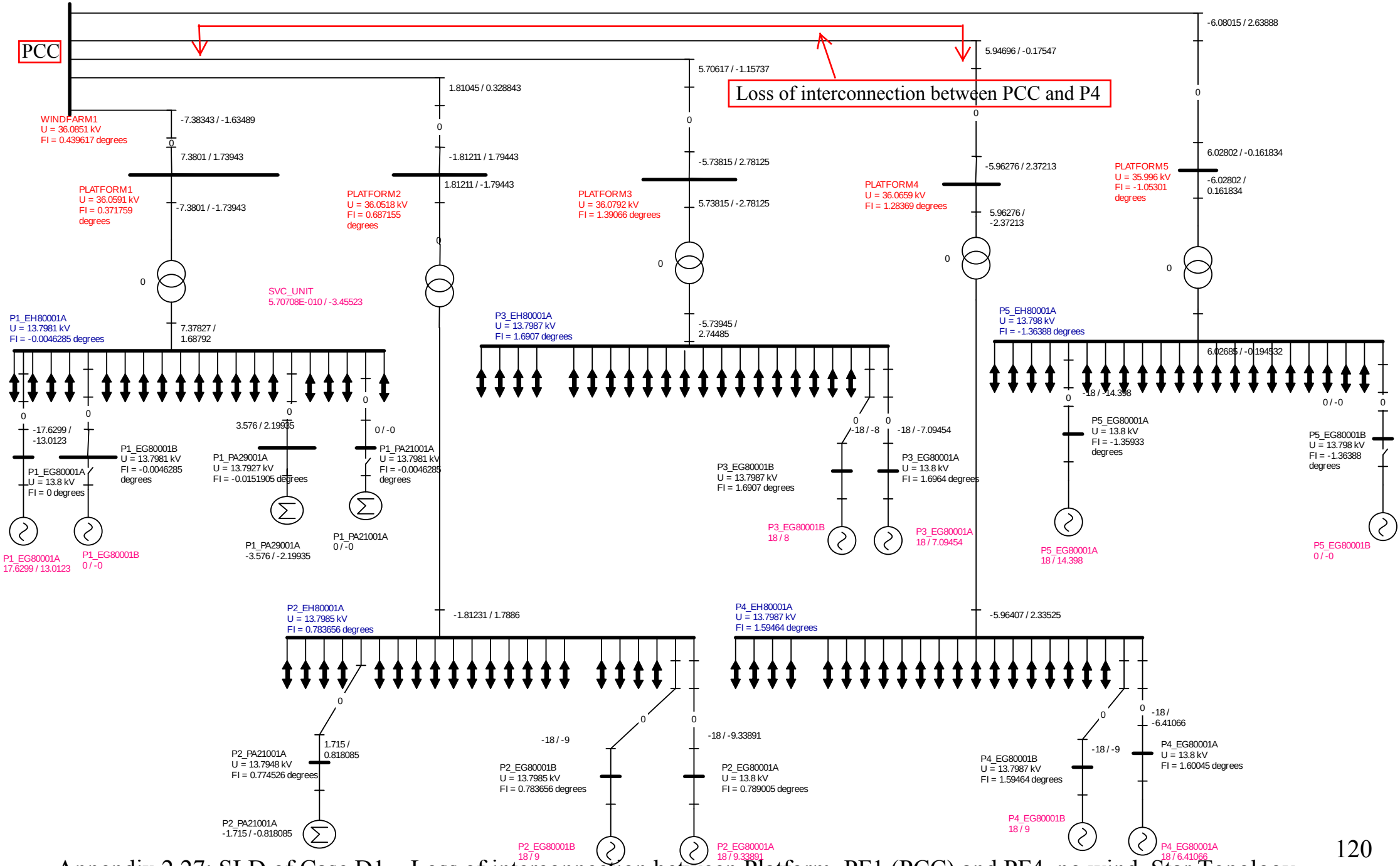

Appendix 2.27: SLD of Case D1 – Loss of interconnection between Platform PF1 (PCC) and PF4, no wind, Star Topology

Case D0: Loss of interconnection cable between PF1 (PCC) and PF4 for "Star" Topology, 36kV Voltage system with no wind included. Diagram represents, frequency variation at different platform buses, load bus voltage variation ref. to 13.8kV in pu, active power and reactive power behavior at different online platform GTs at different platforms.

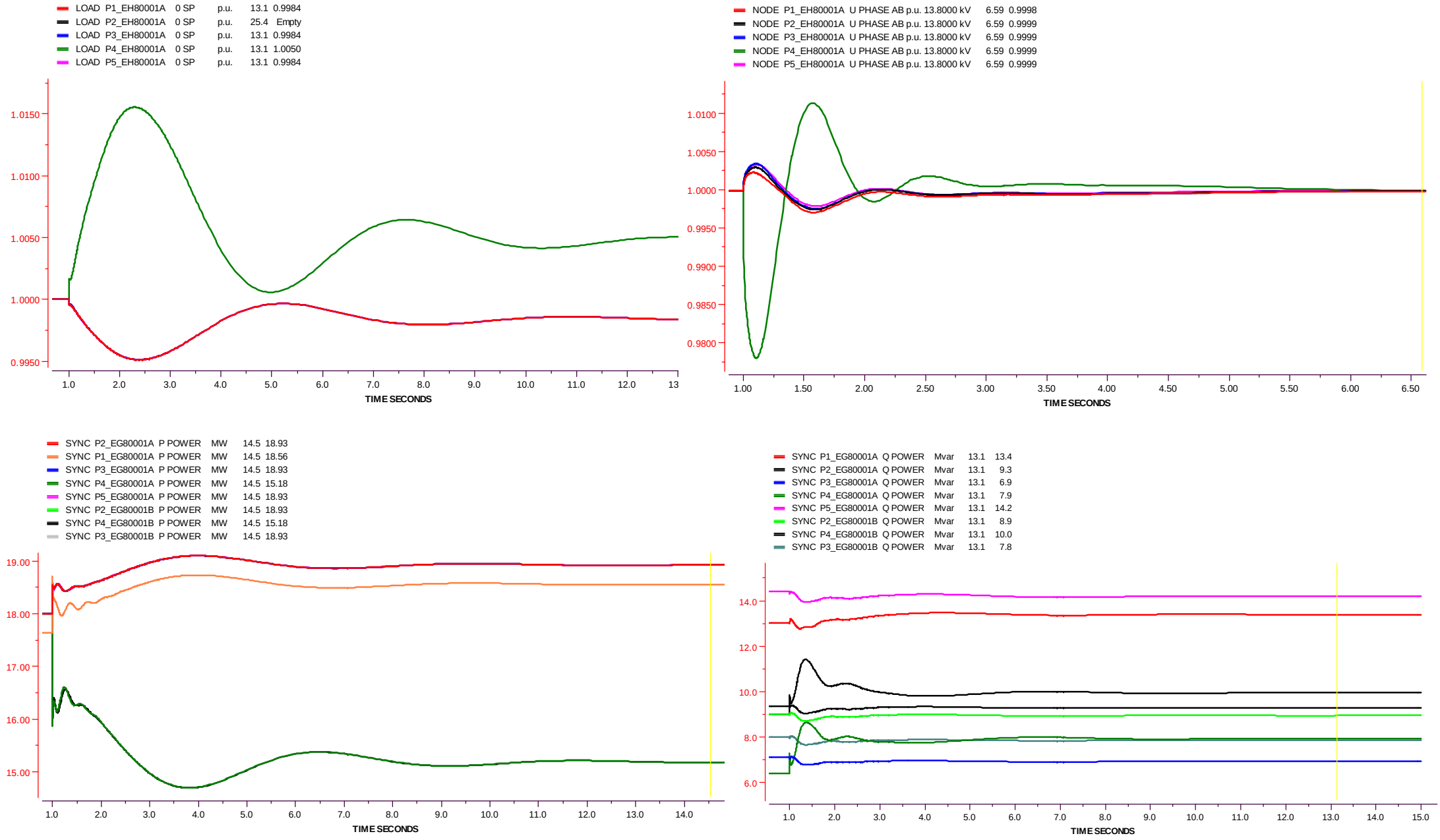

Appendix 2.28: Diagram of Case D1 – Loss of interconnection between Platform PF1 (PCC) and PF4, no wind, Star Topology

Case D1: Loss of interconnection cable between PF1 (PCC) and PF4 for "Star" Topology, 36kV voltage system with 50MW wind power penetration. Single Line Diagram represents, platform load bus voltages of 13.8kV (blue colour), main platform bus voltages (red colour), power generation at different 8 online GTs (purple colour) and power flow situation at network. Note: For simplicity disconnecting cable marked with red arrows in SLD.

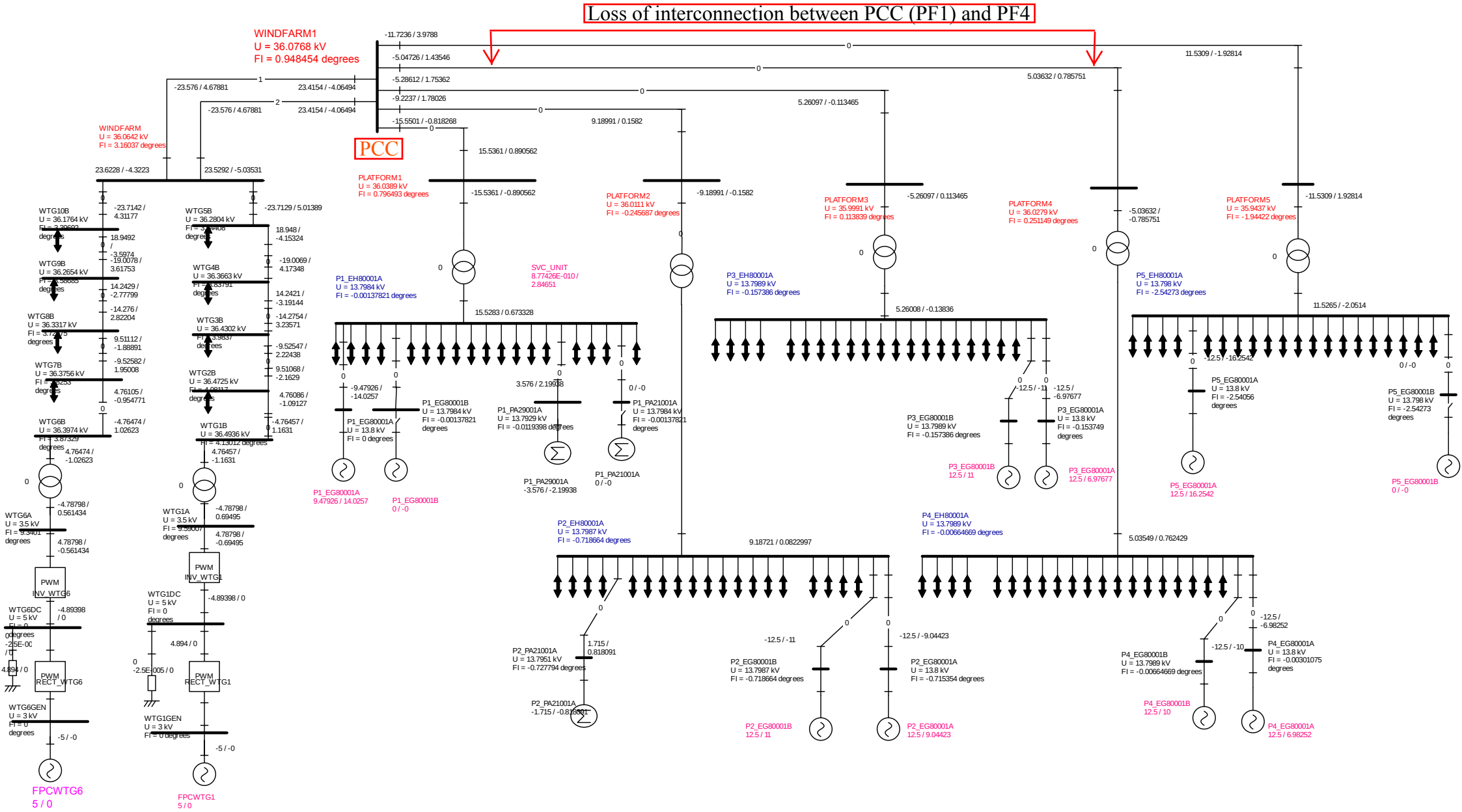

Appendix 2.29: SLD of Case D2 – Loss of interconnection between Platform PF1 (PCC) and PF4, 50MW wind penetration, Star Topology

Case D1: Loss of interconnection cable between PF1 (PCC) and PF4 for "Star" Topology, 36kV Voltage system with 50MW wind penetration. Diagram represents, frequency variation at different platform buses, load bus voltage variation ref. to 13.8kV in pu, active power and reactive power behavior at different online platform GTs at different platforms.

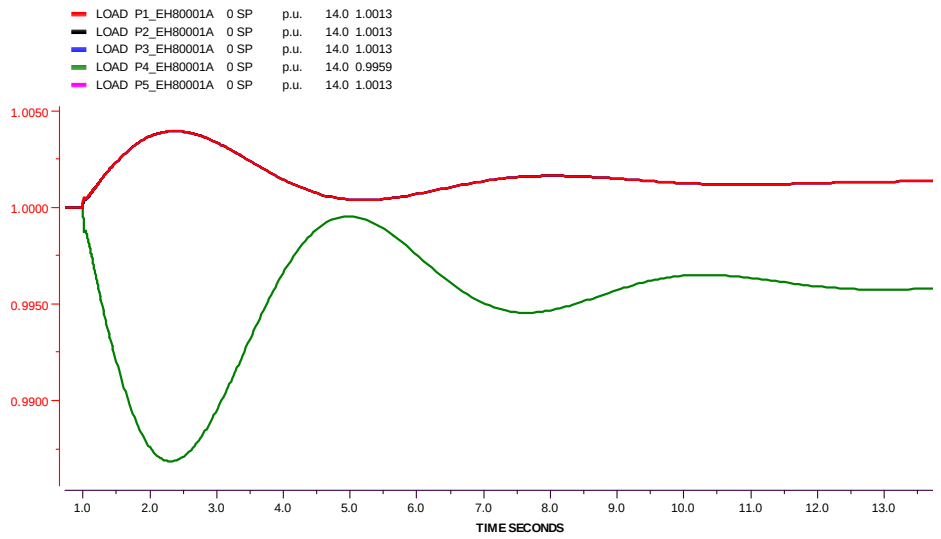

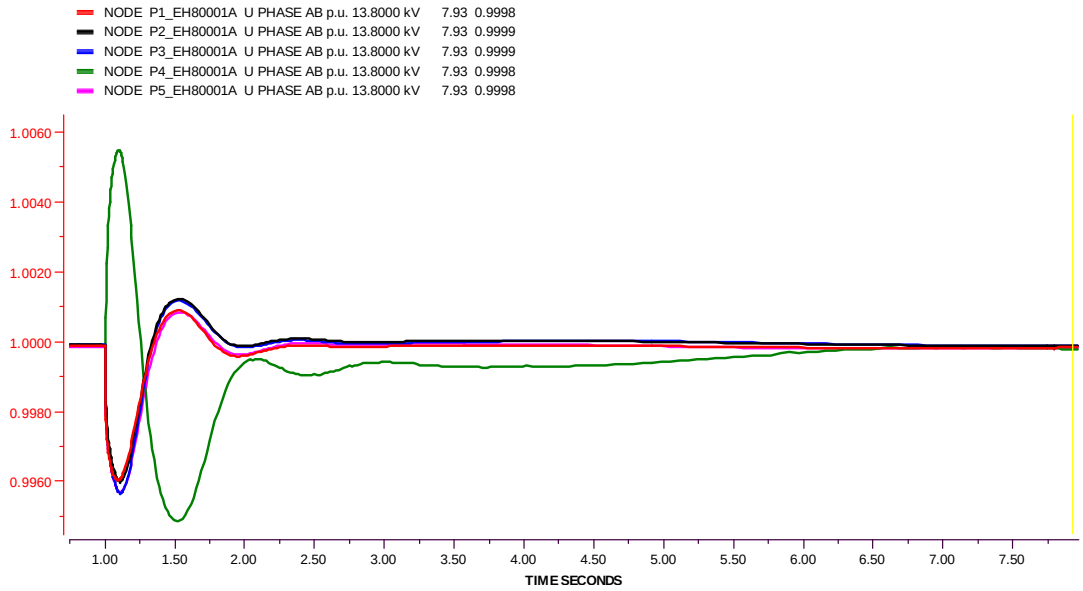

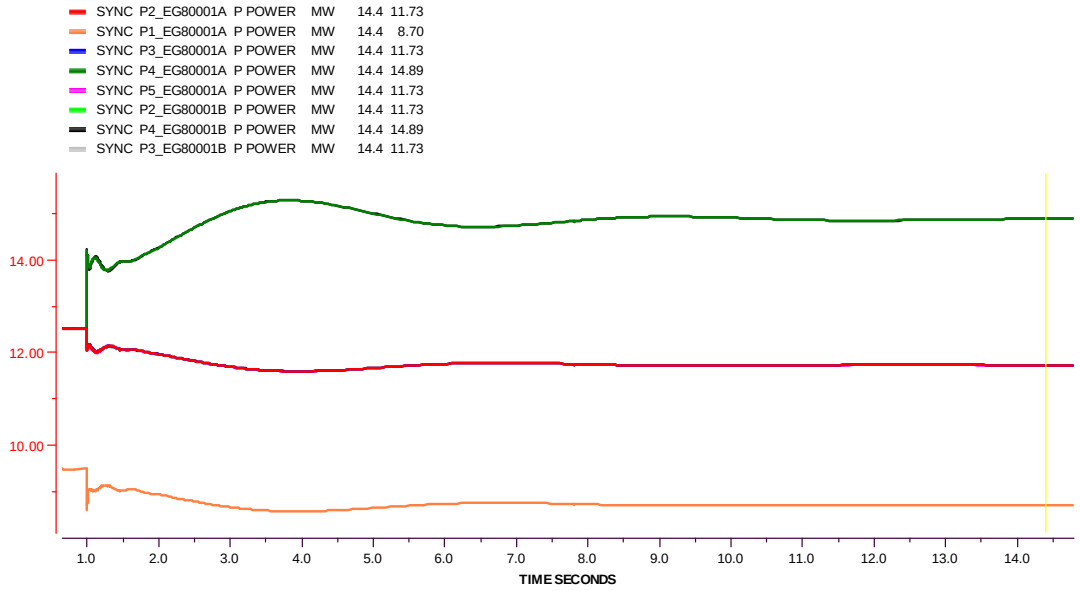

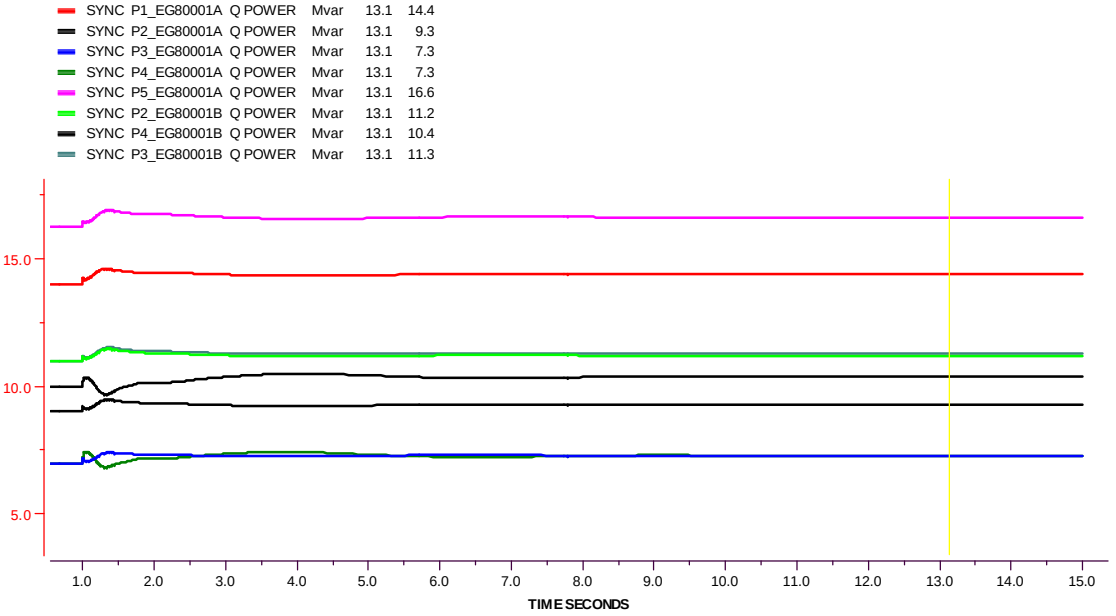

Appendix 2.30: Diagram of Case D2 – Loss of interconnection between Platform PF1 (PCC) and PF4, 50MW wind penetration, Star Topology

Case D2: Loss of interconnection cable between PF1 (PCC) and PF4 for "Star" Topology, 36kV voltage system with 100MW wind power penetration. Single Line Diagram represents, platform load bus voltages of 13.8kV (blue colour), main platform bus voltages (red colour), power generation at different 8 online GTs (purple colour) and power flow situation at network. Note: For simplicity disconnecting cable marked with red arrows in SLD.

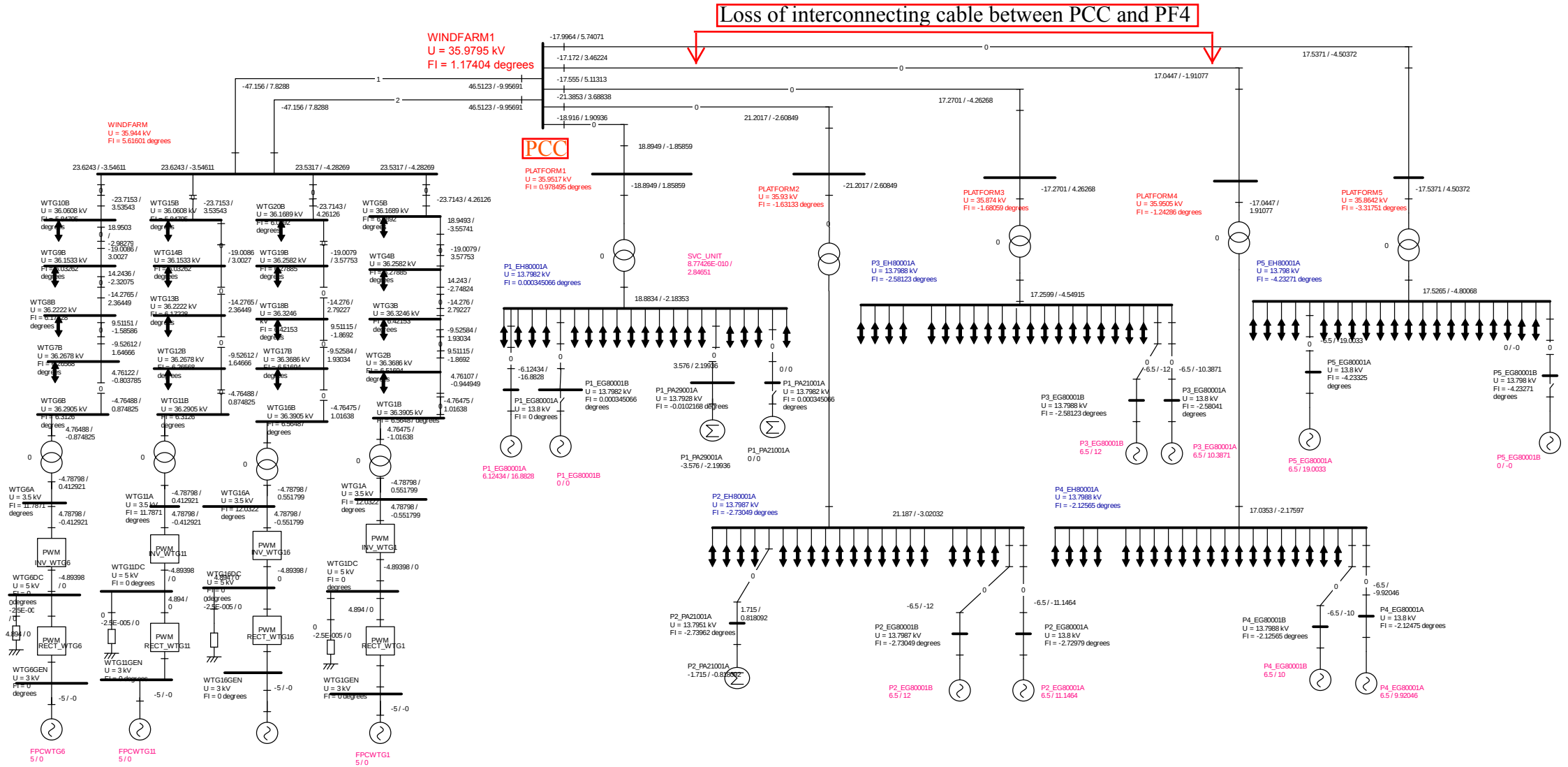

Appendix 2.31: SLD of Case D2 – Loss of interconnection between Platform PF1 (PCC) and PF4, 100MW wind penetration, Star Topology

Case D2: Loss of interconnection cable between PF1 (PCC) and PF4 for "Star" Topology, 36kV Voltage system with 100MW wind included. Diagram represents, frequency variation at different platform buses, load bus voltage variation ref. to 13.8kV in pu, active power and reactive power behavior at different online platform GTs at different platforms.

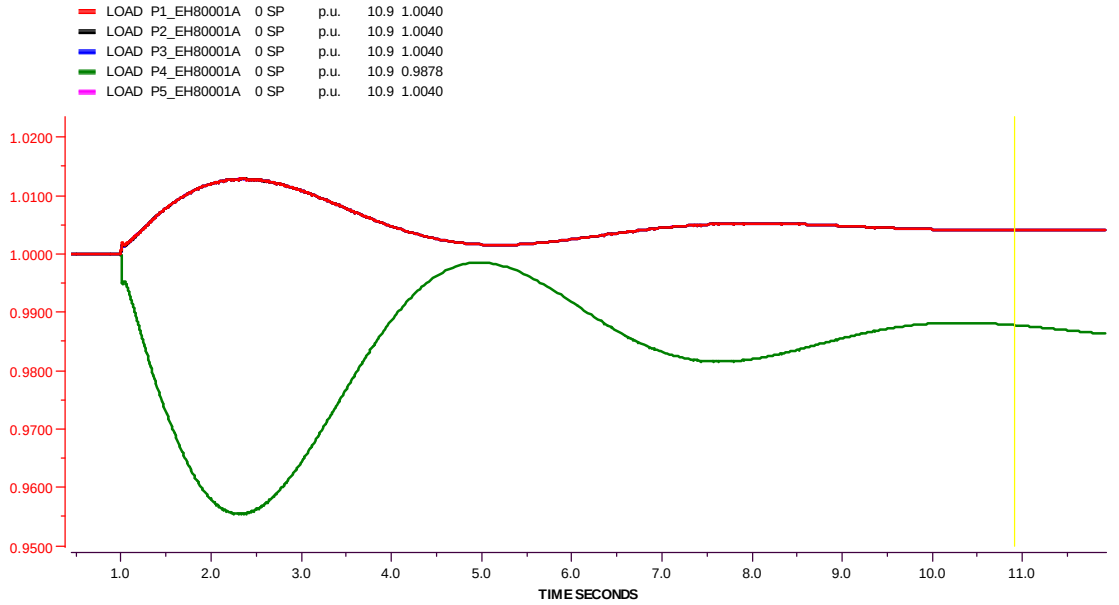

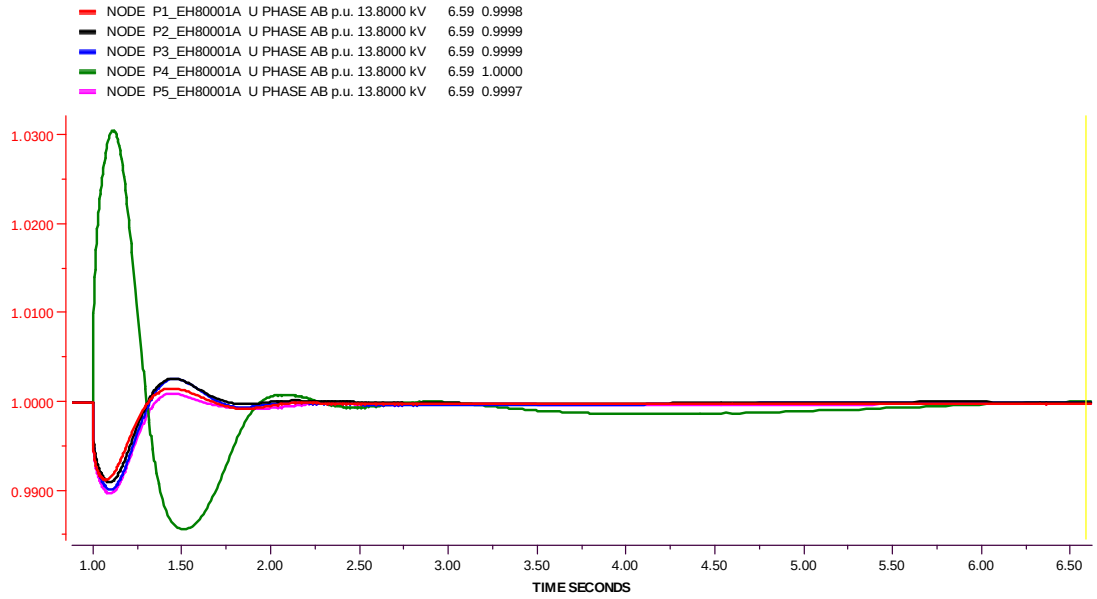

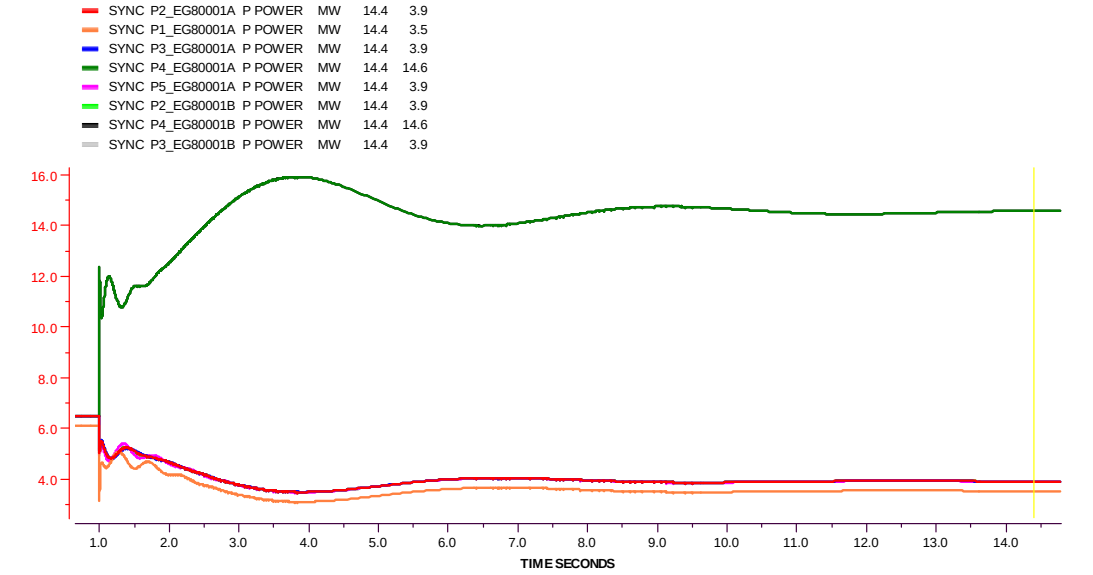

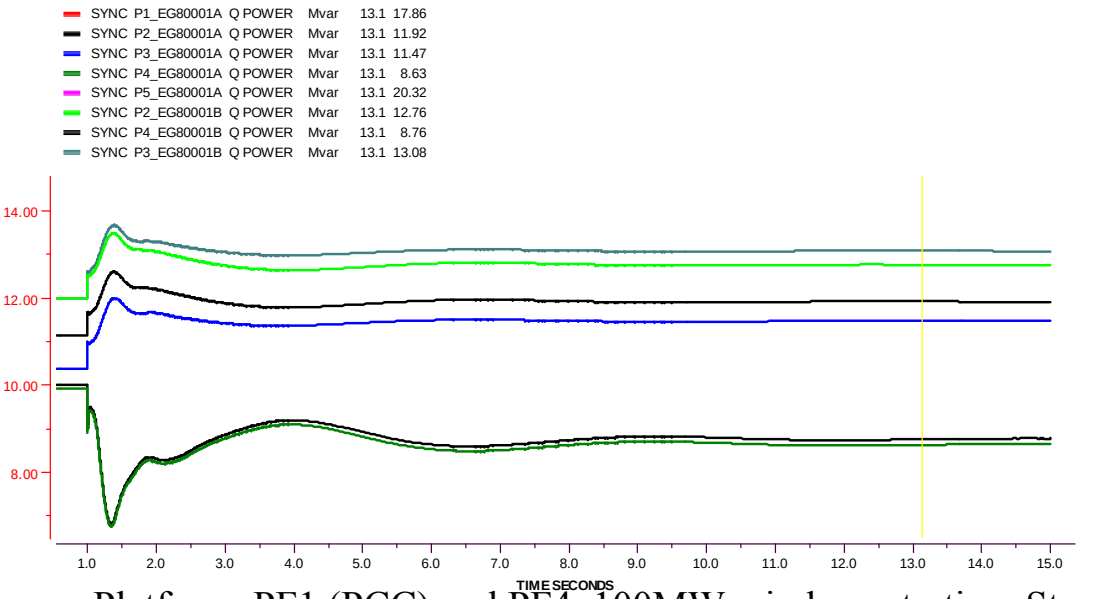

Appendix 2.32: Diagrams of Case D2 – Loss of interconnection between Platform PF1 (PCC) and PF4, 100MW wind penetration, Star Topology